The Requirement for Endothelial Cell Tetrahydrobiopterin in Health and Disease

Surawee Chuaiphichai

Department of Cardiovascular Medicine
&
Magdalen College



A thesis submitted for the degree of Doctor of Philosophy in Cardiovascular Medicine

University of Oxford

Michaelmas Term 2014

Abstract

The Requirement for Endothelial Cell Tetrahydrobiopterin in Health and Disease

Surawee Chuaiphichai

Department of Cardiovascular Medicine and Magdalen College, University of Oxford
Submitted for the degree of D.Phil in Cardiovascular Medicine
Michaelmas Term 2014

Tetrahydrobiopterin (BH4) is an essential cofactor for endothelial nitric oxide synthase (eNOS) function and nitric oxide (NO) generation. Augmentation of BH4 levels can prevent eNOS uncoupling and improve endothelial dysfunction in vascular disease states. However, the physiological requirement for *de-novo* endothelial cell BH4 biosynthesis in eNOS function remains unclear. We generated a novel mouse model with endothelial cell-specific deletion of *GCH1*, encoding GTP cyclohydrolase 1, an essential enzyme for BH4 biosynthesis, to test the cell-autonomous requirement for endothelial BH4 biosynthesis under physiological conditions and disease states *in vivo*.

Mice with a floxed *GCH1* allele (*GCH1*$^{fl/fl}$) were crossed with Tie2cre mice to delete *GCH1* in endothelial cells. *GCH1*$^{fl/fl}$Tie2cre mice demonstrated reduced NO bioactivity and significantly greater $O_2^{\bullet-}$ production. *GCH1*$^{fl/fl}$Tie2cre aortas and mesenteric arteries had impaired endothelium-dependent vasodilatations to acetylcholine. Endothelium-dependent vasodilatations in *GCH1*$^{fl/fl}$Tie2cre aortas were in part mediated by NOS-derived hydrogen peroxide, through soluble guanylate cyclase. *GCH1*$^{fl/fl}$Tie2cre mice had higher systemic blood pressure than wild-type littermates, which was normalised by the NOS inhibitor, L-NAME.

In a lipopolysaccharide (LPS)-induced systemic inflammation model, *GCH1*$^{fl/fl}$Tie2cre mice were partially protected against LPS-induced vascular dysfunction and hypotension compared to wild-type littermates. In the angiotensin II (Ang-II)-induced hypertension model, chronic Ang II infusion with a sub-pressor dose caused hypertension in *GCH1*$^{fl/fl}$Tie2cre mice but did not alter blood pressure in wild-type littermates. Abdominal aortic aneurysms (AAA) in response to Ang II infusion were observed in *GCH1*$^{fl/fl}$Tie2cre but not in wild-type mice. In pregnancy, *GCH1*$^{fl/fl}$Tie2cre mice exhibited a loss of NOS-derived NO mediated vasodilatation, impaired uterine vascular adaptation, increased blood pressure and fetal growth restriction.

Taken together, these studies reveal that endothelial cell *GCH1* and BH4 biosynthesis play a pivotal role in vascular function and blood pressure regulation in health and disease. Therefore, targeting vascular *GCH1* and BH4 biosynthesis may provide a novel therapeutic target for the prevention and treatment of vascular dysfunction in patients with hypertension, AAA formation, septic shock and preeclampsia.

Chapter 1: Introduction 19

1.1 Endothelium and vascular diseases 19

1.2 Endothelium and vascular homeostasis 19

1.2.1 Nitric oxide 20

1.2.2 EDHF 21

1.2.3 Prostacyclin 22

1.3 Oxidative stress and vascular disease 23

1.4 NO synthesis and function 24

1.4.1 NO synthesis 24

1.4.2 Regulation of eNOS function 25

1.5 BH4 biosynthesis and function 26

1.5.1 BH4 biosynthesis 26

1.5.2 Regulation of GTPCH 29

1.6 eNOS regulation by BH4 in vascular disease 29

1.7 Mouse models of BH4 deficient and BH4 overexpression in vascular disease 31

1.7.1 hph-1 mice 31

1.7.2 The *GCH* transgenic mouse (GCH-Tg) 33

1.8 BH4 and other cardiovascular diseases 35

1.8.1 Abdominal aortic aneurysm 35

1.8.2 Septic shock and systemic inflammation....36

1.9 Clinical relevance of BH4 regulation in vascular disease....37

1.10 Hypothesis....38

1.11 Aims....39

Chapter 2: Material and methods....41

2.1 Materials....41

2.1.1 Buffers and Media....41

2.2 Animals....42

2.2.1 Animal handling conditions....42

2.2.2 *GCH1*$^{fl/fl}$Tie2cre mice....43

2.3 DNA techniques....45

2.3.1 DNA extraction....45

2.3.2 Genotyping PCR....45

2.3.3 Procedure of harvesting mouse tissues....49

2.4 Tetrahydrobiopterin assay....49

2.5 Isolation of Murine Endothelial Cells....52

2.6 NO bioactivity measurements....54

2.6.1 Analysis of NO Synthesis by eNOS....54

2.6.2 Nitrite and Nitrate Determination....54

2.6.3 Determination of Aortic NO Production by EPR 55

2.7 Measurement of superoxide and other ROS 56

2.7.1 Quantification of Intracellular Superoxide Production by HPLC 56

2.7.2 Oxidative Fluorescent Microtopography 57

2.7.3 Determination of Aortic H_2O_2 Production 57

2.8 Isometric studies of vasomotor function 58

2.8.1 Wire myograph 58

2.8.2 Mouse mesenteric artery isolation and preparation 59

2.8.3 Isometric tension vasomotor studies in aorta 61

2.8.4 Isometric tension vasomotor studies in mesenteric arteries 61

2.9 Protein extraction and detection 62

2.9.1 Protein lysate preparation 62

2.9.2 Determination of protein content 63

2.9.3 Immunoblotting 63

2.10 Statistical analysis 66

Chapter 3: Characterisation of the Endothelial Cell-Targeted *GCH1* Knockout Mouse 68

3.1 Introduction 68

3.2 Hypothesis and aims 69

3.3 Methods 70

3.4 Results 70

3.4.1 Excision of *GCH1* floxed allele in *GCH1*$^{fl/fl}$Tie2cre mice 70

3.4.2 GTP Cyclohydrolase protein expression and BH4 levels in tissues 72

3.4.3 GTPCH protein expression and BH4 levels in primary endothelial cells 76

3.4.4 Measurement of superoxide production 78

3.4.5 Measurement of NO bioactivity 82

3.5 Discussion 87

Chapter 4: Vascular Function in Endothelial Cell-Specific BH4 Deficient Mice 91

4.1 Introduction 91

4.2 Hypothesis and aims 92

4.3 Methods 94

4.4 Results 94

4.4.1 Vascular function in aorta 94

4.4.2 Vascular function in mesenteric arteries 119

4.5 Discussion 133

Aortas 133

4.5.1 Vascular function in aortas 134

4.5.2 Vascular function in mesenteric arteries 136

Chapter 5: Haemodynamic Regulation in Endothelial Cell-Specific BH4 Deficiency in Health and Disease 143

5.1 Introduction 143

5.2 Hypothesis and aims 145

5.3 Methods 147

5.3.1 Haemodynamic measurements 147

5.3.2 Angiotensin II-induced hypertension 148

5.3.3 LPS-induced systemic inflammation 148

5.4 Results 149

5.4.1 Haemodynamic measurements 149

5.4.2 Haemodynamic responses in anaesthetised mice 153

5.4.3 Haemodynamic responses in conscious mice via tail-cuff method 163

5.4.4 Ang II induced Hypertension 170

5.4.5 LPS-induced hypotension 176

5.5 Discussion 188

5.5.1 Haemodynamic responses under basal physiological condition 189

5.5.2 Haemodynamic responses to Ang II infusion 192

5.5.3 Haemodynamic responses to LPS-induced systemic inflammation 193

Chapter 6: The requirement for endothelial cell BH4 biosynthesis in vascular adaptation to pregnancy.....198

6.1 Introduction 198

6.2 Hypothesis and aims.....201

6.3 Methods 202

6.3.1 Timed mating.....202

6.3.2 BH4 measurement 202

6.3.3 Blood pressure measurement.....204

6.3.4 Statistical analysis 205

6.4 Results.....206

6.4.1 Reproductive outcome.....206

6.4.2 Determination of BH4 levels.....213

6.4.3 Vascular function in uterine arteries.....217

6.4.4 Increased systolic blood pressure in *GCH1*$^{fl/fl}$Tie2cre female mice. 227

6.5 Discussion 231

Chapter 7: General Discussion 238

7.1 Principal findings and implications 238

7.2 Future Work 239

7.3 Concluding Remarks.....241

Chapter 8: References 243

Chapter 9: Appendices 258

9.1 Timing and venue of research 259

9.2 Research funding 259

9.3 Attributions 259

9.4 Acknowledgements 260

9.5 Publications arising from research 261

9.5.1 Publications arising from this thesis 261

9.5.2 Publications arising from other research work 261

9.5.3 Abstracts presented at scientific conferences 262

List of Figures

Figure 1.1 BH4 biosynthesis and metabolism 28

Figure 2.1 Growth curves 44

Figure 2.2 Genotyping of genomic DNA from *GCH1*$^{fl/fl}$Tie2cre and wild-type mice 48

Figure 2.3 Representative chromatograms of BH4 traces 51

Figure 2.4 Primary endothelial cells isolated from lungs 53

Figure 3.1 Generation and characterisation of *GCH1*$^{fl/fl}$Tie2cre mice 71

Figure 3.2 GTPCH protein and BH4 levels in aortas 74

Figure 3.3 BH4 measurements in tissues and plasma 75

Figure 3.4 GTPCH and BH4 levels in primary endothelial cells 77

Figure 3.5 Quantification of superoxide production in endothelial cells 79

Figure 3.6 Superoxide dection in aortic sections 81

Figure 3.7 NOS bioactivity 84

Figure 3.8 NO measurement by EPR 86

Figure 4.1 Vasoconstriction in wild-type and *GCH1*$^{fl/fl}$Tie2cre aortas 96

Figure 4.2 Endothelium-dependent vasodilatation in aortas 97

Figure 4.3 Effect of indomethacin on vascular function in aortas 100

Figure 4.4 H_2O_2-mediated vasodilatation in *GCH1*$^{fl/fl}$Tie2cre aortas 102

Figure 4.5 Effect of catalase on vascular function in aortas 103

Figure 4.6 eNOS-derived H_2O_2 mediated vasodilatation in *GCH1*$^{fl/fl}$Tie2cre aortas 104

Figure 4.7 Mechanism of H_2O_2 mediated vasodilatation in *GCH1*$^{fl/fl}$Tie2cre aortas 106

Figure 4.8 Mechanism of H_2O_2 mediated vasodilatation in *GCH1*$^{fl/fl}$Tie2cre aortas 107

Figure 4.9 H_2O_2 measurements in aortas 109

Figure 4.10 Mechanism of exogenous H_2O_2 mediated vasodilatation in aortas 111

Figure 4.11 Mechanism of exogenous H_2O_2 mediated vasodilatation in aortas 112

Figure 4.12 Effect of BH4 analogue on vascular function in aortas 114

Figure 4.13 Effect of sepiapterin on vascular function in aortas 115

Figure 4.14 eNOS and antioxidant proteins in aortas 117

Figure 4.15 eNOS at Ser1177, eNOS T495 and VASP proteins in aortas 118

Figure 4.16 GTPCH and eNOS proteins in mesenteric arteries 120

Figure 4.17 Vasomotor function in mesenteric arteries 123

Figure 4.18 Endothelium-dependent vasodilatation in mesenteric arteries 124

Figure 4.19 Contribution of prostacyclin, eNOS-derived vasodilators and EDHF in mesenteric arteries 126

Figure 4.20 Contribution of prostacyclin, eNOS-derived vasodilators and EDHF in mesenteric arteries 127

Figure 4.21 eNOS-derived H_2O_2 mediated vasodilatation in mesenteric arteries 129

Figure 4.22 Endothelium-independent vasodilatation in mesenteric arteries.....130

Figure 4.23 Antioxidant protein expression in mesenteric arteries.....132

Figure 5.1 Haemodynamic measurements using tail-cuff plethysmography.....150

Figure 5.2 Invasive haemodynamic measurements using a Millar catheter in anaesthetised mice.....152

Figure 5.3 Effect of phenylephrine on haemodynamic parameters in anaesthetised mice155

Figure 5.4 Effect of indomethacin on haemodynamic parameters in anaesthetised mice.157

Figure 5.5 Effect of NAC on haemodynamic parameters in anaesthetised mice.....159

Figure 5.6 Effect of EUK-8 on haemodynamic parameters in anaesthetised mice.....161

Figure 5.7 Effect of EUK-8 on haemodynamic parameters in anaesthetised mice.....162

Figure 5.8 Effect of NAC (chronic) on haemodynamic measurements.....164

Figure 5.9 Effect of indomethacin (chronic) on haemodynamic measurements.....166

Figure 5.10 Effect of L-NAME (chronic) on haemodynamic measurements.....169

Figure 5.11 Haemodynamic measurements in response to acute angiotensin II.....171

Figure 5.12 Haemodynamic measurements in response to chronic angiotensin II.....173

Figure 5.13 Abdominal aortic aneurysm formation.....175

Figure 5.14 Effect of LPS on haemodynamic parameters in *GCH1*$^{fl/fl}$Tie2cre mice.....178

Figure 5.15 Effect of LPS on vascular reactivity in isolated mesenteric arteries.....180

Figure 5.16 Effect of LPS on vascular reactivity in isolated mesenteric arteries.....181

Figure 5.17 Effect on LPS on vascular reactivity in isolated aortas.....183

Figure 5.18 Total biopterin and BH4 levels in aortas.....185

Figure 5.19 Effect of LPS on vascular reactivity in isolated aortas ex vivo (incubation).187

Figure 6.1 Uterine horn of pregnant mouse.....204

Figure 6.2 Maternal measurements 207

Figure 6.3 Maternal organ weights.....209

Figure 6.4 Fetal measurements.....211

Figure 6.5 Fetal and placental weight from *GCH1*$^{fl/fl}$Tie2cre mothers.....212

Figure 6.6 BH4 levels in uterine arteries.....214

Figure 6.7 BH4 levels in plasma 216

Figure 6.8 Uterine vascular adaptation in pregnancy.....219

Figure 6.9 Uterine vascular adaptation in pregnancy.....220

Figure 6.10 KCl response and diameter size in non-pregnant and pregnant uterine arteries 222

Figure 6.11 Effect of endothelial cell BH4 deficiency on vascular function in non-pregnant uterine arteries 223

Figure 6.12 Effect of endothelial cell BH4 deficiency on vascular function in non-pregnant uterine arteries 225

Figure 6.13 Contribution of prostacyclin, eNOS-derived vasodilators, and EDHF in non-pregnant and pregnant uterine arteries.....226

Figure 6.14 Haemodynamic measurements in *GCH1*$^{fl/fl}$Tie2cre and wild-type female mice 228

Figure 6.15 Haemodynamic measurements during pregnancy 228

List of Tables

Table 1.1 The hph-1 mouse model of systemic BH4 deficiency.....33

Table 1.2 The GCH trasngenic mouse 34

Table 2.1 Buffer and media 41

Table 2.2 Primary and secondary antibodies used for Western blotting.....65

List of Abbreviations

ACh	Acetylcholine
AAA	Abdominal aortic aneurysms
Ang II	Angiotensin II
ApoE	Apolipoprotein E
BCA	Bicinchoninic acid protein assay
BH2	7,8 dihydrobiopterin
BH4	5,6,7,8-tetrahydrobiopterin
BKca	Large-conductance Ca^{2+} activated K^{+} channels
BSA	Bovine serum albumin
Carboxy PTIO salt	2-(4-carboxyphenyl)-4,5-dihydro-4,4,5,5-tetramethyl-1H-imidazolyl-1-oxy-3-oxide, monopotassium salt
CD102	Intercellular adhesion molecule 2 (ICAM-2)
cGMP	Guanosine monophosphate
COX	Cyclooxygenase
Cu,ZnSOD	Copper,zinc-superoxide dismutases
DAHP	2,4, diamino-6-hydroxypyrimidine and N-acetyl-serotonin
DHE	Dihydroethidium
DHFR	Dihydrofolate reductase
DHPR	Dihydropteridine reductase
DMEM	Dulbecco's modified eagle's medium
DNA	Deoxyribo-nucleic acid
DOCA	Deoxycorticosterone acetate
DTT	Dithiothreitol
ecSOD	Extracellular-superoxide dismutases

EDCF	Endothelium-derived constricting factors
EDHF	Endothelium-derived hyperpolarizing factor
EETs	Epoxyeicosatrienoic acids
eNOS	Endothelial nitric oxide synthase
FAD	Flavin adenine dinucleotide
FMN	Flavin mononucleotide
GTPCH	Guanosine triphosphate cyclohydrolase
H2O2	Hydrogen peroxide
H2S	Hydrogen sulphide
hph-1	hyperphenylalaninemic mouse
HPLC	High-performance liquid chromatography
IKca	Lntermediate-conductance Ca^{2+} activated K^{+} channels
iNOS	Inducible nitric oxide synthase
KCl	Potassium chloride
KHB	Krebs-Henseleit buffer
KHB	Kreb's HEPES buffer
L-NAME	Nω-nitro-L-arginine methyl ester
LPS	Lipopolysaccharide
MnSOD	Manganese-superoxide dismutases
NAC	N-acetylcysteine
NADPH	Nicotinamide adenine dinucleotide phosphate
nNOS	Neuronal nitric oxide synthase
NO	Nitric oxide
NOS	Nitric oxide synthase

Nox	NADPH oxidase
O2-	Superoxide Anion
OCT compound	Optimal cutting temperature compound
ODQ	1H-[1,2,4]oxadiazolo[4,3-a]quinoxalin-1-one
ONOO-	Peroxynitrite
PBS	Phosphate buffered saline
PCD	Pterin-4a-carbinolamine dehydratase
PCR	Polymerase chain reaction
PE	Phenylephrine
PEG-catalase	Polyethylene glycol-catalase
PGH2	Prostaglandin H2
PGI2	Prostacyclin
PKG	Protein kinase G
PTPS	6-pyruvol tetrahydropterin synthas
RNA	Ribo-nucleic acid
ROS	Reactive Oxygen Species
SDS	Sodium dodecyl sulphate
sGC	Soluble guanylate cyclase
SKca	Small-conductance Ca^{2+} activated K^{+} channels
SLIGRL	Ser-Leu-Ile-Gly-Arg-Leu-NH_2
SNP	Sodium nitroprusside
SOD	Superoxide Dismutase
SOD	Superoxide dismutases
SR	Sepiapterin reductase
TNF-α	Tumor necrosis factor

VEGF	Vascular endothelial growth factor
WT	Wild type

Chapter 1: Introduction

Chapter 1: Introduction

1.1 Endothelium and vascular diseases

Cardiovascular disease is a major cause of death in the developed world and accounts for one in four of all deaths in the United Sates (Xu et al., 2010), and one in three in the United Kingdom (www.nice.org.uk). It is also emerging as a major health burden in developing countries. The risk factors for cardiovascular disease include atherosclerosis (Landmesser et al., 2004), hypertension (Budhiraja et al., 2004), diabetes (Hink et al., 2001b), obesity, hypercholesterolaemia (Creager et al., 1990), and smoking (Heitzer et al., 1996). These risk factors are all commonly associated with endothelial dysfunction, which is characterized by impaired vascular function with loss of nitric oxide (NO) bioavailability and increased reactive oxygen species (ROS)(Ross, 1999). Impaired endothelial function followed by inflammation of the vascular wall leads to atherosclerotic plaque formation that causes obstruction or occlusion of vessels, ultimately resulting in myocardial infraction and stroke (Libby, 2002; Lusis, 2000).

1.2 Endothelium and vascular homeostasis

The vascular endothelium, a monolayer of cell lining the internal surface of blood vessels, is a key regulator in regulating vascular tone (Kinlay et al., 2001), vasomotor function, inflammation (Hansson, 2005), cellular adhesion (Kubes et al., 1991), platelet activation and thrombosis (Sagripanti and Carpi, 2000). It is now well recognised that the endothelium is not just a passive barrier between the circulating blood and the vessel wall. Endothelium also plays a critical role in maintaining vascular homeostasis by synthesizing and releasing several relaxing and constricting factors in response to different physical and chemical

factors, such as shear stress (Katada and Majima, 2002), hypoxia (Aley et al., 2005) and vasoactive substances. There are three main endothelium-derived vasoactive factors (Figure 1.1): (a) endothelium-derived relaxing factors (EDRF) such as nitric oxide and prostacyclin (Moncada et al., 1976), (b) endothelium-derived constricting factors (EDCF) such as thromboxane A2 (Feletou et al., 2010), and endothelin-1 (Yanagisawa et al., 1988) and (c) endothelium-derived hyperpolarizing factors (EDHF) such as hydrogen peroxide (Matoba et al., 2002; Matoba et al., 2000b; Ray et al., 2011), C-natriuretic peptide (Chauhan et al., 2003; Hobbs et al., 2004) and K^+ (Edwards et al., 1998). The balance between these endothelium-derived vasoactive factors contributes to the physiological maintenance of vascular tone and blood pressure. Imbalance of these factors can lead to endothelial dysfunction and the development of vascular disease states.

1.2.1 Nitric oxide

The major vasoactive factor released from endothelium is nitric oxide (NO), which is produced by endothelial cell nitric oxide synthase (eNOS) (Palmer et al., 1988). NO is a gaseous, lipophilic free radial cellular messenger with a half-life of ~6-30 seconds. It was first discovered by Furchgott and colleagues as endothelium-dependent relaxing factor in rabbit aortas (Furchgott and Zawadzki, 1980). NO plays a central role in the regulation of vascular tone, and blood pressure. NO also has anti-atherogenic properties including anti-inflammatory, anti-thrombotic, anti-proliferative and migratory and antioxidant effects. Endothelium-derived NO dilates all blood vessels by activating soluble guanylate cyclase in vascular smooth muscle cells via binding of NO with the prosthetic heme of the enzyme. This leads to formation of cyclic guanosine monophosphate (cGMP) from guanosine triphosphate (GTP), which in turn activates sGMP-dependent kinases, protein kinase G

(PKG) that decrease intracellular calcium, mediating smooth muscle relaxation (Carvajal et al., 2000; Forstermann et al., 1986 ; Holzmann, 1982). NO has also been shown to evoke smooth muscle hyperpolarization and thus relaxation by activating the K_{ATP} channels (Garland and McPherson, 1992), or K_{ca} channels (Yuill et al., 2011).

1.2.2 EDHF

It has been documented that endothelium-dependent vasodilatation in microvessels is primarily mediated by endothelium-derived hyperpolarizing factor (EDHF). Several reports have demonstrated that EDHF plays a crucial role in maintaining vascular homeostasis in various vascular beds, across various species including humans (Matoba et al., 2002; Matoba et al., 2000a). To date, the precise identity of EDHF is controversial, however, it is well accepted that the common effectors of EDHF pathway are involved in the activation of small, intermediate and large-conductance Ca^{2+} activated K^+ channels (SK_{ca}, IK_{ca} and BK_{ca} channels respectively), which in turn evokes smooth muscle hyperpolarization and relaxation (Dora et al., 2008; Garland, 2010). EDHF evokes smooth muscle hyperpolarization, and relaxation is mediated by NO or prostacyclin-independent signalling pathway (Chen et al., 1988; Plane and Garland, 1996). Currently, the possible candidates for EDHF include hydrogen peroxide (H_2O_2)(Matoba et al., 2000a), hydrogen sulphide (H_2S)(Mustafa et al., 2011), K^+ ions (Edwards et al., 1998), epoxyeicosatrienoic acids (EETs)(Campbell et al., 1996) and myoendothelial gap junctions (Dora et al., 2003).

A large body of evidence suggests that eNOS-derived H_2O_2 is the EDHF in mouse and human mesenteric arteries (Matoba et al., 2002; Matoba et al., 2000a). Reduced eNOS-derived H_2O_2 mediated vasodilatation has been observed in mesenteric arteries of eNOS deficient mice (Matoba et al., 2000b; Takaki et al., 2008a; Takaki et al., 2008b) and

Cu,ZnSOD deficient mice (Morikawa et al., 2003), suggesting eNOS is a major source of endogenous EDHF/H_2O_2 in mouse mesenteric arteries. Emerging evidence suggests that H_2O_2 can mediate endothelium-dependent and independent vasodilation in several vascular beds in multiple species including humans (Matoba et al., 2000a; Rubanyi and Vanhoutte, 1986; Thomas and Ramwell, 1986). It is possible that H_2O_2 may mediate vasodilatation by endothelium-dependent smooth muscle hyperpolarization and vasodilatation, or by activating PKG, and vasodilatation (Burgoyne et al., 2007; Fujimoto et al., 2003; Wolin and Burke, 1987). The mechanisms of H_2O_2-induded vasodilatation are varied depend on vascular beds and species. In human, coronary arteries, H_2O_2 induced vasodilatation through the activation of protein kinase G and subsequently opening of BK_{ca} channels and smooth muscle cell hyperpolarization (Lu et al., 2006).

1.2.3 Prostacyclin

Prostacyclin (PGI_2) is produced mainly in vascular endothelium by prostacyclin synthase from prostaglandin H_2 (PGH_2) and is a powerful vasodilator (Moncada and Vane, 1981), and exhibits properties that prevent platelet aggregation (Moncada et al., 1976). It can also inhibit both proliferation and growth of smooth muscle cells (Libby et al., 1988; Todaka et al., 1999). PGI_2 has a half-life of 42 sec, is then broken down to 6-keto-PGF and has a weak vasodilator effect. PGI_2 is released from endothelial cells in a paracrine manner, and binding to endothelial prostacyclin receptor to cause an increased in intracellular cyclic AMP, which activates protein kinase A, then dephophorylates the myosin light chain and inhibiting myosin light chain kinase, as result smooth muscle relaxation and vasodilatation.

1.3 Oxidative stress and vascular disease

Vascular oxidative stress has been recognised as a key factor in the pathogenesis of vascular disease, characterised by excessive production of reactive oxygen species. Reactive oxygen species (ROS) are highly-reactive free radicals derived from molecular oxygen. These include superoxide anion, peroxynitrite, hydrogen peroxide and hydroxyl anion. Superoxide can be converted to hydrogen peroxide (H_2O_2) by superoxide dismutases (SODs)(Huie and Padmaja, 1993) or is scavenged through the reaction with NO to produce the potent free radical peroxynitrite ($ONOO^-$)(Darley-Usmar et al., 1992). There are three isoforms of SOD: Copper,zinc-SOD (Cu,ZnSOD), Manganese SOD (MnSOD) and extracellular SOD (ecSOD). Cu,ZnSOD is expressed in almost all cell types, which is located in the cytosol and nucleus. It has been shown that Cu,ZnSOD is most abundant SOD isoform in vasculature, which is accountable for 80% of total SOD activity. It is believed that Cu,ZnSOD plays a critical role in dismutating eNOS-derived superoxide anions to H_2O_2, thereby prolonging the half-life of NO. MnSOD is expressed in all almost all cell types, and is located in the mitochondrial matrix while ecSOD is secreted extracellularly. Hydrogen peroxide is then further reduced to water and oxygen by catalase (Yang et al., 2004). Hydrogen peroxide is more stable than superoxide, diffusible and cell membrane permeable. It has been reported that Nox4 and eNOS can produce H_2O_2 under basal physiological conditions as well as in disease states (Ray et al., 2011). Emerging evidence suggests that basal superoxide and H_2O_2 each play important roles in several cellular functions including the modulation of specific redox-sensitive signal transduction pathways (Griendling and Harrison, 1999; Kunsch and Medford, 1999).

Many vascular disease states are associated with an increase in the production of ROS; in particular superoxide anion. Superoxide production reduces vascular NO bioavailability through the near-diffusion rate reaction with superoxide. This produces the potent ROS,

peroxynitrite. There are several sources of superoxide which include eNOS uncoupling, NADPH oxidases, xanthine oxidase, cytochrome p-450, lipoxygenase, and mitochondrial oxidases (Droge, 2002). Increased NADPH oxidase-derived and eNOS-derived superoxide have been documented in various cardiovascular settings such as hypertension (Tojo et al., 2002), atherosclerosis (Warnholtz et al., 1999), diabetes (Kashiwagi et al., 1999); and patients following bypass graft surgery (Guzik et al., 2002a).

1.4 NO synthesis and function

1.4.1 NO synthesis

Nitric oxide (NO), produced by the enzyme NO synthase (NOS), is a key signalling molecule in vascular homeostasis. NOS enzymes are haem-containing oxido-reductases, and exist as homodimers. There are three isoforms of NOS enzymes: neuronal NOS (nNOS, NOS1), inducible NOS (iNOS, NOS2), and endothelial (eNOS, NOS3) named by their main cell type or the order that they were first discovered (Forstermann et al., 1991). These three NOS isoforms share 50-60% amino acid sequence homology (Alderton et al., 2001; Balligand and Cannon, 1997; Groves and Wang, 2000; Kelly and Smith, 1996). eNOS and nNOS are expressed constitutively and produce NO in response to increased intracellular calcium levels, mediated by binding of calcium to calmodulin within the enzyme (Fleming et al., 1998). iNOS is not constitutively expressed but instead is regulated by cytokines and other inflammatory stimuli such as lipopolysaccharide (LPS)(Stuehr et al., 1991). iNOS tightly binds calcium calmodulin and is therefore not sensitive to calcium-dependent calmodulin binding (Cho et al., 1995). All three enzymes produce NO through a 5-step oxidation of its substrate L-arginine to L-citrulline (Moncada et al., 1991).

All three isoforms are active as homodimers. Each monomer of NOS consists of an N-terminal oxygenase domain and a C-terminal reductase domain. The N-terminal oxygenase domain contains the haem group, and binding sites for the substrate, L-arginine, and the cofactor, tetrahydrobiopterin (BH4). The C-terminal reductase domain contains binding sites for calmodulin, flavin mononucleotide (FMN), flavin adenine dinucleotide (FAD), and the electron donor, nicotinamide adenine dinucleotide phosphate (NADPH) (Griffith and Stuehr, 1995). When calcium binds calmodulin (in nNOS and eNOS) this enhances electron transfer from NADPH to the haem where electrons reduce and activate oxygen for NO synthesis (Masters et al., 1996). NOS enzymes hydrolyse L-arginine to N-hydroxy-L-arginine and then oxidise N-hydroxy-L-arginine to L-citrulline and NO (Stuehr and Ikeda-Saito, 1992).

1.4.2 Regulation of eNOS function

eNOS is predominantly expressed in vascular endothelium (Forstermann et al., 1991) but also occurs in a variety of other cell types including cardiomyocytes (Balligand et al 1995), platelets (Thomas and Ramwell, 1986; Wallerath et al., 1997), and neurons (Dinerman et al., 1994). The amino acid sequence of eNOS is highly conserved between mammalian species (approximately 94% identity) (Li et al., 2002)

In cells, eNOS is predominantly localised to invaginations of the plasma membrane called caveolae (Forstermann et al 1991). In basal conditions, eNOS is palmitoylated, myristoylated and tonically inhibited by its interaction with caveolin-1. Stimulation by agonists such as bradykinin, acetylcholine and ATP results in calcium-calmodulin binding, depalmitoylation, and displacement of caveolin-1. This then releases eNOS from the plasma membrane and increasing enzyme activity (Prabhakar et al., 1998). eNOS activation is also

mediated through phosphorylation of key residues. Fluid shear stress, vascular endothelial growth factor (VEGF), estrogen and insulin all activate eNOS by Akt-dependent phosphorylation at Serine 1177 (Chen et al., 1999; Dimmeler et al., 1999a) whereas phosphorylation at Threonine 495 by protein kinase C has been shown to decrease its activity (Fleming and Busse, 2003).

1.5 BH4 biosynthesis and function

1.5.1 BH4 biosynthesis

5,6,7,8-tetrahydrobiopterin (BH4) was first described by Hopkins (Hopkins, 1895) and isolated by Watt (Watt, 1964). It was first identified as a cofactor for the aromatic amino acid hydrolase enzymes which include including phenylalanine hydroxylase (a key enzyme in phenylalanine metabolism), tyrosine-3-hydroxylase (a key enzyme in dopamine synthesis) and tryptophan-5-hydroxylase (a key enzyme in serotonin synthesis). BH4 is also an essential cofactor for all NO synthase (NOS) isoforms as described previously (Kwon et al., 1989; Tayeh and Marletta, 1989). BH4 is synthesised de novo from GTP by a sequential action of three enzymes, the initial and rate-limiting reaction is catalysed by the GTP cyclohydrolase1 (GTPCH). Subsequent steps are catalysed by the enzyme 6-pyruvol tetrahydropterin synthase (PTPS) and sepiapterin reductase (SR). An alternative pathway for BH4 synthesis has been documented in bacteria (Woo et al., 2002) and in drosophila (Krivi and Brown, 1979) whereby 6-pyruvovyl tetrahydropterin is converted to sepiapteirn by SR. Exogenous sepiapterin can be reduced in all cells by sepiapterin reductase to 7,8 dihydrobiopterin (BH2), and further by NADPH-dependent dihydrofolate reductase (DHFR) to form BH4, the so-called ‘salvage pathway’. The principle oxidant species leading to BH4 oxidation to BH2 is peroxynitrite. BH4 is converted into tetrahydrobiopterin-4a-

carbinolamine, which is recycled to BH4 by the actions of pterin-4a-carbinolamine dehydratase (PCD) and dihydropteridine reductase (DHPR) (Crabtree et al., 2008; Nichol et al., 1983). The balance between BH4 biosynthesis from GTPCH, BH4 oxidation to BH2 and recycling from BH2 to BH4 by DHFR determine the net BH4 bioavailability within cells.

Figure 1.1

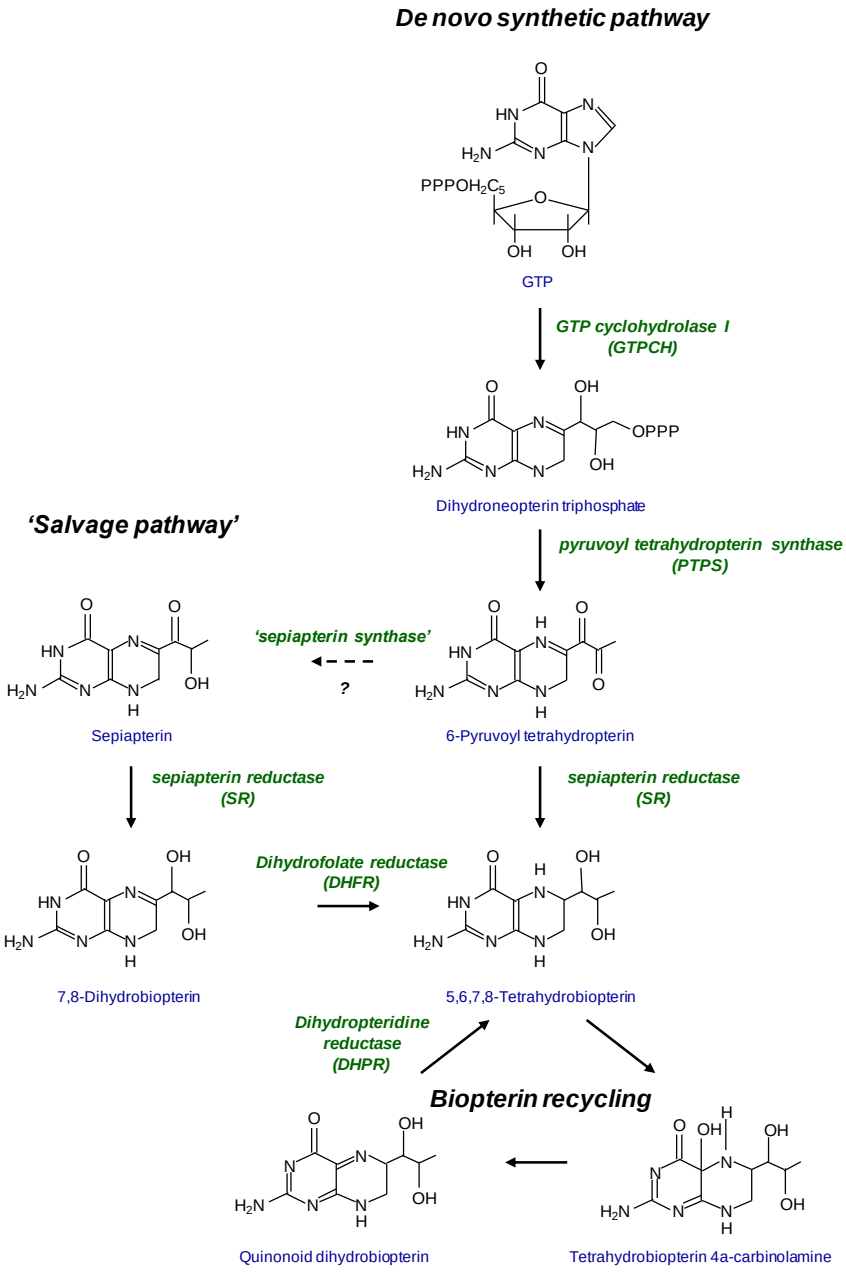


Figure 1.1 BH4 biosynthesis and metabolism

De novo BH4 synthesis occurs from the substrate GTP via a three-step enzymatic pathway. GTPCH, encoded by the *GCH1* gene, is the rate-limiting enzyme. The following steps are catalysed by the enzymes pyruvoyl tetrhydropterin synthase (PTPS) and sepiapterin synthase (SR). An alternative pathway for BH4 synthesis is converted into sepiapterin by SR. Exogenous sepiapterin can be reduced in all cells by SR to BH2, and further by DHFR to form BH4, the so-called 'salvage pathway'. The principle oxidant species leading to BH4 oxidation to BH2 is peroxynitrite. BH4 is converted into tetrahydrobiopterin-4a-carbinolamine, which is recycled to BH4 by the actions of PCD and DHPR.

1.5.2 Regulation of GTPCH

GTPCH, encoded by the *GCH1* gene, forms a homodecamer composed of two pentameric rings with ten active site per multimer. The *GCH1* gene is located on chromosome 14q22.1-q22.2 and consists of 6 exons spanning approximately 30 kilobases and is primarily regulated at the transcriptional level (Thony et al., 2000). Cytokines including tumor necrosis factor (TNF-α) and interferon-γ (Katusic et al., 1998; Linscheid et al., 1998; Werner et al., 1998), hormones including insulin (Ishii et al., 2001), oestrogen (Sun, 2009), mediators/factors such as LPS (Shimizu et al., 1999), and pharmacological agents such as statins (Antoniades et al., 2007) have all been reported to modulate GTPCH transcription, enzyme activity and BH4 levels. The activity of GTPCH activity can also be regulated by phosphorylation at key residues. Phosphorylation of GTPCH at serine 81 in response to shear stress has been shown to increase GTPCH activity (Widder et al., 2007). Ang II and platelet-derived growth factor can regulate GTPCH activity by phosphorylation via protein kinase C-dependent pathway (Lapize et al., 1998).

1.6 eNOS regulation by BH4 in vascular disease

Crystallisation of NOS enzyme indicates the importance of BH4 level on the structure of NOS. Binding of BH4 to NOS shifts the haem iron to a high-spin state, increases affinity for L-arginine and stabilises the dimeric form of the enzyme (Rafikov et al., 2011). Recent studies have shown that *GCH1* expression is the key determinant of endothelial cell BH4 levels and eNOS regulation (Crabtree et al., 2009a; Vasquez-Vivar et al., 2003). When BH4 bioavailability is limiting eNOS becomes enzymatically ‘uncoupled’ from L-arginine oxidation, and superoxide production is produced rather than NO (Vasquez-Vivar et al., 2003; Vasquez-Vivar et al., 1998; Xia et al., 1998). Diminished NO and increased

superoxide productions are key features of endothelial dysfunction. Evidence from experimental and clinical studies have demonstrated that loss of vascular BH4 bioavailability and subsequently eNOS uncoupling, has significant effect on the pathogenesis of endothelial dysfunction, which is a hallmark of cardiovascular disease. Indeed, the BH4 levels in vascular tissue from ApoE knockout mice, diabetic mice and hypercholestolemic rabbits as well as from patients with vascular diseases are markedly decreased and associated with impaired NO-mediated relaxation. Loss of BH4 may result from BH4 oxidation in the presence of increased superoxide production from uncoupled NOS, or other sources such as NADPH oxidase. Landmesser *et al* demonstrated that oxidation of vascular BH4 by NADPH oxidase-derived superoxide, and subsequently the formation peroxynitrite is the key mechanism leading to eNOS uncoupling and reduced NO-mediated vasodilatation in DOCA-salt hypertension mice (Landmesser et al., 2003). It was demonstrated *in vitro* that peroxynitrite causes rapid oxidation of BH4 to the inactive dihydrobiopterin (BH2), which is incapable of acting as a cofactor for eNOS (Milstien and Katusic, 1999). Recent studies by Crabtree *et al* demonstrated that the BH4:BH2 ratio rather BH4 level alone is likely to be the key determinant state of eNOS uncoupling (Crabtree et al., 2008; Crabtree et al., 2009a).

The importance of BH4-dependent eNOS regulation has been demonstrated by the use of eNOS overexpressing mice (eNOS-Tg). eNOS knockout mice have been shown to develop accelerated atherosclerosis compared to ApoE-KO controls. Paradoxically, mice with transgenic overexpression of eNOS-Tg (ApoE-KO/eNOS-Tg) developed more atherosclerotic plaque compared to ApoE-KO controls (Ozaki et al., 2002). Despite similar vascular BH4 levels between the genotypes, increased vascular superoxide generations was observed in ApoE-KO/eNOS-Tg compared to ApoE knockout controls, implying that decreased BH4:eNOS ratio was contributory to the increased superoxide production and

plaque formation observed in ApoE-KO/eNOS-Tg mice. Indeed, supplementation with oral BH4 resulted in a greater reduction in superoxide production and thus atherosclerotic plaque in ApoE-KO/eNOS-Tg mice (Ozaki et al., 2002). These data suggest that strategies to increase eNOS protein without a concomitant augmentation of endothelial cell BH4 levels can lead to eNOS uncoupling and development of vascular disease.

Pharmacological supplementation with BH4 or the BH4 precursor sepiapterin has been shown to restore endothelial function in various vascular diseases models. Supplementation of BH4 has been reported to restore endothelial function in experimental models of diabetes mellitus (Pieper, 1997), atherosclerosis (Hattori et al., 2007), hypertension (Hong et al., 2001), as well as in patients with diabetes mellitus (Heitzer et al., 2000b), hypercholesterolemia (Stroes et al., 1997), coronary artery disease (Maier et al., 2000), hypertension (Higashi et al., 2002) and smoking (Heitzer et al., 2000a; Ueda et al., 2000).

Treatment with an inhibitor of GTPCH, 2,4, diamino-6-hydroxypyrimidine and N-acetyl-serotonin (DAHP) leads to eNOS uncoupling, increased superoxide production and impaired NO-mediated vasodilatation in aortas, endothelial dysfunction and hypertension in rats (Mitchell et al., 2003). Mice with siRNA knock down of *GCH1* exhibit decreased in vascular BH4 levels, eNOS uncoupling, and increased blood pressure (Wang et al., 2008).

1.7 Mouse models of BH4 deficient and BH4 overexpression in vascular disease

1.7.1 Hph-1 mice

The hyperphenylalaninemic (hph-1) mouse, generated by *N*-ethyl- *N*-nitrosourea mutagenesis, has moderate systemic BH4 deficiency due to reduced gene expression from

the *GCH1* locus (Cosentino et al., 2001; Khoo et al., 2005). The precise genetic mutation is not known but lies close to the *GCH1* locus on chromosome 14 but not within the coding region or immediately upstream (Maeda et al., 2000). In hph-1 mice, GTPCH activity is reduced by 80-90% and total biopterins BH4 levels in various tissues including aortas, lung and heart are significantly decreased (Cosentino et al., 2001; Khoo et al., 2005). However, endothelium-dependent vasodilatation to acetylcholine in hph-1 aortas was present and comparable to wild- type controls (Cosentino et al., 2001). Vasodilatation in hph-1 aortas was in part mediated by NOS-derived H_2O_2 production. A single report using tail-cuff recordings in a non-littermate comparison, demonstrated that hph-1 mice have higher systolic blood pressure but a normal heart rate (Cosentino et al., 2001). More recent works reported that hph-1 mice have similar blood pressure to their wild-type littermates (Adlam et al., 2012). A review of the role BH4 plays in vascular disease states using hph-1 as a model is presented in Table 1.1. Systemic BH4 deficiency in hph-1 mice have been shown to associated with various vascular disease states. Increased vascular BH4 levels have been shown to improve endothelial-dependent relaxations in various model of vascular diseases states such as pulmonary hypertension (Khoo et al., 2005; Nandi et al., 2005), AAA formation (Gao et al., 2012), inflammatory pain (Nasser et al 2013), autonomic function (Adlam et al., 2012), vascular injury (Wang et al., 2005), hypoxic pulmonary vasoconstriction (Efrancis et al., 2012) and cerebral microcirculation dysfunction (Santhanam et al., 2012).

Table 1.1

Phenotype	Reference
Hypertensive (compared to non wild-type littermate controls)	Cosentino et al 2001
Normotensive, tachycardia	Adlam et al 2012
Normotensive	Xie HH et al 2010
eNOS uncoupling in cerebral microvessels	Santhanam AV et al 2012
Pulmonary hypertension	Khoo et al 2005
Hypoxic pulmonary vasoconstriction	Francis BN et al 2010
Pulmonary hypertension	Nandi et al 2005
Pulmonary hypertension in new born mice	Belik J et al 2011
Abdominal aortic aneurysm formation in response to Ang II	Gao et al 2012
Abdominal aortic aneurysm formation in response to Ang II	Siu KL et al 2014
Exaggerated intimal hyperplasia after vascular injury	Wang CH et al 2005
Delayed wound healing in STZ-induced diabetes	Tie L et al 2014
Reduced inflammatory pain	Nasser et al 2013

Table 1.1 The hph-1 mouse model of systemic BH4 deficiency.

The importance of BH4 in vascular disease states has been illustrated in a number of studies using hph-1 mice.

1.7.2 The *GCH* transgenic mouse (GCH-Tg)

GCH-Tg mice overexpress *GCH1* specifically within the endothelium (Alp et al., 2004; Alp et al., 2003a) and have been extensively characterised in studies of cardiovascular disease states. GCH-Tg mice have increased BH4 level, and eNOS activity in endothelial-cell rich tissues, including aortas and lungs. GCH-Tg mice exhibit a normal vascular function and blood pressure compared with wild-type littermates, suggesting overexpression of endothelial cell *GCH1* and thus elevated BH4 biosynthesis does not have a detrimental effect or invoke extensive hypotension ({Alp, 2003 #5062}(Adlam et al., 2012)). This increase in endothelial BH4 has been shown to improve endothelial-dependent relaxations in various models of vascular disease states such as diabetes (Tie et al 2009, Alp et al 2003), hypertension (Du et al 2008), atherosclerosis (Alp et al 2007; Alp et al 2004; and vascular

injury (Liao et al 2007; Wang et al 2008; Ali et al 2008, Ali et al 2013). A summary of studies showing the important of the GCH-Tg mouse in vascular disease states is presented in Table 1.2

Table 1.2

Disease	Phenotypes	Reference
Atherosclerosis	Reduced atherosclerotic plaque formation in eNOS-Tg/GCH-Tg/ApoE$^{-/-}$ mice	Takaya et al 2007
Atherosclerosis	Reduced endothelial dysfunction and atherosclerosis in GCH-Tg/ApoE$^{-/-}$mice	Alp et al 2004
Hypertensive	Preserved endothelial function and hypertension in DOCA-salt induced hypertension	Du et al 2008
Diabetes	Accelerated wound healing in STZ/GCH-Tg	Tie et al 2009
Diabetes	Preserved endothelial function	Alp et al 2003
Vascular injury	Reduced neointima formation in carotid arteries	Liao et al 2007
Vascular injury	Reduced vein graft neointima formation in GCH-Tg/ApoE$^{-/-}$ mice	Ali et al 2008
Vascular injury	Reduced neointima formation in GCH-Tg/ApoE$^{-/-}$ mice	Douglas et al 2013
Vascular injury	Reduced vein graft neointima formation in GCH-Tg/ApoE$^{-/-}$ mice	Ali et al 2013
Pulmonary hypertension	Prevent pulmonary hypertension in hph-1/GCH-Tg mice	Khoo et al 2005

Table 1.2 The GCH transgenic mouse

Endothelial specific *GCH* overexpression in the *GCH* transgenic mouse has been shown to be sufficient to restore eNOS coupling and NO bioavailability in various vascular disease states.

.

1.8 BH4 and other cardiovascular diseases

1.8.1 Abdominal aortic aneurysm

Abdominal aortic aneurysm (AAA) is a complex vascular inflammatory disease characterised by a localised degradation of the aortic wall, apoptosis of vascular smooth muscle cells and destruction of the elastic media (Davis et al., 2014). The incidence of AAA increases with age, gender, and smoking (Aggarwal et al., 2011). Although AAA rupture is life threatening, molecular targets for this disease have not yet been identified.

In experimental studies, angiotensin II infusion has been extensively used to induce AAA formation. Doses of Ang II ranging from 0.7 mg/kg/day to 3.0 mg/kg/day have been widely used to induce AAA formation in both C57BL/6 as well as $ApoE^{-/-}$ mice (Ayabe et al., 2006; Daugherty et al., 2000; Fan et al., 2014; Gavazzi et al., 2007; Rateri et al., 2011; Xiong et al., 2009). Increased ROS generation via NADPH oxidases, and activation of pro-inflammatory mediators and cytokines (such as nuclear factor kappa B) have been shown to be a major contributing factor in the development of AAA (Davis et al., 2014; Fan et al., 2014). Recently, important roles for eNOS uncoupling and BH4 deficiency in AAA formation have been documented in hph-1 mice (Gao et al., 2012). Hph-1 mice treated with Ang II (0.7 mg/kg/day) showed increased eNOS uncoupling, increased superoxide production, reduced NO bioactivity, vascular remodelling and AAA formation, which is reversed by supplementation of folic acid (Gao et al., 2012). A recent publication by Gao *et al* demonstrated that circulating BH4 is a biomarker for Ang II-induced AAA in ApoE knockout mice (Siu et al., 2014) and hph-1 mice (Siu and Cai, 2014). Decreased circulating BH4 is correlated with vascular BH4 levels, which is associated with AAA formation in hph-1 mice (Gao et al., 2012). These findings suggest that BH4-dependent eNOS regulation plays an important role in the pathogenesis of AAA.

1.8.2 Septic shock and systemic inflammation

Septic shock carries a high mortality and is characterised by systemic inflammation, decreased peripheral vascular resistance, microvascular leak and decreased cardiac output (Rudyk et al., 2013). Overproduction of NO by iNOS, which is induced by the inflammatory stimuli lipopolysaccharide (LPS) and inflammatory cytokines is likely to be a key mediator of these phenomena. However, administration of NOS inhibitors have been shown to have protective effects (Kilbourn et al., 1990), no protective effects (Evans et al., 1995), and to worsen the outcome ((Billiar et al., 1990) in both experimental models and humans patients with septic shock. These data indicate that the role of NO in sepsis shock is more complicated. This is likely due to the dual roles of iNOS-derived NO in the control of infections, and the putative negative role in mediating mortal hypotension. The synthesis of NO by iNOS requires the cofactor BH4. Pro-inflammatory cytokines and LPS can increase the synthesis of BH4 levels by up-regulating GTPCH mRNA and expression. This is accompanied by an upregulation of iNOS mRNA and protein, which unlike other NOS enzymes is primarily regulated by gene expression. Elevated plasma nitrite/nitrate and circulating biopterins are observed in animal models and patients with septic shock (Bune et al., 1996; Cunha et al., 1994; Galley et al., 2001; Goode et al., 1995; Szabo et al., 1994a; van Amsterdam et al., 1996). Treatment with a NOS inhibitor reduces plasma nitrite/nitrate and increases blood pressure and systemic vascular resistance in humans with septic shock (Petros et al., 1991), although systemic NOS inhibition does not improve survival in these patients. In an experimental model of septic shock, treatment of mice with a GTPCH inhibitor, DAHP reduces BH4 levels, vascular NOS-derived NO generation and preserved blood pressure, despite no change in induction of iNOS (Bune et al., 1996; Shimizu et al., 1998). Thus, targeting vascular *GCH1* and BH4 biosynthesis may provide a novel therapeutic target for the treatment of circulatory collapse in patients with septic shock

1.9 Clinical relevance of BH4 regulation in vascular disease

As already discussed, NO, produced by eNOS, is a critical regulator of vascular homeostasis. Reduced NO-mediated vascular function and increased vascular superoxide generation are key features of endothelial dysfunction, which is a hallmark of a wide range of vascular diseases. Loss of BH4 in the vascular wall is observed in patients and in experimental models of vascular disease, resulting in loss of NO generation and increased ROS production. Augmenting BH4 levels prevents eNOS uncoupling and improves endothelial function in vascular disease states such as hypertension, diabetes mellitus, and atherosclerosis. Although these studies implicate oxidized or dimished BH4 in vascular disease pathogenesis, the physiological requirement for endothelial BH4 in the regulation of eNOS-derived vascular NO generation, or other eNOS-derived signaling mechanisms, remains unknown. Furthermore, investigating whether endothelial cell BH4 synthesis by GTPCH is necessary for physiological eNOS function, as distinct from endothelial cell uptake from plasma or other sources, is important in guiding future therapeutic strategies that target eNOS function in vascular disease states.

1.10 Hypothesis

The central hypothesis of this study is that endothelial cell BH4 availability determines eNOS NO-redox signalling in vascular disease states. Specifically:

- Deficiency in endothelial cell *GCH1* and BH4 biosynthesis will lead to eNOS uncoupling, loss of NO generation and increased ROS production.
- Endothelial cell BH4 is required for eNOS regulation in maintaining vascular function and blood pressure. Deficiency in endothelial cell BH4 biosynthesis will lead to vascular dysfunction and hypertension under physiological conditions.
- Endothelial cell *GCH1* and BH4 biosynthesis plays a critical role in the pathogenesis of aortic abdominal aneurysm in response to Ang II. Deficiency in endothelial cell BH4 biosynthesis will lead to an increased incidence of AAA formation in response to Ang II.
- Endothelial cell *GCH1* and BH4 biosynthesis plays a critical role in systemic inflammation induced by LPS. Deficiency in endothelial cell *GCH1* and BH4 biosynthesis will protect from vascular dysfunction and hypotension in response to LPS.
- Endothelial cell BH4-dependent eNOS regulation plays a pivotal role in vascular adaptations and blood pressure regulation in normal pregnancy. Thus deficiency in endothelial cell BH4 biosynthesis during pregnancy will lead to uterine vascular dysfunction, gestational hypertension and intrauterine growth restriction.

1.11 Aims

- To investigate the requirement for endothelial cell *GCH1* and BH4 biosynthesis in endothelial function, vasomotor function and blood pressure regulation under physiological conditions.
- To investigate the role of endothelial cell *GCH1* and BH4 biosynthesis in the modulation of pathogenesis of AAA in response to angiotensin II.
- To determine the effect of endothelial cell *GCH1* and BH4 deficiency on vasomotor function and blood pressure regulation in response to LPS
- To investigate the requirement for endothelial cell *GCH1* and BH4 biosynthesis on eNOS regulation in vascular adaptation and blood pressure regulation to a normal pregnancy.

Chapter 2:
Material and Methods

Chapter 2: Material and methods

All general material and methods used are contained in this chapter. Some specific techniques are discussed in more detailed in the relevant chapters

2.1 Materials

2.1.1 Buffers and Media

Table 2.1

Buffer/Media	Reagents	Supplier
TAE buffer	2 M Tris Acetate, 100 mM Na2EDTA	National Diagnostics Ltd
DNA lysis buffer	10 mM Tris-HCl pH 8.5, 0.45 % Non-idet P40, 0.45 % Tween-20, 0.2 mg/ml Proteinase K	Sigma-Aldrich, Bioline
PBST	PBS with 0.05 % Tween-20	Lonza, Sigma- Aldrich
MACS buffer	PBS containing 0.5 % BSA and 2 mM EDTA	Lonza, Sigma- Aldrich
DMEM complete growth media (Low glucose 1g or High glucose 4.5g)	DMEM supplemented with 1 % penicillin-streptomycin, 1 % L-glutamine and 10 % foetal bovine serum (FBS)	Lonza, Sigma- Aldrich
Endothelial growth media	EBM-2 supplemented with EMG2 BulletKit (5% FBS, hEGF, VEGF, hFGF-B, R3-IGF-1, hydrocortisone, Gentamycin/Amphotericin-B and ascorbic acid; Lonza, product code CC-3202)	Lonza
Transfer buffer	200mM Tris Base with 2M Glycine	Sigma-Aldrich
Stripping bufer	6.25 mM Tris (pH 6.8) with 2% SDS and 100 mM β-mercaptoethanol	Sigma-Aldrich
Resuspension buffer	50 mM phosphate-buffered saline, 1 mM dithioerythriol, 1 mM EDTA, pH 7.4	Sigma-Aldrich
Acid precipitation buffer	1 M phosphoric acid, 2 M trichloroacetic acid (TCA) and 1 mM dithioerythritol (DTE)	Sigma-Aldrich

Krebs-HEPES buffer	99 mM NaCl, 4.7 mM KCl, 1.2 mM MgSO4, 1 mM KH2PO4, 1.9 mM CaCl2, 25 mM NaHCO3, NaHEPES 20 mM and 11.1 mM glucose	Sigma-Aldrich
Krebs-Henseleit buffer	120 mM NaCl, 4.7 mM KCl, 1.2 mM MgSO4, 1.2 mM KH2PO4, 2.5 mM CaCl2, 25 mM NaHCO3, and 5.5 mM glucose	Sigma-Aldrich
Krebs Ringer's phosphate	145 mM NaCl, 4.8 mM KCl, 1.2 mM MgSO4, 5.7 Na3PO4, 5.5 mM CaCl2, and 5.5 mM glucose	Sigma-Aldrich

Table 2.1 **Buffers and Media.** Buffers and Media are listed with compositions and origin.

2.2 Animals

All animal experiments were conducted in accordance with the UK Home Office Animals (Scientific Procedures) Act 1986 (Project license: PPL 30/3080, Personal license: PIL 60/12451).

2.2.1 Animal handling conditions

All animals were housed in individually ventilated cages at the Functional Genetics Facility, Wellcome Trust Centre for Human Genetics, University of Oxford. Cages were maintained at an ambient temperature of 21°C with a 12-hour light/dark cycle. Mice were provided with standard chow (19.67% protein, 4.13% oil and 3.22% fibre; B&K Universal Ltd, Aldbrough, UK) and water *ad libitum*.

2.2.2 *GCH1$^{fl/fl}$*Tie2cre mice

Endothelial cell-targeted *GCH1* deletion (*GCH$^{fl/fl}$*Tie2cre) mice were generated in house by Dr Nick Alp and Ashley Hale. Exons 2 and 3 of *GCH1*, encoding for the active site of GTPCH I, were flanked by two loxP sites in a targeting construct that was used to produce *GCH1$^{fl/fl}$* mice after homologous recombination in embryonic stem cells. Pups carrying the *GCH1* floxed allele were then back crossed for 8 generations to the C57Bl/6J line. Once back crossed the resultant *GCH1$^{fl/fl}$* animals were bred with Tie2cre transgenic mice to produce *GCH1$^{fl/fl}$*Tie2cre mice where *GCH1* is deleted specifically in endothelial cells, generating a novel mouse model of endothelial cell-specific BH4 deficiency mouse. The Tie2cre transgene is active in the female germline, as such only male animals are used to established breeding pairs to maintain conditional expression. *GCH1$^{fl/fl}$*Tie2cre mice were born in the expected mendelian ratios and had body weights similar to those of wild-type littermates (Figure 2.1). Mouse genotypes were confirmed by PCR.

Figure 2.1

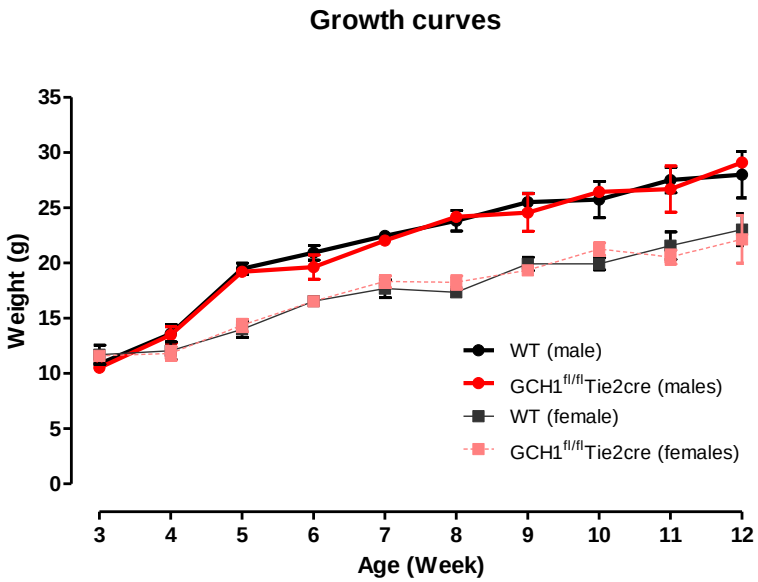


Figure 2.1. Growth curves

WT and *GCH1*$^{fl/fl}$Tie2cre mice, both males and females, were weaned at 3 weeks of age. The mice were weighed weekly from week 3 until week 12. The body weights are comparable between WT and *GCH1*$^{fl/fl}$Tie2cre mice from age of 3 (after weaning) in both males and females. After week 5, males from both genotypes have a significantly greater body weight than female from both genotypes. This data suggests that there is no abnormality in growth in *GCH1*$^{fl/fl}$Tie2cre mice. Data are expressed as mean ± SEM. (n=10 to 14 animals per group).

2.3 DNA techniques

2.3.1 DNA extraction

Mouse ear notches were digested for a minimum of 5 hours at 55°C in 500 µl of DNA lysis buffer (10mM Tris pH 8.5, 0.45% Non-idet P40, 0.45% Tween-20, 0.2mg/ml freshly added Proteinase K). DNA was purified by extraction with 250 µl of 6 M NaCl and then vortexed vigorously before centrifugation at 16,000 g for 7 minutes at room temperature. The clear upper layer (600 µl) was transferred into a new eppendorf tube, 500 µl isopropanol was added. The samples were centrifuged at 16,000 g for 7 minutes at 4 °C to precipitate the DNA. The supernatant was discarded, and the pellets washed with 500 µl 70% ethanol before further centrifugation at 16,000 g for 5 minutes at 4 °C. The supernatant was again discarded, and the DNA pellet was air dried and resuspended in 100 µl DNase free water.

2.3.2 Genotyping PCR

Mice were genotyped by polymerase chain reactions using DNA prepared as above. *GCH1*$^{fl/fl}$Tie2cre mice were genotyped using the primers listed below. Products were run on either a 1.5% agarose gel (Web Scientific) for *GCH1* floxed and *GCH1* excision PCR or 2.5% agarose gel for Tie2cre PCR. Gels were prepared by dissolving agarose in TAE buffer (National Diagnostics) and adding ethidium bromide (Sigma, UK) to a final concentration of 0.004%. Once the gel had set, PCR products were loaded and run at 120 V in TAE buffer for 60 min using BioRad PCR electrophoresis equipment. DNA was visualised using UV illumination. Bioline hyperlandder IV (Bioline) was used to identify the PCR product size.

GCH floxed and GCH excision Genotype PCR:

Primers:	gx5128(F)	5'- GTCCTTGGTCTCAGTAAACTTGCCAGG
	GCH new/rev	5'- GCCCAGCCAAGGATAGATGCA
	Pri5 (F)	5'-GCTCATCCCCCACACTTGTCT

Reaction mix (25µl):	9µl	water
	12.5µl	(2x) Biomix Red (Bioline^{R})
	0.5µl	50mM $MgCl_2$,
	0.25 µl each primer	
	2µl	DNA

Thermocycle sequence: 94 ˚C for 7 min, then

35 cycles of 94 ˚C for 30 sec, 63.5 ˚C for 30 sec, and 68 ˚C for 30 sec, then

68 ˚C for 5 min, then

10 ˚C for 5 min

Product Size:	GCH excised	1392 bp
(on 1.5% agarose gel)	GCH floxed	1030 bp
	Wide-type	906 bp

Tie2Cre Genotyping PCR:

Primers:	S1X A	5'- GCATAACCAGTGAAACAGCATTGCTG
	S1X B	5'-GGACATGTTCAGGGATCGCCAGGCG
	EMcN_HPRTF	5'-CATCGCATAAACTGGGTGTG
	EMcN_HPRTR	5'-TGAATCCCAAGCCATCTAGG

Reaction mix (25µl):	13.6µl Reddy Mix PCR Maxter Mix 1.1 (Theromo Scientific)
	0.15µl each primer
	1.5µl DNA (100ng/µl)
Thermocycle sequence:	94 ˚C for 7 min, then
	30 cycles of 95 ˚C for 30 sec, 55 ˚C for 30 sec, and 72 ˚C for 1 min, then
	72 ˚C for 10 min, then
	10 ˚C for 5 min

Product Size:	Tie2Cre	280 bp
(on 2.5% agarose gel)	Wildtype	229 bp

Figure 2.2

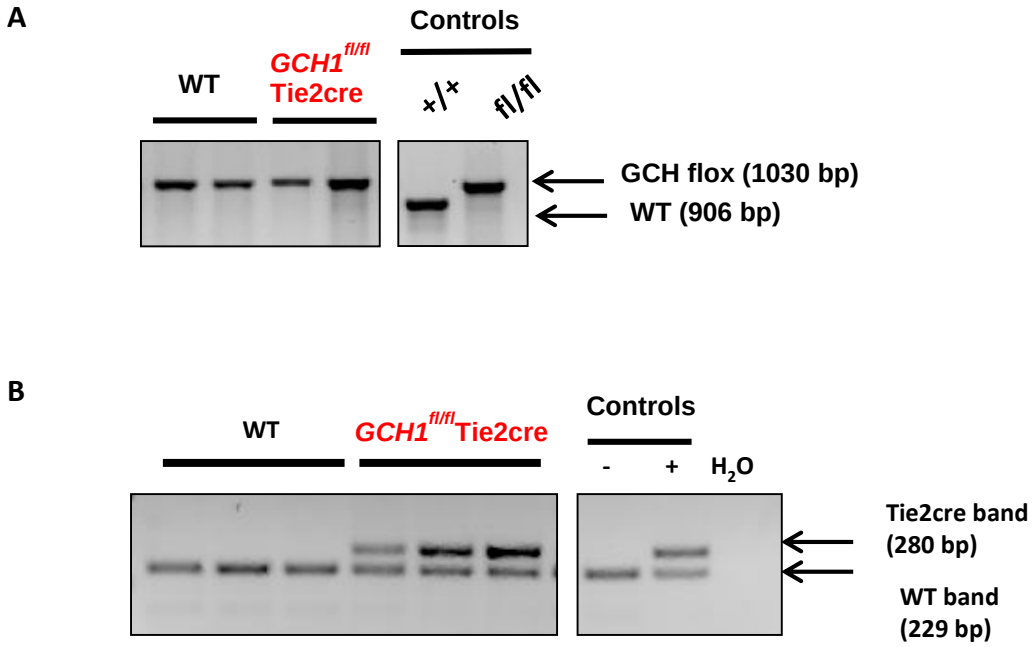


Figure 2.2. Genotyping of genomic DNA from *GCH1*$^{fl/fl}$Tie2cre and wild-type mice.

Gel electrophoresis showing PCR products from wild-type (WT) mice and *GCH1*$^{fl/fl}$Tie2cre mice. **A)** Both WT and *GCH1*$^{fl/fl}$Tie2cre mice used in this project are homozygotes for *GCH1*$^{fl/fl}$, thus a single band of 1030 bp is seen in both genotypes. **B)** PCR product from Tie2cre is 280 bp; the product from wild-type is 229 bp. To exclude contamination control samples with no DNA (H_2O) were included in genotyping experiments.

2.3.3 Procedure of harvesting mouse tissues

Mice were culled using overdose of isofluorane by inhalation. The chest cavity was opened and the systemic circulation was flushed slowly with 5 mls of ice-cold PBS via a needle (G25) inserted into the left ventricle. The needle was then advanced into the right ventricle, and the lungs were flushed with another 5 mls of ice-cold PBS. Thoracic aortas were gently dissected free from the back bone with fine forceps and scissors under microscope and either placed in ice-cold KBH or frozen immediately in dry ice or liquid nitrogen or liquid nitrogen and stored at -80 °C. All organs were harvested and stored to similar manner.

2.4 Tetrahydrobiopterin assay

BH4 and BH2 and biopterin were determined by electrochemical and florescence detection respectively, following sample separation by HPLC (Heales and Hyland, 1989; Howells et al., 1986). The frozen tissues (heart, lung, kidney, and liver) were homogenised in 400 µl ice-cold resuspension buffer (50 mM phosphate-buffered saline, 1 mM dithioerythriol, 1 mM EDTA, pH 7.4). For aortas and primary endothelial cells, samples underwent 2 cycles of freeze-thawed in 100 µl ice-cold resuspension buffer. Following centrifugation at 16,000 g for 10 min at 4°C, the supernatant (180 µl for tissues and 90 µl aortas and primary cells) was transferred to new tube and ice-cold acid precipitation buffer (1 M phosphoric acid, 2 M trichloroacetic acid (TCA) and 1 mM dithioerythritol (DTE)) was added (20 µl for tissues and 10 µl for aortas or primary cells). Following vigorously mixing and centrifugation at 16,000 g for 10 min at 4°C, the supernatant was transferred and injected onto an isocratic HPLC system and quantified using sequential electrochemical detection (Coulochem III, ESA Inc., UK) and fluorescence (JASCO, UK) detection. HPLC separation was performed using a 250 mm ACE C-18 column (Hichrom, UK) and mobile phase comprising of 50 mM

sodium acetate, 5 mM citric acid, 48 µl EDTA and 160 µM DET pH 5.2 (all ultrapure electrochemical HPLC grade) at a flow rate of 1.3 ml/min. Background currents of +500 nA and -50 nA were used for the detection of BH4 on electrochemical cells E1 and E2, respectively. Quantification of BH4 and BH2 and biopterin was obtained by comparison with external standards and normalised to protein concentration, determined by the BCA protein assay as described in Section 2.9. Representative chromatograms show neopterin peaks of aortas and primary endothelial cells from wild-type and *GCH1*$^{fl/fl}$Tie2cre mice (Figure 2.3).

Figure 2.3

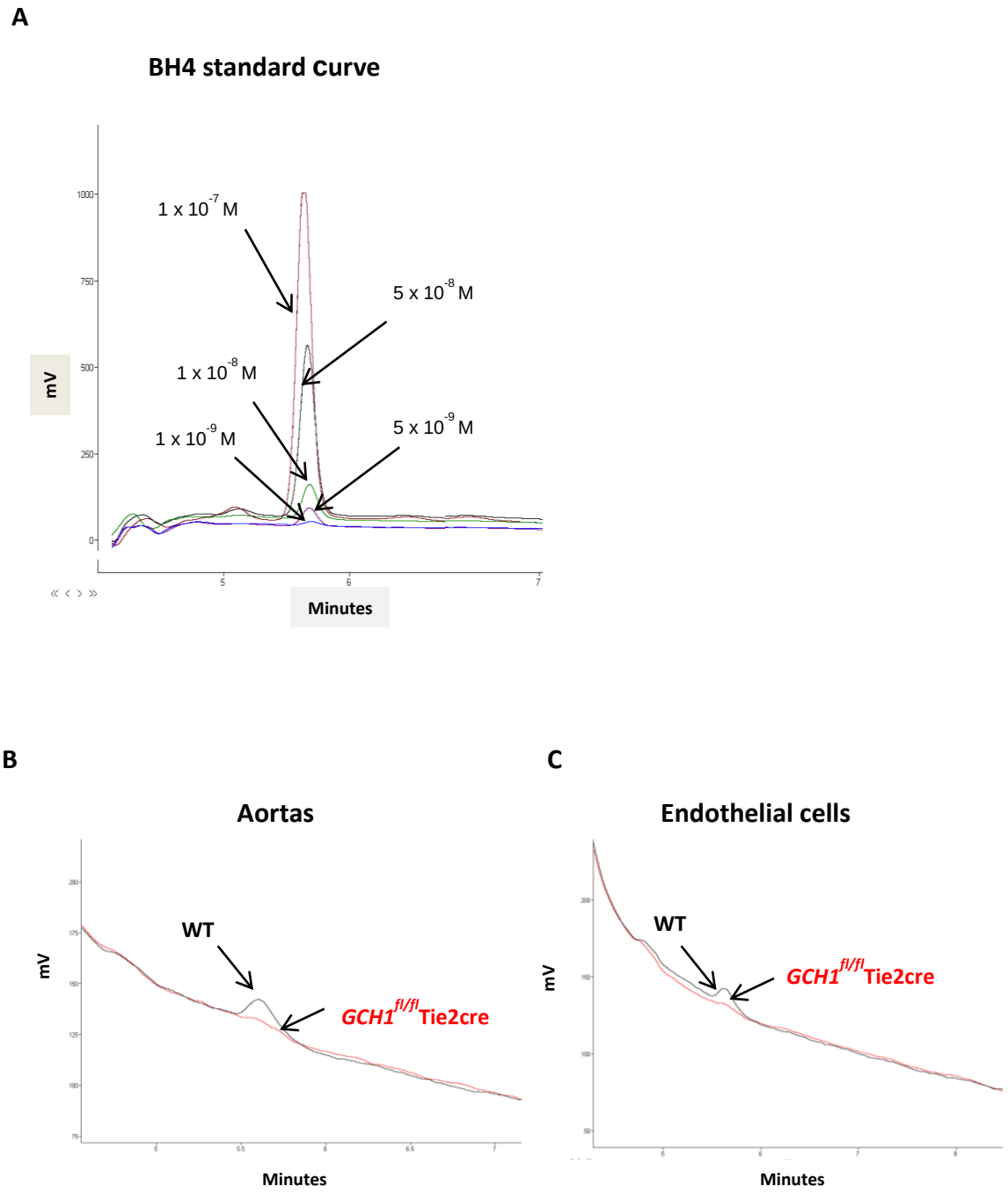


Figure 2.3. Representative chromatograms of BH4 trances.

Traces showing BH4 peaks of a standard curve **(A)**, aortas **(B)** and **(C)** primary endothelial cells from wild-type (WT) and *GCH1*$^{fl/fl}$Tie2cre mice.

2.5 Isolation of Murine Endothelial Cells

Primary endothelial cells were isolated from lungs or hearts of 16-22 week old *GCH1*$^{fl/fl}$Tie2cre and wild-type mice using MACS beads (Miltenyi Biotec), as described previously (Ali et al., 2013). Mice were culled by overdose of inhaled isoflurane as described in section 2.3.3. Perfused lungs or hearts were harvested in ice-cold DMEM under sterile conditions. Lungs/hearts were finely minced and digested in 10 mls DMEM containing 0.18 unit/ml Liberase TM (Roche, Herts, UK) and 0.1 mg/ml Dnase I (Roche, Herts, UK) for 1 hour at 37°C with gentle agitation every 15 minutes. Following digestion, the digested tissue was filtered through 100 μm and 40 μm cell strainers (BD Biosciences, Oxford, UK). The cell suspension was then incubated with rat anti-CD31 (PECAM-1) antibody (BD Biosciences, Oxford, UK) for 15 minutes at 4°C then with anti-rat secondary antibody coated immune magnetic beads for further 15 minutes at 4°C. Bead-bound endothelial cells were selected using a magnetic column. In all experiments, endothelial cells were cultured for 5 days on getatin coated 12 well plates in endothelial basal medium 2 BulletKit^{TM} (Lonza)(Figure 2.4 A). Representative flow cytometry data of primary endothelial cells costained with anti-CD45 and anti-CD31 antibody to show CD31+ and CD45- endothelial cells (Figure 2.4 B). FACS analysis was carried out by Dr Eileen McNeill.

Figure 2.4

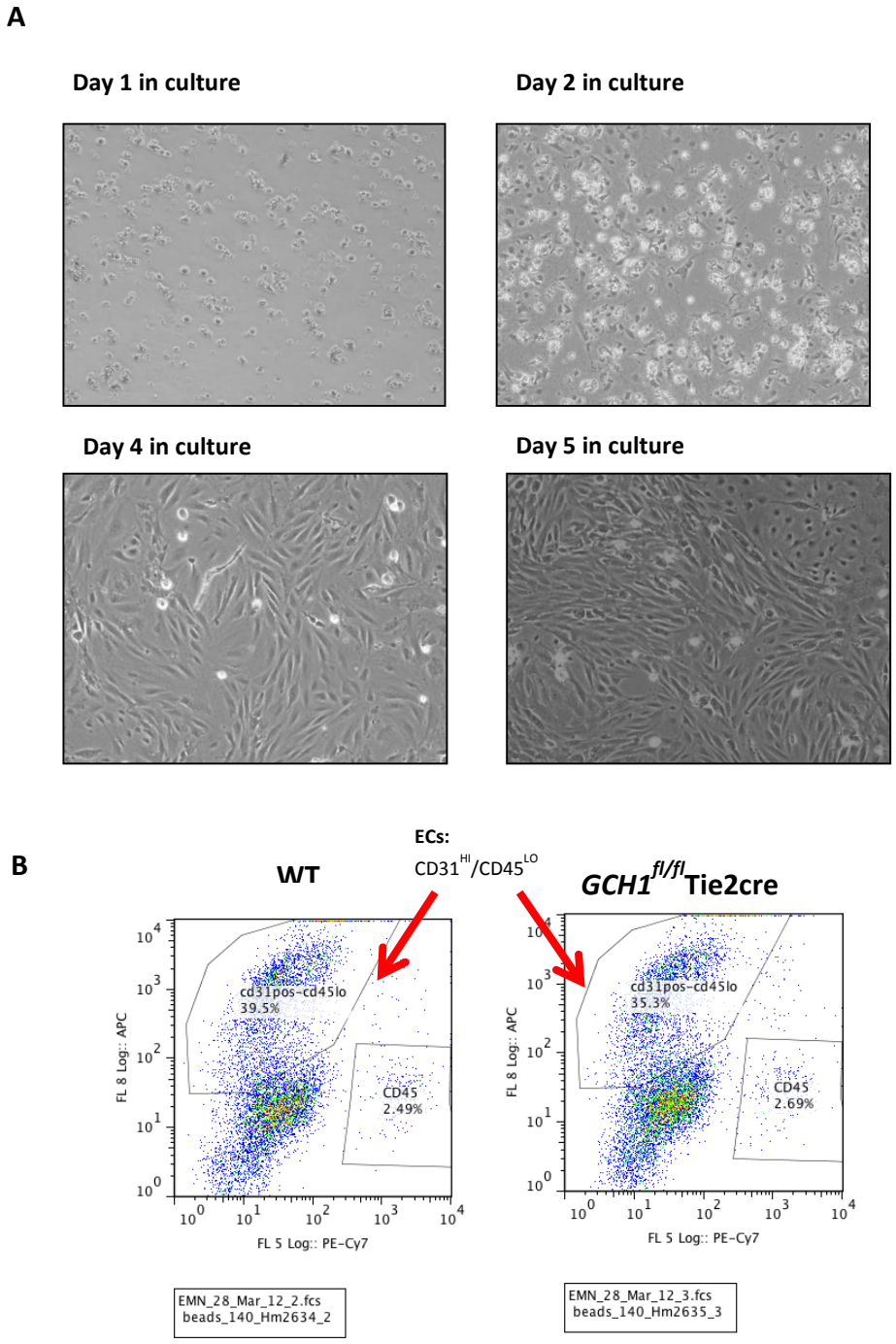


Figure 2.4. Primary endothelial cells isolated from lungs.

A) Phase contrast microscopy of endothelial cell from mouse lungs after 1, 2, 4 and 5 days in culture. **B)** Flow cytometry data of primary endothelial cells costained with anti-CD45 and anti-CD31 antibody to show CD31+ and CD45- endothelial cells.

2.6 NO bioactivity measurements

2.6.1 Analysis of NO Synthesis by eNOS

NO synthesis by eNOS was assessed by conversion of ^{14}C L-arginine to citrulline, followed by HPLC according to methods developed in our laboratory (de Bono et al., 2007). Briefly, primary lungs or hearts endothelial cells were isolated and cultured for 5 days as described in section 2.5. Prior to the assay, endothelial cells were incubated for 4 hours at 37°C in 200 µl Krebs-HEPES buffer containing calcium ionophore (1 µM; to stimulate eNOS activity), ^{14}C L-arginine (2 µl of 50 µCi/mL) and the arginase inhibitor *N*-hydroxy-nor-l-arginine (nor-NOHA) (5 µM), cells were pre-treated with or without N-monomethyl-L-arginine (1 mM, Sigma) for 30 min at 37°C. After incubation, cells were further freeze-thawed three times in 200 µl MilliQ-purified water to release any residual citrulline. 60 µl of 10% trichloroacetic acid was added to deproteinate the samples. 400 µl of supernatant was collected and added to 300 µl distilled water and 100 µl of 10% trichloroacetic acid. Samples were run on a SCX 300 cation-exchange HPLC column (Sigma) with online scintillation detection. Background signals were corrected from samples with ^{14}C L-arginine alone without cells.

2.6.2 Nitrite and Nitrate Determination

Mice were culled by overdose of isofluorane as described in section 2.3.3. Freshly harvested thoracic aortas were harvested in ice-cold Krebs-Henseleit buffer (KHB) buffer. Thoracic aortas were carefully dissected free of adherent tissue under a dissecting microscope. Following incubation in KHB (200 µl) for 20 min at 37°C, aortas were further incubated with or without of L-monomethylarginine (100 µM, Sigma) in Krebs-Henseleit buffer for 20 min at 37°C, then exposed to acetylcholine (1 µM final concentration) for 30 min at 37°C.

Nitrite and nitrate accumulation was measured in samples of buffer using the CLD88 NO analyzer (Ecophysics) and normalized to aortic dry weight.

2.6.3 Determination of Aortic NO Production by EPR

Electron paramagnetic resonance (EPR) spectroscopy was used to quantify aortic NO production, as described previously (Khoo et al., 2004). Mice were culled by overdose isofluorane as described in section 2.3.3. Thoracic aortas were gently dissected free from the back bone with fine forceps and scissors under microscope and placed in 12-well plate containing ice-cold Krebs-HEPES buffer (1ml). Aortas were cleaned of adherent fat under microscope and gently flush the remaining blood out of lumen with 1 ml syrinige (25 G needle) containing ice-cold Krebs-HEPES. Aortas were cut into five to six rings (~2-3 mm) and gently transferred into 96-well plates containing 100 µl ice-cold Krebs-HEPES. Aortic rings were then incubated either in the presence or absence of 1 mM L-NAME at 37°C for 30 minutes. After incubation, 3.5 µl of 0.1 mM A23187 (diluted 10 mM stock 100 fold; 10 µl 1 mM in 990 µl 100% DMSO) was added into each well (3.5 µl 100% DMSO as a control). NaDETC (3.6 mg; Alexis UK) and $FeSO_4$.7H20 (2.25 mg; Sigma, UK) were separated dissolved under argon in two 10 ml volumes of ice-cold Krebs-HEPES on ice for 10 minutes, and rapidly mixed 10 ml of NaDETC with 10 ml of $FeSO_4$.7H20 under argon to obtain colloid iron (II) diethyldithiocarbamate [$Fe(DETC)_2$] solution (0.4 mM), which was immediately added to each well (250 µl, final concentration 285 µM). Aortic rings were incubated at 37°C for 90 minutes in a tissue culture incubator. The plates were stirred gently every 20-30 minutes. After incubation, aortas were transferred into the middle of a column of ice-cold Krebs-HEPES buffer of 1 ml syringe and snap-frozen in liquid nitrogen. After freezing, the syringe was removed from the liquid nitrogen; the remaining barrel filled with

ice-cold Krebs-HEPES and frozen in liquid nitrogen. The syringe was then warmed for 5-10 seconds, and the syringe plunger used to push the frozen column out of the syringe barrel directly into a finger Dewar vacuum flask (Magnettech, Germany) containing liquid nitrogen. EPR spectra were obtained using an X-band EPR spectrometer (Miniscope MS 200; Magnettech). Instrument settings were: centre-field (B_0) 3276G, sweep 115G, microwave power 10 mW, modulation frequency 100 kHz, amplitude modulation 8000 mG, sweep time 60 s, and number of scans 4. Signals were quantified by measuring the total amplitude, after correction of baseline, and after subtracting background signals from incubation with colloid $Fe(DETC)_2$ alone. Values were normalized to aortic dry weight.

2.7 Measurement of superoxide and other ROS

2.7.1 Quantification of Intracellular Superoxide Production by HPLC

Superoxide production was quantified by measuring production 2-hydroxyethidium from dihydroethidium using HPLC (Crabtree and Channon, 2009; Crabtree et al., 2009b). Primary lung or heart endothelial cells were isolated and cultured for 5 days as described in section 2.5. Following 4 hours starvation serum in serum-free DMEM (PAA), endothelial cells were either incubated with or without 100 μM L-NAME (Sigma) for 20 minutes at 37°C. Following incubation, cells were then incubated with 25μM DHE (Invitrogen) for 20 minutes before being harvested for separation of DHE using gradient HPLC system (Jasco, UK) with an ODS3 reverse phase column (250mm, 4.5mm, Hichrom UK) and quantified using a fluorescence detector set at 510 nm (excitation) and 595 nm (emission).

2.7.2 Oxidative Fluorescent Microtopography

Endothelial superoxide production in mouse aortic frozen sections (n=6 per group) was detected using dihydroethidium (DHE) and fluorescent microscopy, as previously described (Bendall et al., 2005). Briefly, thoracic aortas (n = 6 per group) were harvested and frozen in optimal cutting temperature compound (OCT) (VWR International Ltd). Cryosections (30 µm) were cut at -25°C using a cryostat and placed on poly-lysine coated glass slide. Sections were incubated in Krebs-HEPES buffer with or without 1 mM L-NAME for 30 min at 37 °C, then with 2 µM dihydroethidium (Invitrogen) for 5 min at 37°C in darkness. Sections were washed with ice-cold Krebs-HEPES buffer, cover-slipped and placed in darkness. Images (x60) were acquired using a laser confocal microscope, set at identical acquisition settings for all slides (488 nm Excitation and 585 nm Emission). Endothelial superoxide production was quantified using Image-Pro Plus software by measuring the sum of the red intensities of the cells on the luminal side of the internal elastic lamina divided by the length of the vessel. For each ring, mean fluorescence was calculated from each quadrant of the vessels to produce n=1.

2.7.3 Determination of Aortic H_2O_2 Production

Aortic H_2O_2 production was determined by Amplex red assay (Molecular Probes), as described previously (Dikalov et al., 2007). Mice were culled by overdose of isofluorane as described in section 2.3.3. Thoracic aortas were harvested into ice-cold Krebs Ringer's phosphate. Aortas were cleaned of adherent fat under microscope and gently flush out the remaining blood with 1 ml syringe (25 G needle) containing ice-cold Krebs Ringer's phosphate. Aortic rings (6 x 2 mm) were incubated in 50 µl KHB containing 2 µM acetylcholine in a 96-well plate, at 37°C for 60 minutes in dark, either with or without 100

μM L-NAME. Following incubation, 50 μl of Amplex Red reagent mixture containing 20 mM Amplex red, 0.4 U/ml horseradish peroxidase was added. Buffer fluorescence was determined at excitation 530 nm and emission 590 nm. Background fluorescence (without vessels) was subtracted and normalized to aortic dry weight.

2.8 Isometric studies of vasomotor function

2.8.1 Wire myograph

Wire myography is a useful and convenient technique to perform in vitro studies of functional responses and vascular reactivity of vessels as small as 100 μm in diameter (Mulvany et al., 1977)(Figure 2.5). First developed in 1972 by Bevan and Osher (Bevan et al., 1972), it was improved by Mulvany and Halpern in 1976 (Mulvany et al., 1977). They secured both ends of each mounting wire with screws to fixed supports (‘jaw’) to keep the artery under tension, allowing the circumference of the vessels to be kept constant; therefore, the vessels were examined under near isometric conditions. Compounds were added directly to the chamber and vessel tension was monitored for contractile or relaxant responses.

2.8.2 Mouse mesenteric artery isolation and preparation

All myograph experiments described in this thesis were performed using either aortas or mesenteric arteries or uterine arteries. Mice were culled by a Schedule 1 method of humane killing by an overdose of isofluorane as described in section 2.3.3. For mesenteric artery studies, the mesenteric arcade was excised and placed in ice-cold Krebs solution. Mesenteric arcade was gently pinned down on a Sylgard-coated Petri dish filled with ice-cold Krebs buffer. Second-order branches of mesenteric artery were carefully dissected free of adherent tissue under a dissecting microscope (Figure 2.6). The external diameter of the arteries used in this study at 100 mmHg was typically between 150-200 μm. For aortic studies, thoracic aortas were excised and placed in ice-cold Krebs buffer. Aortas were dissected free of adherent tissue under a dissecting microscope. Segments of both mesenteric arteries and aortas were cut to give a final length of 2 mm.

Figure 2.5

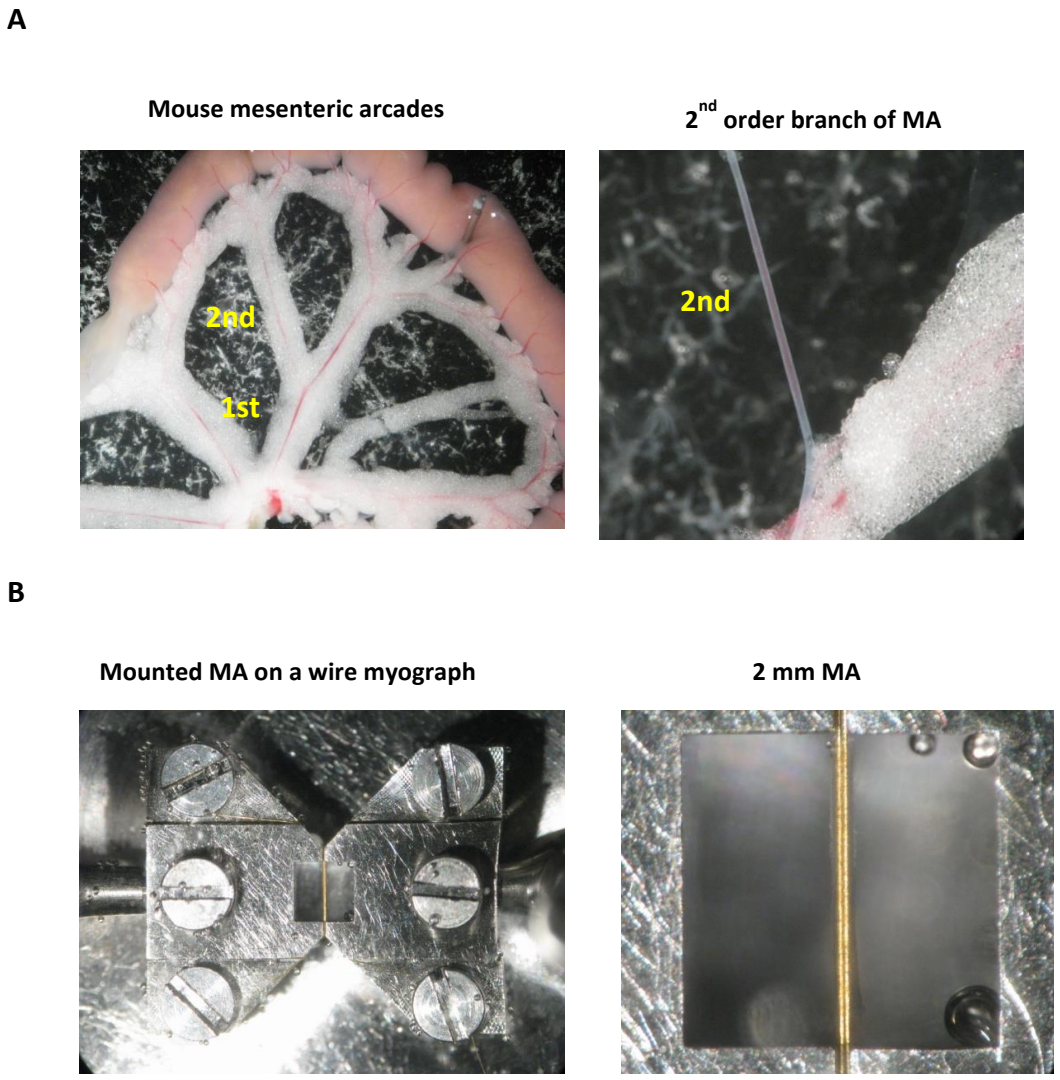


Figure 2.5. Isolation of mesenteric arcade and vessel mounting

A) Photographs of mesenteric arcade pinned down on a Sylgard-coated Petri dish with representation of 1st and 2nd order branch of mesenteric arteries (left), 2nd order mesenteric arteries (right). **B)** Photograph of a second order mouse mesenteric artery mounted in wire myograph jaw.

2.8.3 Isometric tension vasomotor studies in aorta

Vasomotor function was analyzed using isometric tension studies in a wire myograph (Multi-Myograph 610M, Danish Myo Technology, Denmark). Briefly, vascular rings were isolated from the thoracic aorta as described in section 2.3.3. The aortic rings (2 mm) were mounted on a wire myograph using tungsten wires (100 μm diameter; Goodfellows, UK) containing 5 ml of ice-cold Krebs solution gassed with 95% O_2/5% CO_2. After allowing vessels to equilibrate for 30 minutes at 37°C, the optimal tension was to 25 mN. The vessel viability was tested using 60 mM potassium chloride (KCl) (Figure 2.). Concentration-response contraction curves were established using cumulative half-log concentrations of phenylephrine. Vessels were washed three times with fresh Krebs solution, equilibrated for 20 minutes, and then precontracted to approximately 80-90% of maximal tension with PE. Acetylcholine and SLIGRL (Ser-Leu-Ile-Gly-Arg-Leu-NH_2) were used to stimulate endothelium-dependent vasodilatations in increasing cumulative concentrations. Responses were expressed as a percentage of the precontracted tension. Finally, the NO donor sodium nitroprusside (SNP) was used to test endothelium-independent smooth muscle relaxation in the presence of L-NAME.

2.8.4 Isometric tension vasomotor studies in mesenteric arteries

Vasomotor function was analyzed using isometric tension studies in a wire myograph. Second-order branch of mesenteric arteries were isolated from the mesenteric arcade as described in section 2.9.1. Segments of the mesenteric arteries (2 mm) were mounted in a Mulvany-Halpern multi-channel myograph (Model 610M, DMT, Denmark) using gold-plated tungsten wires (15 μm diameter; Goodfellows, UK) in Krebs solution containing 5 ml of ice-cold Krebs solution gassed with 95% O_2/5% CO_2. After allowing vessels to

equilibrate for 30 minutes at 37°C, the vessels were normalised in order to obtain an optimal and standardized stretch according to Laplace's Law. For this, the internal diameter of the vessel was set to a resting tension equivalent to that generated at 0.9 times the diameter of the vessel at 100 mmHg. Concentration-response contraction curves were established using cumulative half-log concentrations of phenylephrine or U46619. Vessels were washed three times with fresh Krebs solution, equilibrated for 20 minutes, and then precontracted to approximately 80-90% of maximal tension with PE or U46619. Acetylcholine and SLIGRL were used to stimulate endothelium-dependent vasodilatations in increasing cumulative concentrations. Responses were expressed as a percentage of the precontracted tension. Finally, the NO donor sodium nitroprusside (SNP) was used to test endothelium-independent smooth muscle relaxation in the presence of L-NAME. To avoid effects of evaporation, bath solutions were changed every 20 minutes.

All pharmacological drugs were pre-incubated at least 20 min before the dose-response curves were determined. PEG-catalase was used at 400 units/ml, apamin at 50 nM, charybdotoxin at 100 nM, 1H-(1,2,4)oxadiazolo[4,3-a]quinoxalin-1-one (ODQ) at 500 nM, indomethacin at 10 µM, L-NAME at 100 µM and sepiapterin at 10 µM. All drugs used were purchased from Sigma Chemical Company except ODQ (Cayman Europe) and SLIGRL (Abcam).

2.9 Protein extraction and detection

2.9.1 Protein lysate preparation

Isolated thoracic aortas and 2nd branches of mesenteric arteries from *GCH1*$^{fl/fl}$Tie2cre mice and wild-type littermates were harvested and snap frozen on dry ice and stored at -80°C as described in Section 2.8.1. Extraction of aortic and mesenteric protein was performed in ice-

cold CellLytic MT mammalian tissue lysis buffer (Sigma-Aldrich, Gillingham, UK) containing complete protease inhibitor (Roche, Herts, UK) and phosphatase inhibitor cocktail (Roche, Herts, UK). Primary endothelial cells were lysed directly in CellLytic MT lysis buffer with protein and phosphatase inhibitors. The wells were scraped with the plunger of 1 ml syringe and lysates were transferred to eppendorf tubes. The sample lysate from aortas and cells underwent three cycles of freeze-thaw. For mesenteric arteries, tissue was homogenised using a glass homogeniser. All samples were centrifuged at 16,000 g for 10 minutes at 4°C. Supernatant was then transferred to a new tube for protein concentration measurements as described in Section 2.9.2. The sample lysates were stored at -20°C.

2.9.2 Determination of protein content

Total protein content in lysate was quantified using the BCA™ Protein Assay kit (Thermo Fisher Scientific, Loughborough, UK) with BSA standards according to the manufacturer's instructions. For the generation of a standard curve, protein standards ranging from 0.125 to 2 mg/ml were prepared from bovine serum albumin (BSA; Sigma-Adrich, UK) using the same buffer as that used for sample preparation (ie. CellLytic MT for western blotting). For the assay itself, 10 µl of standard and samples in duplicates were added to 190 µl of working reagent, incubated for 30 min at 37 C and read in a microplate reader at 562 nm.

2.9.3 Immunoblotting

Western blot analysis was performed to measure protein levels of GTPCH, Phospho-eNOS (Ser1177), Phospho-eNOS (Thr495), eNOS, catalase, MnSOD, EcSOD, Cu/ZnSOD, CD102 and Phospho-VASP (Ser239) and VASP in aortas and primary cells from wild-type and *GCH1*$^{fl/fl}$Tie2cre mice. Protein lysates were added with 4X NuPageR sample buffer

(Invitrogen, Paisley, UK) and 10X reducing agent (Invitrogen, Paisley, UK). Protein lysates (5-15 ug) were loaded into a NuPage 4-12% Bis-Tris gel, transferred to polyvinylidene difluoride (PVDF) membrane (Millipore, Watford, UK). Molecular weight rainbow markers (Amersham, VWR, UK) were loaded to determine product band sizes. Membranes were blocked in 5% milk in PBST for 1 hour at room temperature. Following a 5 minutes wash in PBST, the membranes were then incubated overnight with primary antibodies (Table 1). Protein bands were visualised using HRP-conjugated secondary antibodies (Table 1) and chemiluminescence (Super West Pico Chemiluminescence, Thermo Scientific, Loughborough, UK). Membrane were stripped for 30 minutes at 50°C in 6.25 mM Tris (pH 6.8) with 2% SDS and 100 mM β-mercaptoethanol. Following stripping, membranes were washed for 10 minutes in PBS-T, blocked in PBS-T with 5% milk and incubated with antibodies as described below.

Table 2.2

Target	Conjugate	Specificity	Species	Working Concentration	Product number	Supplier
Primary antibodies						
CD102	-	Mouse	Goat	1:1000	Af774	R&D
GAPDH	-	Mouse	Mouse	1:20000	MAB374	Millpore
eNOS	-	Mouse	Mouse	1:5000	610296	BD Transduction Laboratories
β-tubulin	-	Mouse	Rabbit	1:20000	ab6046	Abcam
Phospho Thr495 eNOS	-	Mouse	Rabbit	1:500	9574	Cell Signalling
Phospho Ser1177 eNOS	-	Mouse	Rabbit	1:500	9571	Cell Signalling
GTPCH	-	Mouse	Rabbit	1:10000	-	Gifted by Prof Steve Gross
Phospho VASP	-	Mouse	Rabbit	1:1000	3114	Cell Signalling
VASP	-	Mouse	Rabbit	1:500	3112	Cell Signalling
Catalase	-	Mouse	Rabbit	1:2500		Calbiochem
MnSOD	-	Mouse	Rabbit	1:2500	SOD111	Stressgen Bioreagents
ecSOD	-	Mouse	Rabbit	1:2500	SOD106	Stressgen Bioreagents
Cu/ZnDOD	-	Mouse	Rabbit	1:2500	SOD101	Stressgen Bioreagents
Seconadary Antibodies						
Rabbit IgG	HRP	Rabbit	Goat	1:5000	W4011	Promega
Mouse IgG	HRP	Mouse	Rabbit	1:5000	W402B	Promega
Goat IgG	HRP	Goat	Donkey	1:5000	sc-2020	Santa Cruz

Table 2.2 Primary and secondary antibodies used for Western Blotting. Antibodies are listed with host and target species, reactivity, working concentrations and origin

2.10 Statistical analysis

Data were analysed using Microsoft Excel (Microsoft, USA) and GraphPad Prism 5 (USA). Data are expressed as the mean ± standard error of the mean (SEM). Between group comparisons of Normally distributed measurements were made using a two-tailed Student's t-test and paired t-test where appropriate. When more than two groups were compared, one-way ANOVA with post-hoc Newman-Keuls Multiple Comparison Test were used. P values of less than 0.05 were regarded as statistically significant.

Chapter 3:

Characterisation of the Endothelial Cell-Targeted *GCH1* Knockout Mouse

Chapter 3: Characterisation of the Endothelial Cell-Targeted *GCH1* Knockout Mouse

3.1 Introduction

Vascular tetrahydrobiopterin (BH4) is a critical cofactor for eNOS enzymatic activity and NO generation. When vascular BH4 bioavailability is limited, as observed in animal models and patients with vascular diseases, NO generation becomes uncoupled from L-arginine oxidation, resulting in superoxide generation rather than NO. Recent evidence suggests that reduced vascular BH4 bioavailability contributes to the pathogenesis of endothelial dysfunction and vascular disease states such as hypertension (Landmesser et al., 2003), diabetes (Heitzer et al., 2000b) and atherosclerosis (Bitar et al., 2005b; Landmesser et al., 2003; Laursen et al., 2001).

Previous studies on the importance of BH4 bioavailability in endothelial cells have used systemic pharmacological inhibition of BH4 biosynthesis by GTPCH or the hph-1 hyperphenylalaninemic mouse, which has moderate systemic BH4 deficiency because of reduced gene expression from the *GCH1* locus (Cosentino et al., 2001; Khoo et al., 2005). However, in the hph-1 mouse, global BH4 deficiency has systemic effects in multiple cell types, such as neurones, and cardiac myocytes, thus confounding the interpretation of endothelial cell BH4 effects on vascular function and blood pressure control by eNOS (Adlam et al., 2012). Therefore, it is unclear whether the deficiency in endothelial cell BH4 alone is sufficient to cause endothelial dysfunction and vascular disease. Furthermore, the physiological requirement for endothelial BH4 in the regulation of eNOS-derived vascular NO generation, or other eNOS-derived signalling mechanisms, remains unanswered. To address this question, a novel mouse model of endothelial cell-targeted *GCH1* knockout (*GCH1*$^{fl/fl}$Tie2cre) was generated.

3.2 Hypothesis and aims

The central hypothesis is that the requirement for endothelial cell *GCH1* and BH4 in vascular disease is cell-specific. I hypothesised that endothelial cell BH4 is required for eNOS function and determines eNOS-derived NO versus eNOS-derived ROS generation. Specifically:

1) Endothelial cell-targeted *GCH1* deletion will result in a significant reduction in GTPCH protein expression and lead to endothelial cell BH4 deficiency.

2) Endothelial cell BH4 deficiency will lead to eNOS uncoupling, loss of NO generation, and increased ROS production.

The main aims of this chapter are:

1) To determine the efficiency of the *GCH1* floxed excision by Tie2cre in primary endothelial cells, endothelial cell-rich tissues and non-endothelial cell-rich tissues from wild-type and *GCH1*$^{fl/fl}$Tie2cre mice.
2) To examine GTPCH expression and BH4 levels in primary endothelial cells and tissues from wild-type and *GCH1*$^{fl/fl}$Tie2cre mice.
3) To investigate the effect of endothelial cell-specific BH4 deficiency on reactive oxygen species generation in primary endothelial cells and aortas from wild-type and *GCH1*$^{fl/fl}$Tie2cre mice.
4) To determine the effect of endothelial cell-specific BH4 deficiency on NO bioactivity in primary endothelial cells and aortas from wild-type and *GCH1*$^{fl/fl}$Tie2cre mice.

3.3 Methods

Most of the methods used in this chapter have been described in Chapter 2. Only methods and reagents used specifically in the experiments for this chapter are described below.

3.4 Results

3.4.1 Excision of *GCH1* floxed allele in *GCH1*$^{fl/fl}$Tie2cre mice

In order to determine the efficiency of excision of the *GCH1* floxed sequence in primary endothelial cells, endothelial cell-rich tissues (heart, lung and aorta), non-endothelial cell-rich tissues (liver and kidney) from *GCH1*$^{fl/fl}$Tie2cre and wild-type littermates, DNA samples were extracted using QIAamp kit (Qaigen, UK). 10 ng of DNA samples from wild-type and *GCH1*$^{fl/fl}$Tie2cre tissues were used and subjected to semi-quantitative PCR using primers for *GCH1* floxed allele and Tie2-cre-excised allele as described in Section 2.3.2 (Figure 3.1). The predicted 1030 bp product of the *GCH1* floxed allele was detected in wild-type mice. In the presence of the Tie2cre transgene a 1392 bp knockout allele was detected. Semi-quantitative PCR demonstrated that there were over 50% of *GCH1* floxed allele being excised by Tie2cre in endothelial cell-rich tissues such as heart, lung and aorta and less than 25% excision was observed in non-endothelial cell-rich tissues such as liver and kidney from *GCH1*$^{fl/fl}$Tie2cre mice. Importantly, there was almost 100% excision of the *GCH1* floxed allele in isolated primary endothelial cells from *GCH1*$^{fl/fl}$Tie2cre mice. Conversely, there was undetectable *GCH1* floxed excision in all tissues and primary endothelial cells from wild-type mice (Figure 3.1). These data suggests efficient excision of *GCH1* floxed allele in endothelial cells from *GCH1*$^{fl/fl}$Tie2cre mice.

Figure 3.1

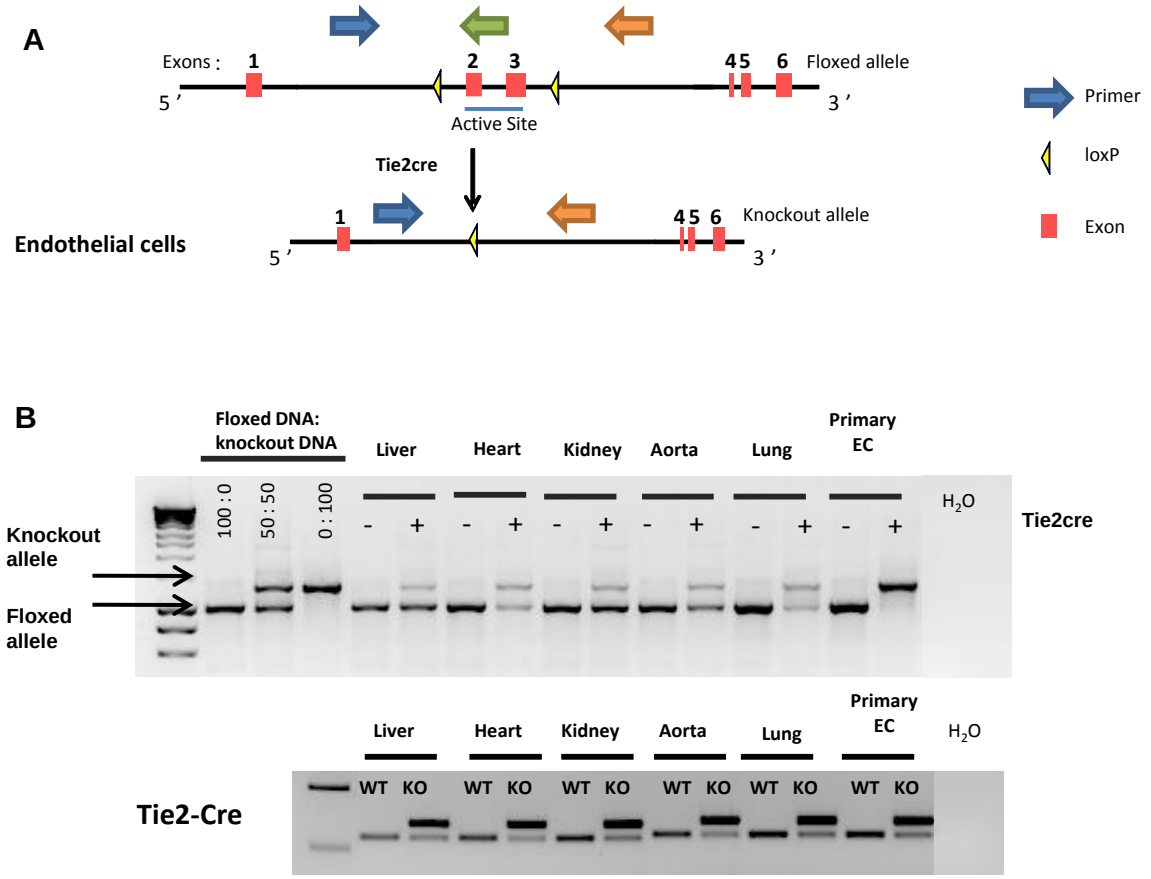


Figure 3.1. Generation and characterisation of *GCH1*$^{fl/fl}$Tie2cre mice.

A) Schematic showing the targeting of the mouse *GCH1* locus with loxP sites flanking the exons (2 and 3) encoding the active site of the GTPCH protein. Arrows show PCR primers for the *GCH1* floxed and Tie2cre-exised allele, *GCH1* floxed allele (blue and green arrows), and deleted allele (blue and orange arrows). **B)** Evaluation of Tie2cre-mediated excision of the loxP flanked DNA in tissues and primary cells derived from *GCH1*$^{fl/fl}$Tie2cre and *GCH1*$^{fl/fl}$ (wild-type) mice. The predicted 1030 bp product was detected in wild-type mice. In the presence of the Tie2cre transgene a 1392 bp knockout allele was detected, with efficient excision in primary endothelial cells.

3.4.2 GTP Cyclohydrolase protein expression and BH4 levels in tissues

After establishing that the *GCH1* floxed allele was efficiently excised in endothelial cells from *GCH1*$^{fl/fl}$Tie2cre mice, I next determined the levels of GTPCH protein expression in vascular tissues such as aortas by western blotting as described in Section 2.9. GTPCH protein expression was substantially reduced in aortas from *GCH1*$^{fl/fl}$Tie2cre mice compared to wild-type controls (P<0.01, Figure 3.2 A) and the endothelial cell-surface marker CD102 and loading control beta-tubulin were present equally in aortas from both *GCH1*$^{fl/fl}$Tie2cre and wild-type mice. In endothelial-denuded aortas, GTPCH protein expression was markedly reduced in wild-type mice but unchanged in *GCH1*$^{fl/fl}$Tie2cre mice, suggesting the majority of GTPCH is expressed in endothelium (Figure 3.2 B). This finding indicates that endothelial cell-targeted *GCH1* deletion led to a marked reduction in endothelial cell GTPCH protein expression in *GCH1*$^{fl/fl}$Tie2cre aortas.

GTPCH is an essential enzyme for de novo BH4 biosynthesis. I therefore determined the levels of BH4 in aortas from *GCH1*$^{fl/fl}$Tie2cre and wild-type mice by HPLC as described in Section 2.4. In *GCH1*$^{fl/fl}$Tie2cre mice, BH4 levels were significantly reduced compared to wild-type controls. BH4 levels were markedly reduced by ~75% in endothelial-denuded aortas from wild-type mice (Figure 3.2 C). In contrast, removal of endothelium in *GCH1*$^{fl/fl}$Tie2cre aortas did not significantly reduce BH4 levels, suggesting the endothelium is the major source of vascular BH4 (P<0.05, Figure 3.2). In *GCH1*$^{fl/fl}$Tie2cre mice, BH4 levels in endothelial cell rich tissues such as the lung and heart were substantially decreased compared to wild-type controls. In non-endothelial cell rich tissues such as liver and kidney, there was no difference in BH4 levels between wild-type and *GCH1*$^{fl/fl}$Tie2cre mice. Importantly, plasma BH4 levels were similar between the groups, indicating that endothelial cell BH4 biosynthesis by GTPCH does not contribute significantly to plasma BH4 levels. Despite marked BH4 deficiency, absolute BH2 levels in aorta, lung, and heart were

comparable between the genotypes, such that the BH4 to BH2 and biopterin ratio was significantly reduced in aortas heart, and lung in *GCH1*$^{fl/fl}$Tie2cre mice (Figure 3.3).

Figure 3.2

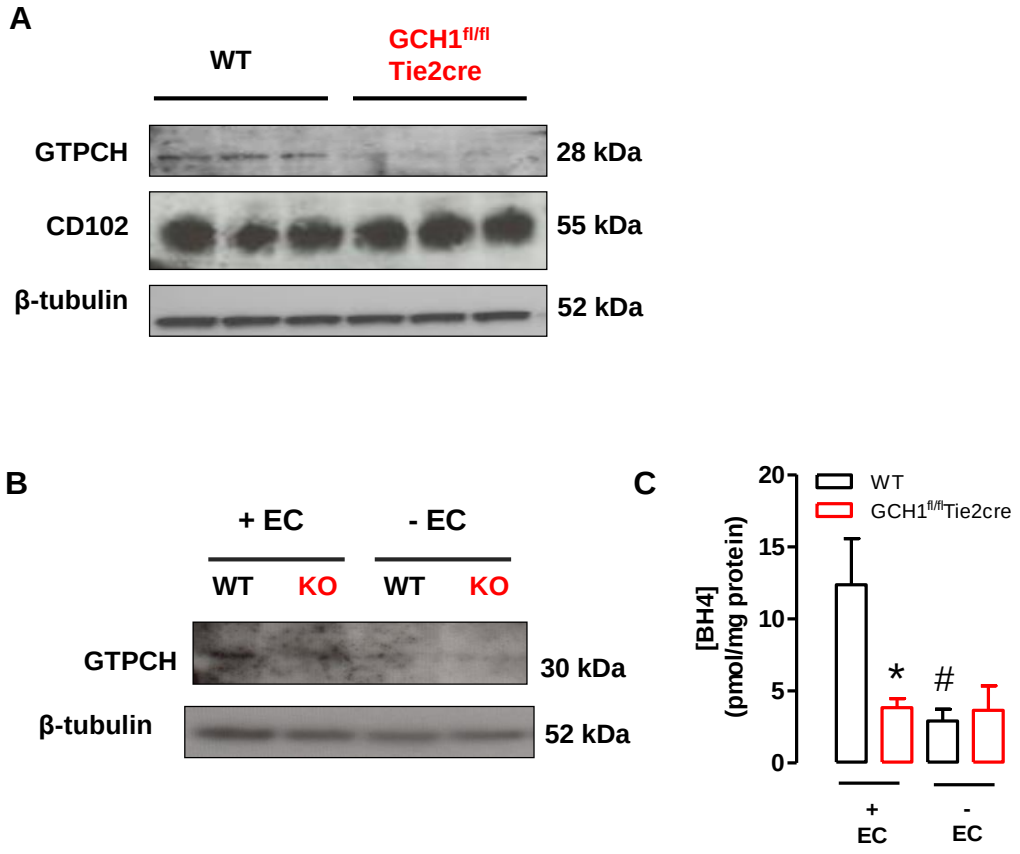


Figure 3.2. GTPCH protein and BH4 levels in aortas

A) Representative western blots for GTPCH protein in aortas from wild-type and *GCH1*$^{fl/fl}$Tie2cre mice. CD102 protein expression was used as endothelium-specific marker and β-tubulin was used as loading control. **B)** Contribution of endothelium GTPCH in mouse aortas. **C)** Contribution of endothelium to vascular BH4 in mouse aortas. Vascular BH4 levels were significantly decreased in wild-type denuded aortas but not in *GCH1*$^{fl/fl}$Tie2cre denuded aortas (**P*<0.05 comparing genotype; #*P*<0.05 comparing treatment; n=5 to 6 animals per group).

Figure 3.3

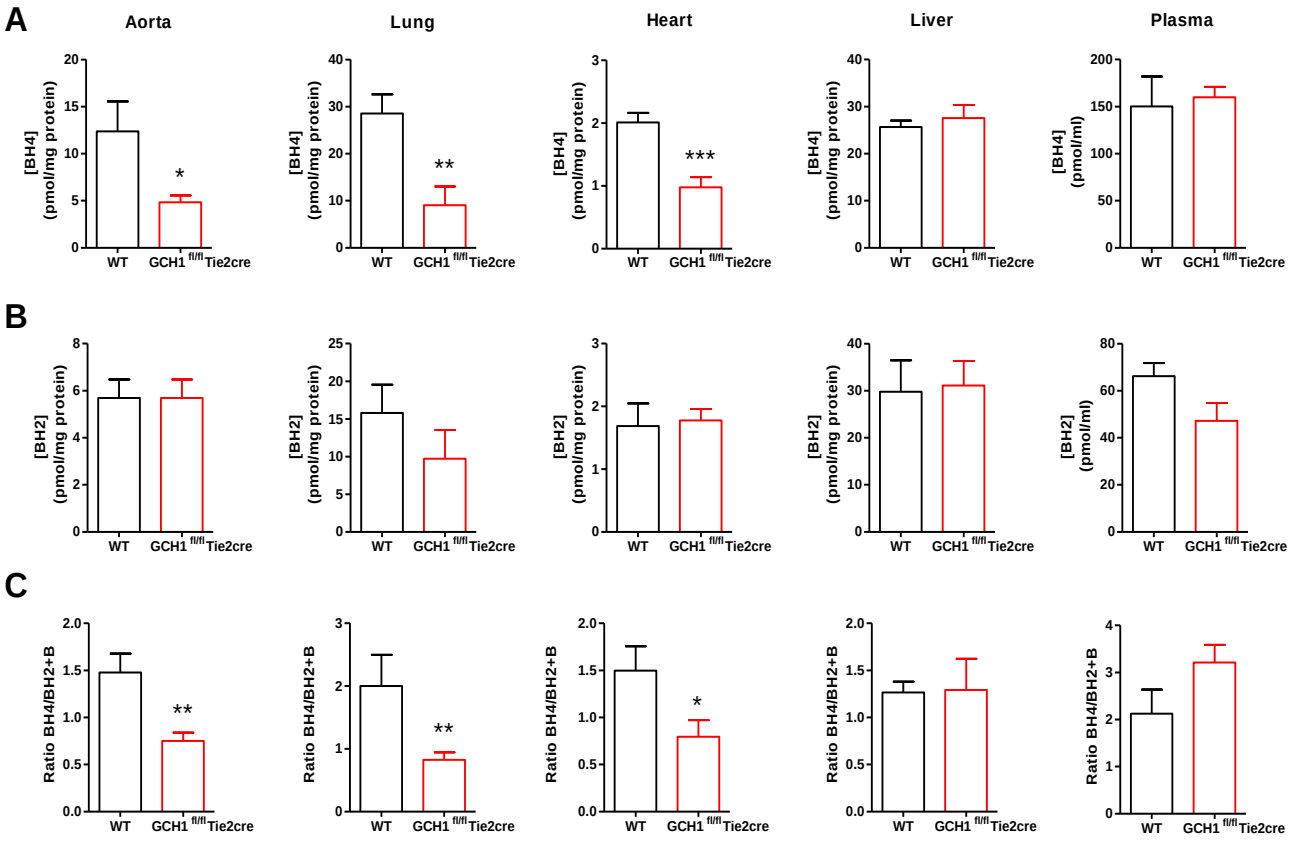


Figure 3.3. BH4 measurements in tissues and plasma
Quantitative analysis of tetrahydrobiopterin (BH4) metabolism in aorta, lung, heart, liver and plasma of wild-type (WT) and *GCH1*$^{fl/fl}$Tie2cre mice. Bar graphs showing levels of **A)** BH4, **B)** 7,8-dihydrobiopterin (BH2), and **C)** BH4/BH2 + biopterin (B) ratio in aorta, lung, heart, liver and plasma of WT and *GCH1*$^{fl/fl}$Tie2cre mice. (**P*<0.05; ***P*<0.01; ****P*<0.001 n=6 to 10 animals per group)

3.4.3 GTPCH protein expression and BH4 levels in primary endothelial cells

To further test the endothelial cell-specificity of *GCH1* deletion, and the effects of endothelial cell loss of BH4 biosynthesis on BH4 levels, I isolated primary endothelial cells using immunomagnetic bead selection as described in section 2.5. Primary endothelial cells were confirmed as CD31+ CD45- by flow cytometry (Figure 3.4 A). In endothelial cells from *GCH1*$^{fl/fl}$Tie2cre mice, GTPCH protein was not detectable by western blotting, whereas GTCPH was readily detected in wild-type endothelial cells, and the endothelial cell-surface markers CD102 and Tie2 were present equally in endothelial cells from both *GCH1*$^{fl/fl}$Tie2cre and wild-type mice (Figure 3.4 B). Measurement of biopterins by HPLC revealed barely-detectable levels of BH4 in primary endothelial cells from *GCH1*$^{fl/fl}$Tie2cre mice (Figure 3.4 C). Taken together, these results demonstrate endothelial cell-specific *GCH1* knockout in *GCH1*$^{fl/fl}$Tie2cre mice, leading to endothelial cell-specific BH4 deficiency. Furthermore, the finding of marked BH4 deficiency in *GCH1*$^{fl/fl}$Tie2cre endothelial cells, despite normal circulating plasma levels, reveals a cell-autonomous requirement for de novo BH4 synthesis in maintenance of endothelial cell BH4 levels.

Figure 3.4

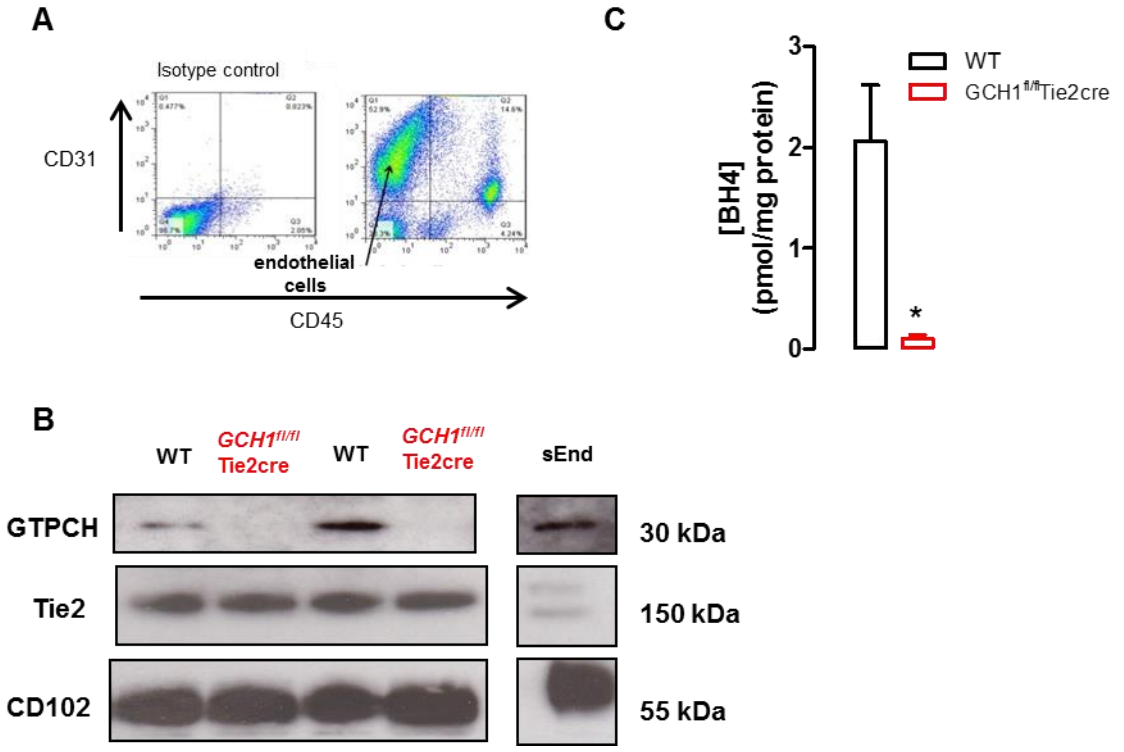


Figure 3.4. GTPCH and BH4 levels in primary endothelial cells

A) Flow cytometry data of primary endothelial cells co-stained with anti CD45 and anti CD31 antibody to show CD31+ and CD45- endothelial cells. **B)** Representative immunoblot of GTPCH levels in primary endothelial cells from WT and *GCH1*$^{fl/fl}$Tie2cre mice. Tie2 and CD102 protein expressions were used as endothelial cell specific markers. sEnd cells were used as positive control for endothelial cells. **C)** BH4 levels in primary endothelial cells from *GCH1*$^{fl/fl}$Tie2cre and wild-type mice (*P<0.05; n=4 animals/group).

3.4.4 Measurement of superoxide production

Previous studies have shown that reduced BH4 bioavailability is associated with eNOS uncoupling, increased superoxide production and reduced NO bioactivity in animal models and patients with vascular disease states. It remains unclear whether deficiency in endothelial cell BH4 alone is sufficient to cause eNOS uncoupling. To address this question, superoxide generation by endothelial cell and aortas from *GCH1*$^{fl/fl}$Tie2cre and wild-type mice were measured using two independent methods.

3.4.4.1 Superoxide measurement using DHE-HPLC

To determine the effects of endothelial cell-specific BH4 deficiency on eNOS function, I first measured basal $O_2^{\bullet-}$ and other reactive oxygen species (ROS) production in isolated primary endothelial cells by quantification of 2-hydroxyethidium (2-HE) and ethidium (E) production from dihydroethidine (DHE), using HPLC as described in Section 2.7.1.

Primary endothelial cells were isolated from the lungs of wild-type and *GCH1*$^{fl/fl}$Tie2cre mice as described in Section 2.5. Cells were cultured for 5 days and then starved for 4 hours in low glucose DMEM then pre-incubated with or without 100 µM of the NOS inhibitor L-NAME for 30 min at 37°C. Cells were further incubated with 25 µM DHE for 20 min before being harvested for the measurement of ROS production by DHE HPLC. The 2-hydroxyethidium and ethidium peaks were quantified as area under the curve (Figure 3.5).

Both 2-HE and ethidium production were significantly elevated in primary endothelial cells from *GCH1*$^{fl/fl}$Tie2cre mice compared with wild-type controls (P<0.05, Figure 3.5). Furthermore, there was significant inhibition of 2-HE and ethidium production in *GCH1*$^{fl/fl}$Tie2cre mice by L-NAME (100 µM), whereas no effect was observed in wild-type endothelial cells, suggesting that eNOS is a source of $O_2^{\bullet-}$ production and other ROS such as H_2O_2 in *GCH1*$^{fl/fl}$Tie2cre endothelial cells.

Figure 3.5

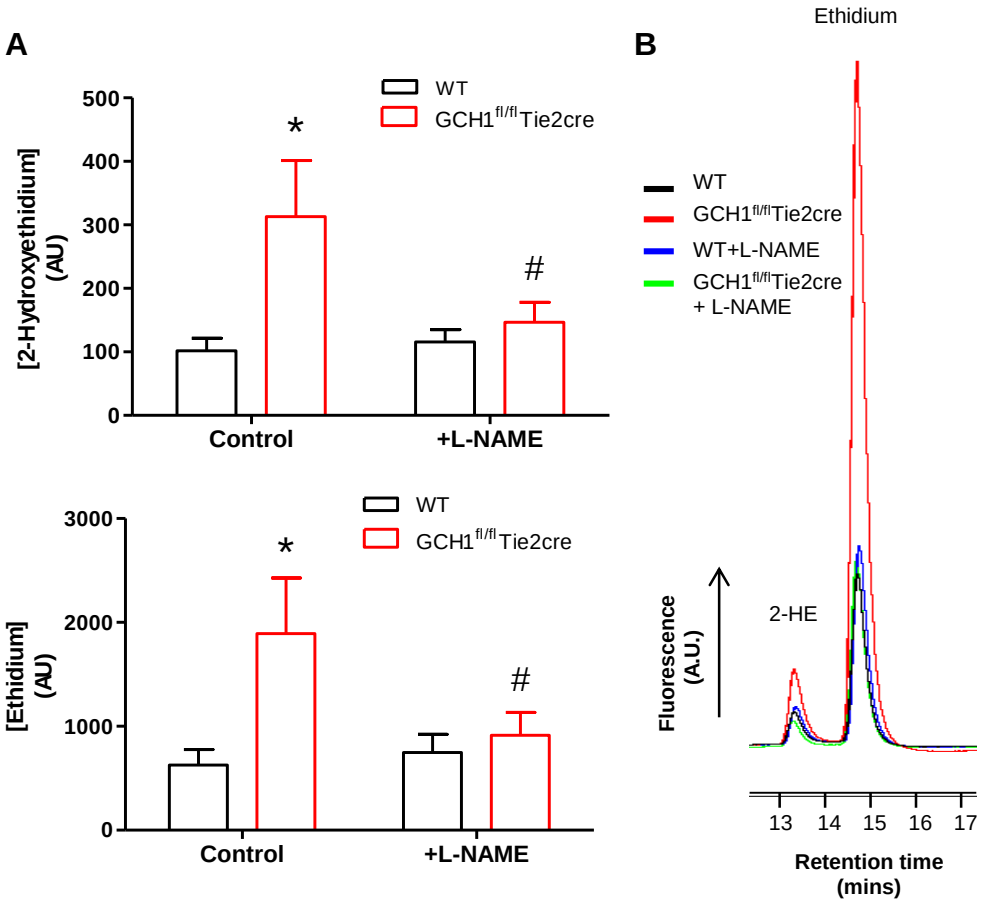


Figure 3.5. Quantification of superoxide production in endothelial cells.
A) Superoxide and other ROS productions detected by DHE high-performance liquid chromatography (HPLC) and quantified by area under the curve of 2-hydroxyethidium (2-HE) and ethidium. Superoxide and other ROS productions as measured by 2-HE and ethidium respectively in primary endothelial cells isolated from *GCH1*$^{fl/fl}$Tie2cre and wild-type mice. Pre-incubation of endothelial cells with L-NAME inhibited the 2-HE and ethidium peaks in *GCH1*$^{fl/fl}$Tie2cre but unaltered in wild-type endothelial cells. Data are expressed as mean ±SEM. A.U. – arbitrary units. (**P*<0.05 comparing genotype, #*P*<0.05 comparing treatment; n=6-7 animals/group). B) Representative trances of 2-HE and ethidium peaks in primary endothelial cells isolated from wild-type and *GCH1*$^{fl/fl}$Tie2cre mice detected by DHE HPLC in the presence and absence of L-NAME.

3.4.4.2 DHE fluorescence

I next determined the spatial distribution of ROS production in aortic tissue sections using dihydroethidium fluorescence microtopography as described in Section 2.7.2. Under basal conditions, *GCH1*$^{fl/fl}$Tie2cre aortas generated 4-fold more endothelium-derived ROS production than wild-type controls (P<0.05, Figure 3.6). In the presence of L-NAME, the level of endothelium-derived ROS production in wild-type aortas was significantly increased compared to untreated wild-type aortas, suggesting a tonic scavenging effect of NO on $O_2^{\bullet-}$ (P<0.01). In contrast, endothelial ROS production in *GCH1*$^{fl/fl}$Tie2cre aortas in the presence of L-NAME was significantly decreased compared to untreated *GCH1*$^{fl/fl}$Tie2cre aortas (P<0.05), indicating a major contribution from eNOS-derived ROS.

Figure 3.6

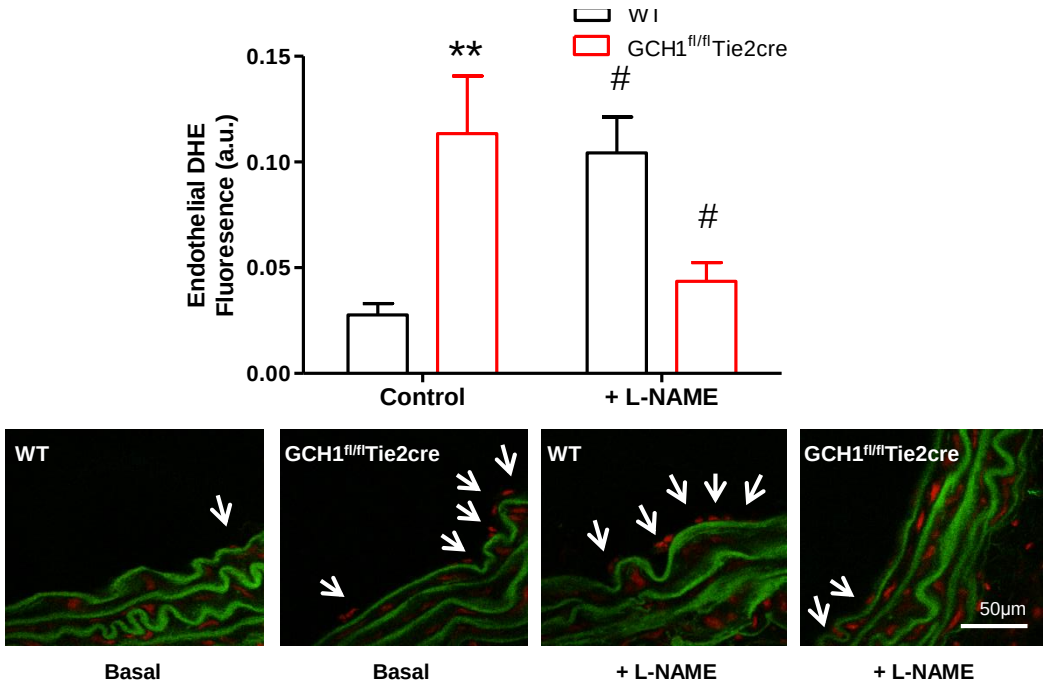


Figure 3.6. Superoxide detection in aortic sections

Endothelium-derived superoxide production was measured by dihydroethidium staining in aortic sections from wild-type and *GCH1*$^{fl/fl}$Tie2cre mice. Endothelium-derived superoxide, quantified in arbitrary units as area of luminal red staining/length of luminal surface, in the absence and presence of 100 μM L-NAME (***P*<0.01 comparing genotype, #*P*<0.05 comparing treatment; n=6 animals/group)

3.4.5 Measurement of NO bioactivity

To determine the effects of endothelial cell BH4 deficiency on NO bioactivity, I measured NO bioactivity in primary endothelial cells and aortas from wild-type and *GCH1*$^{fl/fl}$Tie2cre mice by three independent methods: L-arginine to L-citruline conversion, nitrite/nitrate accumulation by ozone chemiluminescence, and EPR spin trap.

3.4.5.1 L-arginine to L-citrulline conversion assay

First, I measured L-arginine to L-citrulline conversion using HPLC as described in Section 2.6.1. Primary endothelial cells were isolated from the lungs/hearts of wild-type and *GCH1*$^{fl/fl}$Tie2cre mice as described in Section 2.6.1. Cells were cultured for 5 days and at day 5, cells were pre-incubated for 4 hours at 37°C in Krebs-HEPES buffer containing ^{14}C L-arginine (2 μl of 50 μCi/mL) with or without N-monomethyl-L-arginine (1 mM). Background signals were corrected from samples with ^{14}C L-arginine alone without cells. Samples were run on a SCX 300 cation-exchange HPLC column with online scintillation detection. I found that eNOS activity (L-NMA inhibitable) was significantly decreased in endothelial cells from *GCH1*$^{fl/fl}$Tie2cre mice compared to wild-type littermates (P<0.05, Figure 3.7).

3.4.5.2 Nitrite and Nitrate production

Secondly, nitrite and nitrate accumulation by aortas was measured using an NO analyser as described in Section 2.6.2. Briefly, freshly harvested aortas were pre-incubated in the presence or absence of L-monomethylarginine at 37°C for 20 min, then exposed to acetylcholine (1 μM) for 30 min. Nitrite and nitrate accumulation was measured in samples of buffer using the NO analyser and normalized to aortic dry weight. I have shown that nitrite and nitrate accumulation by aortas (L-NMA inhibitable fraction) was significantly reduced in *GCH1*$^{fl/fl}$Tie2cre mice compared to wild-type controls, to levels that were barely detectable above baseline (P<0.05, Figure 3.7).

Figure 3.7

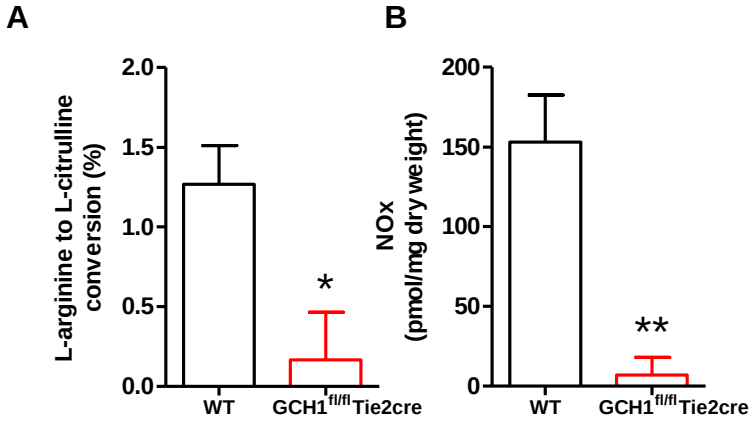


Figure 3.7. NOS bioactivity

A) Conversion of ^{14}C arginine to ^{14}C citrulline was used as a measure of eNOS activity. eNOS activity (L-NMA- inhibitable) was greatly reduced in primary endothelial cells isolated from *GCH1*$^{fl/fl}$Tie2cre mice compared to the wild-type controls (**P*<0.05; n=4 per group). **B)** nitrite/nitrate production in isolated fresh aorta stimulated with 1 μM acetylcholine for 30 min. Nitrite/nitrate production (L-NMA- inhibitable) in stimulated aortas from *GCH1*$^{fl/fl}$Tie2cre mice was significantly decreased compared to wild-type controls (***P*<0.01; n=7-9 animals/group).

3.4.5.3 NO bioactivity by EPR spin trap

Finally, I measured specific NO generation from aortas using EPR detection of NO using the spin-trap colloid $Fe(DETC)_2$ as described in Section 2.6.3. The characteristic NO-$Fe(DETC)_2$ EPR triplet was increased (~6-fold) by stimulation with 1 μM acetylcholine in wild-type mice, and abolished by incubation with L-NAME, but was not detectable in *GCH1*$^{fl/fl}$Tie2cre mice aortas (Figure 3.8). Taken together, these data demonstrate that endothelial cell *GCH1* deletion and BH4 deficiency dramatically reduce vascular NO bioactivity.

Figure 3.8

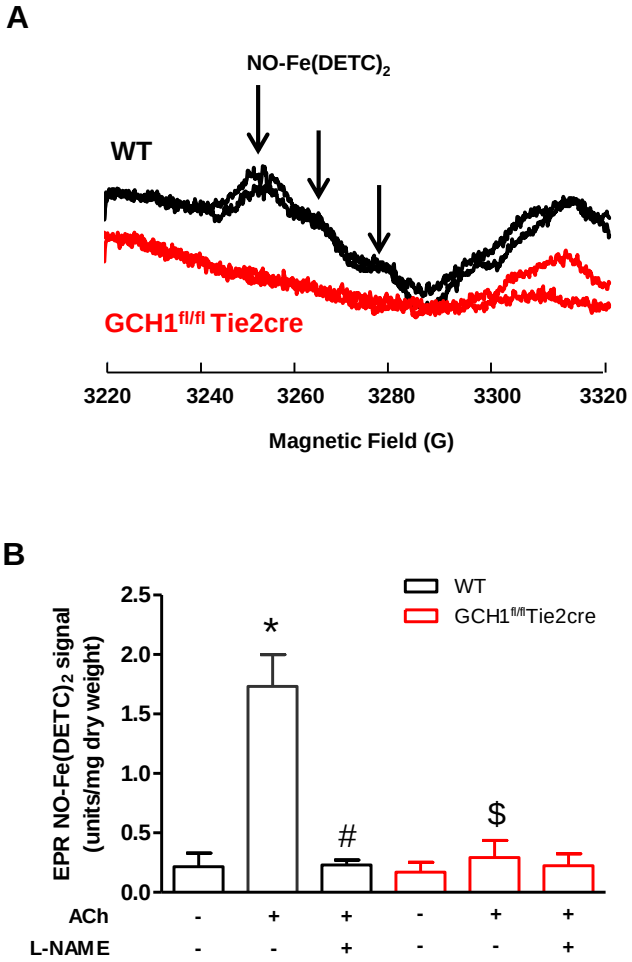


Figure 3.8. NO measurement by EPR

A) Representative EPR spectra of mouse aortas stimulated with 1 μM acetylcholine for 90 min at 37 °C with colloid $Fe(DETC)_2$ (*g* values approximately 2.04). The characteristic triplet peaks associated with $NO\text{-}Fe(DETC)_2$ signal are shown by the vertical arrows. **B)** Quantification of $NO\text{-}Fe(DETC)_2$ signal from *GCH1*$^{fl/fl}$Tie2cre and wild-type aortas with or without stimulated with 1 μM acetylcholine in the presence and absence of 1 mM L-NAME (**P*<0.01 comparing genotype, #*P*<0.01 comparing treatment; n=4-6 animals/group).

3.5 Discussion

In this chapter, I described and characterised a novel mouse model of endothelial cell-targeted *GCH1* deletion. The key findings were:

- Endothelial cell-targeted *GCH1* deletion using Tie2 promoter-Cre expression resulted in efficient *GCH1* excision in isolated primary endothelial cells and in endothelial cell-rich tissues such as lung, heart and aorta.
- Endothelial cell-targeted *GCH1* knockout mice had undetectable GTPCH protein expression in primary endothelial cells and markedly reduced aortic GTPCH.
- Knockout of *GCH1* resulted in a decrease in BH4 levels in primary endothelial cells and in endothelial cell-rich tissues such as lung, heart and aortas. Importantly, plasma BH4 levels were not altered in *GCH1* knockout mice, revealing a cell-autonomous requirement for endothelial GTPCH in de novo BH4 biosynthesis.
- Endothelial cell-specific BH4 deficiency led to eNOS uncoupling with increased superoxide production and loss of endothelial NO generation.

In this chapter, I have shown that endothelial cell-targeted *GCH1* deletion abolished GTPCH protein expression and de novo BH4 biosynthesis in primary endothelial cells. This leads to substantial reductions in GTPCH and BH4 in aortas, demonstrating that the majority of vascular BH4 is contributed by the endothelium, which was confirmed by removal of vascular endothelium that reduced BH4 levels in wild-type but not in $GCH1^{fl/fl}$Tie2cre aortas. Previously studies have shown that the endothelium is a major source of vascular biopterins in mouse aortas (Landmesser et al., 2003) and human vessels (Antoniades et al., 2007). Interestingly, there was no difference in plasma BH4 levels between wild-type and $GCH1^{fl/fl}$Tie2cre mice, suggesting for the first time that the vascular endothelium is not a significant source of circulating biopterins. This finding is consistent with previous studies

by this laboratory that endothelial cell-specific *GCH1* overexpression mice have comparable circulating biopterins to that of their wild-type littermates (Alp et al., 2003a).

Importantly, the maintenance of plasma BH4 levels in *GCH1*$^{fl/fl}$Tie2cre mice was not sufficient to rescue the loss of de novo BH4 biosynthesis in endothelial cells. This novel observation identifies a cell-autonomous requirement for de novo BH4 biosynthesis in the maintenance of endothelial cell BH4 levels *in vivo*. This finding suggests that physiological regulation of endothelial cell BH4 is not influenced by uptake from plasma, despite previous observations that pharmacological administration of supra-physiological dose of BH4 can augment BH4 levels in some tissues.

The physiological requirement for endothelial cell BH4 biosynthesis is reflected in the effect on eNOS function. It had previously been shown that BH4 bioavailability is a determinant of eNOS function and NO generation (Crabtree et al., 2009b; Tatham et al., 2009), and loss of BH4 by oxidation leads to eNOS uncoupling, increased superoxide production and vascular dysfunction in hypertension (Landmesser et al., 2003). However, the physiological requirement for endothelial cell BH4 in these settings remains unclear because loss of vascular BH4 could be a cause of endothelial dysfunction or could be the consequence of vascular disease. I have now shown that deficiency in endothelial cell BH4 is alone sufficient to cause eNOS uncoupling, even in the absence of vascular disease and in the presence of normal plasma BH4 levels.

The absolute dependence of endothelial NO production on endothelial cell BH4 availability was demonstrated by three complementary methods, each indicating highly deficient, or absence endothelial NO bioactivity in *GCH1*$^{fl/fl}$Tie2cre mice when compared to wild-type littermates. These include radiolabeled L-arginine to L-citrulline conversion using HPLC

detection of L-citrulline, nitrite/nitrate accumulation, and EPR detection of NO using $Fe(DETC)_2$ as spin trap.

Several lines of evidence have emerged to show that the intracellular BH4:BH2 ratio, rather than absolute concentrations of BH4, is the key determinant of eNOS uncoupling (Crabtree et al., 2008; Crabtree et al., 2009a). In this study, I have now shown that both BH4 levels and BH4:BH2 ratio were significantly reduced in endothelial cell-rich tissues: heart, lung and aortas from *GCH1*$^{fl/fl}$Tie2cre mice compared to wild-type controls.

Together, the results in this chapter indicate that endothelial cell-targeted *GCH1* deletion leads to endothelial cell BH4 deficiency, despite no significant change in plasma BH4, thus identifying a cell-autonomous requirement for endothelial cell *GCH1* and *de novo* BH4 biosynthesis. Endothelial cell-specific BH4 deficiency leads to eNOS uncoupling, with loss of NO bioactivity and increased superoxide production.

Having confirmed the biochemical phenotype of the *GCH1*$^{fl/fl}$Tie2cre mouse I can next determined the role of endothelial cell BH4 in vascular function.

Chapter 4:

Vascular Function in Endothelial Cell-Specific BH4 Deficient Mice

Chapter 4: Vascular Function in Endothelial Cell-Specific BH4 Deficient Mice

4.1 Introduction

I have shown previously in chapter 3 that:

- Endothelial cell-targeted *GCH1* deletion led to endothelial cell BH4 deficiency, despite no significant change in plasma BH4, thus identifying a cell-autonomous requirement for endothelial cell *GCH1* and de novo BH4 biosynthesis.
- Endothelial cell BH4 deficiency led to eNOS uncoupling, with loss of nitric oxide (NO) bioactivity and increased superoxide production in primary endothelial cell and aortas.

A large body of evidence suggests that reduced vascular BH4 bioavailability, an essential cofactor for eNOS function and NO generation, contributes to the pathogenesis of endothelial dysfunction and vascular disease states. For example, BH4 levels in vascular tissue from diabetic mice, apolipoprotein E knockout mice, hypercholesterolemic rabbits, and patients with diabetes mellitus, are significantly reduced and associated with reduced NO-mediated endothelial function (Bitar et al., 2005a; Heitzer et al., 2000b; Laursen et al., 2001; Spiekermann et al., 2003). Pharmacological supplementation with the BH4 precursor sepiapterin can improve endothelial function in various vascular disease states (Cosentino et al., 2001; Landmesser et al., 2003). Transgenic overexpression of *GCH1* and BH4 biosynthesis in mice is able to improve endothelial function in vascular disease states, such as DOCA-salt hypertension (Du et al., 2008), diabetes mellitus (Alp et al., 2003b) and atherosclerosis (Alp et al., 2004). Although these studies implicate reduced or augmented

BH4 in vascular disease pathogenesis, the physiological requirement for endothelial cell BH4 in regulation of eNOS-derived NO generation, or other eNOS-derived signalling mechanisms, mediating vascular function remains undetermined. To date, it is unknown whether deficiency in endothelial cell BH4 synthesis alone is sufficient to cause vascular dysfunction. To address these questions, I investigated the role of endothelial cell BH4 biosynthesis in vascular function under physiological conditions.

4.2 Hypothesis and aims

In this chapter I aimed to investigate the requirement for endothelial cell BH4 biosynthesis in normal vascular function, by examining the effect of endothelial cell BH4 deficiency on vascular reactivity in conduit and resistance arteries from endothelial cell-targeted *GCH1* knockout mice (*GCH1*$^{fl/fl}$Tie2cre mice).

The main aims of this chapter are:

- To investigate the physiological requirement for endothelial cell BH4 biosynthesis in normal vasomotor function in conduit and resistance arteries using a novel mouse model of endothelial cell BH4 deficiency.
- To determine the contribution of endothelium-derived vasodilators: NO versus prostacyclin versus endothelium-derived hyperpolarizing factor (EDHF), in modulating vasomotor function in conduit and resistance arteries of wild-type and *GCH1*$^{fl/fl}$Tie2cre mice.

I hypothesized that endothelial cell BH4 biosynthesis is required for eNOS function, eNOS-derived NO-ROS production and vascular function. Specifically:

- Deficiency in endothelial cell BH4 biosynthesis will lead to eNOS uncoupling, loss of eNOS-derived NO and increased superoxide/H_2O_2 mediated vasodilatation in conduit and resistance arteries of *GCH1*$^{fl/fl}$Tie2cre mice.
- Endothelial cell BH4 bioavailability is a key determinant of eNOS-derived vasodilators, NO versus ROS/H_2O_2 production, in conduit and resistance arteries.

4.3 Methods

Experimental methods used in this chapter are described in Chapter 2.

4.4 Results

4.4.1 Vascular function in aorta

4.4.1.1 Vascular function in GCH1$^{fl/fl}$Tie2cre aortas

To investigate the requirement for endothelial cell-specific BH4 synthesis in normal vascular function, isometric tension studies in isolated aortic rings from wild-type and *GCH1*$^{fl/fl}$Tie2cre mice were performed using a wire myograph as described in Section 2.8. The maximal vasoconstriction to 60 mM KCl (non-receptor mediated contraction) was comparable between wild-type (6.78±0.27 mN) and *GCH1*$^{fl/fl}$Tie2cre aortas (6.34±0.29 mN)(Figure 4.1 A). Receptor-mediated vasoconstriction to phenylephrine (PE), expressed as percentage contraction to potassium chloride (KCl), was significantly enhanced in *GCH1*$^{fl/fl}$Tie2cre aortas compared to wild-type controls (Figure 4.1 B). This difference was normalised in the presence of the non-selective nitric oxide synthase (NOS) inhibitor L-NAME (10 μM), indicating that the increased constrictor response in *GCH1*$^{fl/fl}$Tie2cre aortas is mediated by tonic eNOS-derived vasodilatation (Figure 4.1 B).

Receptor-mediated endothelium-dependent vasodilatation to acetylcholine was significantly impaired in *GCH1*$^{fl/fl}$Tie2cre aortas compared to wild-type aortas, although the absolute difference was modest (Figure 4.2 A). Endothelium-dependent vasodilatation in response to the protease-activated receptor 2 (PAR2) agonist, SLIGRL (Figure 4.2 B), was also significantly impaired in *GCH1*$^{fl/fl}$Tie2cre aortas, suggesting that the impaired vasodilatation was not due to specific alteration of receptor signalling in endothelial cells of

GCH1$^{fl/fl}$Tie2cre mice. Endothelium-dependent vasodilatation to acetylcholine in both wild-type and *GCH1*$^{fl/fl}$Tie2cre aortas was totally abolished in the presence of L-NAME, indicating that eNOS is the major source of vasodilators in mouse aortas (Figure 4.2 C). Endothelium-independent vasodilatation in response to the nitric oxide donor, sodium nitroprusside (SNP) was similar between the groups, suggesting no major alteration in vascular smooth muscle sensitivity in *GCH1*$^{fl/fl}$Tie2cre aortas (Figure 4.2 D). These findings suggest that deficiency in endothelial cell BH4 biosynthesis leads to loss of eNOS-derived NO-mediated vascular tone and thus impaired vascular function in *GCH1*$^{fl/fl}$Tie2cre aortas.

Figure 4.1

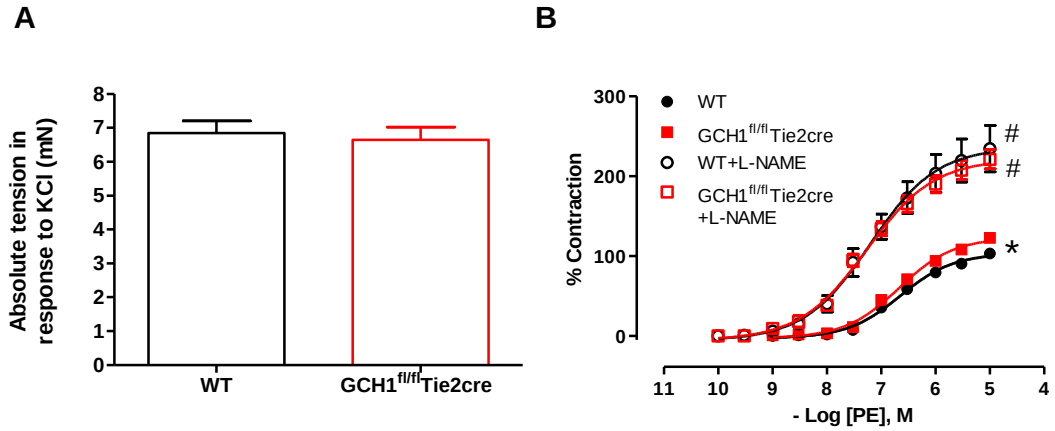


Figure 4.1. Vasoconstriction in wild-type and *GCH1*$^{fl/fl}$Tie2cre aortas.
Isometric tension studies in isolated aortic rings from wild-type (WT) and *GCH1*$^{fl/fl}$Tie2cre mice were determined using a wire myograph. A) Non-receptor-mediated vasoconstriction to KCL (60 mM) response was comparable between wild-type and *GCH1*$^{fl/fl}$Tie2cre aortas. B) Receptor-mediated vasoconstriction to α_1-adrenoceptor phenylephrine (PE), expressed as percentage contraction to KCl, was significantly enhanced in *GCH1*$^{fl/fl}$Tie2cre aortas compared to wild-type aortas, which normalised in the presence of nitric oxide synthase inhibitor, L-NAME (100 μM). Data are expressed as mean ± SEM. (**P<0.05* comparing genotype*; # P<0.001* comparing treatment, n= 16 animals per group).

Figure 4.2

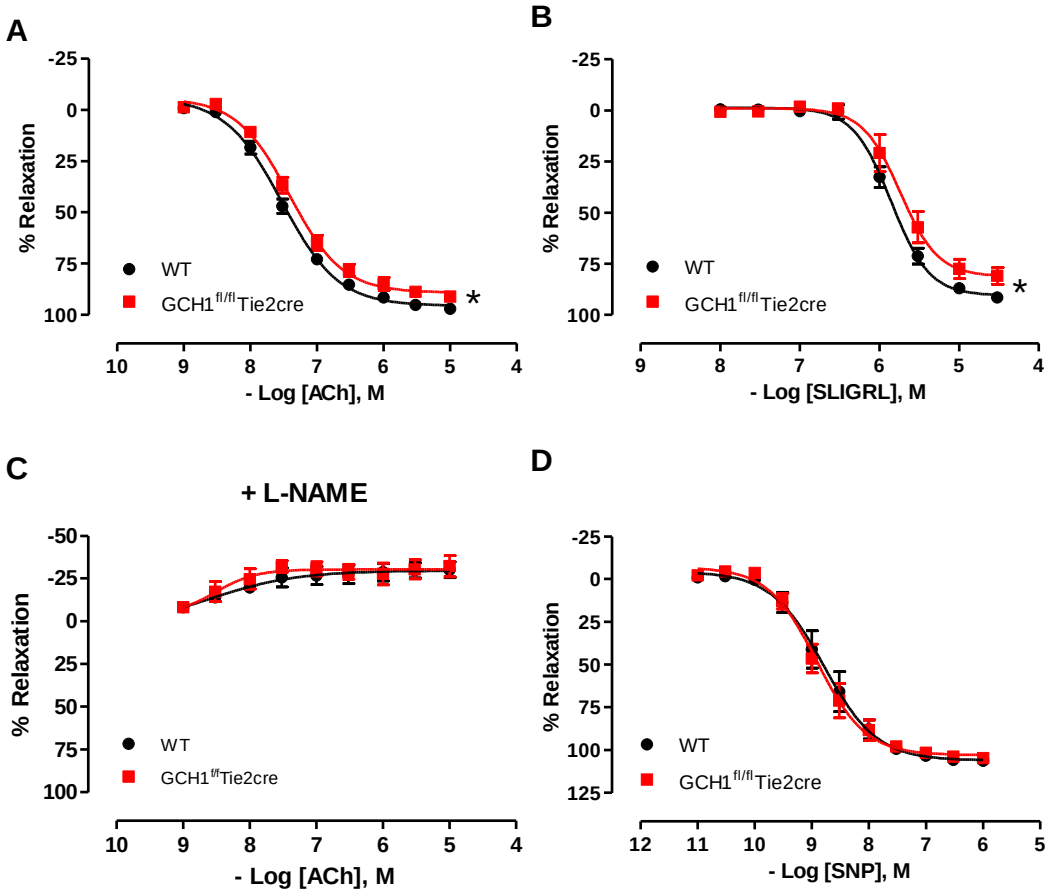


Figure 4.2. Endothelium-dependent vasodilatation in wild-type and *GCH1*$^{fl/fl}$Tie2cre aortas.

Receptor-mediated endothelium-dependent vasodilatations in response to **A)** acetylcholine (ACh) and **B)** SLIGRL were significantly impaired in aortas from *GCH1*$^{fl/fl}$Tie2cre mice compared to wild-type (WT) littermate controls. **C)** In the present of non-selective nitric oxide synthase inhibitor L-NAME (100 μM), acetylcholine-induced vasodilatation was totally abolished in aortas from both genotypes. **D)** Endothelium-independent vasodilatations to nitric oxide donor, sodium nitroprusside (SNP) were comparable between the genotypes. Data are expressed as mean ± SEM. (*$P<0.05$; n= 9 to 10 animals per group).

4.4.1.2 Effect of indomethacin on vascular function in aortas

To examine whether prostaglandin-derived products (eg. prostacyclin) play a role in modulating vasodilatations in mouse aorta, isometric tension studies in isolated aortic rings from wild-type and *GCH1*$^{fl/fl}$Tie2cre aortas were determined with or without the non-selective cyclooxygenase inhibitor, indomethacin (10 μM for 20 minutes). Concentration response curves to vasoconstrictor and vasodilator substances before and after indomethacin treatment were determined and compared.

Ex vivo incubation of aortic rings from wild-type aortas in the presence and absence of indomethacin showed no significant effect on the maximal vasoconstriction to 60 mM KCl, vasoconstriction to phenylephrine, endothelium-dependent vasodilatation to acetylcholine either with or without L-NAME, and endothelium-independent vasodilatation to SNP (Figure 4.3 A, B, C, and D). Indomethacin had no significant effect on resting tension in wild-type aortas (data not shown). This finding suggests that prostaglandin-derived products do not play a significant role in modulating vascular tone and vasodilatation in wild-type aortas.

It has been reported that when vascular eNOS-derived NO generation is compromised, prostaglandin-derived product is up-regulated and compensated endothelium-dependent vasodilatation. To determine whether prostaglandin-derived products play a role in modulating vasodilatation in endothelial cell BH4 deficient aortas, vasomotor function was determined in the presence or absence of indomethacin. The maximal vasoconstriction to KCl, vasoconstriction to phenylephrine, endothelium-dependent vasodilatation to acetylcholine, and endothelium-independent vasodilatations to SNP were comparable between indomethacin-treated *GCH1*$^{fl/fl}$Tie2cre aortas and control untreated aortas (Figure 4.3 E, F, G and H). These findings suggest that deficiency in endothelial cell BH4 biosynthesis is not associated with an upregulation of prostaglandin-derived product

mediated vasodilatation in *GCH1*$^{fl/fl}$Tie2cre aortas, and as a result of this studying all the consequent experiments were performed in the presence of indomethacin to inhibit vascular prostaglandin synthesis.

Figure 4.3

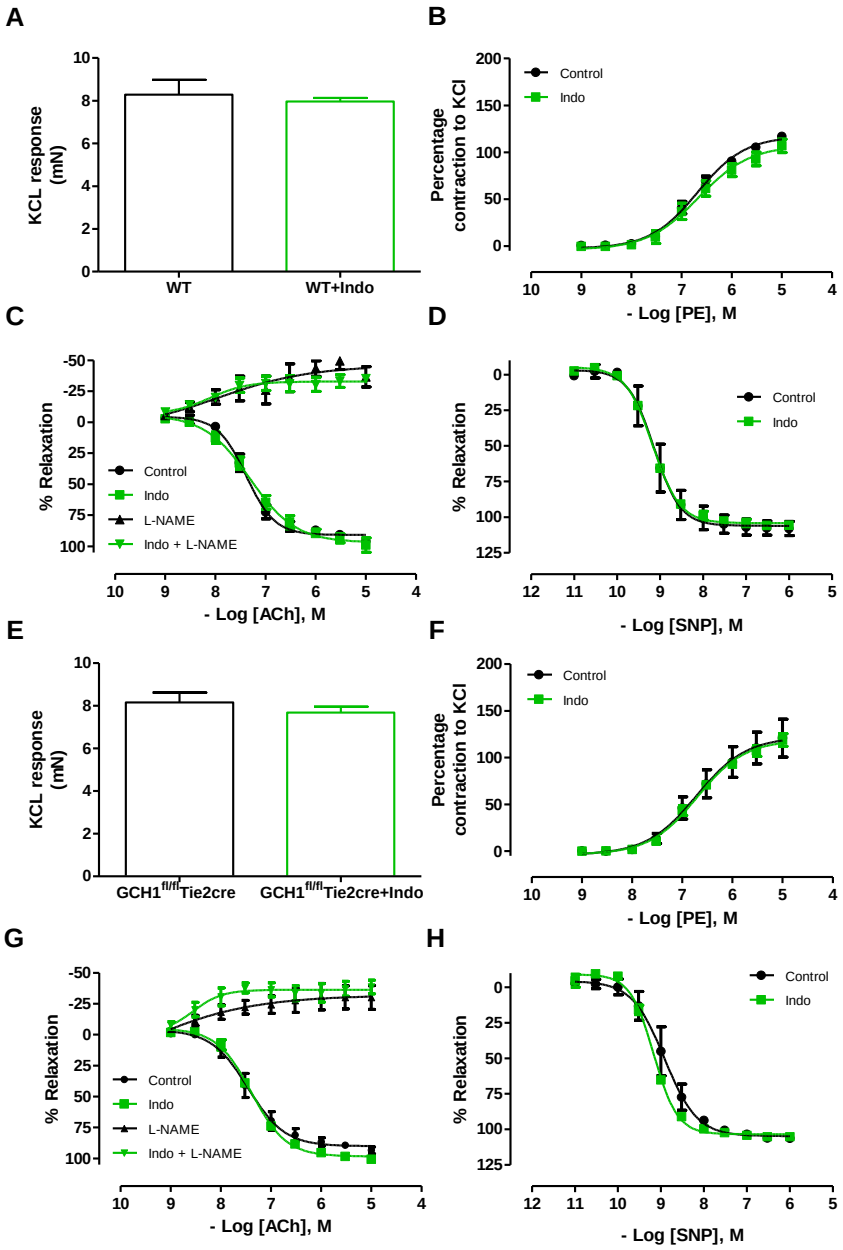


Figure 4.3. Effect of indomethacin on vascular function in aortas.

Isometric tension studies in isolated aortic rings from wild-type (WT) and *GCH1*$^{fl/fl}$Tie2cre mice were determined in the presence or absence of indomethacin (10 µM) using a wire myograph. Indomethacin (Indo) treatment had no significant effect on the maximal contraction to KCl, vasoconstriction to phenylephrine (PE), acetylcholine (ACh)-induced vasodilatation with or without L-NAME, and endothelium-independent vasodilatations to sodium nitroprusside (SNP) in either wild-type aortas **(A-D)** or **(E-H)** *GCH1*$^{fl/fl}$Tie2cre aortas respectively. Data are expressed as mean ± SEM. (n= 4 to 6 animals per group).

4.4.1.3 Hydrogen peroxide-mediated vasodilatation in GCH1$^{fl/fl}$Tie2cre aortas

I next investigated the mechanisms underlying the vasodilator responses in *GCH1$^{fl/fl}$*Tie2cre aortas, given the loss of NO generation and increased ROS production. In the presence of the H_2O_2 scavenger, catalase-polyethylene glycol (PEG-catalase; 400 unit/ml), endothelial-dependent vasodilatations to acetylcholine were significantly inhibited in *GCH1$^{fl/fl}$*Tie2cre aortas but not in wild-type aortas (Figure 4.4 A and B). PEG-catalase treatment also significantly attenuated endothelium-dependent vasodilatation in response to the PAR2 agonist, SLIGRL in *GCH1$^{fl/fl}$*Tie2cre aortas but remained unchanged in wild-type aortas (Figure 4.4 C and D). Incubation of PEG-catalase at 1,000 unit/ml did not further inhibit vasodilatation in *GCH1$^{fl/fl}$*Tie2cre aortas, suggesting that the concentration of PEG-catalase at 400 unit/ml was sufficient to scavenge hydrogen peroxide generation in this preparation (Figure 4.4 E). PEG-catalase treatment had no significant effect on the basal vascular tone, vasoconstriction to phenylephrine, and endothelium-independent vasodilatation to SNP of either wild-type (Figure 4.5 A and C) or *GCH1$^{fl/fl}$*Tie2cre aortas (Figure 4.5 B, and D). In the presence of L-NAME, vasodilatation to acetylcholine was abolished in both groups, and further addition of PEG-catalase did not alter the response in either group, suggesting that eNOS is a predominant source of H_2O_2 (Figure 4.6 A and B).

Figure 4.4

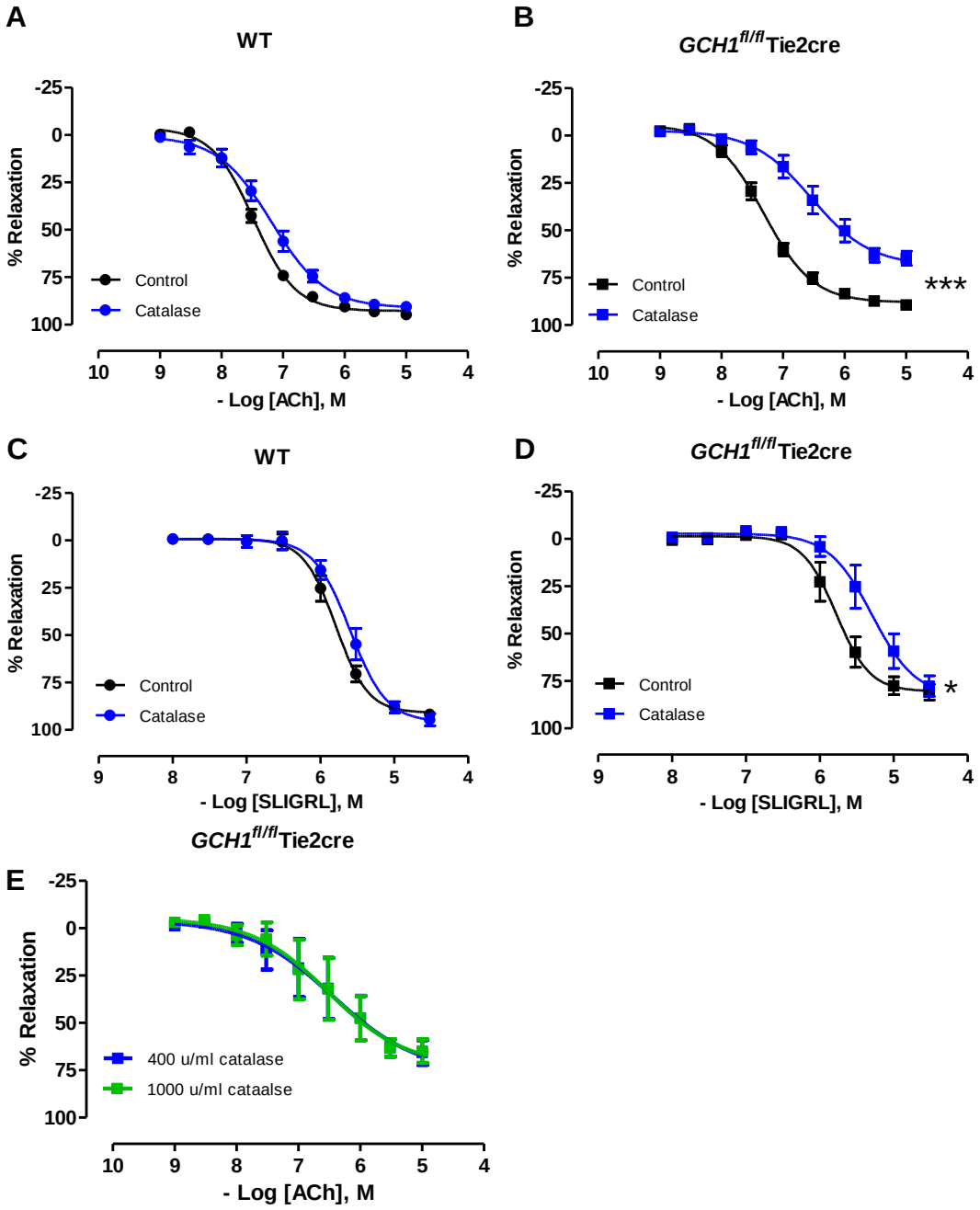


Figure 4.4. H_2O_2-mediated vasodilatation in *GCH1*$^{fl/fl}$Tie2cre aortas

Aortic rings were pre-incubated with or without PEG-catalase (400 unit/ml) for 20 minutes before concentration response curves of acetylcholine (ACh) or SLIGRL were determined. **A and C)** PEG-catalase had no inhibitory effect on vasodilatation in response to ACh and SLIGRL in wild-type (WT) aortas. **B and D)** PEG-catalase significantly attenuated endothelium-dependent vasodilatations to ACh and SLIGRL in *GCH1*$^{fl/fl}$Tie2cre aortas. **E)** Higher concentration of PEG-catalase at 1,000 unit/ml did not further inhibit ACh-induced vasodilatation in *GCH1*$^{fl/fl}$Tie2cre aortas. Data are expressed as mean ± SEM. (**P<0.05; *** P<0.001;* n= 6 to 9 animals per group).

Figure 4.5

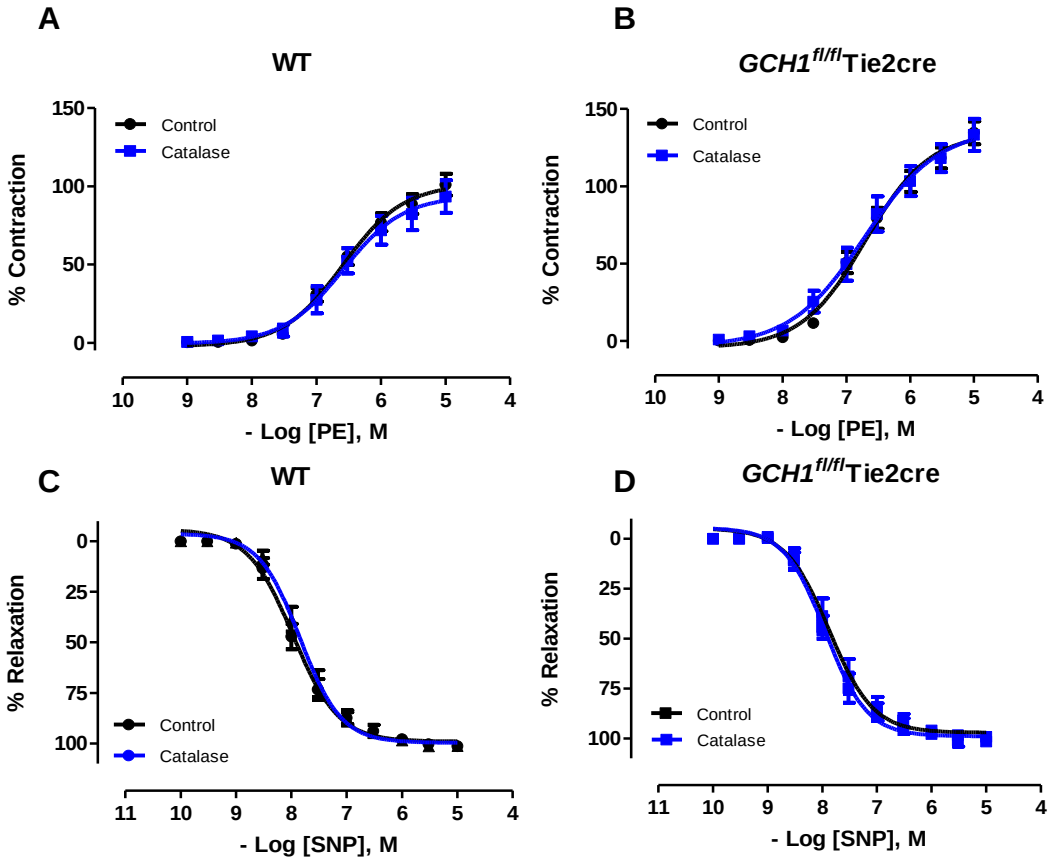


Figure 4.5. Effect of catalase on vascular function in aortas

Aortic rings were pre-incubated with or without PEG-catalase (400 unit/ml) for 20 minutes before concentration response curves of acetylcholine were determined. PEG-catalase treatment had no significant effect on either vasoconstriction to phenylephrine (PE) **(A and B)**, expressed as percentage contraction to KCl or **C and D)** endothelium-independent vasodilatations to sodium nitroprusside (SNP) in aortas of both wild-type (WT) and *GCH1*$^{fl/fl}$Tie2cre mice. Data are expressed as mean ± SEM. (n= 6 to 9 animals per group).

Figure 4.6

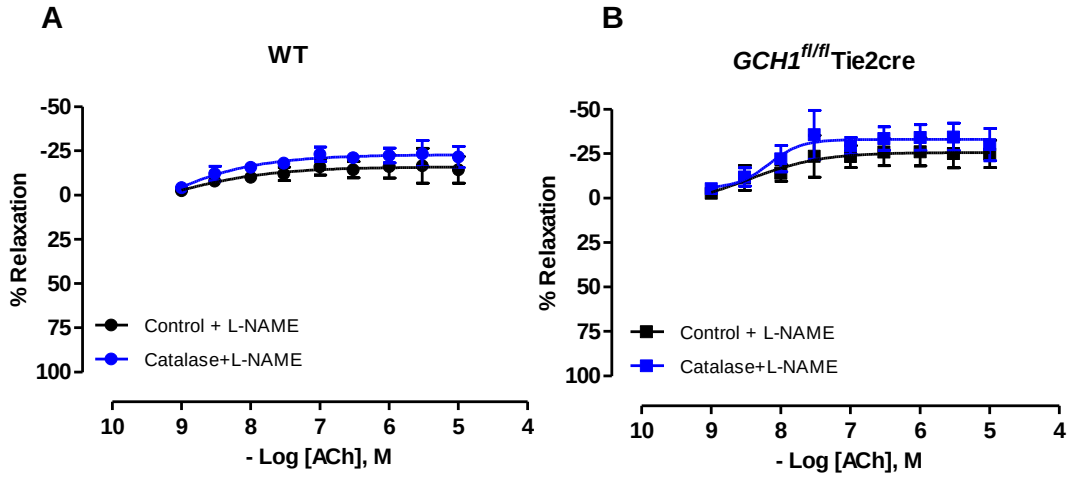


Figure 4.6. eNOS-derived H_2O_2 mediated vasodilatation in *GCH1*$^{fl/fl}$Tie2cre aortas

Aortic rings were pre-incubated with either L-NAME (100 μM) alone or L-NAME with PEG-catalase (400 unit/ml) for 20 minutes before concentration response curves of acetylcholine (ACh) were determined. **A and B)** ACh-induced vasodilatation was totally abolished in the presence of L-NAME of both genotypes, and PEG-catalase treatment has no inhibitory effect on vasodilatation of both wild-type (WT) and *GCH1*$^{fl/fl}$Tie2cre aortas. Data are expressed as mean ± SEM. (n= 6 to 9 animals per group).

4.4.1.4 Mechanism of H_2O_2-mediated vasodilatation in GCH1$^{fl/fl}$Tie2cre aortas

We next investigated the mechanism underlying eNOS-derived H_2O_2-mediated vasodilatation in *GCH1$^{fl/fl}$*Tie2cre aortas. A combination of potassium channels blockers, apamin (small-conductance Ca^{2+} activated K^+ channel blocker) and charybdotoxin (non-selective intermediate and large-conductance Ca^{2+} activated K^+ channels blocker) was used to test K^+ channel-mediated EDHF responses (Busse et al., 2002; Ray et al., 2011). Endothelium-dependent vasodilatation to acetylcholine in *GCH1$^{fl/fl}$*Tie2cre aortas in the presence of apamin and charybdotoxin was similar to wild-type controls (Figure 4.7 A) but was significantly inhibited in the presence of apamin and charybdotoxin with PEG-catalase (Figure 4.7 B). This difference was normalised in the presence of the soluble guanylate cyclase (sGC) inhibitor, 1H-(1,2,4)oxadiazolo[4,3-a]quinoxalin-1-one, ODQ (Figure 4.8 A and B), indicating the involvement of a sGC-dependent pathway. To test the specificity of this finding, vasodilatation to acetylcholine was assessed in the presence of 30 mM extracellular K^+, in order to inhibit the activity of K^+ channels and thus EDHF responses (Ray et al 2011). In the presence of 30 mM extracellular K^+, vasodilatation to acetylcholine in *GCH1$^{fl/fl}$*Tie2cre aortas was similar to wild-type aortas (Figure 4.7 C), but remained significantly inhibited by PEG-catalase (Figure 4.7 D). In the presence of ODQ, acetylcholine-induced vasodilatation in *GCH1$^{fl/fl}$*Tie2cre aortas was inhibited to a similar extent as that observed in the presence of ODQ with PEG-catalase (Figure 4.8 C and D). These findings indicate that eNOS-derived, H_2O_2-mediated vasodilatation in *GCH1$^{fl/fl}$*Tie2cre aortas occurs through a sGC-dependent signalling pathway and not through the activation of EDHF-sensitive components.

Figure 4.7

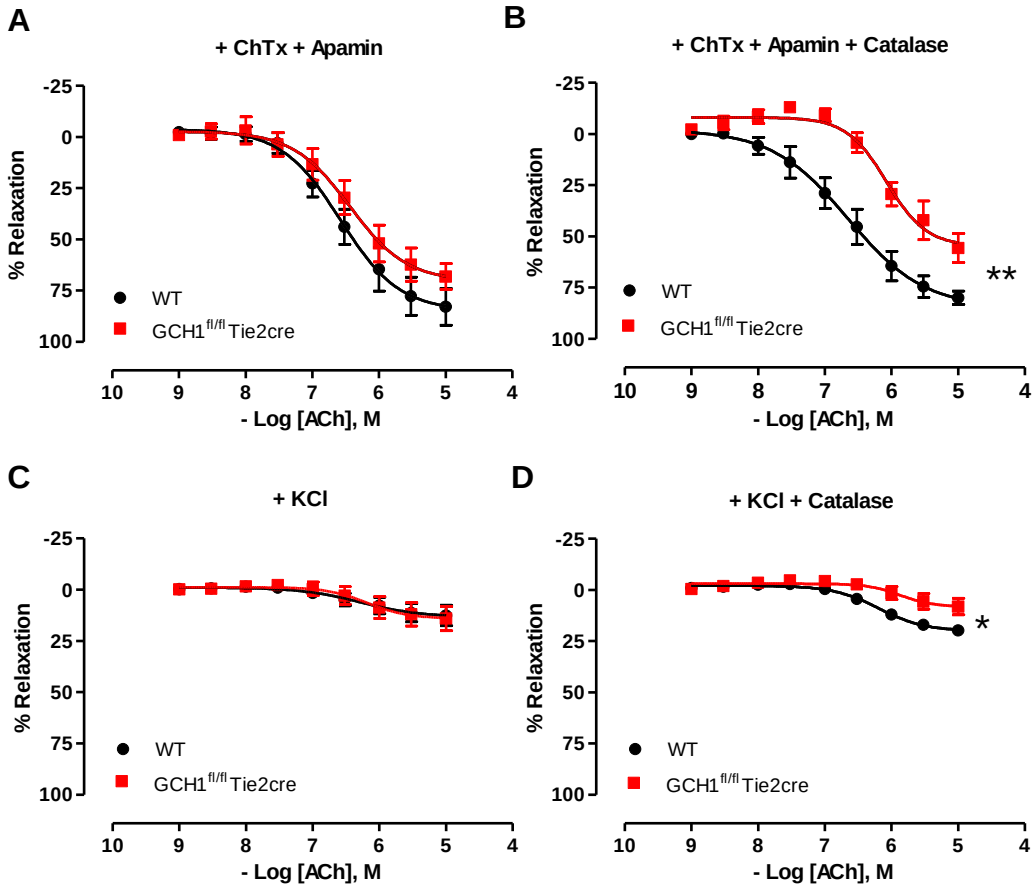


Figure 4.7. Mechanism of H_2O_2 mediated vasodilatation in *GCH1*$^{fl/fl}$Tie2cre aortas.

Endothelium-dependent vasodilatation to acetylcholine (ACh) was assessed in the presence of endothelium-derived hyperpolarizing factor (EDHF) blockers in aortas from wild-type (WT) and *GCH1*$^{fl/fl}$Tie2cre mice. **A and B)** Endothelium-dependent vasodilatation in the presence of charybdotoxin (ChTx; 100 nM) and apamin (50 nM) with or without PEG-catalase (400 unit/ml). **C and D)** Endothelium-dependent vasodilatation to ACh in the presence of 30 mmol/L extracellular potassium chloride (KCl) with or without PEG-catalase. Data are expressed as mean ± SEM. (*$P<0.05$; ** $P<0.01$; n= 6 to 9 animals per group).

Figure 4.8

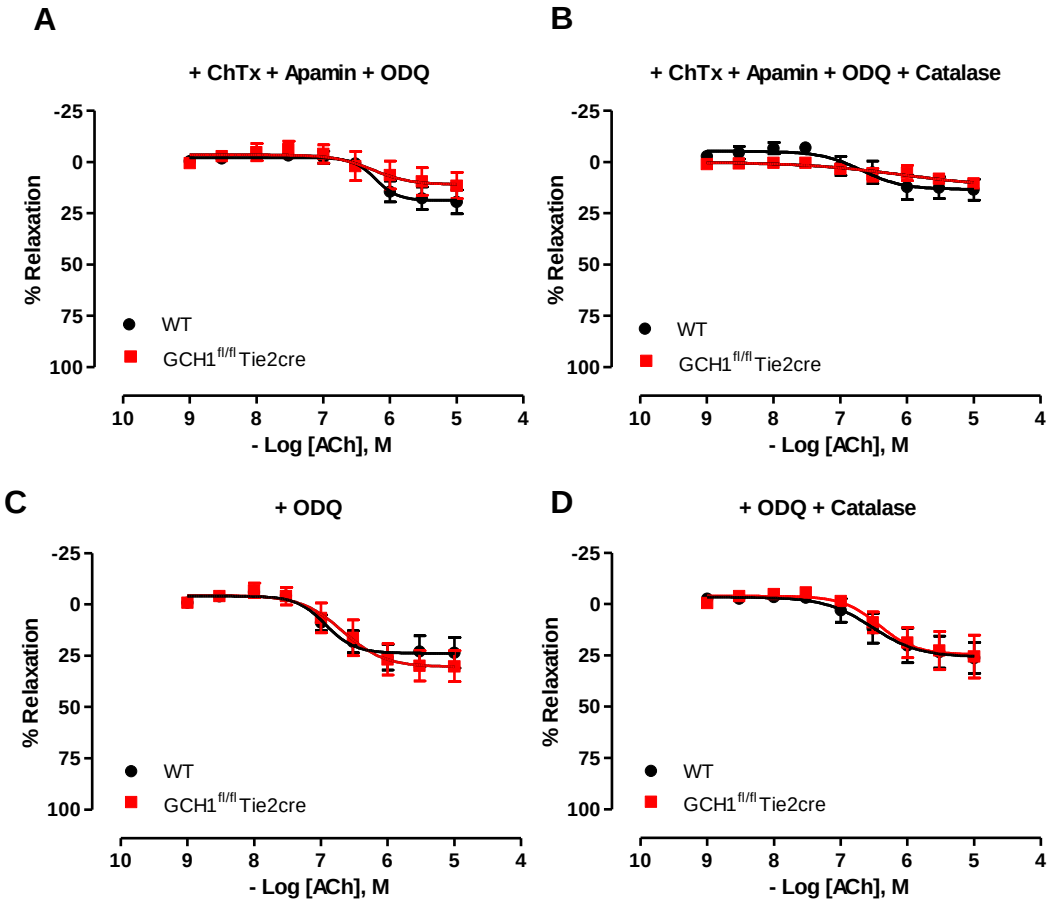


Figure 4.8. Mechanism of H_2O_2 mediated vasodilatation in *GCH1*$^{fl/fl}$Tie2cre aortas.

A and B) Endothelium-dependent vasodilatation in the presence of endothelium-derived hyperpolarizing factor (EDHF) blockers: charybdotoxin (ChTx; 100 nM), apamin (50 nM) and soluble guanylate cyclase inhibitor ODQ (500 nM) with or without PEG-catalase (400 unit/ml). **C and D)** Endothelium-dependent vasodilatation to ACh in the presence of ODQ alone or ODQ with PEG-catalase. Data are expressed as mean ± SEM. (n= 6 to 9 animals per group).

4.4.1.5 Increased eNOS-derived H_2O_2 in GCH1$^{fl/fl}$Tie2cre aortas

We next measured the aortic H_2O_2 production in freshly isolated aortas from wild-type and *GCH1*$^{fl/fl}$Tie2cre mice. Aortic H_2O_2 production was determined by the Amplex red assay as described in Section 2.7.3. The vascular H_2O_2 production was significantly increased in acetylcholine-stimulated aortas (1 μM) from *GCH1*$^{fl/fl}$Tie2cre mice compared to wild-type mice. In the presence of nitric oxide synthase inhibitor, L-NAME (100 μM), increased vascular H_2O_2 production was significantly inhibited in *GCH1*$^{fl/fl}$Tie2cre aortas but was unchanged in wild-type aortas (Figure 4.9 A). This suggests that eNOS is the major source of H_2O_2 in *GCH1*$^{fl/fl}$Tie2cre aortas.

Figure 4.9

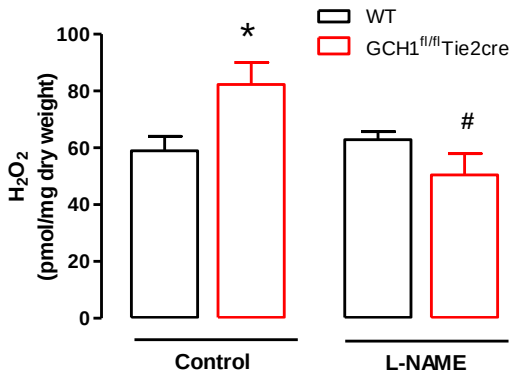


Figure 4.9. H_2O_2 measurement in aortas

H_2O_2 production in aortas from *GCH1*$^{fl/fl}$Tie2cre mice and wild-type (WT) mice was determined by Amplex red assay in the presence with 1 μM acetylcholine with or without treatment of 1 mM L-NAME (**P*<0.05 comparing genotype; #*P*<0.05 comparing between treatment; n=4 to 6 animals per group). Data are expressed as mean ± SEM.

4.4.1.6 Mechanism of exogenous H_2O_2-mediated vasodilatation in mouse aortas

To determine the mechanism underlying H_2O_2-mediated vasodilatation in mouse aortas, concentration response curves of exogenous H_2O_2 in isolated aortic rings from wild-type and *GCH1*$^{fl/fl}$Tie2cre mice were compared. Responses to exogenous H_2O_2-induced vasodilatation in wild-type and *GCH1*$^{fl/fl}$Tie2cre aortas were comparable, but were inhibited in the presence of soluble guanylate cyclase (sGC) inhibitor ODQ (Figure 4.10 A and 4.11 A) and abolished in the presence of ODQ with PEG-catalase or PEG-catalase alone (Figure 4.10 B and D). The combination of apamin and charybdotoxin (EDHF blockers) had no significant effect on H_2O_2 induced vasodilatation in both wild-type and *GCH1*$^{fl/fl}$Tie2cre mice (Figure 4.10 C and 4.11 B). Indeed, this finding is consistent with previous reports by Burgoyne et al (Burgoyne et al., 2012) and suggests that exogenous H_2O_2 induced vasodilatation in mouse aortas occurs through a sGC-dependent signalling pathway and not through the activation of EDHF-sensitive components.

Figure 4.10

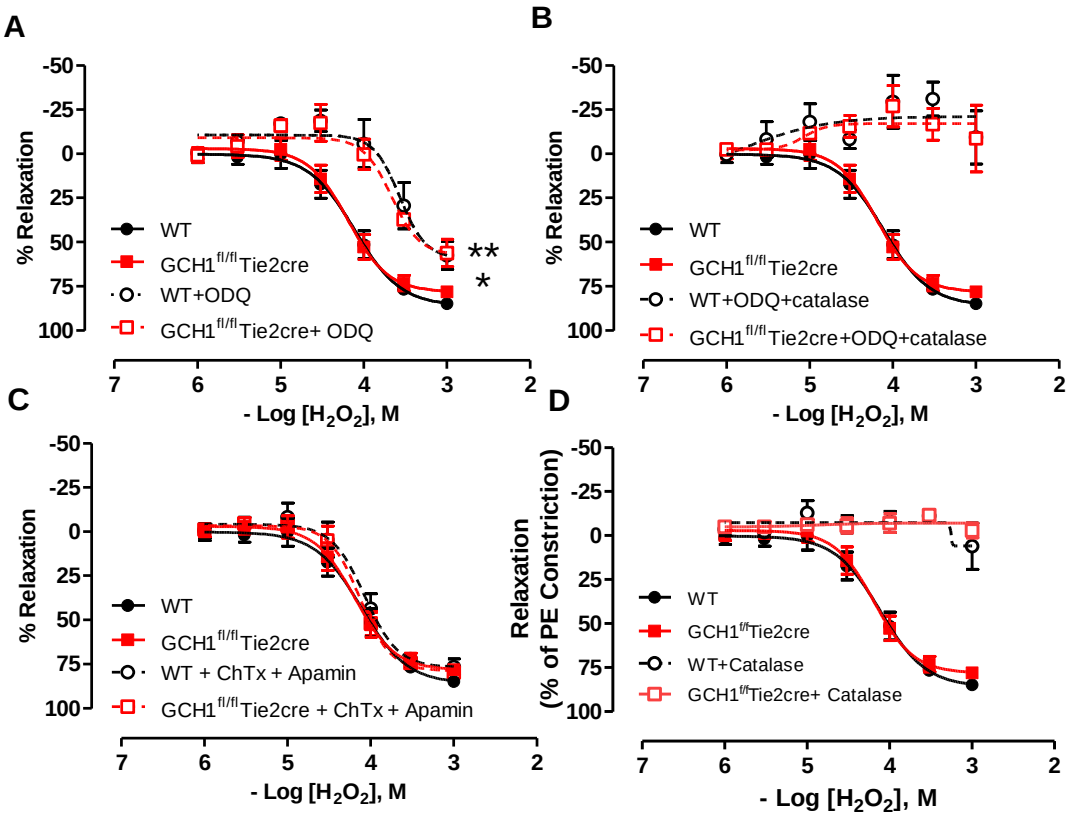


Figure 4.10. Mechanism of exogenous H_2O_2 mediated vasodilatation in aortas.

Isometric tension studies in isolated aortic rings from wild-type and *GCH1*$^{fl/fl}$Tie2cre mice were determined using a wire myograph. **A)** Exogenous H_2O_2-induced vasodilatation in wild-type (WT) and *GCH1*$^{fl/fl}$Tie2cre aortas in the presence of ODQ alone or **B)** ODQ with PEG-catalase (400 unit/ml) or **C)** charybdotoxin (ChTx) with apamin or **D)** PEG-catalase alone. Data are expressed as mean ± SEM. (*$P<0.05$; ** $P<0.01$; n= 4 to 6 animals per group).

Figure 4.11

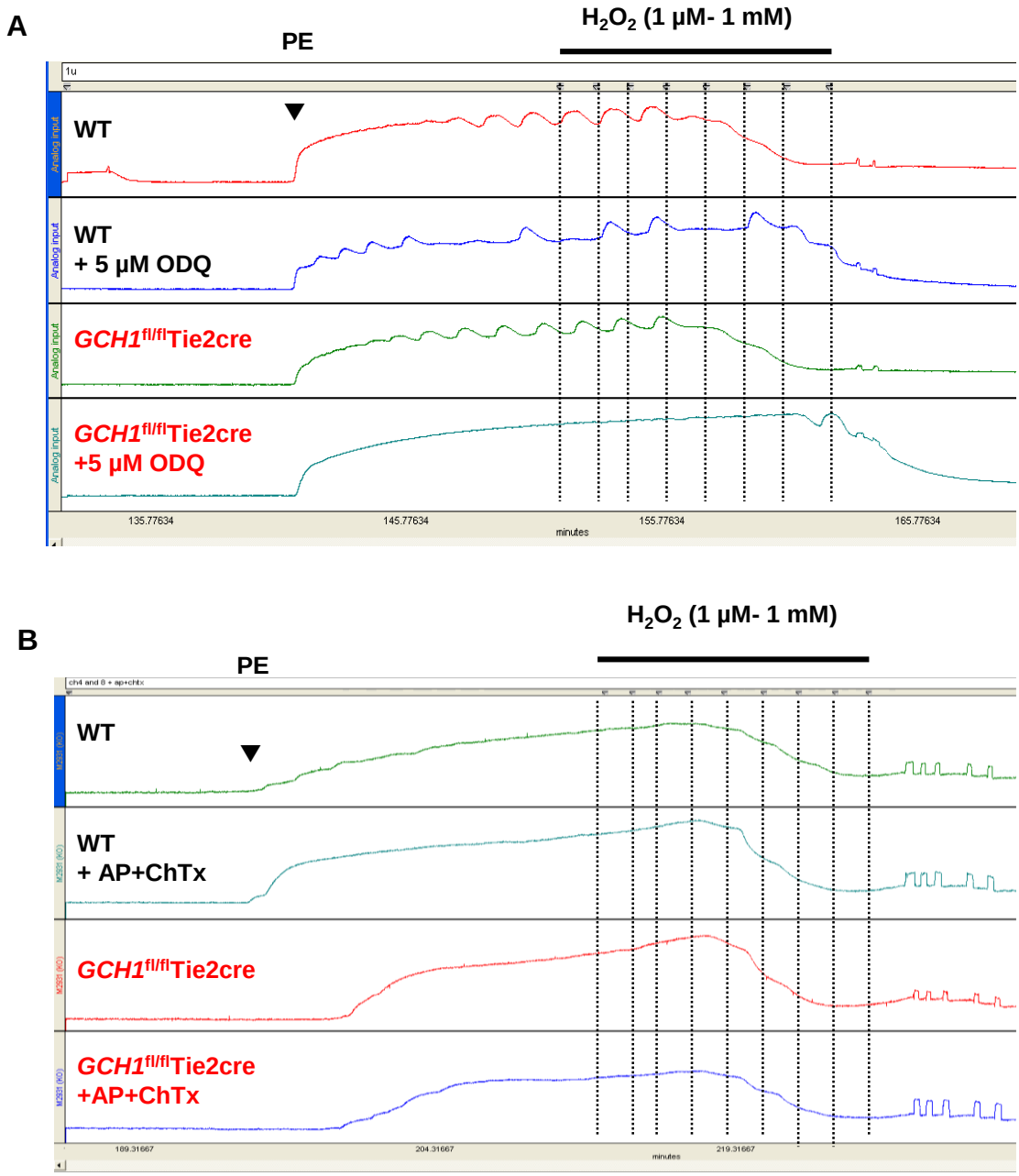


Figure 4.11. Mechanism of exogenous H_2O_2 mediated vasodilatation in mouse aortas.

Original traces demonstrating concentration-dependent vasodilatation evoked by exogenous H_2O_2 in aortic rings preconstricted with phenylephrine (PE) from wild-type (WT) and *GCH1*$^{fl/fl}$Tie2cre aortas. H_2O_2-induced vasodilatation in the presence of **A)** ODQ (5 mM) or **B)** Charybdotoxin (ChTx) and apamin (AP).

4.4.1.7 Ex vivo incubation of sepiapterin on vascular function

To confirm that these effects on vascular function are caused by the deficiency in BH4 I rescued BH4 levels using sepiapterin, which augments BH4 levels via the salvage pathway, independent of *de novo* BH4 biosynthesis by GTPCH. Isometric tension studies of isolated aortic rings from wild-type and *GCH1*$^{fl/fl}$Tie2cre mice were determined using myograph as described in Section 2.8. Concentration response curves to acetylcholine in isolated aortic rings were determined in the presence or absence of PEG-catalase (400 U/ml). Following PEG-catalase treatment, endothelium-dependent vasodilatations were determined in the presence of sepiapterin (10 μM for 20 min).

As observed in Section 4.4.1.3, PEG-catalase significantly inhibited endothelium-dependent vasodilatations in *GCH1*$^{fl/fl}$Tie2cre aortas but had no effect in wild-type aortas (Figure 4.12 A, B, and 4.13 A and B). In the presence of the BH4 analogue sepiapterin, PEG-catalase treatment had no inhibitory effect in endothelium-dependent vasodilatations in either *GCH1*$^{fl/fl}$Tie2cre (Figure 4.12 A and B, Figure 4.13 C) or wild-type aortas. *Ex vivo* incubation of sepiapterin alone did not alter endothelial-dependent vasodilatations of either wild-type or *GCH1*$^{fl/fl}$Tie2cre aortas (Figure 4.12 C and D). These findings suggest that *ex vivo* incubation of sepiapterin restored endothelial vasomotor responses and abolished the effect of PEG-catalase on vasodilatation in *GCH1*$^{fl/fl}$Tie2cre aortas.

Figure 4.12

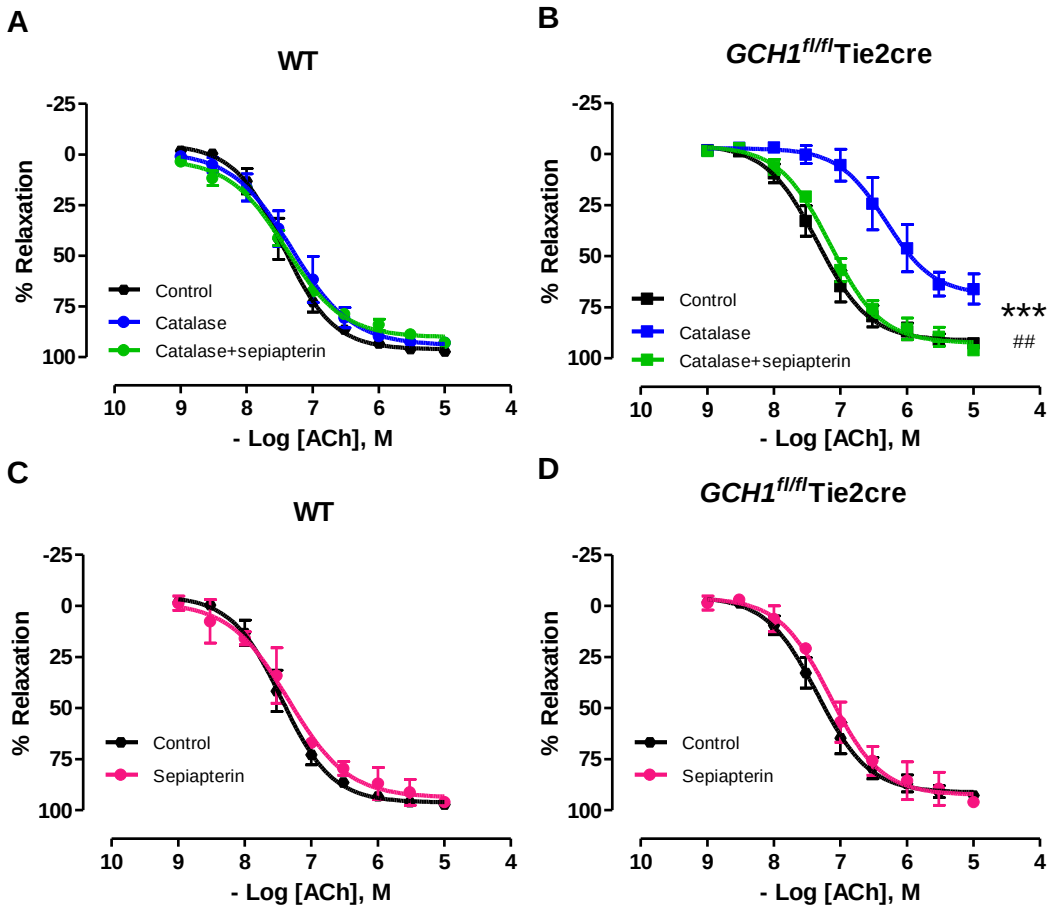


Figure 4.12. Effect of BH4 analogue on vascular function in aortas.

Aortic rings from wild-type (WT) and *GCH1*$^{fl/fl}$Tie2cre aortas were pre-incubated with either PEG-catalase alone, or PEG-catalase with sepiapterin (10 uM) or sepaipterin alone for 30 minutes. **A)** PEG-catalase or PEG-catalase with sepiapterin had no significant effect on vasodilatation in response to acetylcholine (ACh) in wild-type aortas. **B)** PEG-catalase treatment significantly attenuated ACh-induced vasodilatation but not in the presence of PEG-catalase with sepiapterin. **C and D)** Sepiapterin treatment had no significant effect on ACh-induced vasodilatation in both wild-type and *GCH1*$^{fl/fl}$Tie2cre aortas. Data are expressed as mean ± SEM. (*** *P<0.001* comparing control group; ## *P<0.01*, comparing catalase-treated group; n= 4 to 6 animals per group).

Figure 4.13

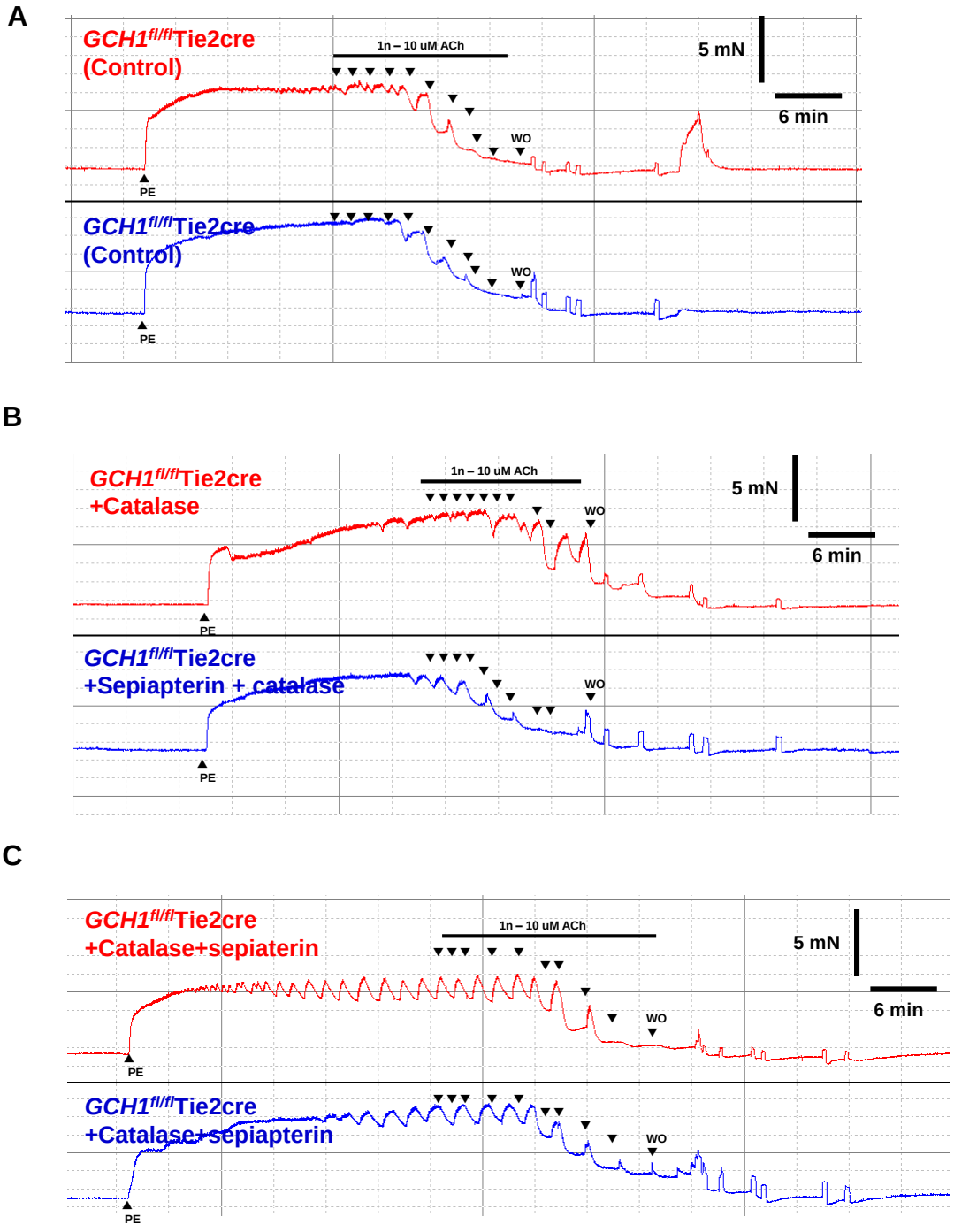


Figure 4.13. Effect of sepiapterin on vascular function in aortas.

A) Original traces demonstrating concentration-dependent vasodilatation in *GCH1*$^{fl/fl}$Tie2cre aortas evoked by acetylcholine (ACh) in aortic rings preconstricted with phenylephrine (PE) or **B)** in the presence of PEG-catalase (400 U/ml) or PEG-catalase with sepiapterin (10 µM), or **C)** PEG-catalase with sepiapterin.

4.4.1.8 Protein expression in GCH1$^{fl/fl}$Tie2cre aortas

Given the enhanced production of H_2O_2 by *GCH1$^{fl/fl}$*Tie2cre aortas, I next investigated whether deficiency in endothelial cell BH4 biosynthesis leads to an alteration in eNOS and antioxidant protein expression. Aortas from wild-type mice and *GCH1$^{fl/fl}$*Tie2cre mice were harvested and protein expression of eNOS, and other antioxidants were determined by immunoblotting as described in Section 2.9. Western blot analysis showed that the level of eNOS protein in *GCH1$^{fl/fl}$*Tie2cre aortas was significantly increased (~2-fold) compared to wild-type controls (Figure 4.14 A; $P<0.001$). The protein levels of antioxidant enzymes Cu/ZnSoD, MnSOD, ecSOD and catalase were similar between the wild-type and *GCH1$^{fl/fl}$*Tie2cre aortas (Figure 4.14 B, C, D and E). Furthermore, the level of phosphorylation of eNOS at Thr495, relative to the total eNOS protein content, was comparable between the groups (Figure 4.15 B). Phosphorylation of eNOS at Ser1177 was significantly reduced in *GCH1$^{fl/fl}$*Tie2cre aortas when normalised to the total eNOS protein content (Figure 4.15 A). The levels of Ser239 phospho-VASP in isolated aortas stimulated with acetylcholine, as determined by immunoblotting, were measured as a readout of PKG activity. There was no significant difference in Ser239 phospho-VASP to total VASP protein between wild-type and *GCH1$^{fl/fl}$*Tie2cre aortas, suggesting that H_2O_2-derived from eNOS uncoupling in *GCH1$^{fl/fl}$*Tie2cre aortas mediated vasodilatation by increasing phosphorylation of VASP at Ser239 (Figure 4.15 C).

Figure 4.14

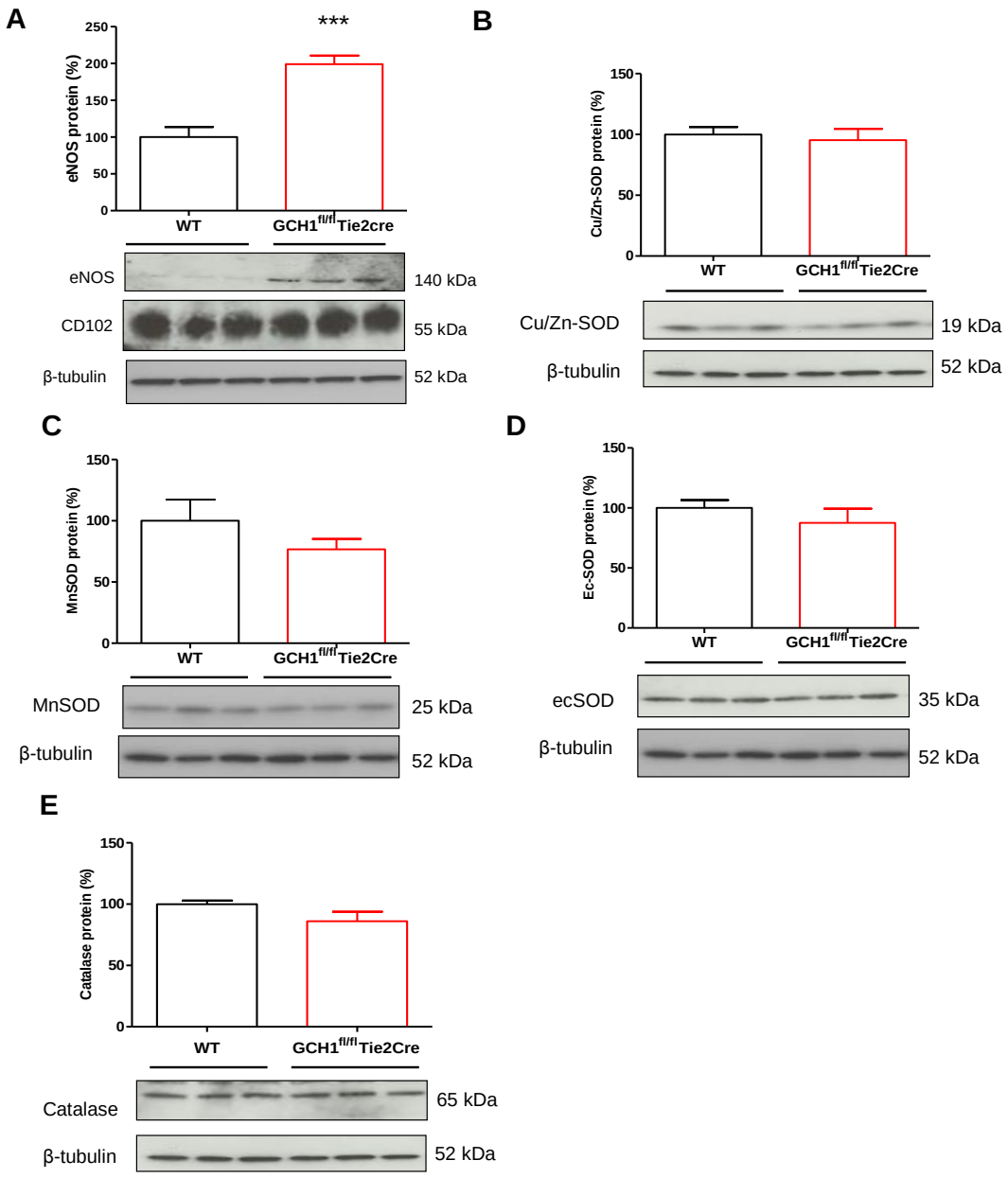


Figure 4.14. eNOS and antioxidant proteins in aortas

A) Representative immunoblots with corresponding quantitative data above showing eNOS protein in wild-type (WT) and *GCH1*$^{fl/fl}$Tie2cre aortas. Corresponding immunoblots for CD102 (endothelial cell marker) and beta-tubulin below. **B-E)** Representative immunoblots for Cu/ZnSoD, MnSOD, ecSOD, and catalase protein expression in wild-type (WT) and *GCH1*$^{fl/fl}$Tie2cre aortas (n=6 per group), with quantitative data, measured as percentage band density, above, and corresponding beta-tubulin immunoblots, below. Antioxidant protein expression were comparable between wild-type and *GCH1*$^{fl/fl}$Tie2cre aortas. Data are expressed as mean ± SEM. (n=6 per group).

Figure 4.15

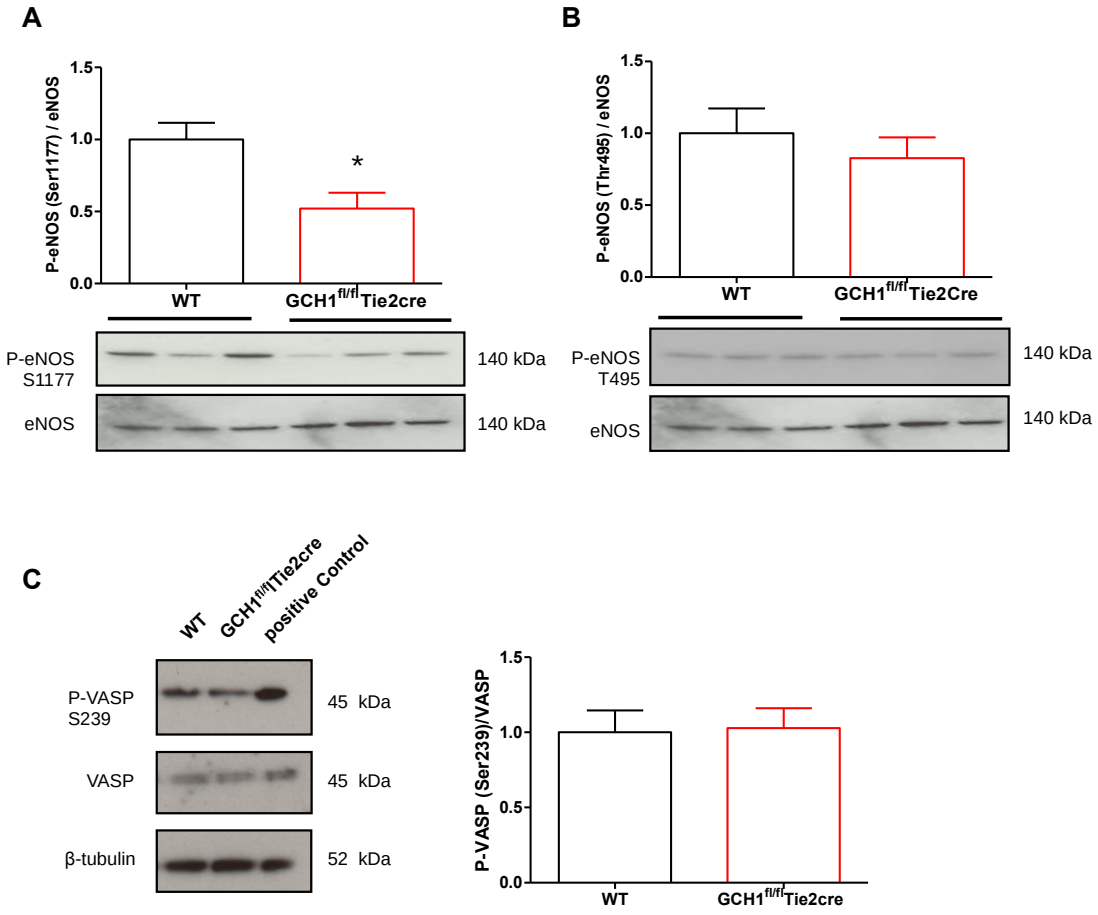


Figure 4.15. eNOS at Ser1177, eNOS T495 and VASP protein in aortas

Representative immunoblots showing **A)** Phosphorylation of eNOS at Ser1177 (P-eNOS S1177) to total eNOS protein in wild-type (WT) and *GCH1*$^{fl/fl}$Tie2cre aortas, **B)** Phosphorylation of eNOS at Thr495 (P-eNOS T495) to total eNOS protein (**P*<0.05; n=6 per group). **C)** Phosphorylation of vasodilator-stimulated phosphoprotein at serine 239 (P-VASP S239) and total VASP in freshly isolated aortas pre-incubated with acetylcholine (ACh, 0.5 µM) for 15 min at 37°C from WT and *GCH1*$^{fl/fl}$Tie2cre mice (left panel). Quantitative data (right panel), measured as band density of P-VASP to total VASP (n=6 per group). β-tubulin was used as loading control. Aortas stimulated with 1 µM sodium nitroprusside were used as positive control for pSer239-VASP. Data are expressed as mean ± SEM.

4.4.2 Vascular function in mesenteric arteries

4.4.2.1 GTPCH and eNOS expression in GCH1$^{fl/fl}$Tie2cre mesenteric arteries

After establishing that the *GCH1* floxed allele was efficiently excised in endothelial cells from *GCH1*$^{fl/fl}$Tie2cre mice, I next determined the levels of GTPCH protein expression in mesenteric arteries by western blotting as described in Section 2.9. Western blot analysis showed that expression of GTPCH protein was barely detectable in mesenteric arteries from *GCH1*$^{fl/fl}$Tie2cre mice, whereas GTPCH was readily detected in wild-type mesenteric arteries. The endothelial cell-surface marker CD102 and loading control β-tubulin were present equally in mesenteric arteries from both wild-type and *GCH1*$^{fl/fl}$Tie2cre mice, suggesting endothelial cell-targeted *GCH1* deletion led to a marked reduction in GTPCH protein expression in mesenteric arteries of *GCH1*$^{fl/fl}$Tie2cre mice (Figure 4.16 A). eNOS protein expression was comparable between wild-type and *GCH1*$^{fl/fl}$Tie2cre mesenteric arteries and endothelial cell-surface marker CD102 and loading control β-tubulin were present equally in mesenteric arteries from both genotypes (Figure 4.16 B), suggesting no major alteration in eNOS protein expression in *GCH1*$^{fl/fl}$Tie2cre mesenteric arteries.

Figure 4.16

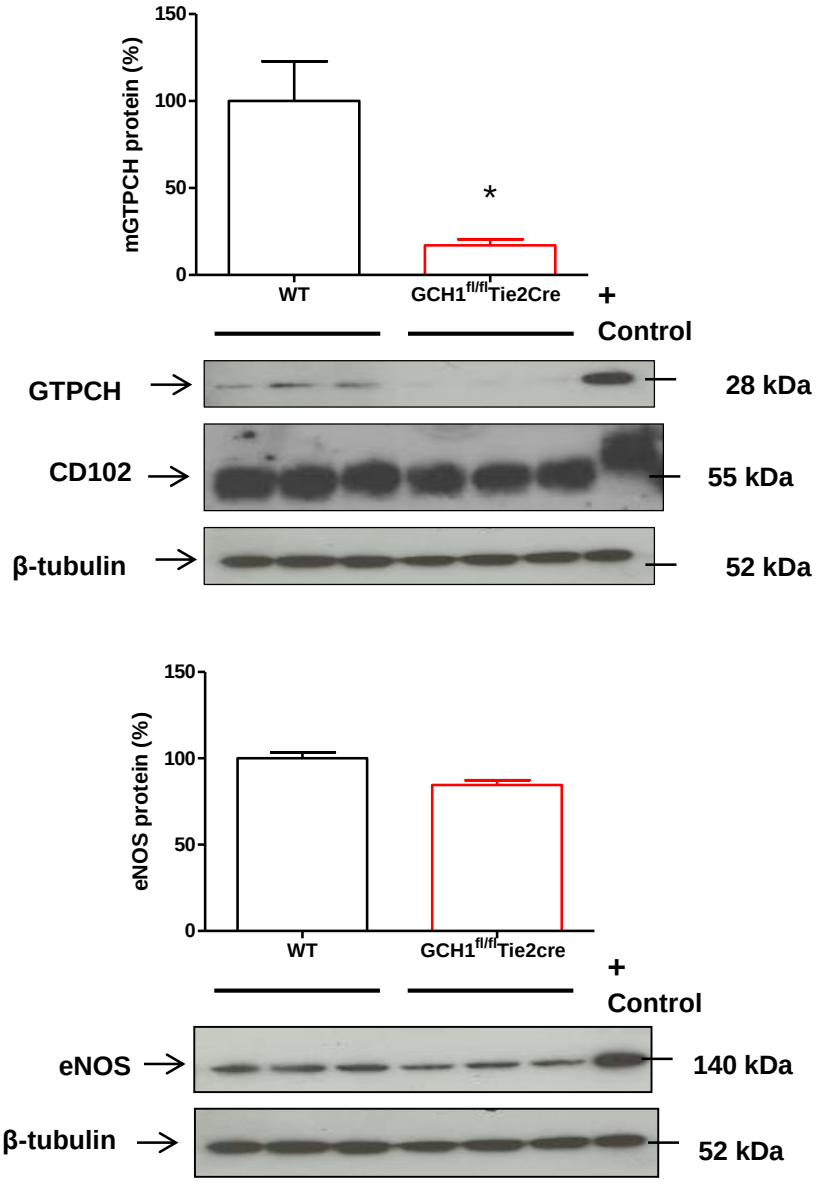


Figure 4.16. GTPCH and eNOS protein in mesenteric arteries

A) Representative immunoblots showing GTPCH protein in wild-type (WT) and *GCH1*$^{fl/fl}$Tie2cre mesenteric arteries (n=6 per group), with quantitative data, measured as percentage band density, above, and corresponding CD102 (endothelial cell marker) and beta-tubulin immunoblots, below (n=6 animals per group). **B)** Representative immunoblots with corresponding quantitative data above showing eNOS protein in wild-type and *GCH1*$^{fl/fl}$Tie2cre mesenteric arteries. Corresponding immunoblots for beta-tubulin below. Endothelial cell line (sEND cells) was used as positive control for GTPCH and eNOS protein. Data are expressed as mean ± SEM. (*P<0.001; n=6 animals per group).

4.4.2.2 Vascular function in mesenteric artery in GCH1$^{fl/fl}$Tie2cre mice

I next investigated the requirement for endothelial cell BH4 biosynthesis in vasomotor function in resistance mesenteric arteries. Mesenteric arcades were harvested as described in Section 2.8. Isometric tension studies in isolated 2nd order mesenteric arteries were performed using a wire myograph as described in Section 2.8.

Diameter sizes of 2nd order mesenteric arteries, as determined by length-tension relationship, were comparable between wild-type (179.3 ± 12.9 μm) and *GCH1$^{fl/fl}$*Tie2cre mice (178.5 ± 9.4 μm)(Figure 4.17 A). No difference was detected between the maximal contraction to KCl of wild-type (1.98 ± 0.23 mN/mm) and *GCH1$^{fl/fl}$*Tie2cre mice (1.72 ± 0.11 mN/mm)(Figure 4.17 B). Receptor-mediated vasoconstrictions to thromboxane A_2 receptor agonist, U46619, were significantly enhanced in *GCH1$^{fl/fl}$*Tie2cre mesenteric arteries compared to wild-type controls (Figure 4.17 C). This difference was normalised in the presence of the nitric oxide synthase inhibitor, L-NAME (Figure 4.17 E), suggesting loss of basal eNOS-derived vasodilators, probably NO, mediated vascular tone in mesenteric arteries of *GCH1$^{fl/fl}$*Tie2cre mice. Receptor-mediated vasoconstrictions to phenylephrine (PE) were also markedly enhanced in *GCH1$^{fl/fl}$*Tie2cre mesenteric arteries compared to wild-type controls (Figure 4.17 D), suggesting that the enhanced vasoconstriction was not due to specific alteration of receptor signalling in endothelial cells of *GCH1$^{fl/fl}$*Tie2cre mice.

Receptor-mediated endothelium-dependent vasodilatations to acetylcholine (Figure 4.18 A and C) and SLIGRL (Figure 4.18 B and D) were both significantly impaired in mesenteric resistance arteries from *GCH1$^{fl/fl}$*Tie2cre mice, suggesting that the impaired vasodilatations were not due to specific alteration of receptor signalling in endothelial cells of *GCH1$^{fl/fl}$*Tie2cre mice. In the presence of L-NAME, endothelium-dependent vasodilatations to both acetylcholine and SLIGRL were almost completely inhibited, suggesting eNOS is the major source of endothelium-derived vasodilators in mesenteric arteries (Figure 4.18 A

and B). Endothelium-independent vasodilatations to the nitric oxide donor, sodium nitruprusside (SNP) were comparable between genotypes (Figure 4.17 F), indicating the impairment of vasodilation in *GCH1*$^{fl/fl}$Tie2cre mesenteric arteries was not due to the alteration of vascular smooth muscle sensitivity. Taken together, deficiency in endothelial cell BH4 biosynthesis leads to a loss of eNOS-derived NO-mediated vascular tone and impaired vasodilatation in *GCH1*$^{fl/fl}$Tie2cre mesenteric arteries. These findings suggest that endothelial cell BH4 plays a pivotal role in maintaining vascular homeostasis in mouse mesenteric arteries.

Figure 4.17

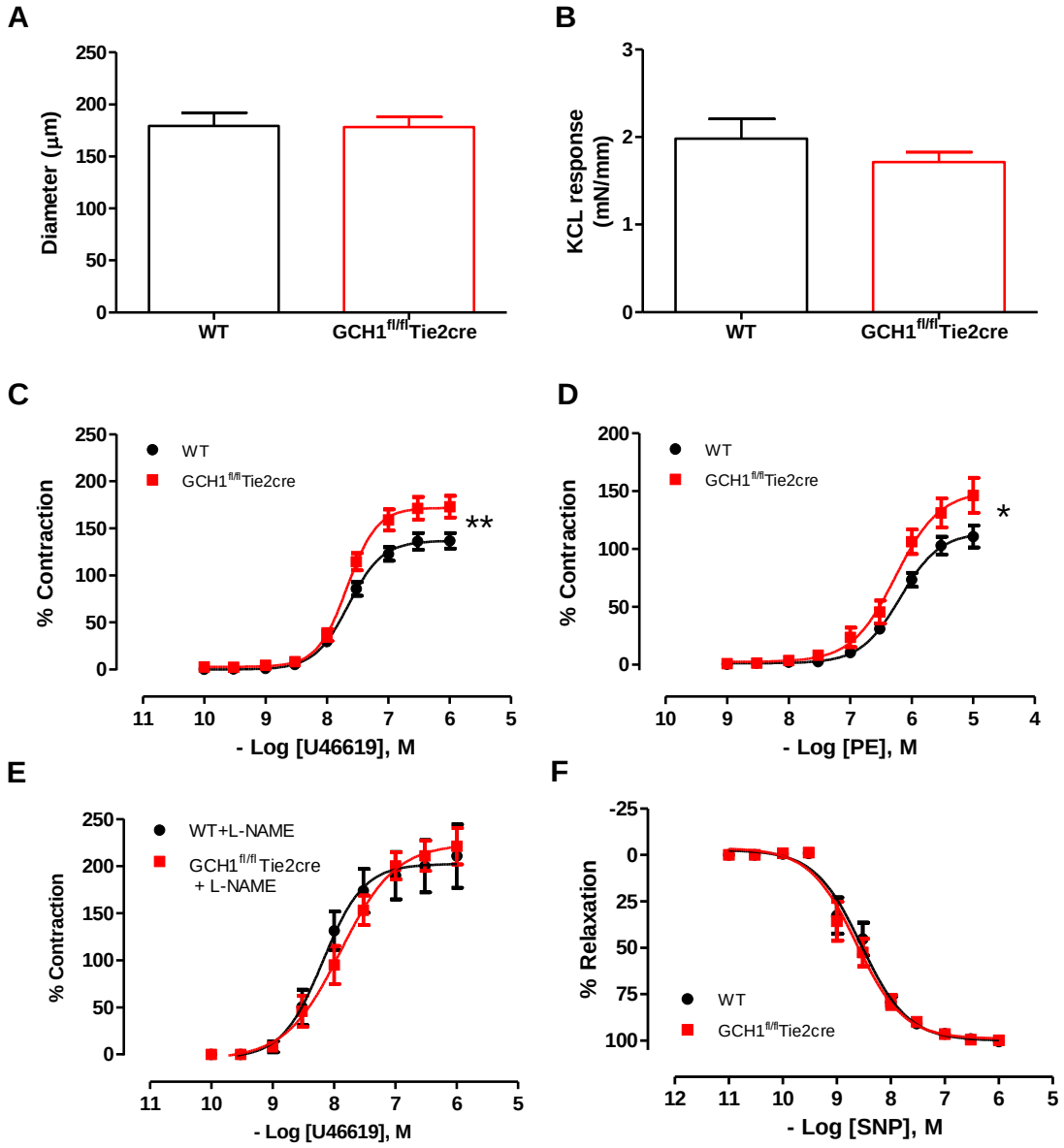


Figure 4.17. Vasomotor function in mesenteric arteries

Isometric tension studies in isolated 2nd order mesenteric arteries from wild-type (WT) and *GCH1*$^{fl/fl}$Tie2cre mice were determined using a wire myograph. **A)** Diameter of mesenteric arteries. **B)** Maximal contraction to 45 mM KCl. **C)** Receptor-mediated vasoconstriction to thromboxane A2 agonist, U46619 and **D)** phenylephrine (PE). **E)** Vasoconstriction to U46619 in the presence of nitric oxide synthase inhibitor, L-NAME (100 µM). F) Endothelium-independent vasodilatation to sodium nitroprusside (SNP). Data are expressed as mean ± SEM. (**P*<0.05, ***P*<0.01; n=14 to18 animals per group).

Figure 4.18

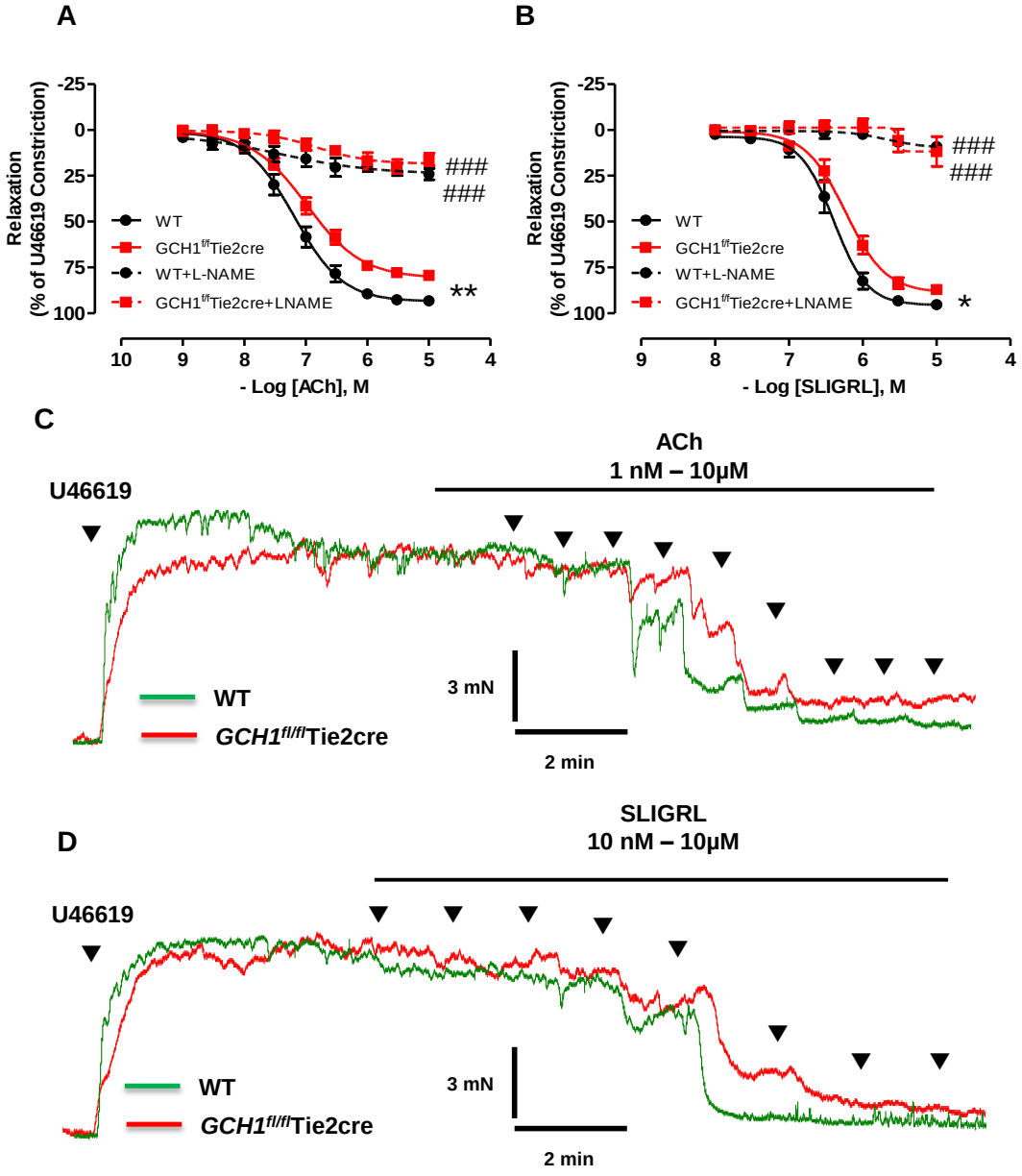


Figure 4.18. Endothelium-dependent vasodilatation in mesenteric arteries.

A) Receptor mediated endothelium-dependent vasodilatation to acetylcholine (ACh) and **B)** to PAR2 agonist, SLIGRL either in the presence or absence of nitric oxide synthase inhibitor, L-NAME (100 µM). **C and D)** Original traces demonstrating concentration-dependent vasodilatation evoked by ACh or SLIGRL respectively. Data are expressed as mean ± SEM. (**P*<0.05, ***P*<0.01; n=14 to18 animals per group).

4.4.2.3 Contribution of vasodilators in mouse mesenteric arteries

The vascular endothelium plays a critical role in maintaining vascular homeostasis by synthesizing and releasing several relaxing factors, such as nitric oxide, prostacyclin and endothelium-derived hyperpolarizing factor (EDHF). However, the precise of contribution of these vasodilators in mouse mesenteric arteries is unclear. To determine the contribution of endothelium-derived vasodilators prostacyclin, nitric oxide and EDHF, isometric tension studies was performed in isolated mesenteric resistance arteries. The contribution of prostacyclin, NO and EDHF were determined by the inhibitory effect of indomethacin (10 μM), L-NAME (100 μM), and EDHF blockers: apamin and charybdotoxin, respectively.

In mesenteric arteries of wild-type mice, endothelium-dependent vasodilatations in response to both acetylcholine and SLIGRL were unaltered by indomethacin but significantly inhibited by indomethacin and L-NAME, and totally abolished by indomethacin, L-NAME combined with apamin and charybdotoxin (Figure 4.19 A and 4.20 A). These data suggest that eNOS-derived vasodilators and EDHF play an important role in modulating vascular function in mouse mesenteric arteries whereas prostaglandin-derived products do not. In mesenteric arteries of *GCH1*$^{fl/fl}$Tie2cre mice, endothelium-dependent vasodilatations in response to both acetylcholine and SLIGRL were significantly inhibited by indomethacin, and markedly attenuated by indomethacin and L-NAME, and totally abolished by indomethacin and L-NAME combined with apamin and charybdotoxin (Figure 4.19 B and 4.20 B). This indicates that a prostaglandin-derived vasodilator, probably prostacyclin, eNOS-derived vasodilators and EDHF all play key roles in maintaining vascular homeostasis in *GCH1*$^{fl/fl}$Tie2cre mesenteric resistance arteries.

Figure 4.19

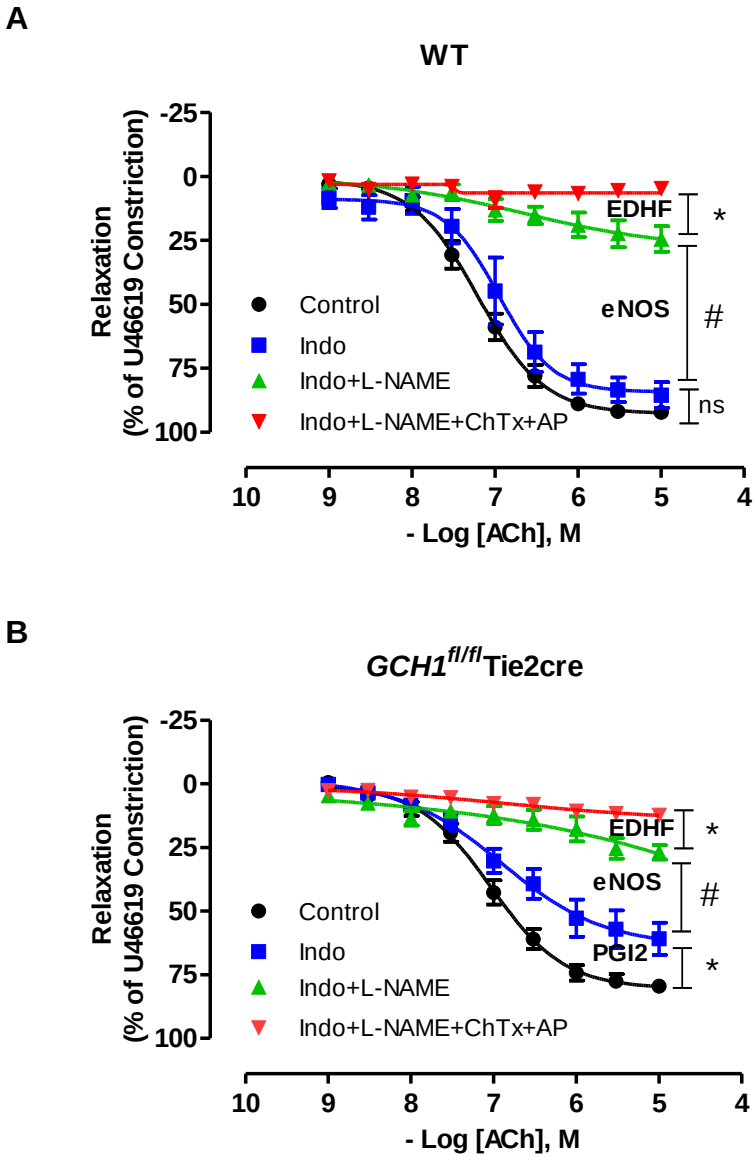


Figure 4.19. Contribution of prostacyclin, eNOS-derived vasodilators, and EDHF in mouse mesenteric arteries.

Isometric tension studies of 2nd order mesenteric arteries from **A)** wild-type (WT) and **B)** *GCH1*$^{fl/fl}$Tie2cre mice were examined using a wire myograph. Endothelium-dependent vasodilatations to acetylcholine (ACh) were determined in the presence of cyclooxygenase inhibitor, indomethacin (10 μM) alone, or indomethacin with nitric oxide synthase inhibitor, L-NAME (100 μM), or indomethacin, L-NAME with EDHF blockers (apamin and charybdotoxin). Data are expressed as mean ± SEM. (**P*<0.05, #*P*<0.001; n=14 to18 animals per group).

Figure 4.20

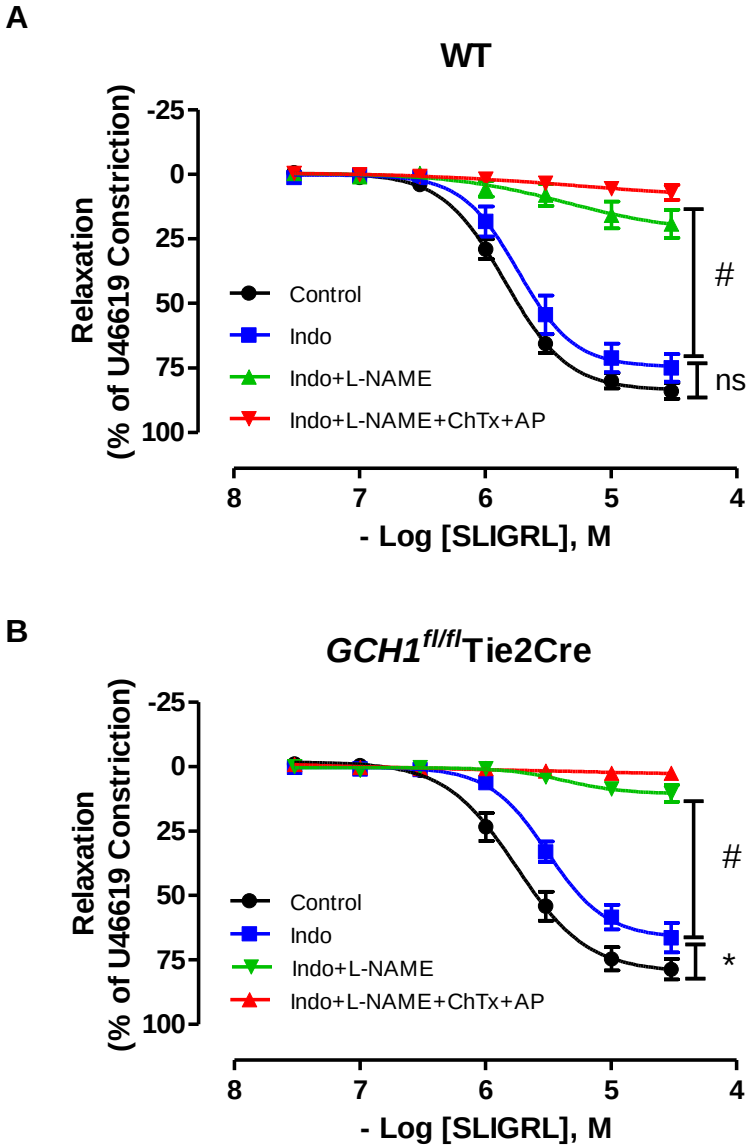


Figure 4.20. Contribution of prostacyclin, eNOS-derived vasodilators, and EDHF in mouse mesenteric arteries.

Isometric tension studies of 2nd order mesenteric arteries from **A)** wild-type (WT) and **B)** *GCH1*$^{fl/fl}$Tie2cre mice were examined using a wire myograph. Endothelium-dependent vasodilatations to SLIGRL were determined in the presence of cyclooxygenase inhibitor, indomethacin (10 μM) alone, or indomethacin with nitric oxide synthase inhibitor, L-NAME (100 μM), or indomethacin, L-NAME with EDHF blockers: apamin and charybdotoxin. Data are expressed as mean ± SEM. (*P<0.05, #P<0.001; n=9 to 10 animals per group).

4.4.2.4 Endothelial NOS-derived H_2O_2-mediated vasodilatation in mouse mesenteric arteries

Several lines of evidence suggest that endothelium-dependent vasodilatation in mouse mesenteric arteries is partly mediated by endothelium-derived H_2O_2 (Matoba et al., 2000b; Prysyazhna et al., 2012). To determine whether this is the case, isometric tension studies in isolated 2nd order mesenteric arteries from wild-type and *GCH1*$^{fl/fl}$Tie2cre mice were determined as described in Section 2.8

In mesenteric arteries, PEG-catalase (400 U/ml for 20 min) significantly inhibited acetylcholine-dependent vasodilatations of both genotypes, indicating that the vasodilatations in mesenteric arteries of wild-type and *GCH1*$^{fl/fl}$Tie2cre is partly mediated by endothelium-derived H_2O_2 (Figure 4.21 A and B). In the presence of L-NAME, acetylcholine-induced vasodilatation was markedly attenuated in both wild-type and *GCH1*$^{fl/fl}$Tie2cre vessels, and addition of catalase had no inhibitory effect on acetylcholine-induced vasodilatation (Figure 4.21 A and B). This suggests that eNOS is likely to be the principle source of H_2O_2 in mesenteric arteries of both wild-type and *GCH1*$^{fl/fl}$Tie2cre mice. Endothelium-independent vasodilatations to exogenous H_2O_2 were comparable between wild-type and *GCH1*$^{fl/fl}$Tie2cre mesenteric arteries (Figure 4.22 B). This finding suggests that eNOS-derived H_2O_2 plays a key role in mediating vasodilatation in mouse mesenteric arteries.

Taken together, endothelium-dependent vasodilation in mesenteric vessels of wild-type mice is primarily mediated by eNOS-derived NO and eNOS-derived H_2O_2, whereas endothelium-dependent vasodilation in *GCH1*$^{fl/fl}$Tie2cre mice mesenteric arteries is mediated by eNOS-derived H_2O_2, and prostacyclin.

Figure 4.21

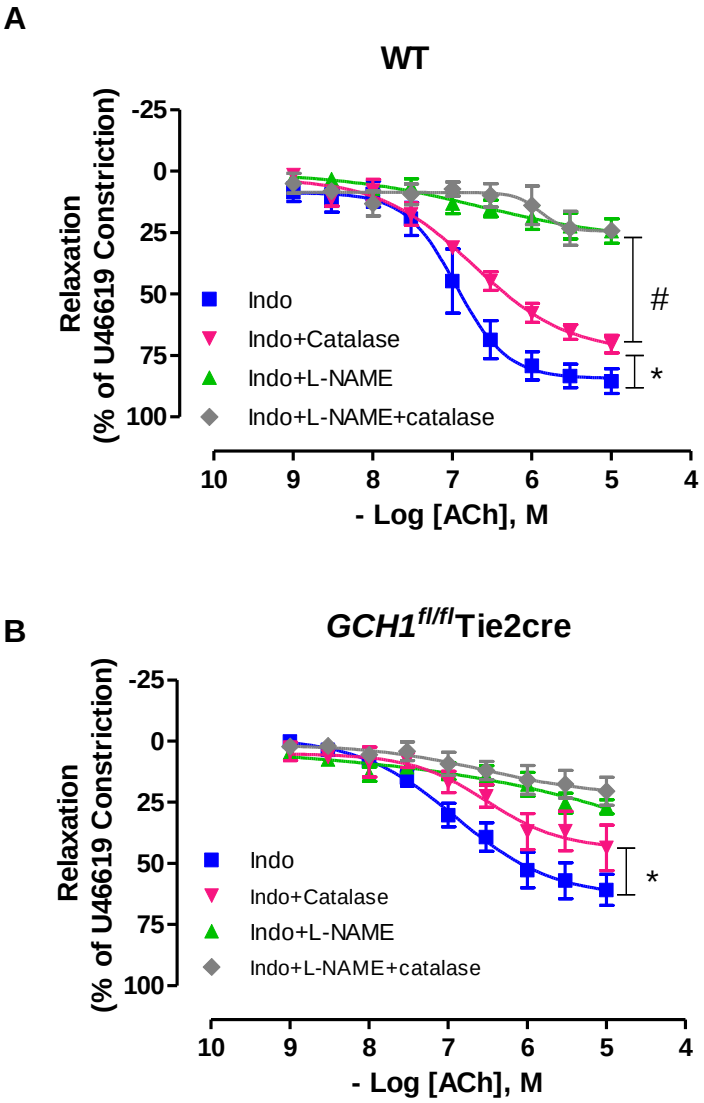


Figure 4.21. eNOS-derived H_2O_2 mediated vasodilatation in mesenteric arteries.

Isometric tension of 2nd order mesenteric arteries from **A)** wild-type (WT) and **B)** *GCH1*$^{fl/fl}$Tie2cre mesenteric arteries was recorded. Endothelium-dependent vasodilatation to acetylcholine (ACh) was determined in the presence of cyclooxygenase inhibitor, indomethacin (10 μM) alone, indomethacin with nitric oxide synthase inhibitor, L-NAME (100 μM), indomethacin with PEG-catalase (400 U/ml), and indomethacin, L-NAME with PEG-catalase. Data are expressed as mean ± SEM. (**P*<0.05, #*P*<0.001; n=14 to18 animals per group).

Figure 4.22

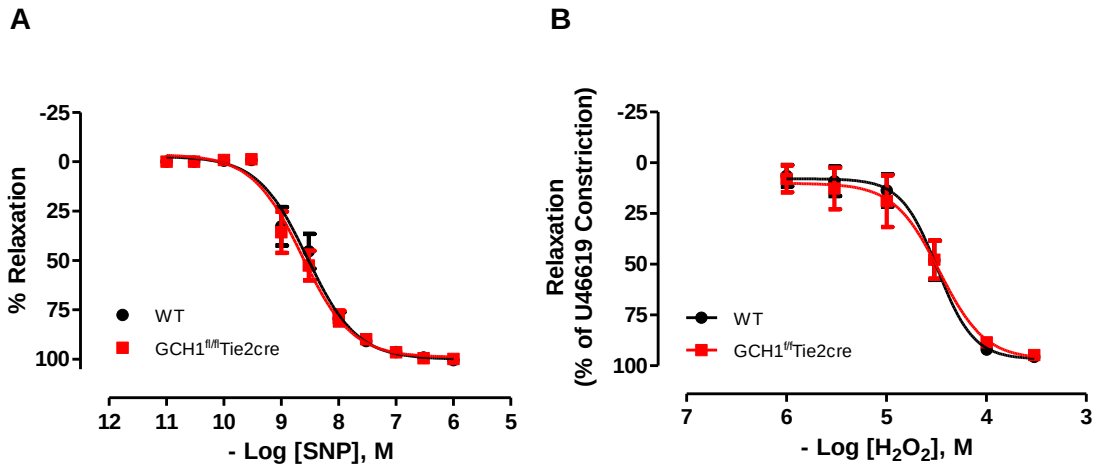


Figure 4.22. Endothelium-independent vasodilatation in mesenteric arteries.

(A) Endothelium-independent vasodilatation to sodium nitroprusside (SNP; n=7 to 9 animals per group) and **B)** hydrogen peroxide (H_2O_2). Data are expressed as mean ± SEM. (n=4 to 5 animals per group).

4.4.2.5 Protein expression in GCH1$^{fl/fl}$Tie2cre mesenteric arteries

I next determined whether endothelial cell BH4 deficiency led to compensatory changes in antioxidant proteins that may influence the vascular response by western blotting as described in Section 2.9. Western blot analysis showed that the protein levels of antioxidant enzymes (cu/znSOD, MnSOD, ecSOD and catalase) were comparable between *GCH1*$^{fl/fl}$Tie2cre and wild-type controls (Figure 4.23 A, B, C and D), indicating that deficiency in endothelial cell BH4 biosynthesis had no significant effect on antioxidant protein expression in mesenteric arteries.

Figure 4.23

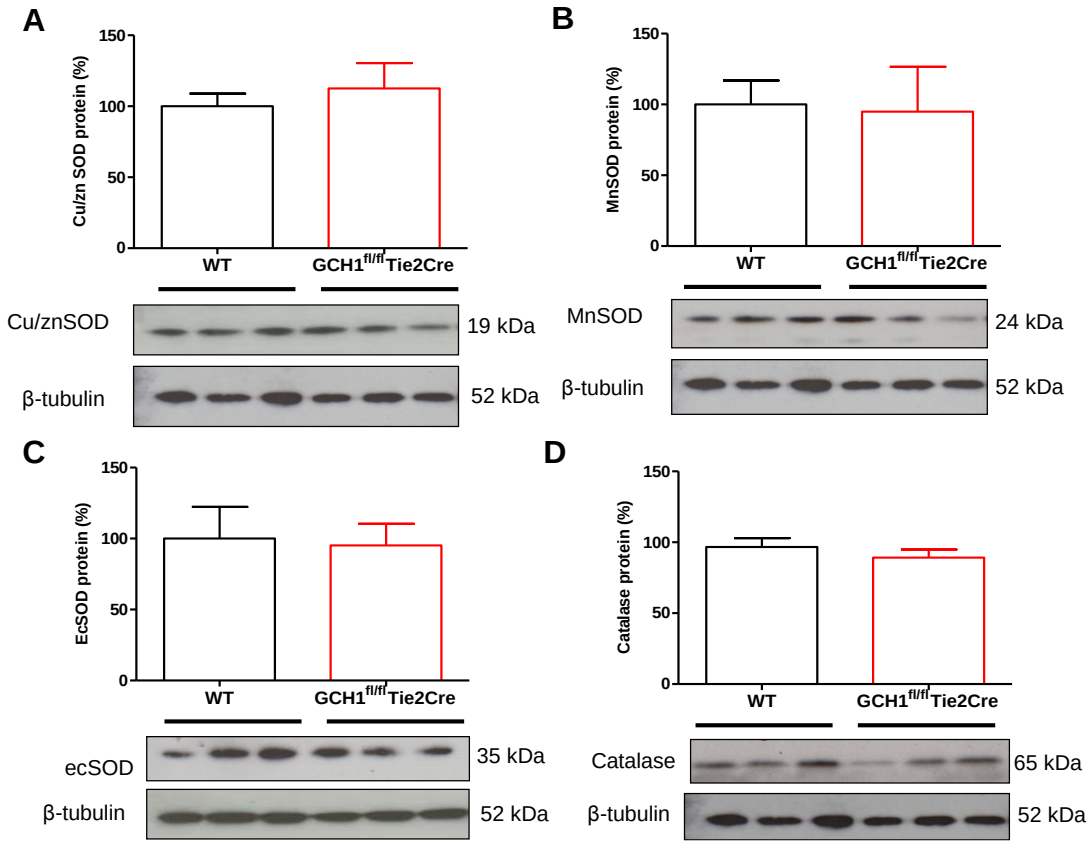


Figure 4.23. Antioxidant protein expression in mesenteric arteries

Representative immunoblots showing **(A)** Cu/ZnSoD, **(B)** MnSOD , **(C)** ecSOD, and **(D)** catalase protein in wild-type (WT) and *GCH1*$^{fl/fl}$Tie2cre mesenteric arteries (n=6 per group), with quantitative data, measured as percentage band density, above, and corresponding beta-tubulin loading control immunoblots, below. The expression of antioxidant proteins in mesenteric arteries were comparable between wild-type and *GCH1*$^{fl/fl}$Tie2cre mice. Data are expressed as mean ± SEM. (n=6 per group).

4.5 Discussion

In this chapter, I investigated the physiological requirement for endothelial cell BH4 biosynthesis in vascular function in conduit and resistance vessels. The key findings were:

Aortas

- Deficiency in endothelial cell BH4 biosynthesis leads to enhanced vasoconstriction and impairment of endothelium-dependent vasodilatation with loss of eNOS-derived NO production in *GCH1*$^{fl/fl}$Tie2cre aortas.
- Endothelium-dependent vasodilatation in *GCH1*$^{fl/fl}$Tie2cre aortas is, in part, mediated by eNOS-derived H_2O_2, acting through the sGC/PKG-dependent signalling pathway.
- *Ex vivo* incubation of *GCH1*$^{fl/fl}$Tie2cre aortas with the BH4 analogue sepiapterin restores endothelial vasomotor responses and abolishes H_2O_2 mediated vasodilatation.

Mesenteric arteries

- In mesenteric arteries of wild-type mice, endothelium-dependent vasodilatation is primarily mediated by eNOS-derived NO and eNOS-derived H_2O_2, suggesting that eNOS-derived vasodilators play a critical role in maintaining vascular homeostasis in mouse mesenteric arteries.
- Deficiency in endothelial cell BH4 biosynthesis leads to a loss of eNOS-derived NO mediated vascular tone and impaired endothelium-dependent vasodilatation in mesenteric resistance arteries.

- Loss of eNOS-derived NO-mediated vasodilatation is associated with up-regulation of prostaglandin-derived vasodilator, which mediates endothelium-dependent vasodilatation in *GCH1*$^{fl/fl}$Tie2cre mesenteric arteries.

4.5.1 Vascular function in aortas

In the first part of this chapter I examined the requirement for endothelial cell BH4 biosynthesis on vascular function in conduit vessels. Despite the clear evidence for loss of endothelial NO generation in *GCH1*$^{fl/fl}$Tie2cre mice (as demonstrated in Section 3.4.5), endothelium-dependent vasodilatation to acetylcholine was only minimally impaired in aortas, suggesting that other eNOS-derived vasodilators are able to mediate vasodilatation when BH4 is limiting. In addition, endothelium-dependent vasodilatation in response to the PAR2 agonist, SLIGRL was also impaired in *GCH1*$^{fl/fl}$Tie2cre aortas, suggesting that the impaired vasodilatation was not due to specific alteration of receptor signalling in endothelial cells of *GCH1*$^{fl/fl}$Tie2cre mice. Endothelium-dependent vasodilatation to acetylcholine in both wild-type and *GCH1*$^{fl/fl}$Tie2cre aortas was abolished and normalised in the presence of L-NAME, indicating that eNOS is the major source of vasodilators in mouse aortas. These findings are consistent with various studies, which demonstrate that endothelium-dependent vasodilatation in mouse aortas is mainly mediated by eNOS-derived NO production (Prysyazhna et al., 2012). In addition, endothelium-independent vasodilatation in response to nitric oxide donor, sodium nitroprusside (SNP) was similar between the groups, suggesting no alteration in vascular smooth muscle sensitivity in *GCH1*$^{fl/fl}$Tie2cre aortas.

Acetylcholine-induced vasodilatation in *GCH1*$^{fl/fl}$Tie2cre aortas is mediated by H_2O_2. This is because PEG-catalase, an enzyme that acts to dismutase H_2O_2, substantially inhibited

vasodilatation in *GCH1*$^{fl/fl}$Tie2cre aortas, and the increased vascular H_2O_2 production in *GCH1*$^{fl/fl}$Tie2cre aortas was inhibited by L-NAME, suggesting eNOS is the principle source of H_2O_2 in *GCH1*$^{fl/fl}$Tie2cre aortas. These observations are consistent with the studies in aortas of mice with deoxycorticosterone acetate-salt hypertension (Landmesser et al., 2003) and in hph-1 mice (Cosentino et al., 2001). However our new findings in *GCH1*$^{fl/fl}$Tie2cre mice overcome the lack of cell specificity in these previous models, and the potentially confounding effects of systemic changes, such as effects of BH4 deficiency on heart rate and sympathetic function in the hph-1 mouse (Adlam et al., 2012).

Evidence suggests that H_2O_2 can mediate endothelium-dependent and endothelium-independent vasodilatation in several vascular beds in multiple species, including humans (Fadel et al., 2003; Matoba et al., 2002; Rosenfeld et al., 2000). H_2O_2 could mediate vasodilatation by endothelium-dependent smooth muscle hyperpolarization and vasodilatation (Busse et al., 2002), or by activating sGC, leading to increased cGMP, or by directly activating PKG, and vasodilatation (Fujimoto et al., 2003; Rudyk et al., 2013; Wolin and Burke, 1987). The mechanisms of H_2O_2-induced vasodilatation are varied depending on the vascular bed and species. These data suggest that H_2O_2 production from uncoupled eNOS in *GCH1*$^{fl/fl}$Tie2cre aortas induces vasodilatation through sGC/PKG rather than through an endothelium-derived hyperpolarizing factor pathway, as evidenced by the lack of inhibition by apamin and charybdotoxin (Ray et al., 2011), or by 30 mmol/L extracellular K^+, to inhibit the activity of Ca^{2+}-activated K^+ channels. In contrast, the soluble guanylate cyclase inhibitor, ODQ, inhibited vasodilatation to acetylcholine in *GCH1*$^{fl/fl}$Tie2cre aortas to a similar extent as that observed in the presence of ODQ with PEG-catalase

The data reveal significantly greater eNOS protein in *GCH1*$^{fl/fl}$Tie2cre aortas, despite impaired vascular responses, which supports previous evidence suggesting, that H_2O_2 can

induce eNOS expression (Landmesser et al., 2003; Youn et al., 2012). These observations are consistent with reduced H_2O_2 production in $Nox4^{-/-}$ mice, which have reduced aortic eNOS expression by 50% (Schroder et al., 2012). An alternative explanation for increased endothelial-derived ROS production may be an alteration in the protein levels of antioxidant enzymes (catalase, MnSOD, Cu/ZnSOD, and extracellular SOD). However, we found that the levels of these antioxidant enzymes were identical in the aortas of *GCH1*$^{fl/fl}$Tie2cre and wild-type mice. Thus, the *GCH1*$^{fl/fl}$Tie2cre mouse reveals a new role for physiological BH4 levels in regulating eNOS-derived H_2O_2 and in turn eNOS expression.

To test the specificity of the observed phenotype for biochemical BH4 deficiency, we performed a rescue experiment using a BH4 precursor, sepiapterin. *Ex vivo* supplementation of *GCH1*$^{fl/fl}$Tie2cre aortas with sepiapterin restored endothelial function, abolishing eNOS-derived H_2O_2 mediated vasodilatation. This result is consistent with previous studies demonstrating that supplementation with sepiapterin in hph-1 mice (Cosentino et al., 2001), hypertensive mice (Landmesser et al., 2003), chronic smokers (Heitzer et al., 2000a), and diabetic patients (Guzik et al., 2002b), improved $NO^{\bullet}$ bioavailability and restored endothelial function. Previous studies of high-level pharmacologic supplementation of exogenous BH4 have been criticised for non-specific antioxidant effects. However, the present studies suggest that exogenous supplementation of BH4, using sepiapterin, can augment endothelial cell BH4 levels, at least in healthy animals. Targeted cell-specific mouse models of *GCH1* deletion will be useful in future studies to test the effectiveness of *in vivo* strategies to restore or supplement cellular BH4 levels.

4.5.2 Vascular function in mesenteric arteries

In this chapter, we examined the requirement for endothelial cell BH4 biosynthesis on vascular function in resistance arteries. We have shown that deficiency in endothelial cell

BH4 biosynthesis in mesenteric arteries leads to a loss of eNOS-derived NO, enhanced vasoconstriction and impaired endothelium-dependent vasodilatation in *GCH1*$^{fl/fl}$Tie2cre mice. This observation is consistent with previous reports, which have demonstrated that reduced vascular BH4 bioavailability leads to eNOS uncoupling and loss of NO-mediated vasodilatations in mesenteric arteries of DOCA-salt hypertension mice (Du et al., 2008). This effect was prevented in transgenic mice with endothelial-specific GTPCH overexpression (GCH-Tg)-DOCA-salt hypertension mice (Du et al., 2008). Although these studies implicate reduced or augmented BH4 in vascular disease pathogenesis, the physiological requirement for endothelial cell BH4 biosynthesis in the regulation of eNOS-derived vasodilator in vasomotor function remains unknown. In the present study, we have demonstrated for the first time that deficiency in endothelial cell BH4 biosynthesis is alone sufficient to cause vascular dysfunction in resistance arteries even in the absence of vascular disease. These findings suggest that endothelial cell *GCH1*/BH4 biosynthesis plays a pivotal role in maintaining vascular homeostasis in mesenteric resistance arteries.

It is unlikely that down regulation of eNOS protein expression is responsible for reduced NO-mediated vasodilatation because eNOS expression was unaltered in *GCH1*$^{fl/fl}$Tie2cre mesenteric arteries. Despite impairment of vascular function in *GCH1*$^{fl/fl}$Tie2cre mesenteric arteries, diameter sizes and maximal contraction to KCl were comparable between the genotypes. Endothelium-independent vasodilatations in response to sodium nitroprusside and exogenous H_2O_2 were comparable, indicating that vasodilatation properties of vascular smooth muscle cells were preserved in *GCH1*$^{fl/fl}$Tie2cre mice and wild-type littermate controls.

Interestingly, endothelium-dependent vasodilatations in both wild-type and *GCH1*$^{fl/fl}$Tie2cre mesenteric arteries were, in part, mediated by eNOS-derived H_2O_2 production. This finding

is consistent with previous reports in mouse and human mesenteric arteries and porcine coronary arteries. eNOS deficient mice have markedly reduced eNOS-derived H_2O_2-mediated vasodilation in mesenteric arteries (Matoba et al., 2000a; Takaki et al., 2008b). Furthermore, mice with deficiency in Cu/ZnSOD lack eNOS-derived H_2O_2 generation and exhibit impaired acetylcholine-induced vasodilation in mesenteric arteries, further suggesting the role of eNOS-derived H_2O_2 mediated vasodilation in mesenteric arteries. Interestingly, in the present studies, the relative contribution of H_2O_2-mediated vasodilation, which would be expected to be enhanced in endothelial cell BH4 deficiency mice, was comparable between mesenteric arteries of wild-type and *GCH1*$^{fl/fl}$Tie2cre mice. It is unlikely that alteration in the antioxidant protein expression contributed to this observation because the antioxidant proteins (MnSOD, Cu/ZnSOD, ecSOD and catalase) were all comparable between *GCH1*$^{fl/fl}$Tie2cre and wild-type mesenteric arteries. This finding suggests that eNOS-derived H_2O_2 mediated vasodilatations are unlikely to be influenced or affected by the endothelial cell BH4 bioavailability in mesenteric arteries. I remain uncertain as to why eNOS-derived H_2O_2 levels were unaltered in *GCH1*$^{fl/fl}$Tie2cre mesenteric arteries despite being increased in *GCH1*$^{fl/fl}$Tie2cre aortas. One explanation would be that the level of eNOS-derived H_2O_2 production is highly regulated in mouse mesenteric arteries compared to aortas. Consistent with this idea, Burgoyne *et al* have demonstrated that the protein level of catalase in mouse mesenteric arteries is 5-fold greater than that of aortas (Burgoyne et al., 2012). The low level of catalase protein in aortas could explain the phenomenal result observed in *GCH1*$^{fl/fl}$Tie2cre mice where aortic eNOS-derived H_2O_2 production is markedly increased and mediated vasodilatation. In contrast to this finding, others have reported that endothelium-dependent vasodilatation in mouse mesenteric arteries is mainly mediated by eNOS-derived H_2O_2 which acts as EDHF. The discrepancy may be due to the difference in vessel size studies (2^{nd} versus 3^{rd} order mesenteric arteries) or type

of inhibitor used (eg. L-NAME versus L-NNA). Indeed, it has been reported that L-NNA, an inhibitor of nitric oxide synthase, inhibits NO generation from coupled NOS but not superoxide production from uncoupled NOS (Vasquez-Vivar et al., 2002a). In contrast, both NO and superoxide generation derived from NOS have been reported be to fully inhibited by L-NAME (Bendall et al., 2005; Khoo et al., 2004; Vasquez-Vivar et al., 2002b). Therefore, it is likely that when L-NNA is used, the scavenger effect of eNOS-derived NO is reduced thereby increasing superoxide and H_2O_2 generation, which are able to mediate vasodilatation in mouse mesenteric arteries. In the current study using L-NAME, we have demonstrated that eNOS-derived NO and eNOS-derived H_2O_2 are likely to be the key mediators in modulating endothelium-dependent vasodilatation in mouse mesenteric arteries, a finding consistent with the recent study by Prysyazhna et al (Prysyazhna et al., 2012).

Furthermore, endothelium-dependent vasodilatation in *GCH1*$^{fl/fl}$Tie2cre mesenteric arteries is in part mediated by a prostaglandin-derived vasodilator, probably prostacyclin. Despite up-regulation of prostaglandins-derived vasodilator, endothelium-dependent vasodilatation in *GCH1*$^{fl/fl}$Tie2cre mesenteric arteries was markedly impaired compared to wild-type controls. This finding suggests that when eNOS-derived NO generation is compromised, prostaglandin-derived vasodilator is up-regulated and partially compensated in endothelium-dependent vasodilatation in *GCH1*$^{fl/fl}$Tie2cre mesenteric arteries. This observation is consistent with previous reports, which have demonstrated that prostacyclin is upregulated in mesenteric arteries of eNOS knockout mice (Chataigneau et al., 1999; Matoba et al., 2000b). It has been suggested that endogenous eNOS-derived NO acts as an inhibitor of prostacyclin synthesis. Indeed, Barker *et al* have demonstrated that treatment of isolated rings of human saphenous vein with NOS inhibitor, increases the release of endogenous prostacyclin, which decreases in the presence of nitrogylcerin (Barker et al., 1996). Beverelli

et al showed that chronic treatment with NOS inhibitor increases prostacyclin production by upregulation of cyclooxynease type 1 in coronary arteries (Beverelli et al., 1997). These findings suggest that endothelial cell BH4/eNOS-derived NO bioavailability plays a role in regulating the synthesis of endogenous prostacyclin.

In the presence of indomethacin, L-NAME substantially attenuated acetylcholine-dependent vasodilatation and the combination of indomethacin, L-NAME with EDHF blockers, apamin and charybdotoxin resulted in full blockage of vasodilatation in both wild-type and *GCH1*$^{fl/fl}$Tie2cre vessels. These findings suggest that endothelium-dependent vasodilatation in wild-type mesenteric arteries is mainly mediated by eNOS-derived NO and eNOS-derived H_2O_2. In contrast, endothelium-dependent vasodilatation in *GCH1*$^{fl/fl}$Tie2cre mesenteric arteries is partly mediated by prostaglandin-derived vasodilator and eNOS-derived H_2O_2. In this study, we also observed the remaining vasodilatations, which are not inhibited by indomethacin or by the combination of indomethacin with L-NAME or by indomethacin combined with L-NAME and catalase, but totally abolished in the presence of additional EDHF blockers: apamin and charybdotoxin. This suggests that non-eNOS/prostaglandin-derived vasodilators mediate vasodilatations in mesenteric arteries of both genotypes. Currently, the possible candidates for this EDHF include hydrogen sulphide (H_2S), K^+ ions (Edwards et al., 1998), epoxyeicosatrienoic acids, and myoendothelial gap junctions (Dora et al., 2003). The nature of EDHF in this study is unlikely to be affected by the levels of endothelial cell BH4 because the relative contribution of this EDHF-mediated vasodilatation was similar between wild-type and *GCH1*$^{fl/fl}$Tie2cre mesenteric arteries.

In summary, we describe for the first time that selective deficiency in endothelial cell BH4 biosynthesis, by targeted *GCH1* deletion, is alone sufficient to cause eNOS uncoupling, loss of eNOS-derived NO, impaired vascular function in both conduit and resistant vessels even

in the absence of vascular disease. This endothelial cell-autonomous requirement for BH4 biosynthesis is pivotal in maintaining eNOS-mediated NO versus H_2O_2 signalling in vascular physiology.

Having demonstrated the critical role of endothelial cell BH4 biosynthesis in vasomotor function in aortas and mesenteric arteries from *GCH1*$^{fl/fl}$Tie2cre mouse, I next determined the role of endothelial cell BH4 in blood pressure regulation.

Chapter 5:

Haemodynamic Regulation in Endothelial Cell-Specific BH4 Deficiency in Health and Disease

Chapter 5: Haemodynamic Regulation in Endothelial Cell-Specific BH4 Deficiency in Health and Disease

5.1 Introduction

I have previously shown in chapter 3 and 4 that:

- Endothelium-targeted *GCH1* deletion led to endothelial cell BH4 deficiency, eNOS uncoupling, increased superoxide production, and reduced NO bioavailability.
- Deficiency in endothelial cell BH4 biosynthesis led to an impairment of vascular function in both conduit and resistance vessels from *GCH1*$^{fl/fl}$Tie2cre mice.

Several lines of evidence demonstrated that reduced vascular BH4 bioavailability is associated with vascular disease states such as hypertension, diabetes and atherosclerosis in both experimental models and clinical studies (Antoniades et al., 2011a; Bitar et al., 2005a; Heitzer et al., 2000b; Laursen et al., 2001). To date, it remains unknown whether reduced vascular BH4 bioavailability is the cause, or occurs as a consequence of vascular disease. Landmesser *et al* demonstrated that oxidation of vascular BH4 by NADPH oxidase-derived superoxide is the key mechanism underlying the cause of eNOS uncoupling and hypertension in DOCA-salt induced hypertension model (Landmesser et al., 2003). Du *et al* demonstrated that mice with endothelium-targeted *GCH1* overexpression are partially protected from hypertension in DOCA-salt-induced hypertension (Du et al., 2008). In contrast to reduced vascular BH4 bioavailability, increased vascular BH4 bioavailability has been implicated in the pathogenesis of vascular disease with systemic inflammation such as sepsis (Bune et al., 1996) (Shimizu S et al 1998). These findings demonstrate the critical role of vascular *GCH1* and BH4 bioavailability in the pathogenesis of vascular disease.

Previous studies investigating the importance of BH4 biosynthesis have used either systemic pharmacological inhibitors of GTPCH such as 2,4, diamino-6-hydroxypyrimidine and N-acetyl-serotonin (DAHP), or the hph-1 hyperphenylalaninemic mouse that has moderate systemic BH4 deficiency because of reduced gene expression from the *GCH1* locus (Cosentino et al., 2001; Khoo et al., 2005). The previous study by Cosentino *et al* found that hph-1 mice are hypertensive compared with wild-type non-littermate controls (Cosentino et al., 2001). However, recent reports have demonstrated no difference in systolic blood pressure between hph-1 mice and wild-type littermate controls (Adlam et al., 2012);Santhanam, 2012 #5551}. In addition, global BH4 deficiency in hph-1 mice has systemic effects in multiple cell types, such as neurotransmitter synthesis and autonomic function, thus confounding the interpretation of endothelial cell BH4 on vascular function and blood pressure regulation control by eNOS. To date, the specific physiological requirement for endothelial cell BH4 biosynthesis on blood pressure regulation in vivo has yet to be investigated.

5.2 Hypothesis and aims

The aim of this chapter was to investigate the requirement for endothelial cell BH4 biosynthesis on blood pressure regulation in endothelial cell-targeted *GCH1* knockout mice (*GCH1*$^{fl/fl}$Tie2ce mice) in normal physiology, and disease states. Specifically the experiments in this chapter had the following aims:

- To characterise the baseline blood pressure of the *GCH1*$^{fl/fl}$Tie2cre mice by two independent methods.
- To determine the requirement for endothelial cell BH4 biosynthesis in haemodynamic responses to NOS inhibition, antioxidants, vasoconstrictor and cyclooxygenase inhibition.
- To investigate the role of endothelial cell BH4 biosynthesis on blood pressure regulation in response to angiotensin II.
- To investigate whether deficiency in endothelial cell *GCH1* and subsequent endothelial cell BH4 biosynthesis provides an alternative therapeutic mechanism to regulate vascular NOS-derived NO overproduction and haemodynamic alteration in lipopolysaccharide (LPS)-induced systemic inflammation.

I hypothesized that endothelial cell *GCH1* and BH4 biosynthesis is required for eNOS function and blood pressure regulation. Specifically:

- Endothelial cell *GCH1* and BH4 biosynthesis is required for eNOS regulation and blood pressure regulation under basal physiological conditions in vivo. Thus, deficiency in endothelial cell BH4 will lead to increased blood pressure.
- Deficiency in endothelial cell BH4 biosynthesis will lead to increased blood pressure compared to wild-type controls in response to chronic Ang II infusion.

- Deficiency in endothelial cell *GCH1* and thus BH4 biosynthesis will result in a reduction in NOS-derived NO generation in vascular endothelium in response to LPS, which in turn will protect from vascular dysfunction and hypotension in response to LPS.

5.3 Methods

Most of the methods used in this chapter have been described in Chapter 2. Only methods and reagents used specifically in the experiments for this chapter are described below.

5.3.1 Haemodynamic measurements

5.3.1.1 Non-invasive approach using tail-cuff method

Systolic blood pressure and heart rate was determined using a computerized tail-cuff system (Visitech, USA) in conscious mice. Experiments were performed between the hours of 8 and 12 am. The animal tails were pulled and passed through a cylindrical latex tail-cuff and taped down to reduced movement. A blood pressure sensor was then placed over the tail. Twenty readings were taken per mouse of which the first 5 readings were discarded. The remaining 15 readings were used to calculate the mean systolic blood pressure and heart rate in each mouse.

5.3.1.1 Invasive approach using Millar catheter method

Systolic blood pressure and heart rate were measured in wild-type and *GCH1*$^{fl/fl}$Tie2cre mice by a direct invasive approach under general anaesthesia using the Millar catheter system. Mice were anaesthetised using inhalational isofluorane vaporised on oxygen. Anaesthetised mice were transferred to a warming pad at temperature of 36.5°C with maintenance anaesthesia provided via a nose cone. The left carotid artery was isolated via a midline incision in the neck and a 1.5F Millar catheter was introduced into the carotid artery and in to the aorta. Experimental anaesthesia was monitored to maintain a respiratory rate of 60 to

70 per minutes. Following a 15-minute equilibration period, a 15 minute trace of intra-arterial blood pressure was recorded as a baseline measurement.

5.3.2 Angiotensin II-induced hypertension

5.3.2.1 Insertion of osmotic mini-pumps

Subcutaneous osmotic mini-pumps (Alzet Model 1002, 14 days: Charles River) were used for saline or angiotensin II (Ang II) infusion (Sigma-Aldrich, Gillingham, UK). Male *GCH1*$^{fl/fl}$Tie2cre and wild-type mice (16-22 week-old mice) were anaesthetised by inhalation of 2% isofluorane in 95% oxygen. Mice received buprenorphine at the time of surgery. Osmotic mini-pumps containing either sterile saline or Ang II (0.4 mg/kg/day) were implanted subcutaneously in the midscapular region. Mini-pump surgery was performed by Dr Gillian Douglas. Mice were monitored throughout the study for adverse effects such as muscle weakness or wound breakdown. Animals showing signs of discomfort, distress or significant weight loss that could not be alleviated were culled by a Schedule 1 method.

5.3.3 LPS-induced systemic inflammation

LPS (1 mg/kg of body weight, Sigma-Aldrich, Gillingham, UK) or sterile saline was administrated to 16-22-week-old male wild-type and *GCH1*$^{fl/fl}$Tie2cre mice via intraperitoneal route. Mice were monitored throughout the study for adverse effects. LPS administration is expected to cause a systemic inflammation and hypotension, which may lead to hypothermia. To counteract this, mice were maintained in a heated recovery cage and were given a subcutaneous injection of saline. 24-hour post injection, mice were culled and tissues were collected. LPS administration was performed by Dr Eileen McNeill.

5.4 Results

5.4.1 Haemodynamic measurements

5.4.1.1 Tail-cuff plethysmography

Given the striking changes in eNOS coupling and vasomotor function in aortas and mesenteric arteries from *GCH1*$^{fl/fl}$Tie2cre mice, I next determined the requirement for endothelial cell BH4 synthesis in blood pressure regulation in vivo, by measuring arterial blood pressure in conscious mice using tail-cuff plethysmography. Male wild-type and *GCH1*$^{fl/fl}$Tie2cre mice (16-22 week-old) were subjected to non-invasive tail-cuff recordings as described in section 5.3.1.1. Following 5 days training, baseline blood pressure measurements were recorded for 3 days and the results averaged. *GCH1*$^{fl/fl}$Tie2cre mice had significantly higher systolic blood pressure (103.4 ± 1.3 mmHg; $P<0.001$) than wild-type littermates (96.4 ± 0.8 mmHg)(Figure 5.1 A). Heart rate was significantly reduced in *GCH1*$^{fl/fl}$Tie2cre mice (722 ± 5 beat per minute; $P<0.05$) compared to wild-type littermates (734 ± 3 beat per minute) (Figure 5.1 B).

Figure 5.1

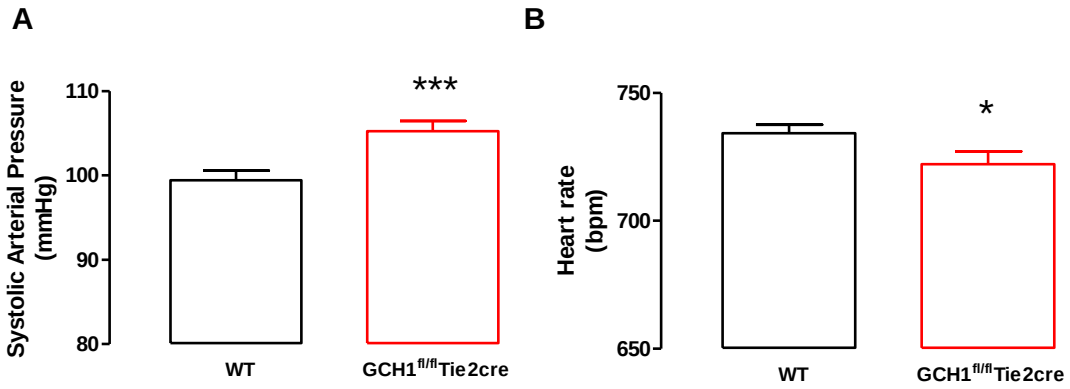


Figure 5.1. Haemodynamic measurements using tail-cuff plethysmography.

16-22 week-old mice were subjected to non-invasive tail-cuff recordings. Following 5 days training, basal haemodynamic measurements were recorded over 3 consecutive days and results averaged. **A)** Systolic blood pressure, expressed in mmHg. *GCH1*$^{fl/fl}$Tie2cre mice have significantly higher systolic blood pressure than wild-type littermates. **B)** Heart rate, expressed in beats per minute (bpm). *GCH1*$^{fl/fl}$Tie2cre mice have significantly lower heart rate than wild-type littermates. Data are expressed as mean ± SEM. (*$P<0.05$, ***$P<0.001$; n=35 to 37 animals per group).

5.4.1.2 Millar catheter (invasive method)

In a further cohort of mice, an alternative method was used to measure blood pressure. 16-22 week-old male mice were subjected to haemodynamic study using a Millar catheter inserted into the left carotid artery as described in section 5.3.1.2. Following 15 minutes equilibration basal haemodynamic parameters were recorded over a 15-minute period and blood pressure was determined. Under anaesthesia, *GCH1*$^{fl/fl}$Tie2cre mice had significantly higher systolic blood pressure compared to wild-type littermates (106.2 ± 1.7 mmHg versus 101.4 ± 1.3 mmHg; $P<0.05$)(Figure 5.2 A). Previously study using tail-cuff method in conscious mice in Section 5.4.1.3 demonstrated that *GCH1*$^{fl/fl}$Tie2cre mice had significantly lower heart rate compared to wild-type littermates. However, in this study, no difference was detected between heart rate of either wild-type (457 ± 9 bmp) or *GCH1*$^{fl/fl}$Tie2cre mice (474 ± 7 bpm)(Figure 5.2 B). No difference in heart rate between the genotypes may be due to the effect of anaesthetic agent isofluorane which is known to act as cardiovascular and respiratory suppressants and hence can directly influence haemodynamic parameters (Zuurbier et al., 2002). The respiratory rate during the study was comparable between wild-type (61 ± 3 per min) and *GCH1*$^{fl/fl}$Tie2cre mice (62 ± 5 per min)(Figure 5.2 C), indicating similar level of anaesthetic depth between the genotypes.

Taken together, this finding suggests that deficiency in endothelial cell *GCH1* and thus BH4 biosynthesis lead to a mild-hypertension and bradycardia in *GCH1*$^{fl/fl}$Tie2cre mice.

Figure 5.2

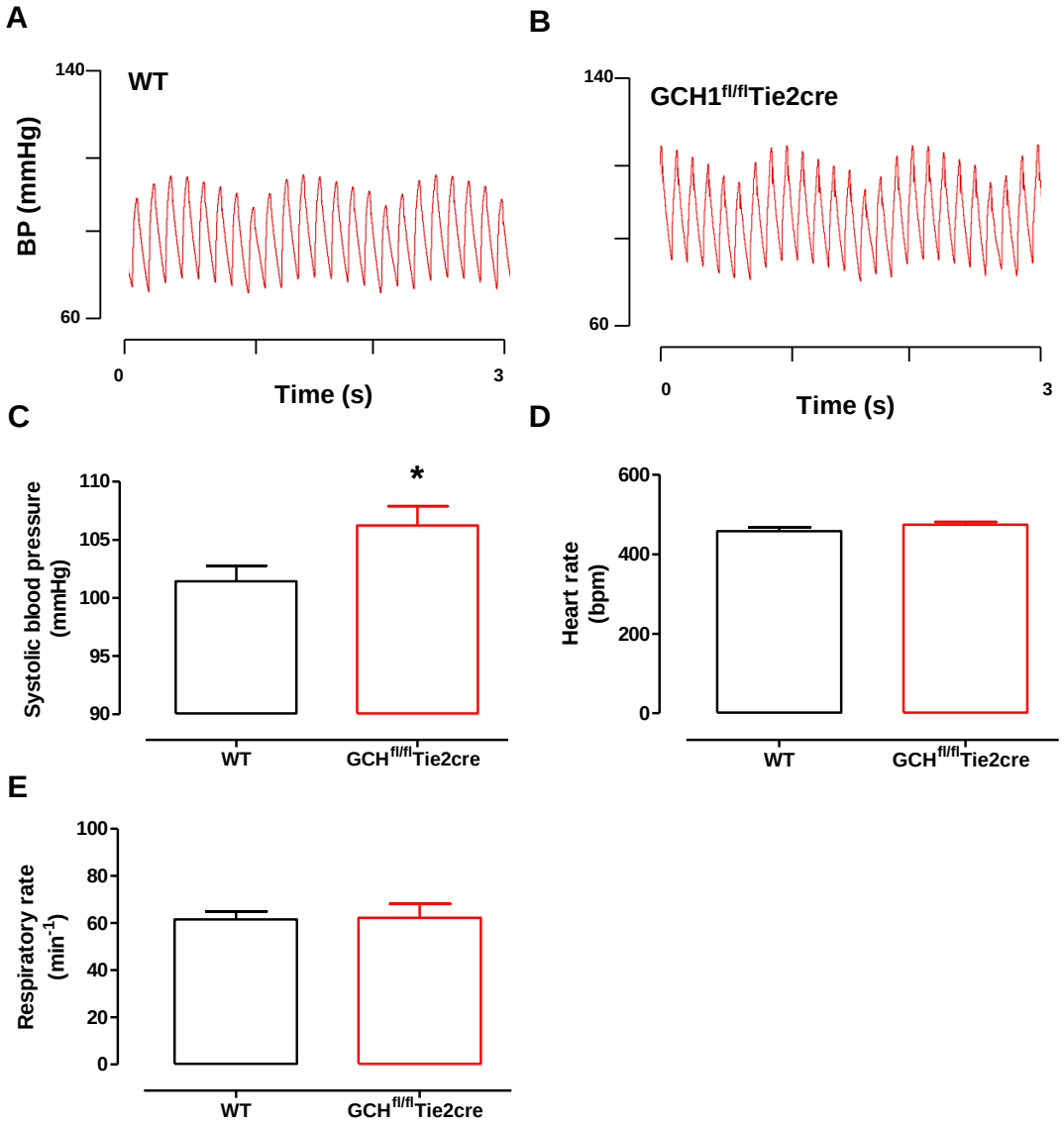


Figure 5.2. Invasive haemodynamic measurements in using Millar catheter in anaesthetised mice.

16-22 week-old mice were subjected to invasive Millar catheter haemodynamic recordings. **A)** Representative traces of blood pressure in wild-type and **B)** *GCH1*$^{fl/fl}$Tie2cre mice. **C)** Systolic blood pressure, expressed in mmHg. *GCH1*$^{fl/fl}$Tie2cre mice have significantly higher systolic blood pressure than wild-type littermates. **D)** Heart rate, expressed in beats per minute (bpm). **E)** Respiratory rate, expressed in per minute (min^{-1}). Data are expressed as mean ± SEM. (*$P<0.05$; n=13 to 16 animals per group).

5.4.2 Haemodynamic responses in anaesthetised mice

5.4.2.1 Acute administration of phenylephrine

I have previously shown that deficiency in endothelial cell BH4 biosynthesis leads to vascular dysfunction with enhancement of vasoconstriction and impairment of vasodilatation in isolated mesenteric resistance arteries of *GCH1*$^{fl/fl}$Tie2cre mice. To determine whether this is the case in vivo, I measured changes in arterial blood pressure in response to the vasoconstrictor phenylephrine (Sigma-Aldrich, Gillingham, UK) in anaesthetized mice, using a Millar catheter in the left carotid artery as described in section 5.3.1.2. Following 15 min equilibration and 15 min baseline recording, a serial intraperitoneal bolus dose of phenylephrine (0.1-10 μmol/kg) was administrated in wild-type and *GCH1*$^{fl/fl}$Tie2cre mice. It has been shown that phenylephrine has a rapid onset of action within 5 min post injection in anaesthetised mice (Adlam et al., 2012), therefore, haemodynamic responses were recorded over 5 minute period and haemodynamic parameters were determined.

Administration of phenylephrine at 0.1 μmol/kg of body weight had no significant effect on systolic blood pressure of both wild-type and *GCH1*$^{fl/fl}$Tie2cre mice. Treatment of phenylephrine at 1 μmol/kg of body weight caused a significantly greater increase in systolic blood pressure in *GCH1*$^{fl/fl}$Tie2cre mice (11.74 ± 2.46 mmHg; $P<0.05$) compared with wild-type controls (0.06 ± 1.69 mmHg) and after administration of 10 μmol/kg body weight of phenylephrine (25.42 ± 2.61 mmHg versus 10.24 ± 4.84 mmHg; $P<0.01$)(Figure 5.3 A). This finding suggests that there is an increase in responsiveness to low doses of phenylephrine in *GCH1*$^{fl/fl}$Tie2cre mice. Administration of phenylephrine at 0.1 and 1 μmol/kg of body weight had no significant effect on heart rate of either genotype but administration of 10 μmol/kg phenylephrine significantly reduced heart rate (Figure 5.3 B),

a finding consistent with previous report (Adlam D. 2012 *DPhil. Thesis, University of Oxford*).

Figure 5.3

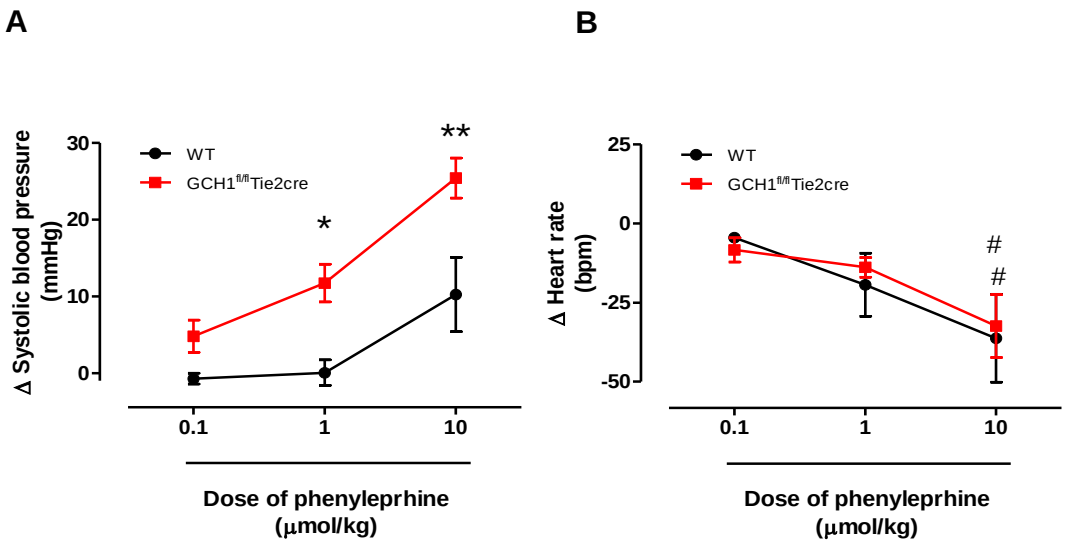


Figure 5.3. Effect of phenylephrine on haemodynamic parameters in anaesthetised mice.

16-22 week-old mice were subjected to invasive Millar catheter haemodynamic recordings. **A)** change in systolic blood pressure, expressed in mmHg, in response to serial intraperitoneal bolus doses of phenylephrine (PE; 0.1-10 µmol/kg). PE caused a significantly higher increase in systolic blood pressure in *GCH1*$^{fl/fl}$Tie2cre when compared with that in wild-type controls after administration of 1 µmol/kg. **B)** Change in heart rate, expressed in beats per minute (bpm). Data are expressed as mean ± SEM. (**P<0.05; **P<0.01* comparing wild-type*; # P<0.05* comparing treatment; n=5 to 6 animals per group).

5.4.2.2 Effect of indomethacin on haemodynamic responses

I have previously shown in section 4.4.2.3 that endothelium-dependent vasodilatation was in part mediated by a prostaglandin-derived vasodilator in isolated mesenteric resistance arteries of *GCH1*$^{fl/fl}$Tie2cre mice. To determine whether this is the case in vivo, I measured changes in arterial blood pressure in response to non-selective cyclooxygenase inhibitor indomethacin (Sigma-Aldrich, Gillingham, UK) in anaesthetized mice, using a Millar catheter in left carotid arteries as described in section 5.3.1.2. Following 15 minutes equilibration and 15 min baseline recording, a single dose of either indomethacin (5 mg/kg dissolved in 5% ethanol in saline) or control (5% ethanol in saline) was administrated via intraperitoneal route. Haemodynamic response was recorded over a 15-minute period and haemodynamic parameters were determined.

Administration of indomethacin significantly reduced systolic blood pressure in wild-type mice but did not alter blood pressure in *GCH1*$^{fl/fl}$Tie2cre mice (Figure 5.4 A and B). Indomethacin had no significant effect on heart rate of either wild-type or *GCH1*$^{fl/fl}$Tie2cre mice (Figure 5.4 C). In the control group, 5% ethanol in saline (vehicle control) had no significant effect on either blood pressure or heart rate of wild-type and *GCH1*$^{fl/fl}$Tie2cre mice (data not shown), demonstrating that reduced systolic blood pressure in wild-type mice is solely due to the effect of indomethacin. There was no difference in respiratory rate during experimental procedure between wild-type (69 ± 3 breaths per min) and *GCH1*$^{fl/fl}$Tie2cre mice (70 ± 3 breaths per min)(Figure 5.4 D), indicating similar level of anaesthetic depth between the genotypes.

Figure 5.4

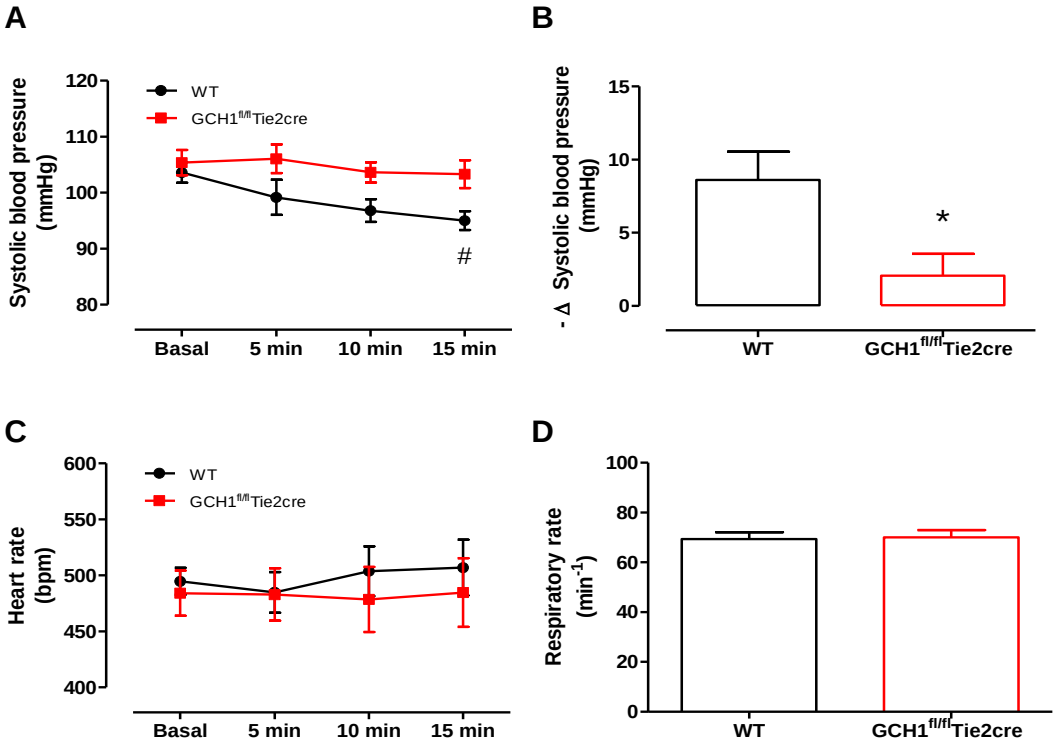


Figure 5.4. Effect of indomethacin on haemodynamic parameters in anaesthetised mice.

16-22 week-old mice were subjected to invasive Millar catheter haemodynamic recordings. Following 15 min baseline blood pressure recording, a single dose of indomethacin (5 mg/kg IP) was administrated. **A)** Systolic blood pressure, expressed in mmHg. Acute administration of indomethacin significantly reduced systolic blood pressure in wild-type mice but unaltered in *GCH1*$^{fl/fl}$Tie2cre mice. **B)** Mean quantitative data for the change (Δ) in systolic blood pressure following indomethacin administration. **C)** Heart rate, expressed in beats per minute (bpm). No differences were detected in heart rate of wild-type and *GCH1*$^{fl/fl}$Tie2cre mice either before or after indomethacin administration. **D)** Respiratory rate, expressed per minute (min^{-1}). Respiratory rate was comparable between wild-type and *GCH1*$^{fl/fl}$Tie2cre mice. Data are expressed as mean ± SEM. (*$P<0.05$; n=6 to 9 animals per group).

5.4.2.3 Effect of N-acetylcysteine (NAC) on haemodynamic responses

To investigate the role of reactive oxygen species from uncoupled eNOS on haemodynamic response in vivo, I next administered the non-selective antioxidant, *N*-acetylcysteine (NAC; Sigma-Aldrich, Gillingham, UK) in anaesthetised wild-type and *GCH1*$^{fl/fl}$Tie2cre mice. Haemodynamic parameters were recorded using the Millar catheter method in the left carotid arteries as described in section 5.3.1.2. Following 15 minutes equilibration and 15 minutes baseline recording, a single dose of either NAC (50 mg/kg) or saline was infused via jugular vein. The response was recorded over a 15-minute period and haemodynamic responses were calculated.

Administration of NAC caused a significantly greater decrease in systolic blood pressure in wild-type mice (-6.8 ± 1.7 mmHg) when compared with that in *GCH1*$^{fl/fl}$Tie2cre mice (-1.9 ± 1.1 mmHg; $P<0.05$) (Figure 5.5 A and B). No differences were detected in heart rate between wild-type and *GCH1*$^{fl/fl}$Tie2cre mice either before or after NAC treatment (Figure 5.5 C). In the control group, administration of saline (vehicle control) did not alter blood pressure or heart rate of either wild-type or *GCH1*$^{fl/fl}$Tie2cre mice (data not shown). There was no difference in respiratory rate during experimental procedure between wild-type and *GCH1*$^{fl/fl}$Tie2cre mice (Figure 5.5 D), indicating similar level of anaesthetic depth between the genotypes.

Figure 5.5

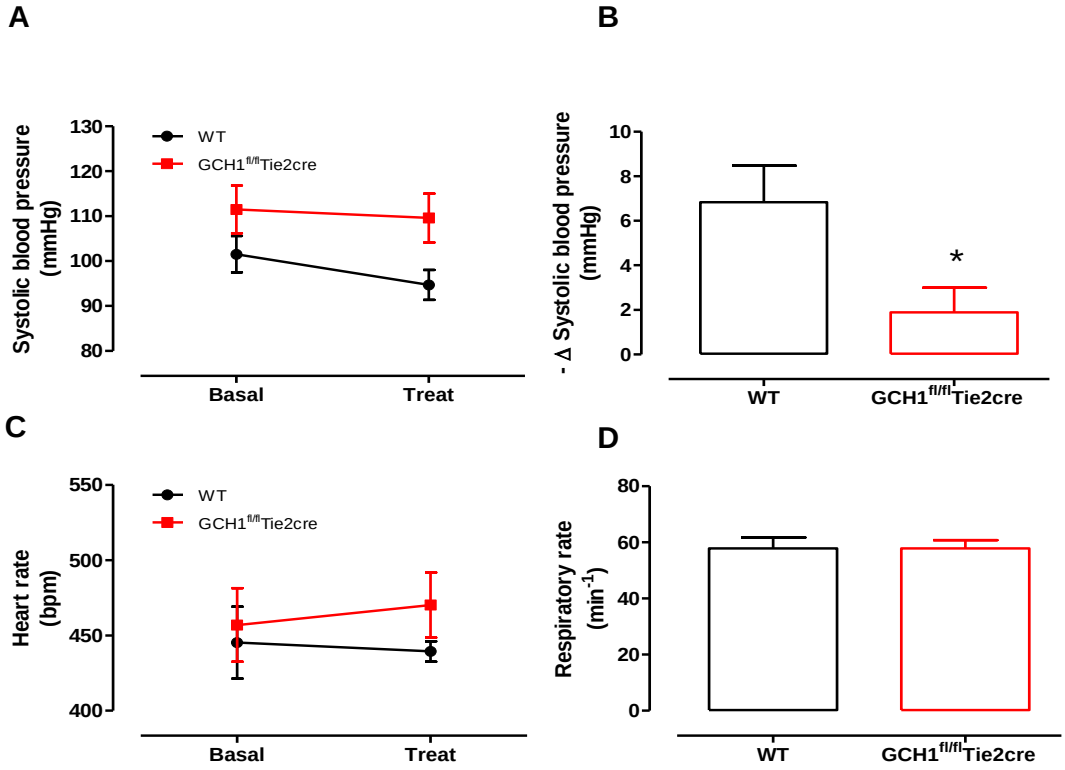


Figure 5.5. Effect of NAC on haemodynamic parameters in anaesthetised mice.

16-22 week-old mice were subjected to invasive Millar catheter haemodynamic recordings. Following 15 min baseline blood pressure recording, a single dose of N-acetylcysteine (NAC; 50 mg/kg IP) was administrated. **A)** Systolic blood pressure, expressed in mmHg. **B)** Mean quantitative data for the change (Δ) in systolic blood pressure following NAC administration. Acute administration of NAC caused a significantly greater decrease in systolic blood pressure in wild-type mice compared with *GCH1*$^{fl/fl}$Tie2cre mice. **C)** Heart rate, expressed in beat per minute (bpm). No difference was detected in heart rate of wild-type and *GCH1*$^{fl/fl}$Tie2cre mice either before or after NAC administration. **D)** Respiratory rate, expressed per minute (min^{-1}). Respiratory rate was comparable between wild-type and *GCH1*$^{fl/fl}$Tie2cre mice. Data are expressed as mean ± SEM. (*$P<0.05$; n=6 animals per group).

5.4.2.4 Effect of EUK-8 on haemodynamic responses

To further investigate the role of ROS from uncoupled eNOS on haemodynamic response in vivo, I next administered the Salen-manganese-based SOD/catalase mimetic, EUK-8 (Cayman Chemical, Cambridge Bioscience Ltd, UK) in anaesthetised mice of both genotypes. Haemodynamic parameters were recorded using a Millar catheter in left carotid arteries as described in section 5.3.1.2. Following 15 minutes equilibration and 15 minutes baseline recording, a single dose of either EUK-8 (25 mg/kg) or control was administrated via the intraperitoneal route. Haemodynamic responses were recorded over a 15-minute period.

Acute administration of EUK-8 significantly reduced systolic blood pressure in wild-type mice, whereas blood pressure was unaltered in *GCH1*$^{fl/fl}$Tie2cre mice (Figure 5.6 A and B). This finding suggests that EUK-8 may act to reduce blood pressure in wild-type mice, where BH4 bioavailability is not limited, due to the scavenging of basal ROS production, which in turn increases NO bioavailability. No differences were detected in heart rate between wild-type and *GCH1*$^{fl/fl}$Tie2cre mice either before or after EUK-8 treatment (Figure 5.6 C and Figure 5.7). There was no difference in respiratory rate during experimental procedure between wild-type and *GCH1*$^{fl/fl}$Tie2cre mice (Figure 5.6 D and Figure 5.7).

Figure 5.6

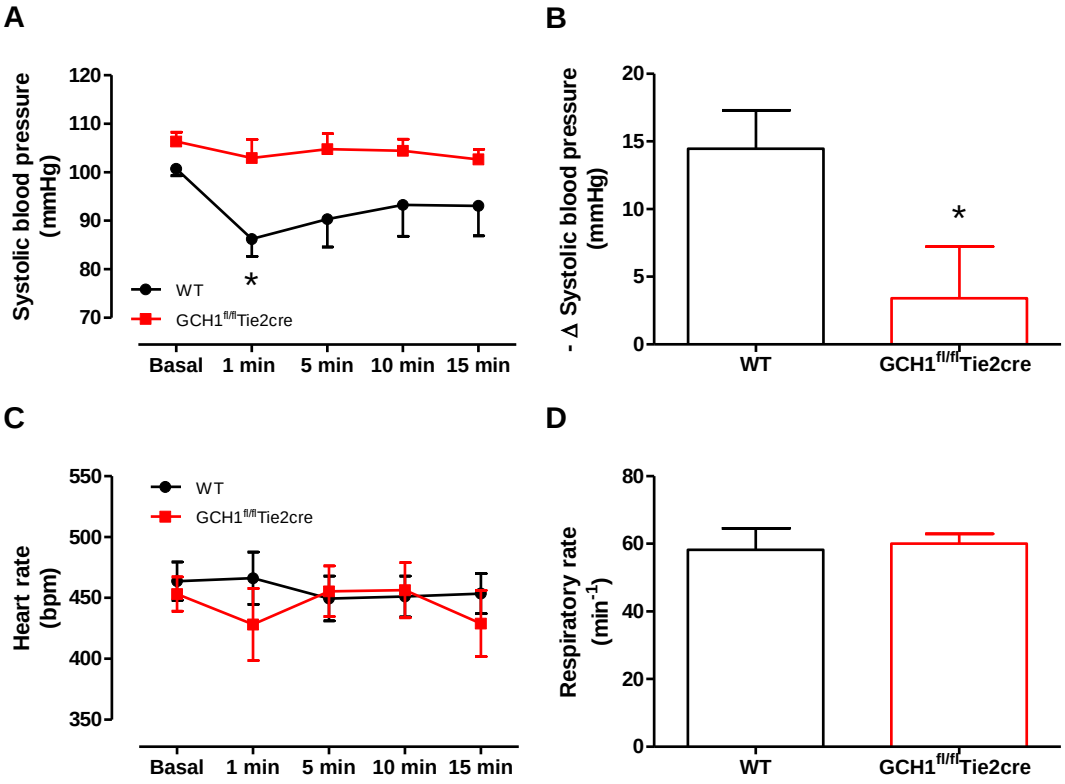


Figure 5.6. Effect of EUK-8 on haemodynamic parameters in anaesthetised mice.

16-22 week-old mice were subjected to invasive Millar catheter haemodynamic recordings. **A)** Systolic blood pressure, expressed in mmHg, in wild-type and *GCH1*$^{fl/fl}$Tie2cre mice before and after a single dose of EUK-8 (25 mg/kg IP) administration. **B)** Mean quantitative data for the change (Δ) in systolic blood pressure following EUK-8 administration (after 1 min). **C)** Heart rate, expressed in beats per minute (bpm). No differences were detected in heart rate of wild-type and *GCH1*$^{fl/fl}$Tie2cre mice either before or after EUK-8 administration. **D)** Respiratory rate, expressed per minute (min^{-1}). Respiratory rate was comparable between wild-type and *GCH1*$^{fl/fl}$Tie2cre mice. Data are expressed as mean ± SEM. (*$P<0.05$; n=6 to 9 animals per group).

Figure 5.7

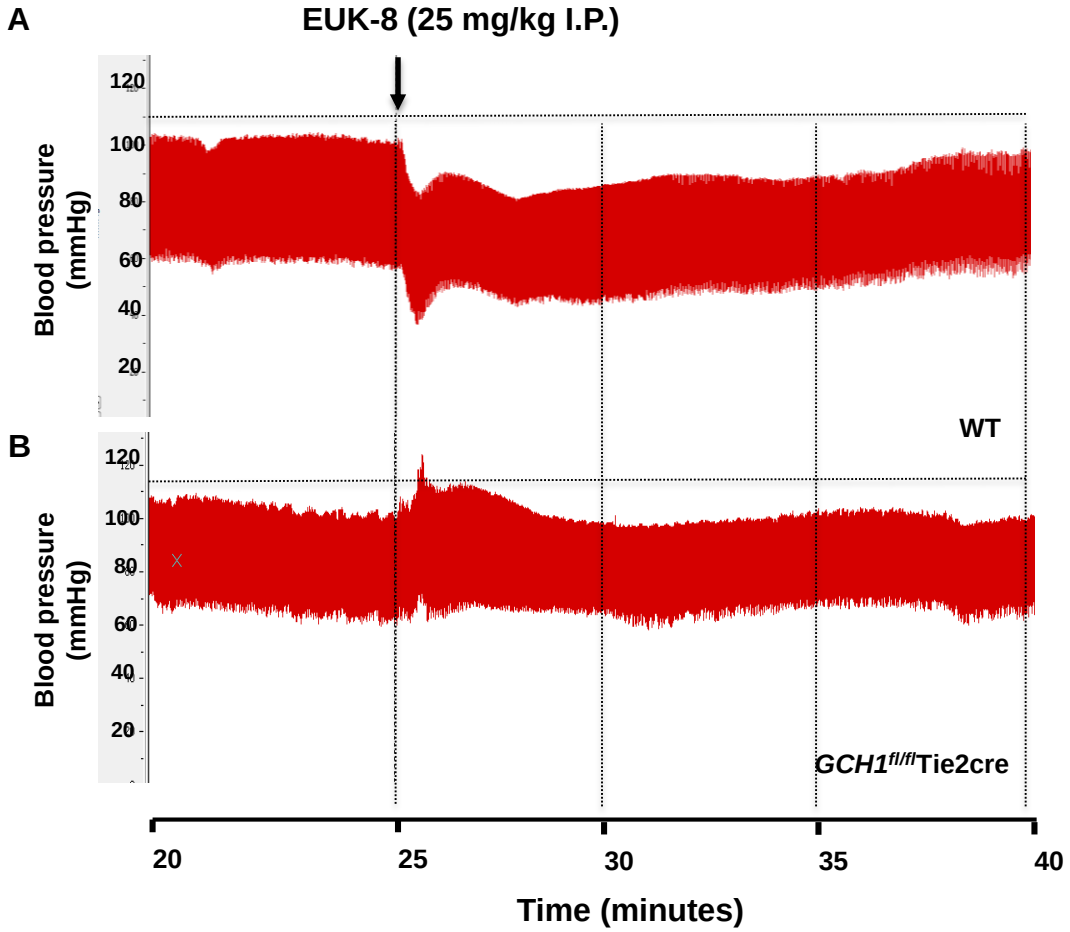


Figure 5.7. Effect of EUK-8 on haemodynamic parameters in anaesthetised mice.

Representative continuous blood pressure trace, measured using a Millar catheter, from a wild-type (WT)(above) and *GCH1*$^{fl/fl}$Tie2cre (below) mouse before and after a bolus dose of EUK-8 (25 mg/kg IP).

5.4.3 Haemodynamic responses in conscious mice via tail-cuff method

5.4.3.1 Chronic treatment of NAC (tail-cuff)

To determine the role ROS from uncoupled eNOS on blood pressure regulation in a conscious mice *in vivo*, I subjected wild-type and *GCH1*$^{fl/fl}$Tie2cre mice to systemic ROS scavenger by non-specific antioxidant N-acetylcysteine (NAC; Sigma-Aldrich, Gillingham, UK). Blood pressure was determined by tail-cuff method as described in Section 5.3.1.1. Following 5 days training and 3 days baseline recordings, wild-type and *GCH1*$^{fl/fl}$Tie2cre mice either received NAC in drinking water (5 g/l) or water control for 7 days. Blood pressure was recorded for 7 days. Following 7 days of treatment, NAC in drinking water was replaced with a normal drinking water (washout) for 7 days and blood pressure was again determined.

Chronic treatment of NAC in drinking for 7 days had no significant effect on systolic blood pressure or heart rate in either wild-type and *GCH1*$^{fl/fl}$Tie2cre mice (Figure 5.8 A and B). In water control group, no significant change in either blood pressure or heart rate of wild-type and *GCH1*$^{fl/fl}$Tie2cre mice was detected (Figure 5.8 C and D). NAC-treated mice of both genotypes showed a tendency toward a decrease in daily consumption of drinking water, but the difference did not reach statistical significance (Figure 5.8 E). No differences in the percentage body weight lost between control and NAC groups of both genotypes (Figure 5.8 F). This finding indicates that chronic treatment of non-specific antioxidant agent NAC in drinking water has no effect haemodynamic parameter in mice.

Figure 5.8

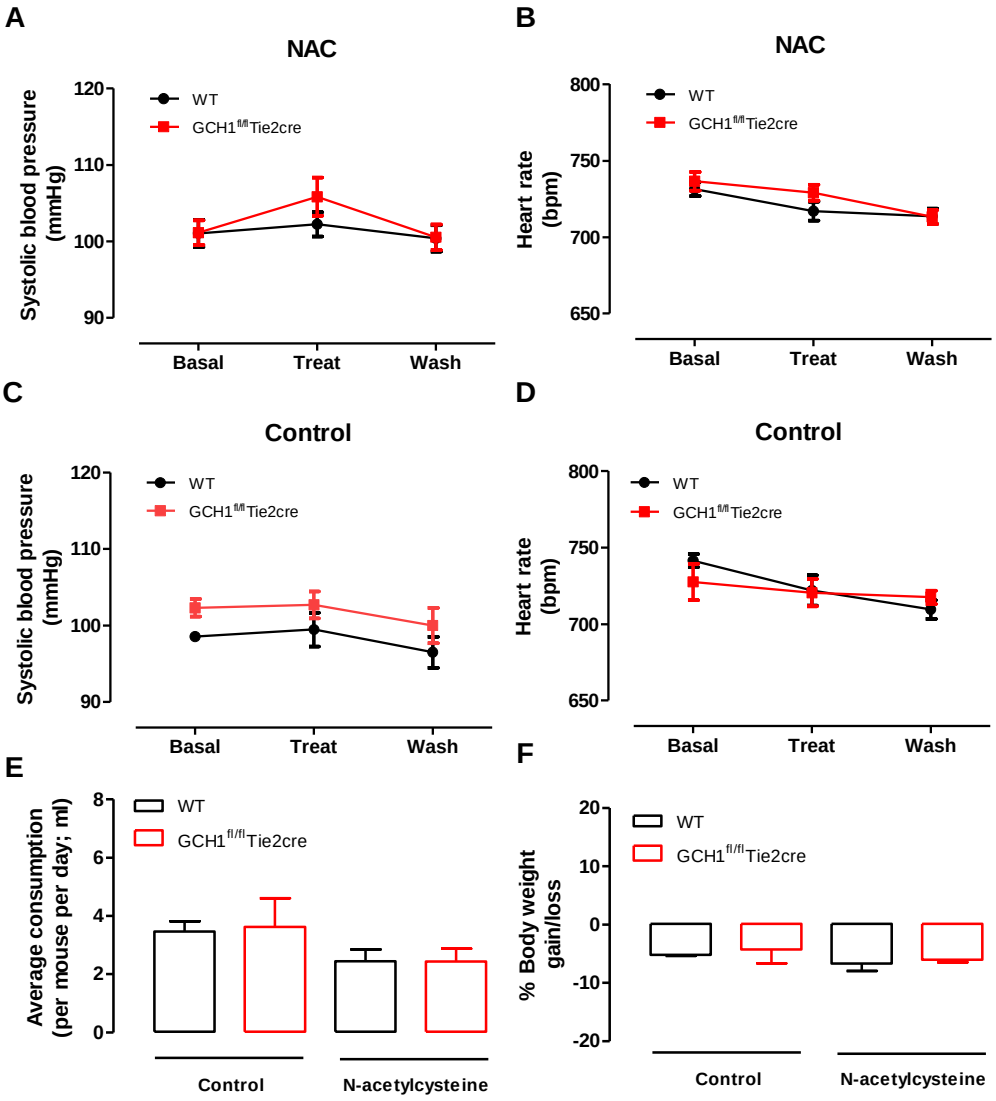


Figure 5.8. Effect N-acetylcysteine (chronic) on haemodynamic measurements

16-22 week-old mice either received NAC (5 g/L) in drinking water or water control alone for 7 days, were subjected to non-invasive tail-cuff recordings. Basal blood pressure and heart rate were recorded over 3 days and results averaged. Blood pressure and heart rate were recorded on day 7 of treatment (treat) and again on day 7 after NAC withdrawal (wash). **A and B)** NAC treatment had no significant effect on either blood pressure or heart rate of wild-type and *GCH1*$^{fl/fl}$Tie2cre mice. **C and D)** Blood pressure and heart rate of wild-type and *GCH1*$^{fl/fl}$Tie2cre mice in control group. **E)** Daily consumption of drinking water per mouse, expressed in ml. There was no difference in drinking water consumption between control and NAC group of both genotypes. **F)** There were no differences in the percentage body weight lost between control and NAC groups of both genotypes. Data are expressed as mean ± SEM. (n=6 animals per group).

5.4.3.2 Effect of chronic treatment of indomethacin (tail-cuff)

To determine the effect of prostaglandin-derived products on haemodynamic responses *in vivo*, wild-type and *GCH1*$^{fl/fl}$Tie2cre mice were subjected to systemic cyclooxygenase (COX) inhibition by indomethacin treatment (Sigma-Aldrich, Gillingham, UK) for 7 days. Haemodynamic responses were determined by the tail-cuff method as described in Section 5.3.1.1. Following 5 days training and 3 days basal recordings, wild-type and *GCH1*$^{fl/fl}$Tie2cre mice received either indomethacin (30 mg/l dissolved in 1% ethanol) or control (1% ethanol) in drinking water for 7 days. Blood pressures were recorded for 7 days and again 7 days after withdrawal of indomethacin treatment.

Indomethacin treated wild-type mice showed a tendency toward decrease in systolic blood pressure after 7 days of treatment, but the difference did not reach statistical significance. Seven days after withdrawal of indomethacin treatment, systolic blood pressure was returned to similar to the in pre-treatment state (Figure 5.9 A). In *GCH1*$^{fl/fl}$Tie2cre mice, chronic administration of indomethacin had no significant effect on systolic blood pressure either before or, during, or after treatment (Figure 5.9 A). Chronic treatment of indomethacin in drinking water for 7 days significantly reduced heart rate of both genotypes, which returned to a baseline after withdrawal of treatment (Figure 5.9 B). In the control group, no significant change was detected in either blood pressure or heart rate of wild-type and *GCH1*$^{fl/fl}$Tie2cre mice either before, during or after indomethacin treatment (Figure 5.9 C and D). Mean of daily consumption of drinking water per mouse, expressed in ml, was comparable between control group and indomethacin group (Figure 5.9 E). No differences were observed in the percentage body weight lost between control and indomethacin groups of both genotypes (Figure 5.9 F). This finding suggests that chronic treatment with indomethacin in drinking water for 7 days has little effect on haemodynamic response in both genotypes.

Figure 5.9

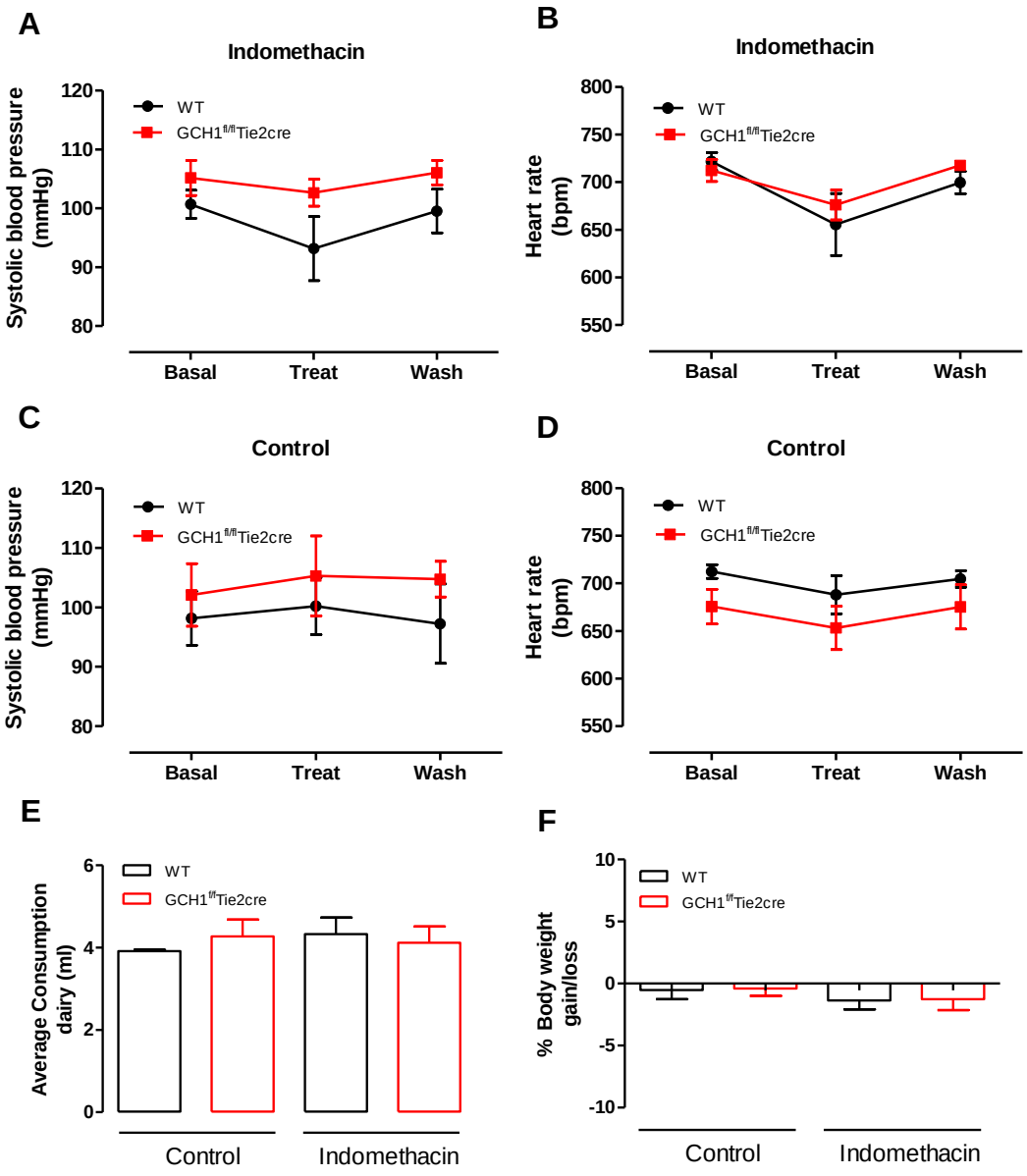


Figure 5.9. Effect indomethacin (chronic) on haemodynamic measurements

16-22 week-old mice either received indomethacin (30 µg/l) in drinking water or control for 7 days, were subjected to non-invasive tail-cuff recordings. Following 3 days basal blood pressure recordings, blood pressure was recorded on day 7 of treatment and again on day 7 after indomethacin withdrawal (wash). **A and B)** Indomethacin treatment had no significant effect on either blood pressure or heart rate of wild-type and *GCH1*$^{fl/fl}$Tie2cre mice. **C and D)** Blood pressure and heart rate of wild-type and *GCH1*$^{fl/fl}$Tie2cre mice in control group. **E)** Daily consumption of drinking water per mouse, expressed in ml. There no difference in drinking water consumption between control and indomethacin group of both genotypes. **F)** The percentage weight loss was significantly increased in mice of both genotypes treated with indomethacin compared to control mice of both genotypes. Data are expressed as mean ± SEM. (n=6 animals per group).

5.4.3.3 Effect of chronic treatment of L-NAME

To determine whether the difference in systolic blood pressure could be mediated by NOS, wild-type and *GCH1*$^{fl/fl}$Tie2cre mice were subjected to systemic NOS inhibition by L-NAME (Sigma-Aldrich, Gillingham, UK) in the drinking water for 7 days. Blood pressure was determined by tail-cuff method as described in Section 5.3.1.1. Following 5 days training, basal haemodynamic measurements were performed over 3 days and results averaged. It has been shown previously that administration of L-NAME (1 mg/kg) in drinking water caused an increase in systolic blood pressure and a reduction in heart rate after 7 days of treatment (Adlam D. 2012 *DPhil. Thesis, University of Oxford*). For this reason I decided to treat mice with 1 mg/kg of L-NAME in drinking water for 7 days. Blood pressures were determined on day 7 of L-NAME treatment.

As expected, *GCH1*$^{fl/fl}$Tie2cre mice have significantly higher basal systolic blood pressure than wild-type littermates at baseline (102.4 ± 1.99 mmHg vs 95.88 ± 1.28 mmHg; $P<0.05$)(Figure 5.10 A). Heart rate was also significantly reduced in *GCH1*$^{fl/fl}$Tie2cre mice compared to wild-type littermates (757 ± 4 bpm vs 737 ± 6 bpm; $P<0.05$)(Figure 5.10 B). After L-NAME treatment for 7 days, systolic blood pressure was significantly increased in both genotypes, such that blood pressures were no longer different between *GCH1*$^{fl/fl}$Tie2cre mice (113.4 ± 1.8 mmHg) and wild-type (114.3 ± 1.1 mmHg)(Figure 5.4 A), suggesting that increased blood pressure in *GCH1*$^{fl/fl}$Tie2cre mice is NOS-mediated. In addition, NOS inhibition significantly reduced heart rates in L-NAME treated mice of both genotypes, but the difference is still maintained, suggesting the resting bradycardia in *GCH1*$^{fl/fl}$Tie2cre mice may not be NOS-mediated (Figure 5.10 B). Systolic blood pressure and heart rate of both genotypes remained unaltered in the control group (Figure 5.10 C and D). No differences in daily consumption of drinking water between control (4.06 ± 0.37 ml in WT versus 4.09 ± 0.34 ml in *GCH1*$^{fl/fl}$Tie2cre) and L-NAME groups (3.98 ± 0.39 ml in wild-type versus 3.77±

0.51 ml in *GCH1*$^{fl/fl}$Tie2cre) was observed. No differences in body weight loss were detected between control and L-NAME groups of both genotypes (Figure 5.10 E and F).

Figure 5.10

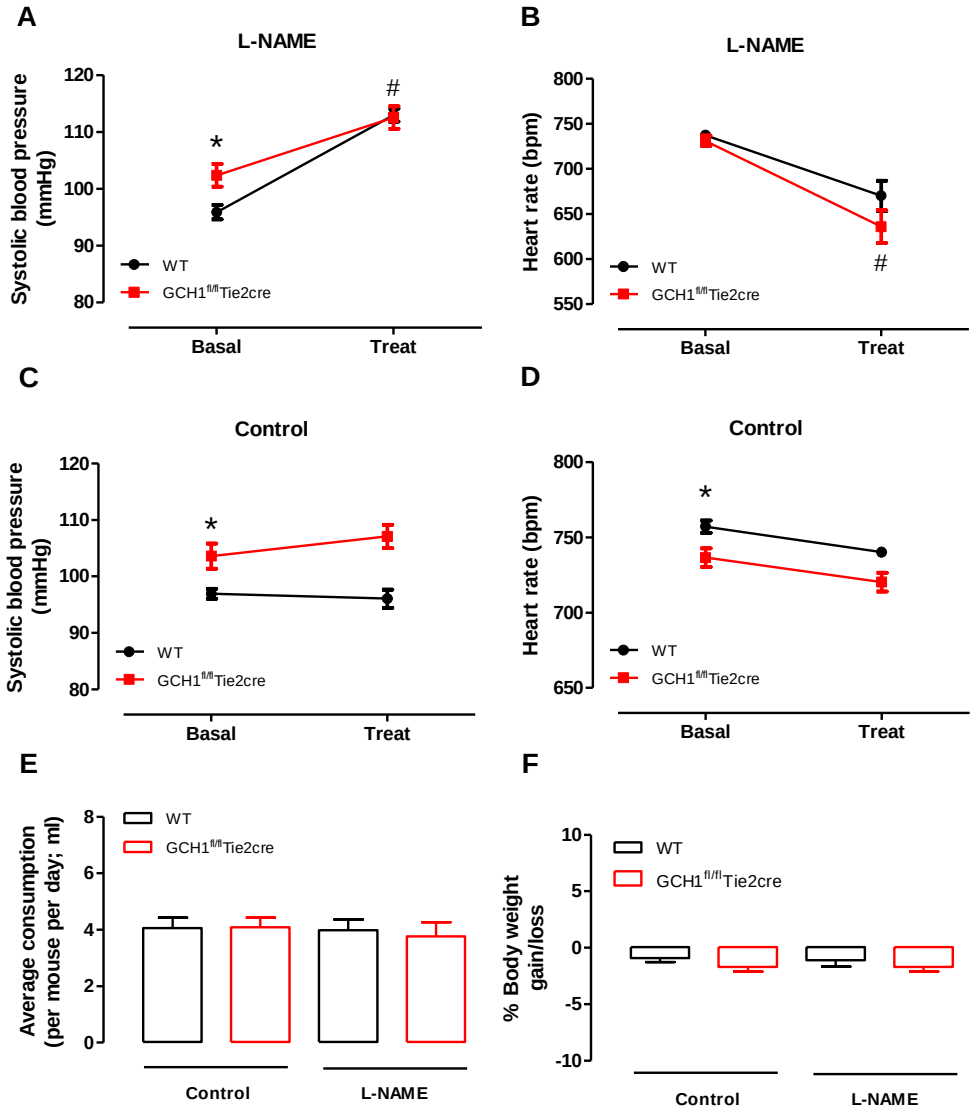


Figure 5.10. Effect L-NAME (chronic) on haemodynamic measurements

Basal haemodynamic measurements were performed over 5 days and results averaged. The measurements were recorded on day 7 of treatment (treat). **A and B)** Systolic blood pressure and heart rate respectively, in control group of both genotypes. **C and D)** Systolic blood pressure and heart rate respectively, in L-NAME group of wild-type and *GCH1*$^{fl/fl}$Tie2cre mice. **E)** Treatment consumption, expressed in ml. No differences were detected between genotypes of both control and L-NAME groups. F) No differences in body weight between control and L-NAME groups of both genotypes. Data are expressed as mean ± SEM. (**P<0.05* comparing genotypes, *#P<0.05* comparing treatment; n=6 animals per group).

5.4.4 Ang II induced Hypertension

5.4.4.1 Haemodynamic response to acute Ang II infusion in anaesthetised mice

To investigate the of role endothelial cell BH4 biosynthesis on the blood pressure response to angiotensin II (Ang II), haemodynamic parameters were measured using a Millar catheter in the left carotid artery as described previously in Section 5.3.1.2. Following 15 min baseline recording, a single dose of angiotensin II (10 μg/kg) was administrated via the intraperitoneal route. Haemodynamic responses were taken over a 5-minute period and blood pressure was determined. Acute administration of Ang-II caused a significantly greater increase in systolic blood pressure in *GCH1*$^{fl/fl}$Tie2cre mice (7.0 ± 1.2 mmHg) compared with wild-type mice (2.4 ± 0.4 mmHg; $P<0.01$) (Figure 5.11 A and B), suggesting a lower threshold for Ang II sensitivity. Ang II administration markedly significantly reduced heart rates in both wild-type (- 11 ± 3 beat per min) and *GCH1*$^{fl/fl}$Tie2cre mice (-12 ± 4 beat per min) (Figure 5.11 C)

Figure 5.11

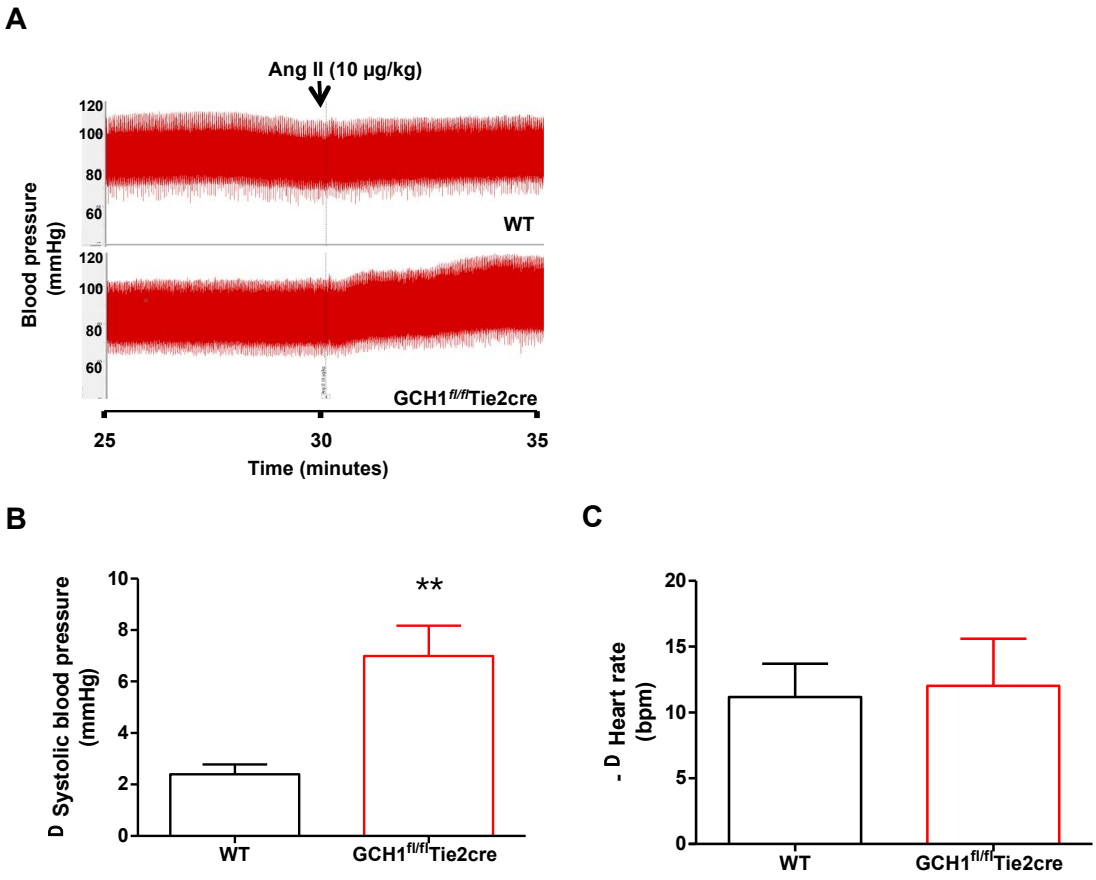


Figure 5.11. Haemodynamic measurements in response to acute angiotensin II

A) Representative continuous blood pressure traces, measured by Millar catheter, from a wild-type and *GCH1*$^{fl/fl}$Tie2cre mice before and after a bolus injection of 10 µg/kg angiotensin II (Ang II) with quantitative data for change in systolic blood pressure following Ang II administration. **B)** Ang II caused a significantly greater increase in systolic blood pressure in *GCH1*$^{fl/fl}$Tie2cre mice when compared with that in wild-type controls. **C)** Ang II markedly decreased heart rate in both wild-type and *GCH1*$^{fl/fl}$Tie2cre mice. Data are expressed as mean ± SEM. (***P<0.01;* n=6 animals per group).

5.4.4.2 Haemodynamic response to chronic in vivo Ang II infusion (tail-cuff method)

I next determined the effect of endothelial cell BH4 deficiency on blood pressure regulation in response to chronic Ang II-infusion in vivo. The haemodynamic measurements were determined using non-invasive tail-cuff method as described in section 5.3.1.1. Following 5 days training period and 3 days baseline recordings, osmotic minipumps filled with either angiotensin II (0.4 mg/kg/day) or saline (PBS) was implanted in wild-type and *GCH1*$^{fl/fl}$Tie2cre mice as described in section 5.3.2.1. After 24 hour surgical recovery period, blood pressure recordings were recorded on day 3, 5, 7 10 and 12.

As expect, basal systolic blood pressure was significantly increased in *GCH1*$^{fl/fl}$Tie2cre mice (108±1 mmHg) compared with wild-type littermate controls (101±2 mmHg; $P<0.05$)(Figure 5.12 A). On day 3 of Ang-II infusion, systolic blood pressure was significantly increased in *GCH1*$^{fl/fl}$Tie2cre mice (132 ± 10 mmHg; $P<0.01$) but unchanged in wild-type mice (102± 2 mmHg). After day 3, the increased systolic blood pressure was maintained throughout the study in Ang II infused *GCH1*$^{fl/fl}$Tie2cre mice. In contrast, Ang II infusion did not have a significant effect on systolic blood pressure of wild-type mice in the study (Figure 5.12 A). Basal heart rate was significantly reduced in *GCH1*$^{fl/fl}$Tie2cre mice (657 ± 18 bpm) compared to wild-type littermates (698± 9 bpm)(Figure 5.12 B). After 3 days of Ang II infusion, heart rate in *GCH1*$^{fl/fl}$Tie2cre mice was significantly reduced (551 ± 23 bpm)($P<0.01$) compared to basal readings but remained unchanged in wild-type mice (703 ± 21 bpm)(Figure 5.12 B). Heart rates were remained lower throughout Ang II infusion in *GCH1*$^{fl/fl}$Tie2cre mice but were unaltered in wild-type mice (Figure 5.12 B). In control mice, saline infusion had no significant effect on either systolic blood pressure or heart rates of wild-type and *GCH1*$^{fl/fl}$Tie2cre mice (Figure 5.12 C and D).

Figure 5.12

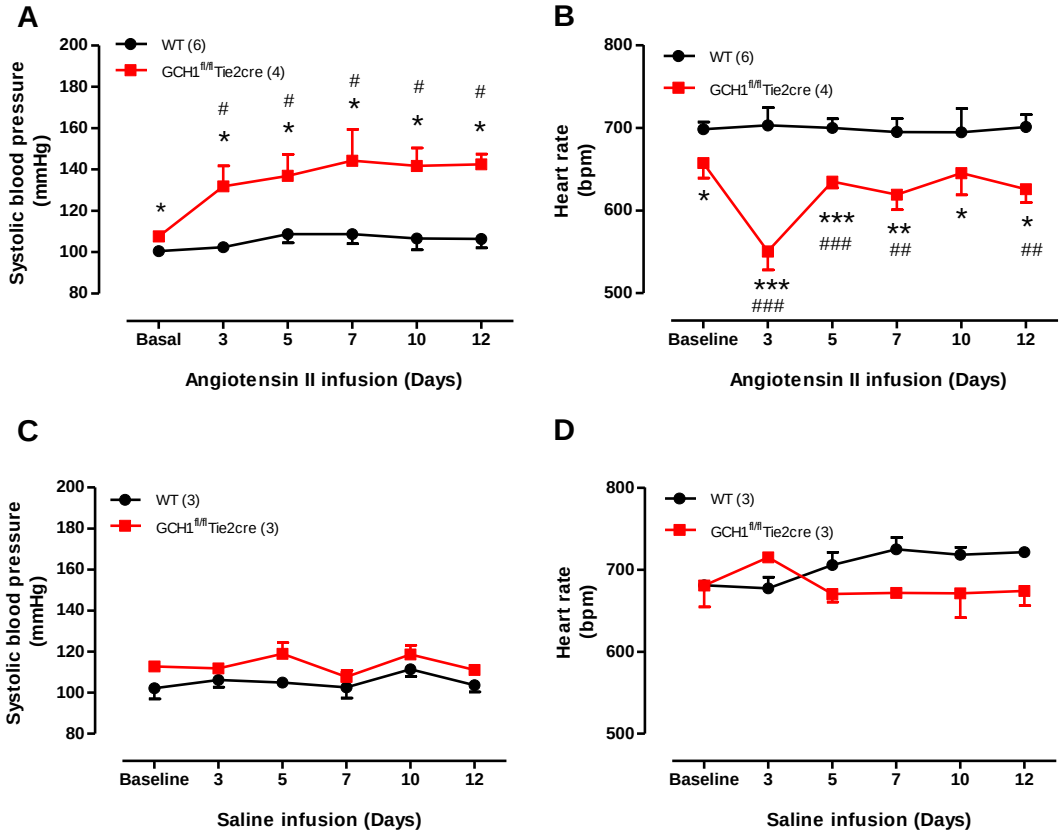


Figure 5.12. Haemodynamic measurements in response to chronic angiotensin II infusion

Osmotic minipumps containing angiotensin II (Ang II; 0.4 mg/kg/day) or saline was implanted in male wild-type and *GCH1*$^{fl/fl}$Tie2cre mice (16-22 week-old). Mice were subjected to non-invasive tail-cuff recordings for 14 days. **A)** Systolic blood pressure significantly increased in *GCH1*$^{fl/fl}$Tie2cre mice after 3 days of Ang II infusion, but unaltered in wild-type mice. **B)** Heart rate significantly reduced in *GCH1*$^{fl/fl}$Tie2cre mice after 3 days of Ang II infusion, but unaltered in wild-type mice. **C and D)** Systolic blood pressure and heart rate respectively in saline-infused mice. Data are expressed as mean ± SEM. (**P<0.05, **P<0.01, ***P<0.01* comparing genotypes, *#P<0.05, ##P<0.01, ###P<0.001* comparing treatment; n=6 animals per group).

5.4.4.3 Ang II induced AAA formation in GCH1$^{fl/fl}$Tie2cre mice

During 14 days of Ang-II infusion study, 40% of Ang II-infused *GCH1$^{fl/fl}$*Tie2cre mice were found dead with abdominal aortic aneurysm (AAA) rupture (2/5). Among the survivors, 33% developed AAA formation (1/3), resulting in an incidence of aneurysm of 60% (3/5). In contrast, none of the Ang II-infused wild-type mice died or developed AAA formation, and importantly none of the saline (control)-infused wild-type or *GCH1$^{fl/fl}$*Tie2cre mice died or developed AAA formation (Figure 5.13 A and B).

Figure 5.13

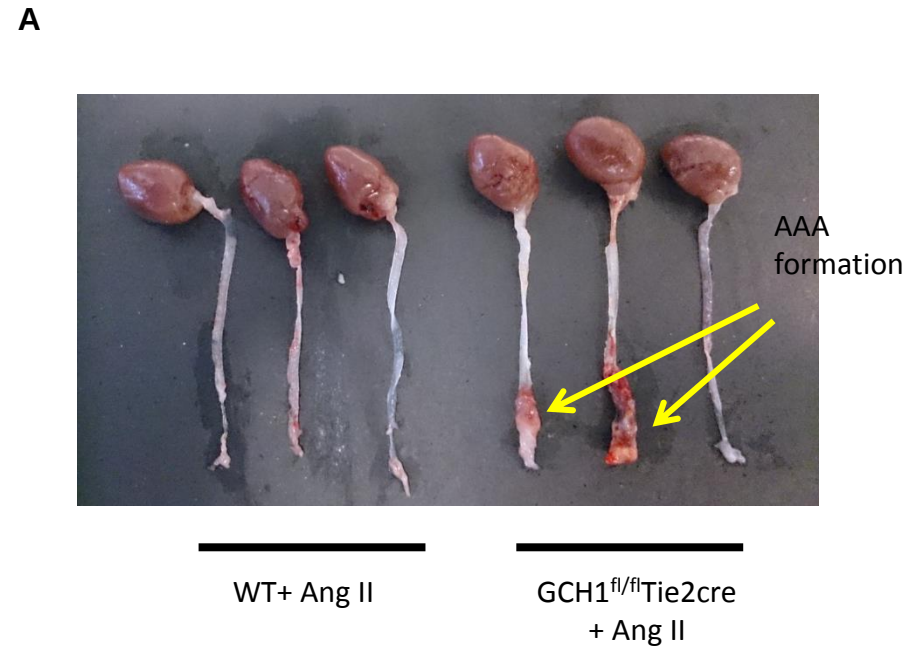


Figure 5.13. Abdominal Aortic Aneurysm formation

GCH1$^{fl/fl}$Tie2cre and wild-type mice were treated with 0.4 mg/kg/day Angiotensin II infusion for 14 days. Ang II treatment causes aortic aneurysms in *GCH1*$^{fl/fl}$Tie2cre mice but aneurysms are not seen in Ang II treated wild-type. **A)** Representative appearance of abdominal aortic aneurysm (AAA) formation. **B)** AAA formation rates in Ang II-infused *GCH1*$^{fl/fl}$Tie2cre mice and Ang II-infused wild-type mice. Only Ang II-infused *GCH1*$^{fl/fl}$Tie2cre mice developed AAA. (*$P<0.05$, n=5 to 6 animals per group)

5.4.5 LPS-induced hypotension

It has been shown previously that administration of LPS causes an increase in vascular *GCH1* mRNA, GTPCH expression and BH4 levels in (Cunha et al., 1994) and rats (Szabo et al., 1994b). This is accompanied by an increase in iNOS mRNA and protein expression in the vascular endothelium and smooth muscle cells, which in turn increases vascular NO generation, causing hypotension. In this study, I investigated whether deficiency in endothelial cell *GCH1* and thus endothelial cell BH4 biosynthesis provides an alternative therapeutic mechanism to regulate vascular NOS-derived NO overproduction and haemodynamic in LPS-induced systemic inflammation.

5.4.5.1 Haemodynamic response to LPS

Haemodynamic parameters in conscious mice were recorded using tail-cuff plethysmography as described in Section 5.3.1.1. Following training and basal blood pressure recordings, $GCH1^{fl/fl}$Tie2cre and wild-type littermates (16-22 week-old) were administrated with a single dose of either 1 mg/kg LPS or saline control via intraperitoneal route as described in Section 5.3.2.2. Blood pressures were determined at 6-hour and 24-hours post administration. Administration of 1 mg/kg LPS is not associated with mortality in this study.

As expected, basal systolic blood pressure was significantly increased in $GCH1^{fl/fl}$Tie2cre mice (105.8 ± 2.2 mmHg) compared to wild-type littermates (98.8 ± 2.0 mmHg; $P<0.05$). Six hours post LPS injection, systolic blood pressures were significantly decreased in both wild-type (80.1 ± 3.2 mmHg; $P<0.01$) and $GCH1^{fl/fl}$Tie2cre mice (95.3 ± 2.9 mmHg; $P<0.05$)(Figure 5.14 A), but with a greater reduction in wild-type mice (-20.8 ± 3.7 mmHg) compared to $GCH1^{fl/fl}$Tie2cre mice (-7.9 ± 4.2 mmHg; $P<0.05$)(Figure 5.14 C). 24-hours

post injection, the decrease in systolic blood pressure was also significantly greater in wild-type-treated LPS-mice (-24.3 ± 3.0 mmHg) compared to *GCH1*$^{fl/fl}$Tie2cre mice (-12.5 ± 2.8 mmHg; $P<0.05$). Administration of LPS significantly reduced heart rate of both genotypes at 6-hour post injection (from 680 ± 12 bpm to 603 ± 17 bpm in wild-type mice and from 694 ± 10 bmp to 598 ± 15 bpm) and 24-hour post injection (592 ± 22 bpm in wild-type mice and 572 ± 20 bpm in *GCH1*$^{fl/fl}$Tie2cre mice)(Figure 5.14 B). In the control group, saline-treated mice had no significant effect on either systolic blood pressures or heart rates in both genotypes (data not shown).

Figure 5.14

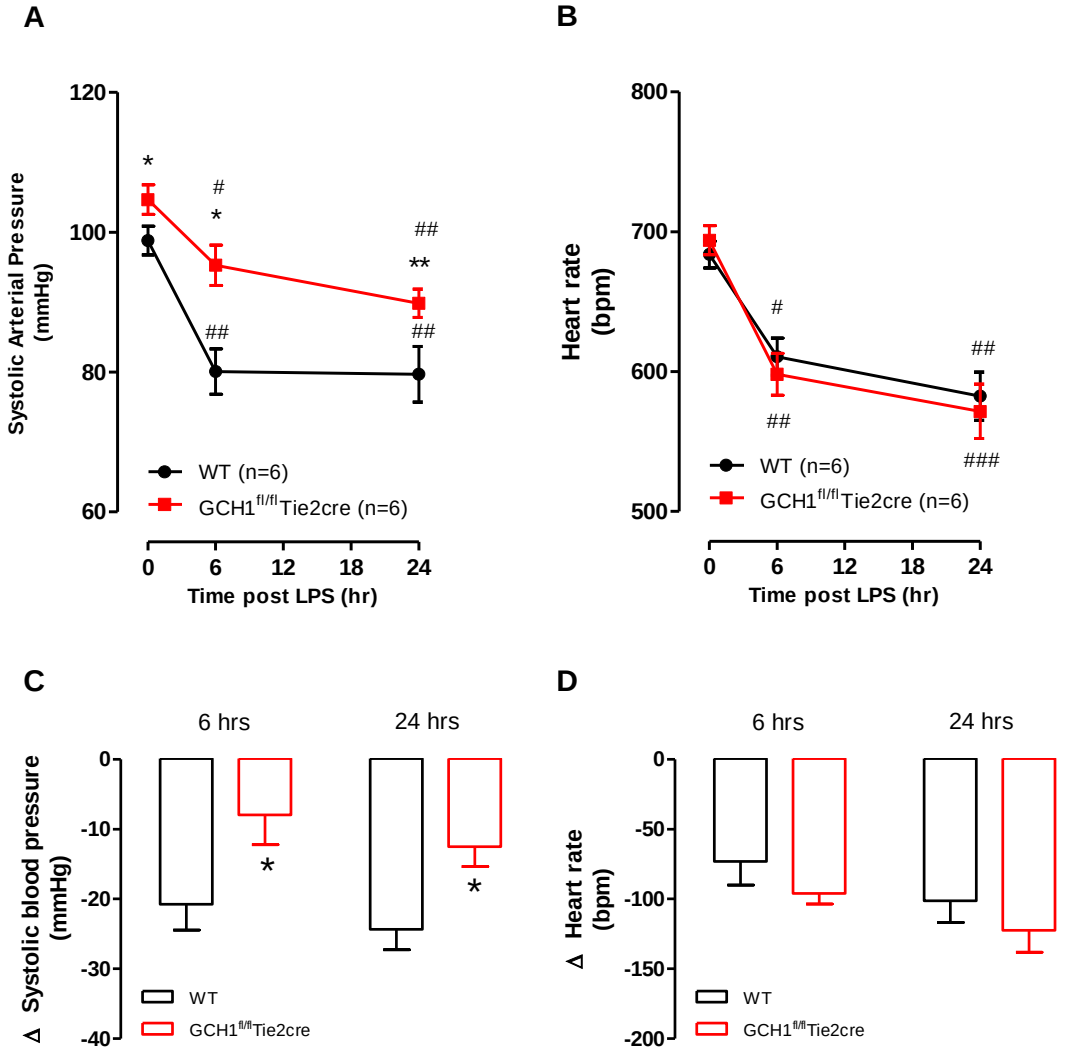


Figure 5.14. Effect of LPS on haemodynamic parameters in *GCH1$^{fl/fl}$*Tie2cre mice.

16-22 week-old mice from both genotypes, either received a single dose of 1 mg/kg (IP.) lipopolysaccharide (LPS) or saline control was subjected to non-invasive tail-cuff recordings. Basal haemodynamic measurements were performed over 3 days and results averaged. The measurements were recorded at 6-hour and 24-hour post LPS administration. **A)** Systolic blood pressure and **B)** heart rate. Data are expressed as mean ± SEM. (**P<0.05, **P<0.01* comparing genotypes, *#P<0.05, ##P<0.01* comparing treatment*;* n=6 animals per group).

5.4.5.2 Effect of LPS administration on vascular reactivity in mesenteric arteries

To investigate whether a reduction in blood pressure is related to changes in contractile response in resistance vasculature, wild-type and *GCH1*$^{fl/fl}$Tie2cre mice were injected with either 1 mg/kg LPS or saline control. 24 hours post injection, mice from both control and LPS group were culled and the mesenteric arcade was collected as described in Section 2.8.1. Vascular reactivity of isolated 2nd order mesenteric arteries was determined using wire myograph as described in Section 2.8.4.

In wild-type mesenteric arteries, LPS administration significantly attenuated contractile response to α-adrenoceptor agonist phenylephrine (PE) in mesenteric arteries from wild-type mice (Figure 5.15 A). This blunted contractile response was prevented in the presence of L-NAME (Figure 5.15 C), such that there was no longer a difference in vasoconstriction between saline-treated wild-type mice and LPS-treated wild-type mice, indicating that increased basal NOS-derived NO is responsible for the decreased vasoconstrictor response in mesenteric arteries from LPS-treated wild-type. Similar findings were also observed when thromboxane A2 agonist U46619 is used (Figure 5.16 A and C), suggesting that the blunted vasoconstrictor response was not due to specific alteration of receptor signalling on endothelial cells.

In *GCH1*$^{fl/fl}$Tie2cre mesenteric arteries, LPS-treated *GCH1*$^{fl/fl}$Tie2cre mice had no significant alteration in vasoconstrictor response to either PE or U46619 (Figure 5.15 B and 5.16 B). L-NAME treatment had little effect on contractile response in LPS-treated *GCH1*$^{fl/fl}$Tie2cre mice (Figure 5.15 D and 5.16 D).

Figure 5.15

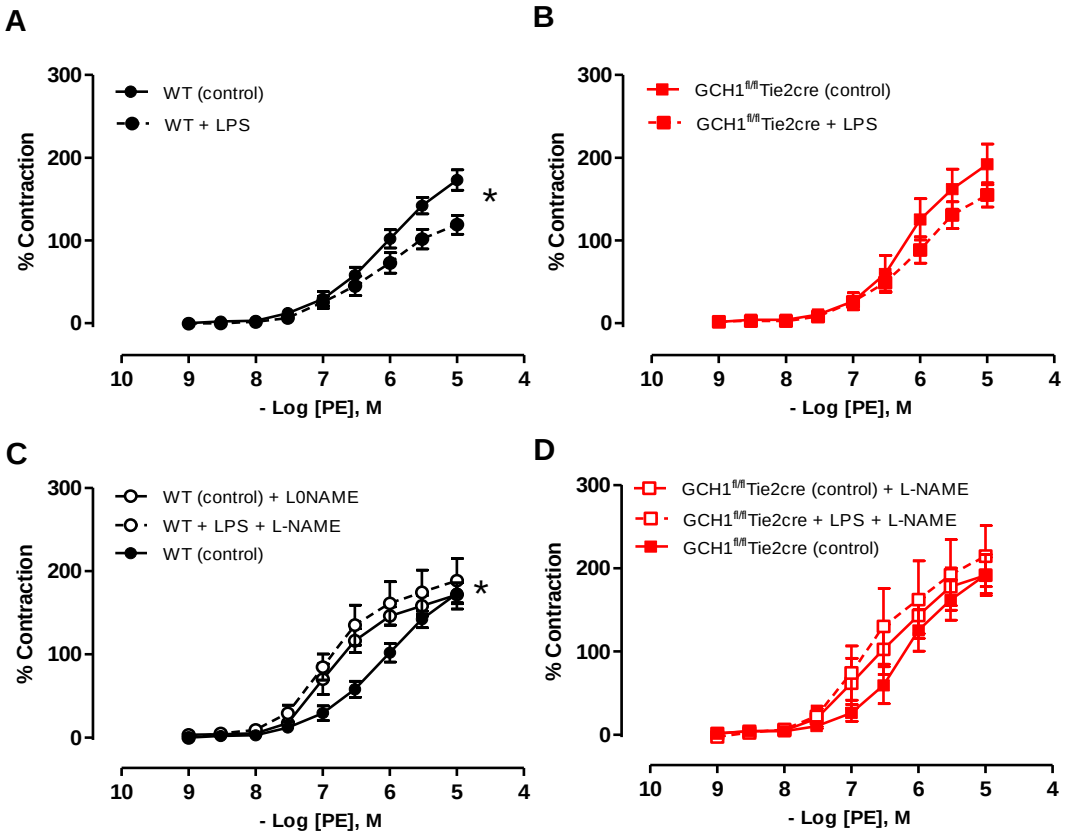


Figure 5.15. Effect of LPS on vascular reactivity in isolated mesenteric arteries.

Vasoconstriction to phenylephrine (PE), expressed in percentage contraction to KCl. **A)** Increased vasoconstriction to PE was significantly blunted in LPS treated wild-type (WT) mice compared to control WT mice. **B)** No differences were detected between control *GCH1*$^{fl/fl}$Tie2cre mesenteric arteries and LPS-treated *GCH1*$^{fl/fl}$Tie2cre mesenteric arteries. **C and D)** In the presence of nitric oxide synthase inhibitor (100 mM; L-NAME), vasoconstrictions were increased and normalised in both control and LPS groups of both genotypes compared to wild-type aortas. Data are expressed as mean ± SEM. (*$P<0.05$; n=8 to 10 animals per group).

Figure 5.16

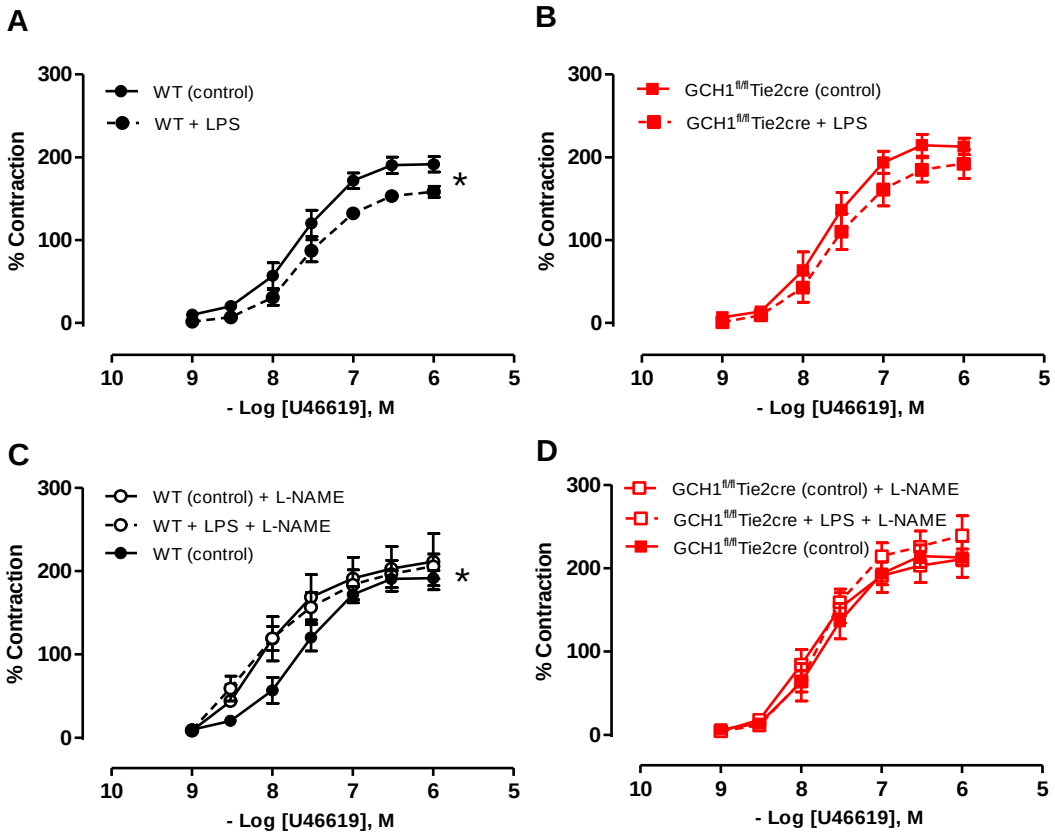


Figure 5.16. Effect of LPS on vascular reactivity in isolated mesenteric arteries.

Vasoconstriction to U46619 expressed in percentage contraction to KCl. **A)** Increased vasoconstriction to U46619 was significantly blunted in LPS treated wild-type (WT) mice compared to control WT mice. **B)** No differences were detected between control *GCH1*$^{fl/fl}$Tie2cre mesenteric arteries and LPS-treated *GCH1*$^{fl/fl}$Tie2cre mesenteric arteries. **C and D)** In the presence of nitric oxide synthase inhibitor (100 mM; L-NAME), vasoconstrictions were increased and normalised in both control and LPS groups of both genotypes. Data are expressed as mean ± SEM. (*$P<0.05$; n=8 to 10 animals per group)

5.4.5.3 Effect of LPS administration on vascular reactivity in aortas

I next determined the effect of systemic inflammation on vascular reactivity in conduit vessels. Wild-type and *GCH1*$^{fl/fl}$Tie2cre mice were injected with either 1 mg/kg LPS or saline control for 24 hours. Following 24 hours post injection, saline and LPS treated mice were culled and thoracic aortas were excised and collected as described in Section 2.8.1. Vascular reactivity of isolated aortic rings was determined using wire myograph as described in Section 2.8.3.

Administration of LPS at 1 mg/kg of body weight for 24 hours had no significant effect on vascular reactivity to either phenylephrine or U46619 of both genotypes compared to saline-treated group (Figure 5.17 A and B). In the presence of L-NAME, contractile responses were significantly increased in all groups compared to untreated groups (Figure 5.17 C and D). This finding suggests that administration of LPS at 1 mg/kg is not sufficient to alter vascular reactivity in either genotype.

Figure 5.17

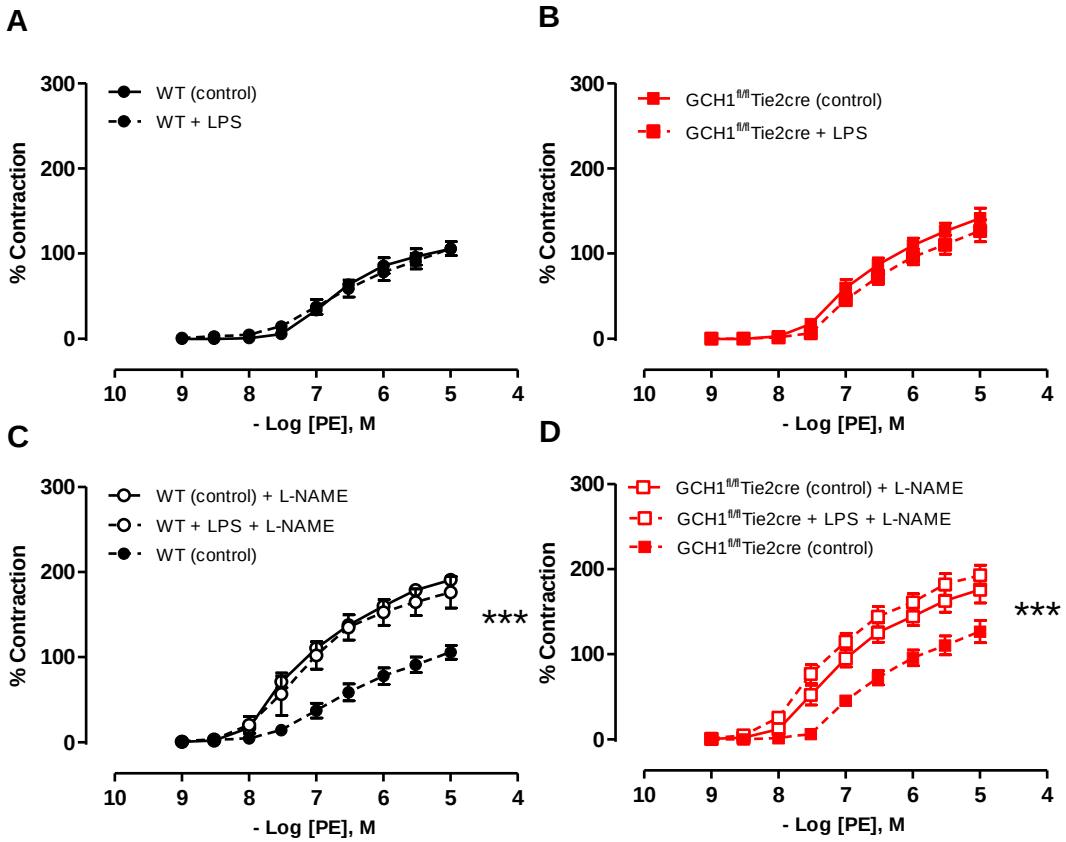


Figure 5.17. Effect of LPS on vascular reactivity in isolated aortas.

Vasoconstriction to PE expressed in percentage contraction to KCl. LPS treatment has no significant effect on vascular constrictor response of either **A)** wild-type or **B)** *GCH1*$^{fl/fl}$Tie2cre aortas. **C and D)** In the presence of nitric oxide synthase inhibitor (100 mM; L-NAME), vasoconstrictions were increased and normalised in both control and LPS groups of both genotypes. Data are expressed as mean ± SEM. (*$P<0.05$, ***$P<0.001$; n=5 to 6 animals per group)

5.4.5.4 Aortic BH4 Levels of LPS-treated mice

It has been previously shown that administration of LPS results in an increase in GTPCH protein expression and BH4 levels in vascular tissues such as aorta. To determine vascular BH4 levels in response to systemic LPS treatment, wild-type and *GCH1*$^{fl/fl}$Tie2cre mice were administrated with a single dose of either 1 mg/kg LPS or saline control. 24-hours post injection, mice were culled and aortas were collected for biopterin measurement as described in Section 2.4.

In the saline treated group, there was a marked reduction in total biopterin and BH4 levels in *GCH1*$^{fl/fl}$Tie2cre aortas (2.67 ± 0.17 pmol/mg) compared with wild-type aortas (9.11 ± 0.89 pmol/mg; $P<0.05$) (Figure 5.18). Following LPS treatment, the total biopterin and BH4 levels were significantly increased in aortas from both wild-type and *GCH1*$^{fl/fl}$Tie2cre mice (11.30 ± 1.29 pmol/mg), but to a greater extent in wild-type mice (25.29 ± 2.03 pmol/mg)($P<0.001$) (Figure 5.18).

Figure 5.18

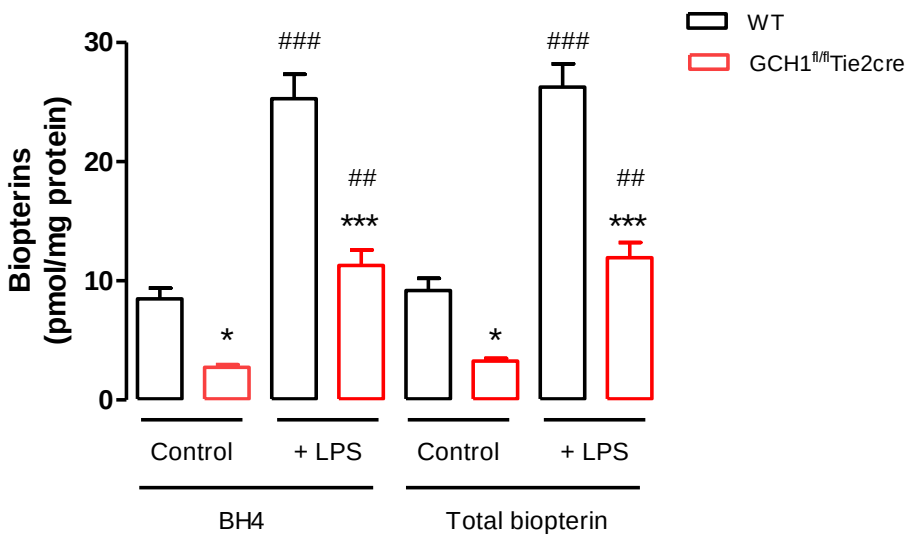


Figure 5.18. Total biopterin and BH4 levels in aortas.

16-22 week-old mice from both genotypes received either a single dose of 1 mg/kg (IP.) LPS or PBS (control). After 24 hours, aortas from control and LPS groups were harvested. Total biopterin and BH4 in aortas were determined using HPLC. In control group, total biopterin and BH4 in aortas was significantly reduced in *GCH1*$^{fl/fl}$Tie2cre aortas compared to wild-type aortas. LPS treatment significantly increased total biopterin and BH4 levels in aortas of both genotypes but the differences still maintained. Data are expressed as mean ± SEM. (*$P<0.05$, ***$P<0.001$ comparing genotypes, ##$P<0.01$, ###$P<0.001$ comparing treatment; n=3 to 6 aortas per group).

5.4.5.5 Ex vivo LPS treatment in aortas

It has been shown previously that administration of LPS causes an attenuation of a contractile function in mouse aortas (Lund et al., 2007). Due to the severity limit on our home office licence, we are unable to determine the effect of LPS at higher dose in vivo (ie. in the LPS-induced septic shock model). To determine the effect of endothelial cell BH4 deficiency on vascular function in response to high dose of LPS, isolated mouse aortic rings from *GCH1*$^{fl/fl}$Tie2cre and wild-type mice were incubated in DMEM with or without 1 µg/ml of LPS for 24 hours. Following 24 hours incubation, vasocontractile responses to phenylephrine were determined using a wire myograph as described in Section 2.8.3.

In wild-type aortas, incubation with LPS significantly blunted vascular contractility in response to phenylephrine (PE) compared to saline-treated wild-type controls. In *GCH1*$^{fl/fl}$Tie2cre aortas, incubation with LPS had no significant effect on vasocontractility compared to saline-treated *GCH1*$^{fl/fl}$Tie2cre aortas (5.19 A and B).

Figure 5.19

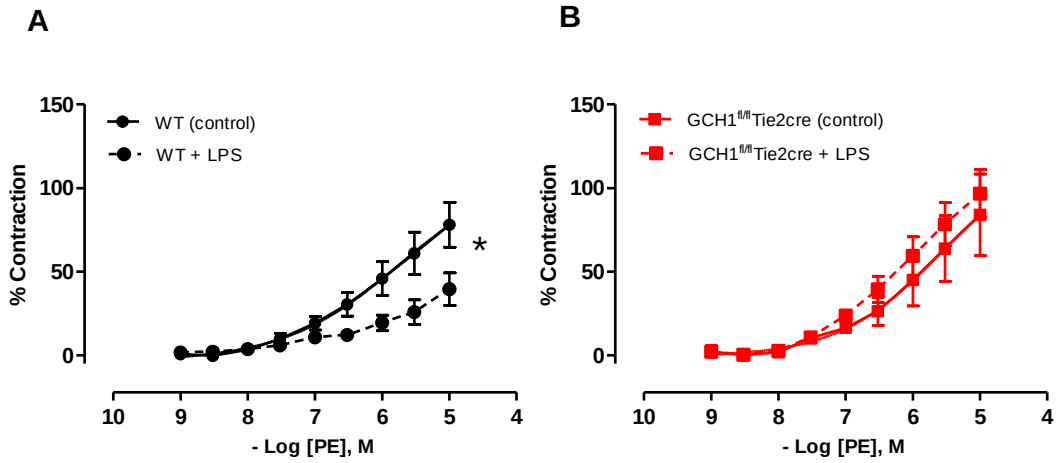


Figure 5.19. Effect of LPS on vascular reactivity in isolated aortas *ex vivo* (incubation)

Aortic rings from wild-type (WT) and *GCH1*$^{fl/fl}$Tie2cre mice were harvested and incubated in either DMDM media alone or DMDM containing 1 µg/ml of LPS for 24 hours. Vascular reactivity in aortas were determined using wire myograph. Vasoconstriction to phenylephrine (PE), expressed in percentage contraction to KCl. **A)** Increased PE-induced vasoconstriction was significantly blunted in LPS-treated wild-type aortas compared to untreated wild-type aortas. **B)** LPS treatments have no significant effect on vasoconstriction to PE of *GCH1*$^{fl/fl}$Tie2cre aortas. Data are expressed as mean ± SEM. (*$P<0.05$, n=5 to 6 aortas per group)

5.5 Discussion

In this chapter, I investigated the physiological requirement for endothelial cell BH4 biosynthesis in blood pressure regulation in both health and disease. The key findings were:

- Deficiency in endothelial cell BH4 biosynthesis led to mild hypertension in *GCH1*$^{fl/fl}$Tie2cre mice compared to wild-type littermate controls.
- The blood pressure difference in *GCH1*$^{fl/fl}$Tie2cre mice was abolished by chronic administration of a NOS inhibitor, suggesting increased blood pressure in *GCH1*$^{fl/fl}$Tie2cre mice is NOS mediated.
- Acute administration of either phenylephrine or angiotensin II in anaesthetised mice caused a further augmented systolic blood pressure in *GCH1*$^{fl/fl}$Tie2cre mice compared to wild-type littermate controls.
- Acute administration of either antioxidant drugs (NAC and EUK-8) or indomethacin had no effect on blood pressure in *GCH1*$^{fl/fl}$Tie2cre mice but significantly reduced blood pressure in wild-type littermate controls.
- Chronic treatment of either NAC or indomethacin had no significant effect on blood pressure in either wild-type or *GCH1*$^{fl/fl}$Tie2cre mice.
- Chronic Ang II infusion with a sub-pressor dose caused hypertension in *GCH1*$^{fl/fl}$Tie2cre mice but did not alter blood pressure in wild-type littermates.
- Chronic Ang II infusion with a sub-pressor dose led abdominal aortic aneurysm formation in *GCH1*$^{fl/fl}$Tie2cre mice but not in wild-type mice.
- Deficiency in endothelial cell *GCH1* and BH4 biosynthesis partially protects mice from LPS-induced vascular dysfunction and hypotension.

5.5.1 Haemodynamic responses under basal physiological condition

In the first part of this chapter I have demonstrated that the endothelial cell-specific BH4 deficiency, resulting from *GCH1* deletion leads to a mild hypertension in *GCH1*$^{fl/fl}$Tie2cre mice. This finding is compatible with other studies of vascular function in resistance vessels from *GCH1*$^{fl/fl}$Tie2cre mice. The loss of basal eNOS-derived NO is likely to be responsible for a mild-hypertensive phenotype in *GCH1*$^{fl/fl}$Tie2cre mice. In line with this finding, administration of phenylephrine under anaesthesia caused a greater increase in systolic blood pressure in *GCH1*$^{fl/fl}$Tie2cre mice but did not affect in wild-type mice, further demonstrating the loss of tonic eNOS-derived NO generation regulated blood pressure in *GCH1*$^{fl/fl}$Tie2cre mice. Indeed, chronic administration of nitric oxide synthase inhibitor, L-NAME in drinking water increased and normalised blood pressure, such that blood pressure is no longer different between wild-type and *GCH1*$^{fl/fl}$Tie2cre mice, further indicating that increased blood pressure in *GCH1*$^{fl/fl}$Tie2cre mice is eNOS-mediated. Consistent with this idea, eNOS mice, but not nNOS knockout (Sallstrom J, 2006) or iNOS (Noronha et al., 2005) knockout mice, have impaired NOS-mediated endothelium-dependent vasodilatation and increased blood pressure (Stauss et al., 1999; Yang et al., 1999), demonstrating the critical role of eNOS-derived NO in regulation of vascular tone and blood pressure.

Increased systolic blood pressure in *GCH1*$^{fl/fl}$Tie2cre mice is accompanied by a marked reduction in heart rate (~10 to 15 beats per minute lower than wild-type littermates). Reduced heart rate has been reported in eNOS knockout mice (Stauss et al., 1999). These findings suggest that the baroreceptor reflex mechanisms responding to increased blood pressure are likely to be responsible for a reduction in heart rate in *GCH1*$^{fl/fl}$Tie2cre mice. Consistent with this idea, administration of NOS inhibitors increases blood pressure and reduces heart rates in mice, rats (Widdop et al., 1992), dogs, (Elsner et al., 1992) and humans (Stamler et al., 1994).

Previous studies have demonstrated that reduced vascular BH4 bioavailability is associated with vascular disease states such as hypertension, diabetes and atherosclerosis in both experimental models and clinical studies (Antoniades et al., 2011b; Bitar et al., 2005b; Heitzer et al., 2000a; Landmesser et al., 2003; Laursen et al., 2001). It remains unknown whether reduced vascular BH4 bioavailability is the cause or is a consequence of vascular disease. In this study, I have shown for the first time that deficiency in endothelial cell BH4 biosynthesis is alone sufficient to cause vascular dysfunction and hypertension, even in the absence of vascular disease, suggesting that endothelial cell *GCH1* and thus BH4 biosynthesis play a pivotal role in eNOS function and blood pressure regulation.

Acute administration of an antioxidant, the superoxide dimutase (SOD) mimetic EUK-8 in anesthetized mice markedly reduced blood pressure in wild-type mice but had no significant effect in *GCH1*$^{fl/fl}$Tie2cre mice. Consistent with this finding, acute administration of non-selective antioxidant N-acetylcysteine in anesthetized mice also decreased blood pressure in wild-type but again had no effect in *GCH1*$^{fl/fl}$Tie2cre mice. EUK-8 and NAC may act to reduce blood pressure in wild-type mice, where BH4 bioavailability is not limited, due to the scavenging of basal ROS production, which in turn increases NO bioavailability. Indeed, treatment of mice with either EUK-8 or NAC has been reported to reduce systolic blood pressure (Ray et al., 2011). In contrast to wild-type mice, *GCH1*$^{fl/fl}$Tie2cre mice have limited endothelial NO bioactivity and vasodilatations that are already dependent on eNOS-derived H_2O_2 and prostacyclin, such that the SOD mimetic alone has no significant effect on blood pressure. In contrast to acute antioxidants, chronic treatment with NAC in drinking water for 7 days had no significant effect on blood pressure in both wild-type and *GCH1*$^{fl/fl}$Tie2cre mice. These findings suggest that administration of antioxidants may be beneficial for a short term rather than a longer term treatment. Consistent with this finding, studies using

non-selective antioxidant drugs in large-scale clinical trials have shown no benefit as treatments of cardiovascular disease (Channon, 2012).

Although prostaglandin-derived vasodilators play some compensatory roles, as demonstrated in isometric tension studies of mesenteric arteries, the extent of the compensation was not enough to prevent basal blood pressure elevation in *GCH1*$^{fl/fl}$Tie2cre mice. Acute administration of the cyclooxygenase inhibitor indomethacin in anesthetized mice markedly reduces systolic blood pressure in wild-type mice but has no significant effect on *GCH1*$^{fl/fl}$Tie2cre mice. It is possible that reduced basal prostaglandin-derived vasoconstrictors are attributable to a reduction in blood pressure in wild-type mice, since I have shown previously that endothelium-dependent vasodilatation in resistance arteries of *GCH1*$^{fl/fl}$Tie2cre mice was in part mediated by a prostaglandin-derived vasodilator, likely to be prostacyclin. It is therefore likely that administration of indomethacin to *GCH1*$^{fl/fl}$Tie2cre mice reduces the synthesis of both prostaglandin-derived vasoconstrictors as well as prostaglandin-derived vasodilators, such that the effect of reduced vasoconstrictor and reduced vasodilator cancelled each other out. In contrast to acute treatment of indomethacin, chronic treatment of indomethacin had no significant effect on blood pressure in both wild-type and *GCH1*$^{fl/fl}$Tie2cre mice, a finding consistent with previous reports (Muirhead et al., 1976). Notably, it has been reported that prostacyclin receptor-deficient mice are normotensive (Murata et al., 1997)

Taken together, I describe for the first time that selective deficiency in endothelial cell BH4 biosynthesis, through targeted *GCH1* deletion, is alone sufficient to cause eNOS uncoupling, vascular dysfunction and hypertension even in the absence of vascular disease, and importantly, all in the presence of normal plasma and systemic BH4 levels. These findings suggest that targeting endothelial cell BH4 biosynthesis rather than systemic BH4 levels may be more relevant to the development and treatment of vascular diseases.

5.5.2 Haemodynamic responses to Ang II infusion

In the second part of this chapter I have investigated the requirement of endothelial cell BH4 biosynthesis in the regulation of blood pressure in response to chronic angiotensin II (Ang II) infusion. I have shown that chronic treatment with Ang II at a sub-pressor dose (0.4 mg/kg/day) caused a significant increase in blood pressure in *GCH1*$^{fl/fl}$Tie2cre mice but had no significant effect in wild-type littermate controls. In line with this finding, administration of Ang II under anaesthesia caused a greater increase in systolic blood pressure in *GCH1*$^{fl/fl}$Tie2cre mice when compared with that in wild-type controls, demonstrating that reduced vascular NO bioactivity is likely to contribute to the initial pressor response to Ang II infusion.

Surprisingly, Ang II infusion even at a sub-pressor dose results in an increased incidence of aortic abdominal aneurysm (AAA) formation in *GCH1*$^{fl/fl}$Tie2cre mice (~60%) but not in wild-type mice. To my knowledge, this is the first study that demonstrates that sub-pressor dose of Ang II infusion at 0.4 mg/kg/day is sufficient to cause AAA formation when endothelial cell BH4 bioavailability is limited, suggesting the critical role of endothelial cell BH4 biosynthesis in the pathogenesis of AAA formation. It is possible that the increased blood pressure in response to Ang II may contribute to the development of AAA formation in *GCH1*$^{fl/fl}$Tie2cre mice. However, a large body of literature suggests that increased blood pressure is unlikely to be the major risk factor for the development of AAA formation or AAA rupture (Fan et al., 2014; Gao et al., 2012). Indeed, a similar dose of Ang II infusion at 0.4 mg/kg/day caused an increase in blood pressure in Ang II-infused Nox2 mice without the development of AAA formation (Bendall et al., 2007), thus suggesting that increased blood pressure in response to Ang II is unlikely to contribute to an increased incidence of AAA formation in *GCH1*$^{fl/fl}$Tie2cre mice.

Important roles for eNOS uncoupling and BH4 deficiency in AAA formation have been recently reported in hph-1 mice with moderate systemic BH4 deficiency. Hph-1 mice treated with Ang II at 0.7 mg/kg/day, show increased eNOS uncoupling, increased superoxide, reduced NO bioactivity, vascular remodelling and AAA formation (Gao et al., 2012). As discussion previously, hph-1 mouse has a global BH4 deficiency, affecting all cells with all tissues, thus it is impossible to dissect out where BH4 deficiency is acting to produce AAA formation. However, my new finding in *GCH1*$^{fl/fl}$Tie2cre mice overcome the lack of cell specificity in hph-1 mice and the potential confounding effects of systemic changes and altered sympathetic function (Adlam et al., 2012).

In summary, I describe for the first time that selective deficiency in endothelial cell BH4 biosynthesis leads to an increased incidence of AAA formation in *GCH1*$^{fl/fl}$Tie2cre mice in response to Ang II infusion, even at the sub-pressor dose of Ang II, demonstrating the pivotal role of endothelial cell BH4 biosynthesis in the pathogenesis of AAA formation. Thus, targeting endothelial cell *GCH1* and BH4 biosynthesis may provide a novel therapeutic target for the treatment of AAA formation or rupture.

5.5.3 Haemodynamic responses to LPS-induced systemic inflammation

A large body of evidence has demonstrated that administration of LPS causes an increase in vascular *GCH1* mRNA, GTPCH expression and BH4 levels. This is accompanied by an increase in vascular iNOS mRNA and protein expression, which in turn elevates vascular NOS-derived NO generation and reduces blood pressure (Bune et al., 1996; Shimizu et al., 1998). Previous studies have shown that increased GTPCH expression, biopterins and thus vascular NOS-derived NO generation are inhibited in LPS-treated rats following administrated with a GTPCH inhibitor (Bune et al., 1996; Shimizu et al., 1998). These

findings suggest that inhibiting the activity of GTPCH and hence the synthesis of BH4 may be beneficial for therapeutic treatment of systemic inflammatory conditions such as sepsis. The role of endothelial cell BH4-dependent NOS regulation in the pathogenesis of LPS-induced systemic inflammation has yet to determined.

The aim of this study was to use a genetic approach to investigate whether deficiency in endothelial cell *GCH1*, and subsequent endothelial cell BH4 biosynthesis provides an alternative therapeutic mechanism to regulate vascular NOS-derived NO overproduction and haemodynamic response in LPS-induced systemic inflammation. In this study, administration of LPS markedly reduces concentration-dependent vasoconstriction to both phenylephrine and U46619 in mesenteric arteries from wild-type mice. This reduced vasoconstriction is inhibited by L-NAME, suggesting that increased vascular NOS-derived NO generation is responsible for the blunted vasoconstrictor response. Consistent with this finding, administration of mice with LPS increases vascular NOS-derived NO production and reduces vasoconstrictor response in mouse resistance arteries (Chiao et al., 2013). In contrast to wild-type mesenteric arteries, administration of *GCH1*$^{fl/fl}$Tie2cre mice with LPS had no significant effect on vasoconstriction to either phenylephrine or U46619, suggesting that the inability to induce endothelial cell *GCH1* expression, BH4 biosynthesis and thus NOS-derived NO generation is likely to be the mechanism underlying the blunted decrease in vasoconstrictor response in mesenteric arteries from LPS-treated *GCH1*$^{fl/fl}$Tie2cre mice. Consistent with this hypothesis, reduced biopterins levels and NOS-derived NO production in response to LPS treatment is inhibited in rats co-treated with DAHP, an inhibitor of GTP cyclohydrolase (Bune et al., 1996).

Despite increased aortic BH4 levels in LPS-treated wild-type mice and partially increased BH4 levels in LPS-treated *GCH1*$^{fl/fl}$Tie2cre mice, aortic vasoconstrictions in response to both U46619 and phenylephrine were comparable to that of saline-treated group. A previous

study has demonstrated that administration of LPS at higher dose (40 mg/kg) reduces vasoconstrictor response in isolated mouse aortas (Lund et al., 2007). It is likely that the dose of LPS used in this study (1 mg/kg) is not sufficient to cause vascular hyporeactivity in aortas. This finding suggests that a low dose of LPS with 1 mg/kg is sufficient to induce vascular dysfunction in resistance vessels but not in conduit vessels. Unfortunately, due to the severity limit on our home office licence, we are unable to determine the effect of LPS at higher dose in vivo (ie. in the LPS-induced septic shock model). To determine the effect of endothelial cell BH4 deficiency on vascular function in response to high dose of LPS, isolated mouse aortic rings from *GCH1*$^{fl/fl}$Tie2cre and wild-type mice were incubated with LPS. Treatment of isolated mouse aortic rings with LPS for 24 hours markedly reduced vasoconstriction in response to phenylephrine in wild-type aortic rings but *GCH1*$^{fl/fl}$Tie2cre rings were unaltered, suggesting that at higher dose, deficiency in endothelial cell *GCH1* and BH4 biosynthesis is protective against LPS-induced vascular dysfunction in isolated aortas.

It is known that administration of LPS causes an increase in plasma nitrite/nitrate and a decrease in blood pressure in mice (Cunha et al., 1994) and rats (Szabo et al., 1994b). Treatment of mice with L-NAME reduced plasma nitrite/nitrate and increases blood pressure and systemic vascular resistance in human patients with septic shock (Petros et al., 1991).These findings suggest that NOS induction contribute to the pathogenesis of LPS-induced hypotension and septic shock. Indeed, both eNOS deficient mice and iNOS deficient mice are protected against LPS-induced hypotension (Connelly et al., 2005), suggesting the important role of both eNOS and iNOS in the pathogenesis of LPS-induced hypotension.

In this study, I have demonstrated for the first time that deficiency in endothelial cell *GCH1* and thus BH4 biosynthesis is partially protective against LPS-induced hypotension in *GCH1*$^{fl/fl}$Tie2cre mice compared to wild-type littermate controls. This finding supports other

observations from vascular function studies in resistance vessels from LPS-treated mice. The lack of endothelial cell *GCH1*, BH4 levels and thus NOS-derived NO, in response to LPS, is likely to be responsible for the partial reduction in hypotension in *GCH1*$^{fl/fl}$Tie2cre mice. The drop in blood pressure in LPS-treated *GCH1*$^{fl/fl}$Tie2cre mice that is still observed is likely to be induced by the overproduction of NOS-derived NO from non-endothelial cell, probably vascular smooth muscle cells. This finding suggests that endothelial cells and vascular smooth muscle cells are likely to be the main source NOS-derived NO generation in response to low dose of LPS. It has yet to be determined whether *GCH1*$^{fl/fl}$Tie2cre mice are protected from vascular dysfunction and hypotension in LPS-induced model of septic shock.

Taken together, I have demonstrated for the first time that deficiency in endothelial cell *GCH1* and BH4 biosynthesis partially protects against LPS-induced vascular dysfunction and hypotension. These findings suggest that endothelial cell BH4 biosynthesis plays a critical role in the pathogenesis of this LPS-induced model of systemic inflammation. Thus, targeting endothelial cell *GCH1* and BH4 biosynthesis might provide a novel therapeutic target for the treatment of circulatory collapse in patients with septic shock.

Chapter 6:

The Requirement for Endothelial Cell BH4 Biosynthesis in Vascular Adaptation to Pregnancy

Chapter 6: The requirement for endothelial cell BH4 biosynthesis in vascular adaptation to pregnancy

6.1 Introduction

Hypertensive disorders of pregnancy such as preeclampsia and gestational hypertension are associated with a higher risk of cardiovascular disease for both mother and offspring in later life. Women with these complications during pregnancy have a 4-fold increased risk of developing hypertension (Bellamy et al., 2007; McDonald et al., 2008) and a 2-fold increased risk of developing stroke after pregnancy (Bellamy et al., 2007). Offspring from mothers with hypertensive disorders of pregnancy are also likely to have a higher risk of hypertension and other cardiovascular disease in later in life (Ferreira et al., 2009; Kajantie et al., 2009). Therefore, understanding the mechanisms underlying vascular adaptations and blood pressure regulations during pregnancy are of importance.

The maternal cardiovascular system undergoes remarkable changes in pregnancy in order to provide the growing fetus with sufficient oxygen and nutrition. By term, the uteroplacental bed receives more than 12% of cardiac output. The increase in uterine blood flow is associated with a marked reduction in uteroplacental vascular resistance. Outward remodelling and vasodilatation of more proximal uterine arteries, together with trophoblast invasion and remodelling of spiral arteries, contribute to this adaptive response (Kelly et al., 2000). Failure of this vascular adaptation is associated with adverse outcomes including intrauterine growth restriction (IUGR) and hypertensive related disorders of pregnancy such as pre-eclampsia and gestational hypertension.

Nitric oxide (NO) is a key mediator of vascular adaptation. Increased uterine artery calibre is associated with both enhanced eNOS expression and activity, and NO bioavailability (Cooke and Davidge, 2003; Nelson et al., 2000; Sullivan et al., 2006). Increases in uterine artery blood flow and shear stress enhance eNOS expression (Dimmeler et al., 1999b; Kublickiene et al., 1997) and this may contribute to structural arterial remodelling via NO-dependent upregulation of matrix metalloproteinase (MMP) expression (Dumont et al., 2007; Kelly et al., 2003; Tronc et al., 2000). The impaired remodelling observed in uterine arteries of pregnant eNOS-knockout mice may be due to reduced activation of MMPs (van der Heijden et al., 2005).

There is less certainty regarding the role of eNOS coupling and NO bioavailability in the uterine circulation in pre-eclampsia and IUGR. NO-dependent flow-mediated vasodilation is reduced or abolished in myometrial arteries isolated from pre-eclamptic pregnancies; indeed, increased shear leads to paradoxical vasoconstriction in these arteries (Kublickiene et al., 2000). In pre-eclampsia there are no data regarding eNOS expression in uterine arteries, and conflicting reports of decreased (Beinder et al., 1999), unchanged (Conrad and Davis, 1995) or increased (Myatt et al., 1996; Rutherford et al., 1995) eNOS expression or activity in spiral arteries and placental vessels. Although this disparity may reflect variation in experimental design, it is unlikely that reduced NO bioavailability can be explained simply by loss of eNOS protein or activity. In other vascular disease states such as diabetes, hypertension or heart failure, expression of eNOS protein levels are increased yet NO bioavailability remains reduced (Bauersachs et al., 1999; Cosentino et al., 1997; Hink et al., 2001a). Similar findings have been reported in placental villous arteries (Myatt et al., 1996) and small subcutaneous arteries isolated from women with pre-eclampsia (Roggensack et al., 1999), suggesting a role for uncoupled eNOS in the pathogenesis of this condition. Markers of oxidative stress are present in the placenta and maternal circulation of patients

with pre-eclampsia (Raijmakers et al., 2004), yet in a landmark clinical trial the antioxidants vitamin C and vitamin E failed to prevent the development of pre-eclampsia in high risk pregnancies (Poston et al., 2006), and simple strategies attempting to restore or augment NO with NO donors in pre-eclampsia have been disappointing (Meher and Duley, 2007).

One possible explanation for these results is the failure to specifically target eNOS uncoupling and consequent altered NO/ROS signalling. Recent data from a rat model of pre-eclampsia (PE) demonstrate normalization of eNOS uncoupling with restoration of endothelial function in aorta and mesenteric vessels *ex vivo* by scavenging ROS or enhancing BH4 levels (Mitchell et al., 2007), although vascular BH4 levels were not directly measured in this study. Accordingly, there remains a pressing need to determine the importance of endothelial cell BH4-eNOS interactions in the vascular adaptation to pregnancy and preeclampsia. To date, the physiological requirement of endothelial cell BH4 biosynthesis in eNOS regulation in uteroplacental vascular adaptation and blood pressure regulation to pregnancy is unclear. To address this question, a novel mouse model of endothelial cell-targeted *GCH1* knockout was used.

6.2 Hypothesis and aims

The central hypothesis of this chapter is that endothelial cell BH4-dependent NOS regulation is a key mediator of vascular adaptation in pregnancy. Specifically:

1) NOS-derived vasodilators determine physiological vascular adaptations in pregnancy.
2) Endothelial cell-specific BH4 deficiency in pregnancy will lead to abnormal uterine adaptations with enhanced vasoconstriction and impaired endothelium-dependent vasodilatation.
3) Endothelial cell BH4-dependent NOS regulation plays a critical role in blood pressure regulation during pregnancy. Thus, deficiency in endothelial cell BH4 biosynthesis during pregnancy will lead to gestational hypertension and intrauterine growth restriction.

The main aims of this chapter are:

1) To examine uterine vascular adaptation to a normal pregnancy by studying vascular reactivity in uterine arteries from non-pregnant wild-type and pregnant wild-type mice.
2) To investigate the requirement of endothelial cell BH4 biosynthesis in uterine vascular adaptation to pregnancy by studying vascular reactivity in uterine arteries from pregnant wild-type and pregnant *GCH1*$^{fl/fl}$Tie2cre mice.
3) To examine the requirement of endothelial cell BH4 biosynthesis in blood pressure regulation during pregnancy in wild-type and *GCH1*$^{fl/fl}$Tie2cre mice.
4) To determine whether *GCH1*$^{fl/fl}$Tie2cre mice demonstrate characteristics of pre-eclampsia and intrauterine growth restriction.

6.3 Methods

Most of the methods used in this chapter have described in Chapter 2. Only methods and reagents used specifically in the experiments for this chapter are described below.

6.3.1 Timed mating

Pregnancy was achieved by mating virgin *GCH1*$^{fl/fl}$Tie2cre and wild-type females (aged between 10-16 weeks old) with a wild-type male. To evaluate the gestation day, vaginal plugs were checked for the following morning. The 0.5 day of gestation (E0.5) is considered to be the day that vaginal plug is found. Plugged females were then removed into a new cage (typically 4-6 plugged females per cage). Body weights of plugged *GCH1*$^{fl/fl}$Tie2cre and wild-type mice were determined throughout gestation (E0, E2.5, E5.5, E7.5, E10.5, E12.5, E15.5, E16.5, E17.5 and E18.5). Urine samples from non-pregnant and pregnant (at E18.5) *GCH1*$^{fl/fl}$Tie2cre and wild-type females were collected and stored at -80 °C for biochemistry analysis. Unless otherwise stated, all tissues were harvested and collected for experiments at either preconception or E18.5 day of gestation (late gestation, two days prior to normal term delivery).

6.3.2 BH4 measurement

Biopterin levels in plasma and uterine arteries from non-pregnant and pregnant *GCH1*$^{fl/fl}$Tie2cre and wild-type mice were determined as described in Section 2.4. Mice were culled by overdose of inhalation of isoflurane as described in Section 2.3.3. For plasma, whole blood samples (~ 500 μl) were collected in a heparin-treated syringe with a needle (G27) and placed on ice. Whole blood samples were then centrifuged for 3,000 rpm for 10 min at 4 °C. Plasma samples (supernatant fraction) were then collected in a new tube and

stored at -80 °C. For uterine arteries, uterine horns were collected in ice-cold Krebs. Main uterine arteries (without uterine branches) were then dissected and isolated under the microscope, then collected and stored at -80 °C.

6.3.3 Vascular function studies

Vascular function in uterine arteries from both non-pregnant and pregnant (E18.5) *GCH1*$^{fl/fl}$Tie2cre and wild-type mice were examined using a wire myograph as described previously in chapter 2. Briefly, mice were culled by overdose of inhalation of isoflurane. The uterine horns were removed by surgical laparotomy (Figure 6.1) and placed into ice-cold Krebs and uterine arteries were carefully dissected and isolated under a microscope. The 2-mm rings of uterine arteries were then mounted in a wire myograph using tungsten golden wires (15μm in diameter). The procedure was then followed as described in Section 2.8.

Figure 6.1

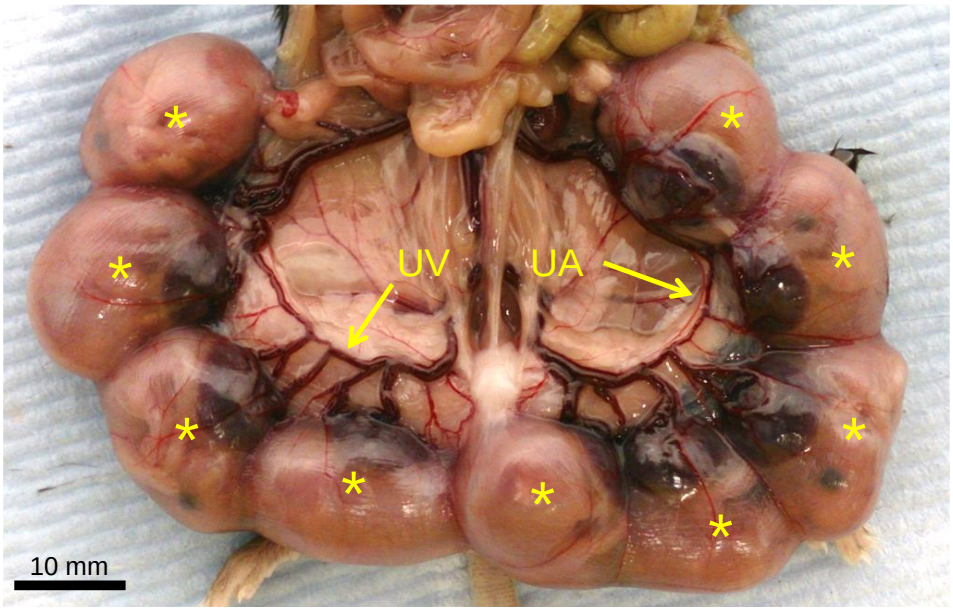


Figure 6.1. Uterine horn of pregnant mouse.

Representative image of uterine horns of adult female mouse at E18.5 day of gestation. * fetus were identified in the litter and numbered off to permit identification of implantation site. Scale bar equivalent to 10 mm. UA= uterine arteries, UV= uterine veins.

6.3.3 Blood pressure measurement

The systolic blood pressure and heart rate were measured using an automated computerised tail-cuff system in conscious mice as described previously in chapter 2. Prior to timed mating, *GCH1*$^{fl/fl}$Tie2cre and wild-type females were trained on BP machine for 5 consecutive days following 3 days of baseline measurements. Following vaginal plug, blood pressure and heart rate measurements in both *GCH1*$^{fl/fl}$Tie2cre and wild-type mice were recorded at gestation day: E2.5, E5.5, E7.5, E10.5, E12.5, E15.5, E16.5, E17.5 and E18.5. All recordings were performed between 08:00 and 12:00 h.

6.3.4 Statistical analysis

Data are expressed as mean ± SEM. Comparisons between wild-type and *GCH1*$^{fl/fl}$Tie2cre were made by two-tailed unpaired *Student's* t test. Concentration-response curves were compared by ANOVA for repeated measurements followed by Bonferroni post-hoc test. A p-value of less than 0.05 was considered statistically significant.

6.4 Results

6.4.1 Reproductive outcome

6.4.1.1 Maternal weight gain and litter size

To determine the effect of endothelial cell BH4 deficiency on maternal weight gain during pregnancy, body weights of *GCH1*$^{fl/fl}$Tie2cre and wild-type littermates (10-16 week-old) were determined at preconception (before timed mating) and throughout pregnancy. Preconception body weights were comparable between wild-type and *GCH1*$^{fl/fl}$Tie2cre mice. During E2.5 to E12.5 day of gestation, increased maternal weights were comparable between wild-type and *GCH1*$^{fl/fl}$Tie2cre mice. After E12.5 day of gestation, increased maternal weight gain was significantly blunted in *GCH1*$^{fl/fl}$Tie2cre mice compared to wild-type mice and the difference was maintained throughout pregnancy (Figure 6.2 A). There was no significant differences in either litter size between wild-type and *GCH1*$^{fl/fl}$Tie2cre mice at E18.5 day of gestation or at birth (Figure 6.2 B). The onset of parturition were comparable between wild-type and *GCH1*$^{fl/fl}$Tie2cre mice (Figure 6.2 C). There was no significant differences in protein concentration in uterine samples between non-pregnant and pregnant both genotypes (Figure 6.2 D).

Figure 6.2

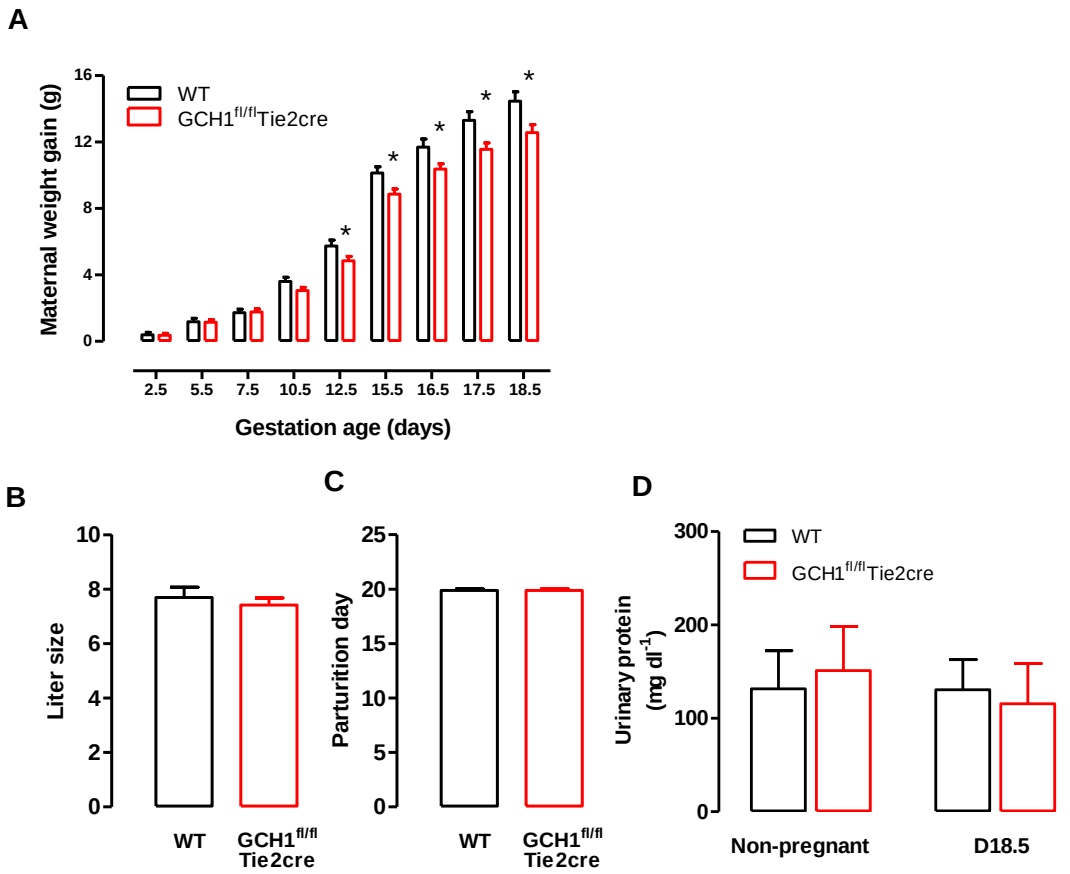


Figure 6.2. Maternal measurements.

A) Maternal weight gain by wild-type and *GCH1*$^{fl/fl}$Tie2cre mice was determined prior to and throughout gestation. *GCH1*$^{fl/fl}$Tie2cre mothers gained significantly less weight during gestation compared to wild-type mothers. (**P<0.05;* n= 15 to 20 animals per group). **B)** litter sizes, **C)** On set of parturition, **D)** Urine samples were collected from non-pregnant and pregnant (at E18.5) wild-type and *GCH1*$^{fl/fl}$Tie2cre mice. Protein concentration in uterine samples were determined using bicinchoninic acid (BCA) Protein Assay. No different in protein in urine between non-pregnant and pregnant wild-type and *GCH1*$^{fl/fl}$Tie2cre mice (n=5 to 7 animals per group). Data are expressed as mean ± SEM.

6.4.1.2 Maternal organ weights during pregnancy

It has been reported that increased organ weights of tissues such as liver, heart and lung are important for normal pregnancy in rats. To determine whether this is the case in mice, organs (heart, lung, liver, kidney and spleen) from wild-type and *GCH1*$^{fl/fl}$Tie2cre mice were harvested and weighed at preconception and at E18.5 day of gestation. In non-pregnant mice, there were no significant differences in organ weights (heart, lung, kidney, liver and spleen) between wild-type and *GCH1*$^{fl/fl}$Tie2cre mice (Figure 6.3 A-E), suggesting endothelial cell BH4 deficiency does not lead to abnormal growth of these organs in *GCH1*$^{fl/fl}$Tie2cre mice. At E18.5 day of gestation, heart, lung and liver weights from both pregnant wild-type and *GCH1*$^{fl/fl}$Tie2cre mice were significantly increased by approximately 20%, 10% and 80% respectively. In contrast, kidney and spleen weights from both pregnant wild-type and *GCH1*$^{fl/fl}$Tie2cre mice were comparable to that of non-pregnant wild-type and *GCH1*$^{fl/fl}$Tie2cre mice (Figure 6.3 A-E).

Figure 6.3

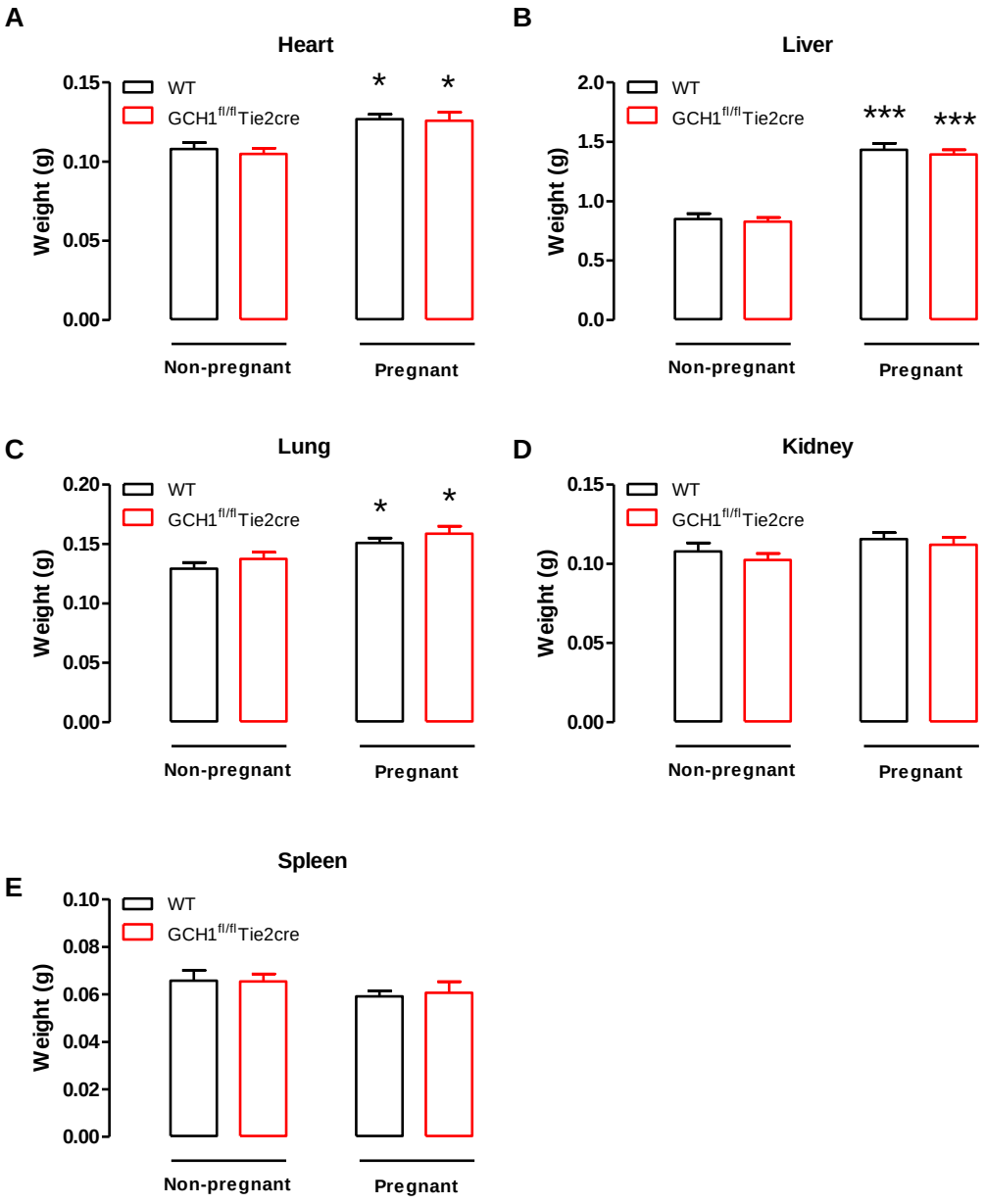


Figure 6.3. Maternal organ weights

Organs from either non-pregnant virgin wild-type (WT) and *GCH1*$^{fl/fl}$Tie2cre mice or pregnant wild-type and *GCH1*$^{fl/fl}$Tie2cre mice at E18.5 days of gestation were collected and weighed. **A-C)** Heart, lung and liver weight were significantly increased in pregnant mice of both genotypes compared to non-pregnant mice of both genotypes. **D-E)** No differences were detected in either kidney or spleen weights of pregnant mice and non-pregnant mice. Data are expressed as mean ± SEM. (**P<0.05;* *** *P<0.001*, n= 10 to14 animals per group)

6.4.1.3 Fetal measurements

To determine whether reduced maternal weight gain in *GCH1*$^{fl/fl}$Tie2cre mice was associated with intrauterine growth restriction, foetal and placental weights were determined at E18.5 day of gestation. At E18.5 day of gestation, mean weight of fetuses from *GCH1*$^{fl/fl}$Tie2cre dams were ~10% lower than that of fetuses from wild-type dams ($P<0.01$)(Figure 6.4 A and D). This reduction was associated with a significantly decreased crown-to-rump length of fetuses from *GCH1*$^{fl/fl}$Tie2cre mice compared to that from wild-type mice ($P<0.05$) (Figure 6.4 B). Placental weight from *GCH1*$^{fl/fl}$Tie2cre dams at E18.5 day of gestation was significantly reduced (~10%) compared to that of litters from wild-type controls ($P<0.01$) (Figure 6.4 C and D). Mean body weight of offspring at birth from *GCH1*$^{fl/fl}$Tie2cre dams was also significantly lower than that of offspring from wild-type dams ($P<0.05$) (Figure 6.4 E and F).

To examine whether reduced fetal and placental weights in *GCH1*$^{fl/fl}$Tie2cre mothers was caused by the maternal genotype or the genotype of the fetuses themselves, genotypes of fetuses from *GCH1*$^{fl/fl}$Tie2cre dams were determined. The mean foetal and placental weight of wild-type fetuses from *GCH1*$^{fl/fl}$Tie2cre dams was comparable to that of *GCH1*$^{fl/fl}$Tie2cre fetuses from *GCH1*$^{fl/fl}$Tie2cre dams (Figure 6.5 A and B).

Figure 6.4

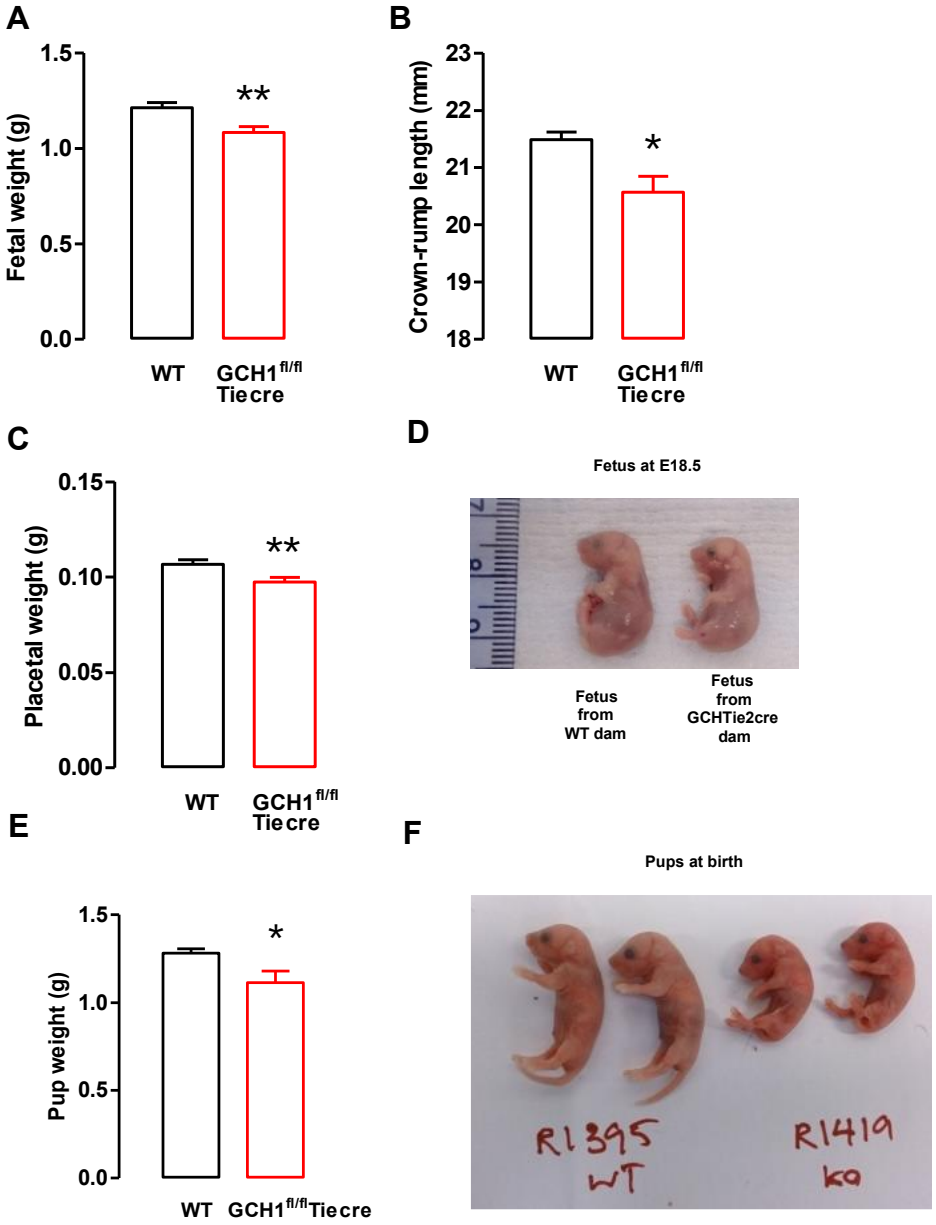


Figure 6.4. Fetal measurements.

A-D) Fetuses and placentas from wild-type and *GCH1*$^{fl/fl}$Tie2cre mothers were collected and weighed at E18.5 of gestation (*$P<0.05$; ** $P<0.01$, n= 72 to 85 pups from 10 to 13 litters per group). **E-F)** Offspring weights from wild-type and *GCH1*$^{fl/fl}$Tie2cre mothers were determined at birth. Averaged per litter of animals (*$P<0.05$, n= 51 to 75 pups from 7 to 10 litter per group). Data are expressed as mean ± SEM averaged per litters of animals.

Figure 6.5

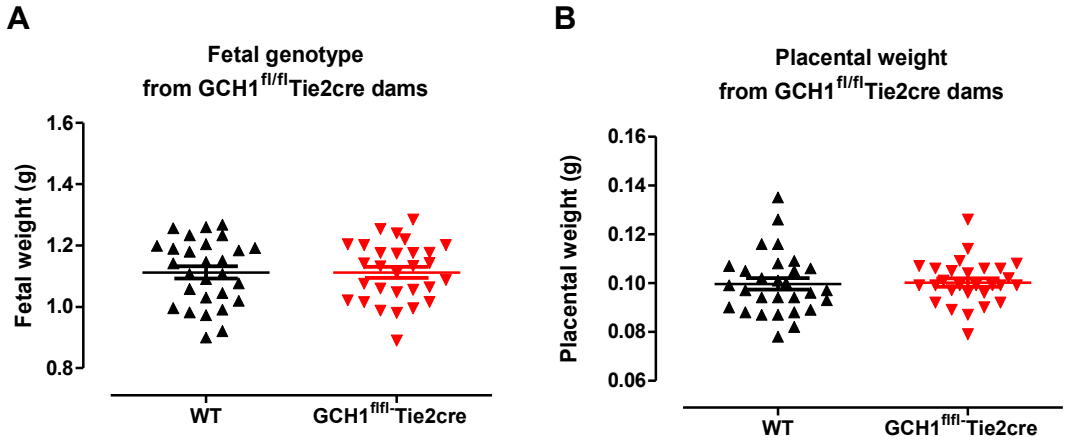


Figure 6.5. Fetal and placental weight from *GCH1*$^{fl/fl}$Tie2cre mothers.

Fetal and placental weights from *GCH1*$^{fl/fl}$Tie2cre mothers were determined according to fetus genotype. **A and B)** no difference in fetal and placental weights between wild-type fetus and *GCH1*$^{fl/fl}$Tie2cre fetus from *GCH1*$^{fl/fl}$Tie2cre mothers. Data are expressed as mean ± SEM. (n=29 to 30 fetuses per group from 6 litters)

6.4.2 Determination of BH4 levels

6.4.2.1 BH4 levels in uterine arteries.

In chapter 3 and 4, I have previously shown that biopterin and BH4 levels were greatly reduced in vascular tissues such as aortas from *GCH1*$^{fl/fl}$Tie2cre mice compared to wild-type littermates. Whether biopterin and BH4 levels are also reduced in uterine arteries has yet to be determined. To address this question, the main uterine arteries from both uterine horns of non-pregnant and pregnant (at E18.5) mice were collected. The total biopterins and BH4 levels were determined as described in Section 2.4. In non-pregnant mice, the total biopterins and BH4 levels in uterine arteries from *GCH1*$^{fl/fl}$Tie2cre mice were significantly lower compared to that of wild-type mice ($P<0.05$) (Figure 6.6 A). The total biopterins and BH4 levels were significantly (~6-fold) increased in uterine arteries from pregnant wild-type compared to non-pregnant wild-type mice ($P<0.05$) (Figure 6.6 A). Pregnant *GCH1*$^{fl/fl}$Tie2cre mice showed a tendency towards an increase in total biopterins and BH4 levels in uterine arteries, but the difference did not reach statistical significance. This increase in vascular BH4 levels was accompanied by increased BH4:BH2+B ratio in pregnant wild-type but unchanged in pregnant *GCH1*$^{fl/fl}$Tie2cre mice ($P<0.01$) (Figure 6.6 B).

Figure 6.6

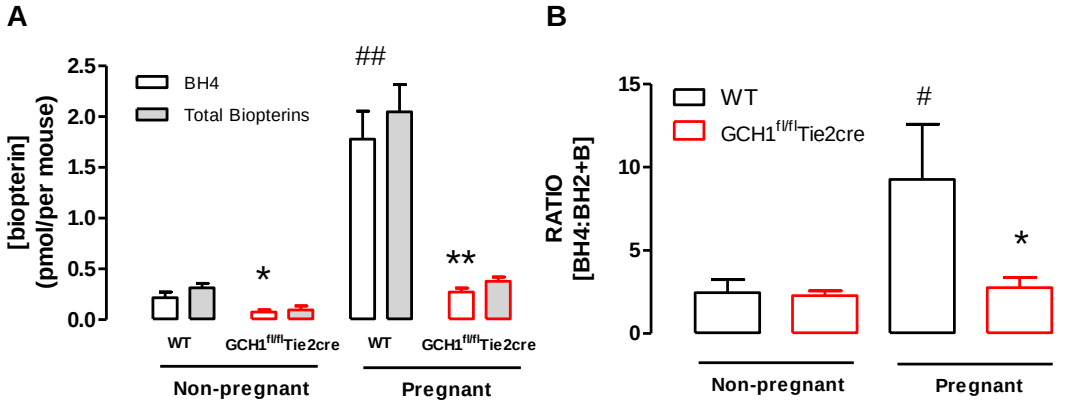


Figure 6.6. BH4 levels in uterine arteries.

Total biopterins and BH4 levels in uterine arteries determined by HPLC. **A)** In non-pregnant mice, total biopterins and BH4 levels were significantly lower in uterine arteries from *GCH1*$^{fl/fl}$Tie2cre compared to wild-type mice. In pregnant mice, total bioperins and BH4 levels were significantly increased in wild-type but not significantly changed in *GCH1*$^{fl/fl}$Tie2cre uterine arteries. **B)** BH4 to BH2+B ratio was significantly increased in pregnant wild-type mice but unaltered in pregnant *GCH1*$^{fl/fl}$Tie2cre mice. Data are expressed as mean ± SEM. (*$P<0.05$, **$P<0.01$ comparing wild-type, #$P<0.05$, ##$P<0.01$ comparing treatment; n=4 to 6 animals per group).

6.4.2.2 BH4 levels in plasma.

In non-pregnant mice, the plasma biopterins and BH4 levels were comparable between non-pregnant wild-type and *GCH1*$^{fl/fl}$Tie2cre female mice (Figure 6.7 A). In pregnant mice, the total plasma biopterins and BH4 levels were significantly reduced in both pregnant wild-type and *GCH1*$^{fl/fl}$Tie2cre dams but to a lesser extent in *GCH1*$^{fl/fl}$Tie2cre dams ($P<0.001$) (Figure 6.7 A). The BH4:BH2+B ratio in pregnant *GCH1*$^{fl/fl}$Tie2cre mice was significantly reduced compared to non-pregnant *GCH1*$^{fl/fl}$Tie2cre mice ($P<0.001$) or pregnant wild-type mice ($P<0.05$) (Figure 6.7 B).

Figure 6.7

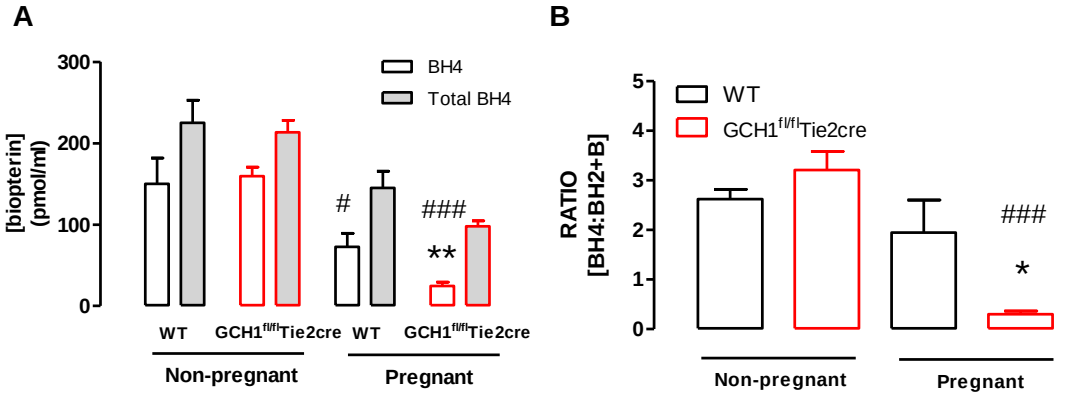


Figure 6.7. BH4 levels in plasma.

Total biopterins and BH4 levels in plasma determined by HPLC. **A)** In non-pregnant mice, total biopterins and BH4 levels were comparable between in plasma from *GCH1*$^{fl/fl}$Tie2cre compared to wild-type mice. In pregnant mice, total bioperins and BH4 levels were significantly reduced in both wild-type and *GCH1*$^{fl/fl}$Tie2cre mice compared to non-pregnant mice. Pregnant *GCH1*$^{fl/fl}$Tie2cre mice showed significantly lower levels of BH4 in plasma compared to pregnant wild-type controls. **B)** BH4 to BH2+B ratio was significantly decreased in pregnant *GCH1*$^{fl/fl}$Tie2cre mice but unaltered in pregnant wild-type mice. Data are expressed as mean ± SEM. (*$P<0.05$, **$P<0.01$ comparing wild-type, ###$P<0.001$ comparing treatment; n=5 to 7 animals per group).

6.4.3 Vascular function in uterine arteries

It has been documented that maternal vasculature, in particular, uterine and spiral arteries, undergoes dramatic changes during pregnancy in order to supply adequate nutrients and oxygen to the growing fetus. During pregnancy, increased NOS-derived NO mediated vasodilatation in uteroplacental circulation occurs in humans, mice, and rats (Anumba et al., 1999; Miller et al., 1999; Sladek et al., 1997; Williams et al., 1997). Increased prostacyclin and EDHF-mediated vasodilatation have also been reported in pregnant rats and humans. However, the precise nature of these vasodilators in mouse uterine arteries during pregnancy is unclear. To address this question, isometric tension studies using a wire myograph were performed in isolated uterine arteries from non-pregnant and pregnant (at E18.5) wild-type mice and vascular reactivity was compared.

6.4.3.1 Vascular adaptation to pregnancy in mice

Firstly, lumen diameter of uterine arteries was significantly increased in pregnant mice compared to non-pregnant mice (244.2±17.1 μm versus 155±10.2 μm*; P<0.01*) (Figure 6.8 A). Vasoconstriction in response to KCl was significantly increased (~2-fold) in uterine arteries from pregnant wild-type mice compared to non-pregnant wild-type mice (*P<0.05*; 6±0.7 mN versus 3.0±0.5 mN)(Figure 6.8 B).

6.4.3.2 Contribution of NO vs Prostacyclin vs EDHF in pregnant uterine artery

In the present study, I have shown that increased vasoconstriction to U46619 was significantly blunted in uterine arteries from pregnant mice compared to non-pregnant mice (*P<0.01*)(Figure 6.8 C). Vasoconstriction to U46619, expressed as a percentage of the KCl response, was also significantly reduced in uterine arteries from pregnant mice compared to non-pregnant mice (*P<0.001*)(Figure 6.8 D). Endothelium-dependent vasodilation in response to acetylcholine was significantly enhanced in uterine arteries from pregnant mice compared to non-pregnant mice (*P<0.05*)(Figure 6.9 A). In the presence of NOS inhibitor L-NAME, endothelium-dependent vasodilatation was significantly blunted in both uterine arteries from pregnant and non-pregnant mice, but the difference was maintained, indicating NOS-mediated vasodilation in both non-pregnant and pregnant UA (Figure 6.9. B). In the presence of L-NAME and non-selective cyclooxygenase (COX) inhibitor, indomethacin, endothelium-dependent vasodilatation to acetylcholine was comparable to that of uterine arteries treated with L-NAME alone (Figure 6.9 C). Endothelium-dependent vasodilatation to acetylcholine was totally abolished in the presence of L-NAME, indomethacin, and EDHF blockers (apamin, and charybdotoxin) (Figure 6.9 D). Endothelium-independent vasodilatation in response to nitric oxide donor, sodium nitroprusside (SNP) was also significantly enhanced in pregnant uterine arteries compared to non-pregnant uterine arteries (*P<0.01*)(Figure 6.9 E), suggesting enhanced vascular smooth muscle sensitivity to NO during pregnancy.

Figure 6.8

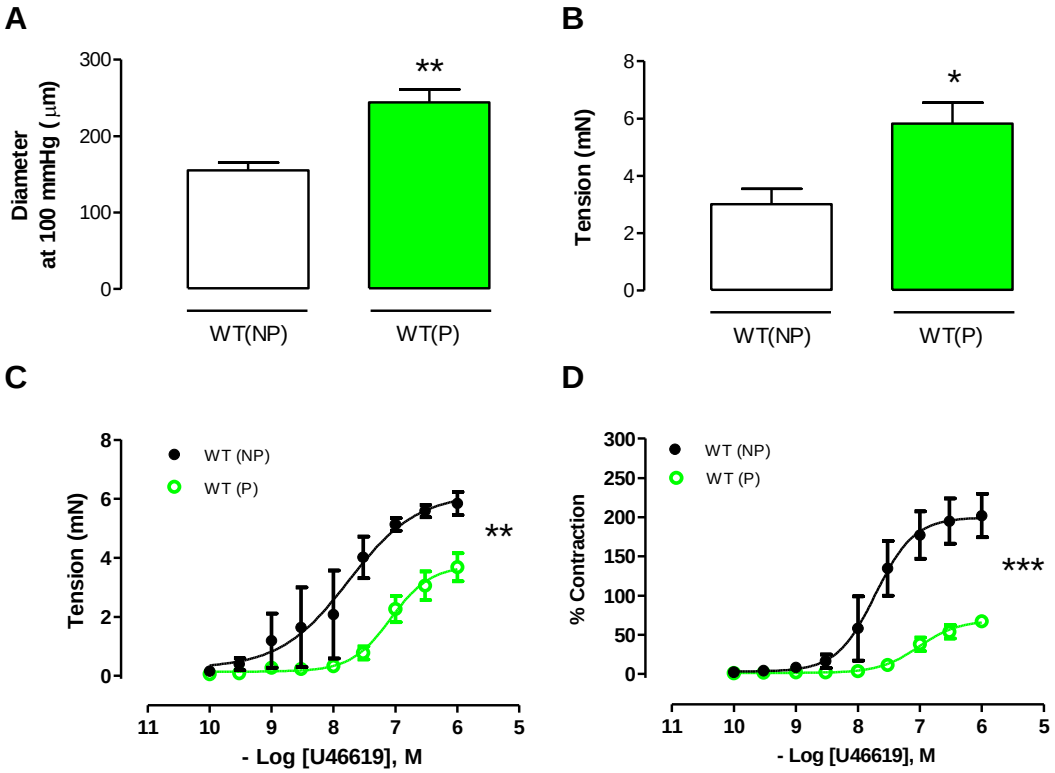


Figure 6.8. Uterine vascular adaptation in pregnancy

Vascular function of isolated uterine arteries (UA) from non-pregnant (NP) and pregnant (P) (at E18.5) wild-type mice was determined using a wire myograph. **A)** Lumen diameter of UA from pregnant mice was significantly increased compared to UA from non-pregnant mice. **B)** Vasoconstriction in response to KCl was significantly elevated in pregnant UA compared to non-pregnant arteries. **C and D)** Absolute constriction (mN) and percentage contraction to U46619 in response were significantly blunted in UA from pregnant mice compared to non-pregnant mice. Data are expressed as mean ± SEM. (**P<0.05, ** P<0.01, *** P<0.001*; n=5 to 6 animals per group).

Figure 6.9

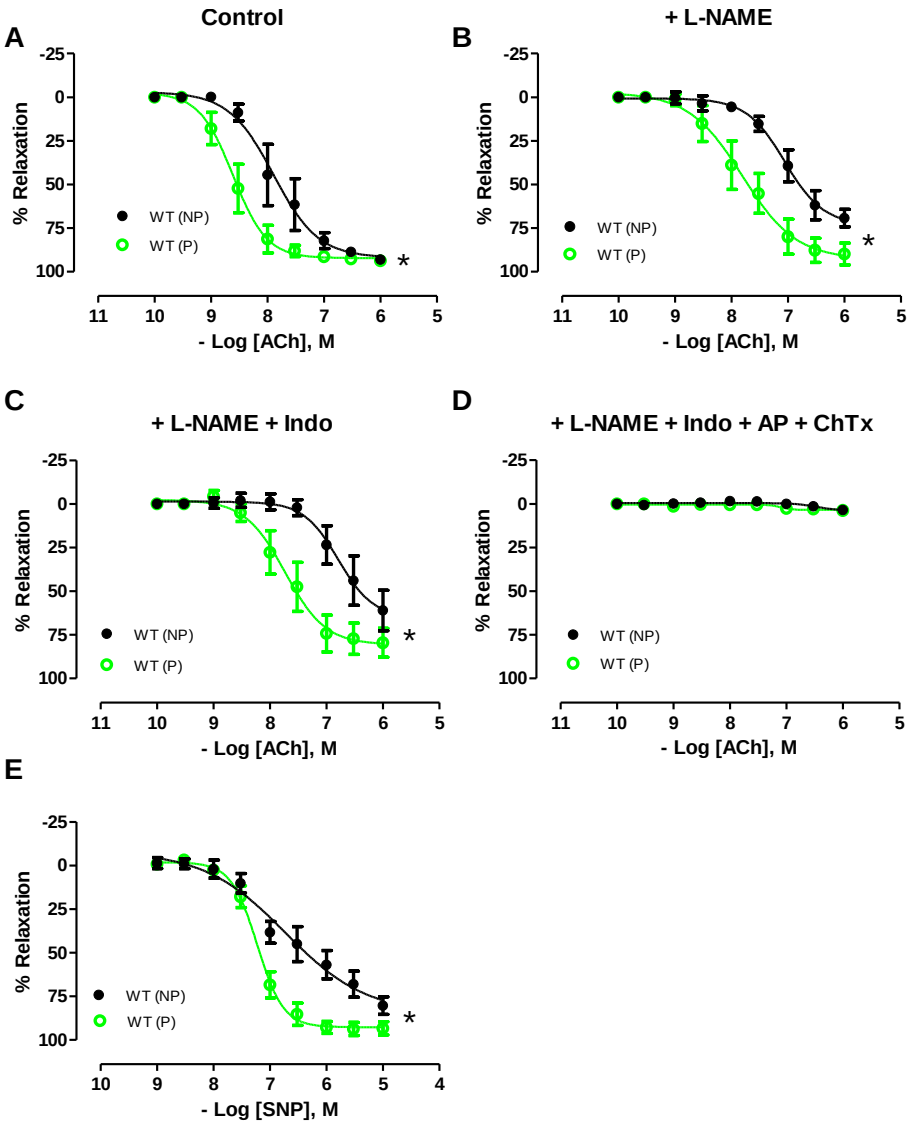


Figure 6.9. Uterine vascular adaptation in pregnancy.

Vascular function of isolated uterine arteries (UA) from non-pregnant (NP) and pregnant (P) (at E18.5) wild-type mice (WT) was determined using a wire myograph. **A)** Endothelium-dependent vasodilatation to acetylcholine (ACh) was significantly enhanced in pregnant UA compared to non-pregnant UA. **B)** In the present of L-NAME, endothelium-dependent vasodilatation was significantly inhibited in both non-pregnant and pregnant UA, but the difference still maintained. **C)** In the presence of L-NAME, indomethacin (Indo) has no significant effect on vasodilatation in both non-pregnant and pregnant wild-type UA. **D)** In the present of L-NAME, indomethacin, apamin (AP) and charybdotoxin (ChTx), endothelium-dependent vasodilatation was totally abolished in both UA. **E)** Endothelium-independent vasodilatation in response to the nitric oxide donor, sodium nitroprusside (SNP), was significantly enhanced in UA from pregnant mice compared to UA from non-pregnant mice. Data are expressed as mean ± SEM. (**P<0.05, ** P<0.01, ***P<0.001;* n=5 to 6 animals per group)

6.4.3.3 Vascular function in uterine arteries from non-pregnant wild-type and GCH1$^{fl/fl}$Tie2cre mice.

To determine the requirement of endothelial cell BH4 biosynthesis in vascular adaptation in uterine arteries, isometric tension studies were performed in isolated uterine arteries from non-pregnant wild-type and *GCH1*$^{fl/fl}$Tie2cre mice using a wire myograph as described in Section 2.8.

In non-pregnant mice, the arterial lumen diameter, as determined by length-tension relationship, and the KCl response were comparable between uterine arteries from wild-type and *GCH1*$^{fl/fl}$Tie2cre mice (Figure 6.10 A). Despite endothelial cell BH4 deficiency in *GCH1*$^{fl/fl}$Tie2cre uterine arteries, vasoconstrictions to U46619, endothelium-dependent vasodilatations to acetylcholine, and endothelium-independent vasodilatations to nitric oxide donor sodium nitruprusside (SNP), were all comparable between wild-type and *GCH1*$^{fl/fl}$Tie2cre mice (Figure 6.11 A, B and F). Endothelium-dependent vasodilatations to acetylcholine were comparable between wild-type and *GCH1*$^{fl/fl}$Tie2cre mice in the presence of either L-NAME (Figure 6.11 C) alone, or L-NAME and indomethacin (Figure 6.11 D), or L-NAME, indomethacin and apamin and charbydotoxin (Figure 6.11 E).

Figure 6.10

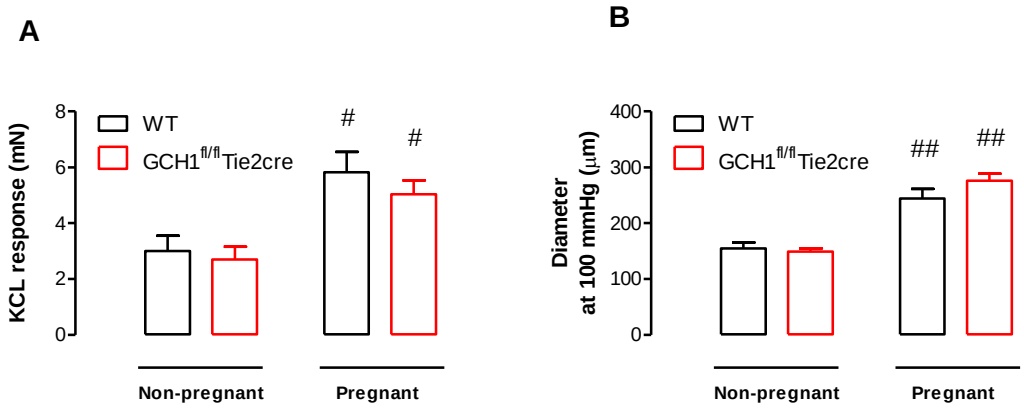


Figure 6.10. KCl response and diameter size in non-pregnant and pregnant uterine arteries

Vascular function of isolated uterine arteries (UA) from non-pregnant (NP) and pregnant (P) (at E18.5) mice of both genotypes was determined using a wire myograph. **A)** Vasoconstrictions in response to KCL (45 mM) were significantly increased in pregnant UA from both genotypes. **B)** Diameters of uterine arteries, as determined by length-tension relationship at 100 mmHg, were significantly increased in pregnant UA from both genotypes. Data are expressed as mean ± SEM. (*#P<0.01; ##P<0.001* comparing treatment; n=5 to 6 animals per group).

Figure 6.11

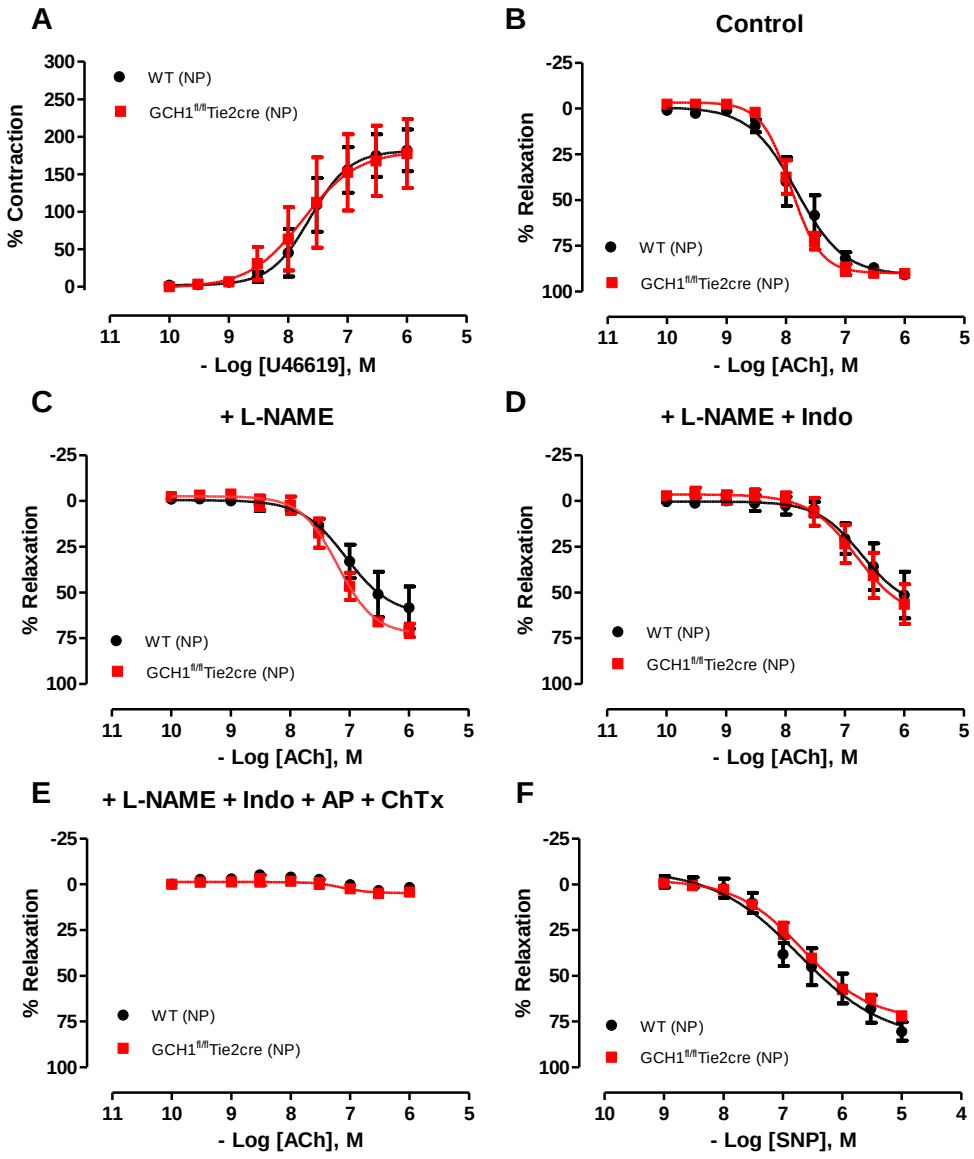


Figure 6.11. Effect of endothelial cell BH4 deficiency on vascular function in non-pregnant uterine arteries. Vascular function of isolated uterine arteries (UA) from non-pregnant (NP) wild-type and NP *GCH1*$^{fl/fl}$Tie2cre mice was determined using a wire myograph. Vasoconstriction, endothelium-dependent and independent vasodilatations were comparable between UA from non-pregnant wild-type and *GCH1*$^{fl/fl}$Tie2cre mice. A) Vasoconstriction to U46619. B) Endothelium-dependent vasodilatation to acetylcholine (ACh), C) Endothelium-dependent vasodilatation to ACh in the presence of L-NAME, D) L-NAME and indomethacin (Indo), E) L-NAME, indomethacin, apamin (AP) and charybdotoxin (ChTx). F) Endothelium-independent vasodilatation in response to the nitric oxide donor, sodium nitroprusside (SNP). Data are expressed as mean ± SEM. (n=5 to 6 animals per group

6.4.3.4 Vascular function in uterine arteries from pregnant wild-type and GCH1$^{fl/fl}$Tie2cre mice.

In pregnant mice, the lumen diameter of uterine arteries, as determined by length-tension relationship, from both pregnant wild-type and *GCH1*$^{fl/fl}$Tie2cre dams was significantly increased compared to non-pregnant wild-type and *GCH1*$^{fl/fl}$Tie2cre mice (Figure 6.10 B). This was accompanied by a greater KCl response in uterine arteries from pregnant wild-type and *GCH1*$^{fl/fl}$Tie2cre mice (Figure 6.10 A).

Vasoconstriction to U46619 was significantly decreased in uterine arteries from wild-type mice compared to *GCH1*$^{fl/fl}$Tie2cre mice (Figure 6.12 A; $P<0.01$). This difference was abolished in the presence of nitric oxide inhibitor L-NAME (Figure 6.2 A). Endothelium-dependent vasodilatation was significantly enhanced in wild-type uterine arteries compared to *GCH1*$^{fl/fl}$Tie2cre uterine arteries (Figure 6.12 B; $P<0.01$). In the presence of L-NAME, endothelium-dependent vasodilatation was significantly inhibited in wild-type uterine arteries but unaltered in *GCH1*$^{fl/fl}$Tie2cre uterine arteries (Figure 6.12 C) such that the vasodilation was no longer different between the genotypes. In the presence of L-NAME, indomethacin had a significant effect on endothelium-dependent vasodilation in both wild-type and *GCH1*$^{fl/fl}$Tie2cre uterine arteries (Figure 6.12 D). Endothelium-dependent vasodilation was totally abolished in both genotypes in the presence of L-NAME, indomethacin and EDHF blocker (apamin and charybdotoxin) (Figure 6.12 E), suggesting the role of EDHF-mediated vasodilator during pregnancy. No difference was detected in endothelium-independent vasodilatation to SNP between wild-type and *GCH1*$^{fl/fl}$Tie2cre uterine arteries (Figure 6.12 F). The contributions of prostacyclin, eNOS-derived vasodilator and EDHF in uterine arteries from non-pregnant and pregnant wild-type and *GCH1*$^{fl/fl}$Tie2cre mice were summarised in Figure 6.13.

Figure 6.12

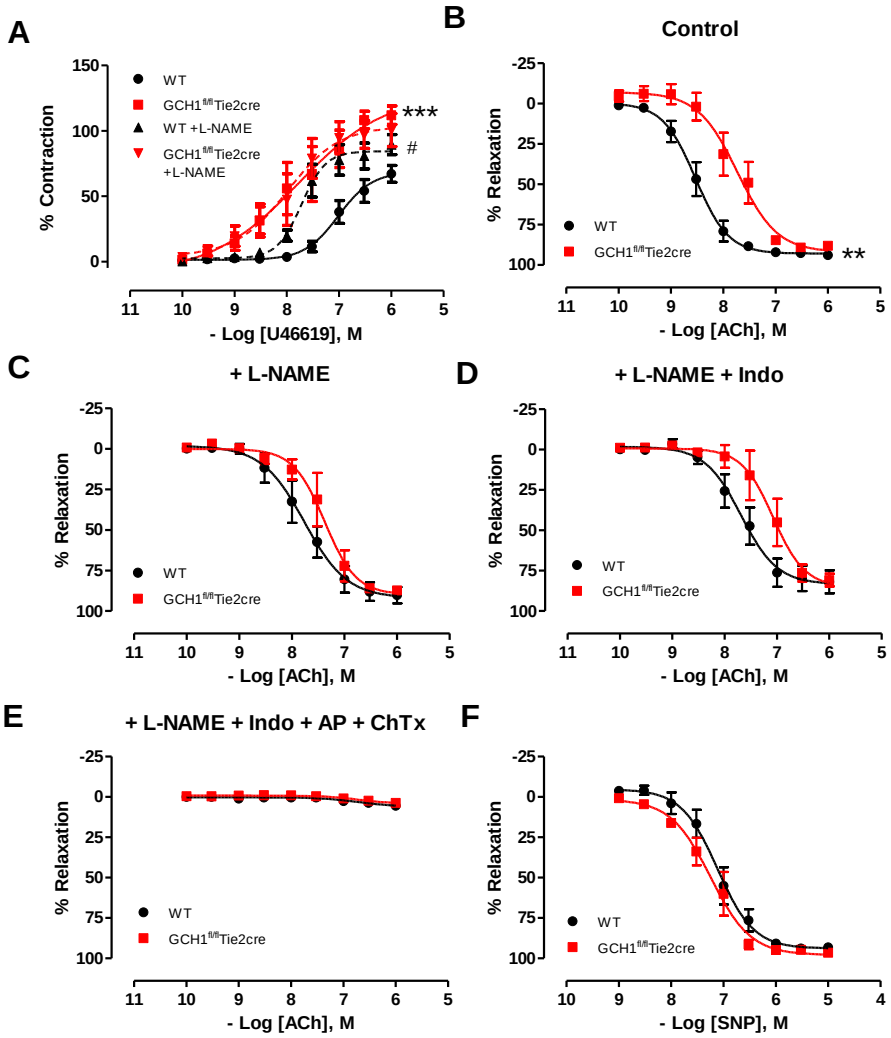


Figure 6.12. Effect of endothelial cell BH4 deficiency on vascular function in pregnant uterine arteries. Vascular function of isolated uterine arteries from pregnant (at E18.5) wild-type (WT) and *GCH1*$^{fl/fl}$Tie2cre mice was determined using a wire myograph (section). A) Percentage contraction in response to U46619 in the presence or absence of non-selective NOS inhibitor, L-NAME. B) Endothelium-dependent vasodilatation to acetylcholine (ACh) alone, C) in presence of L-NAME, D) L-NAME with indomethacin (Indo), E) L-NAME, indomethacin, apamin (AP) and charybdotoxin (ChTx). F) Endothelium-independent vasodilatation in response to the nitric oxide donor, sodium nitroprusside (SNP). Data are expressed as mean ± SEM. (*$P<0.05$, ** $P<0.01$ *** $P<0.001$ comparing genotype; #$P<0.001$ comparing treatment; n=5 to 6 animals per group).

Figure 6.13

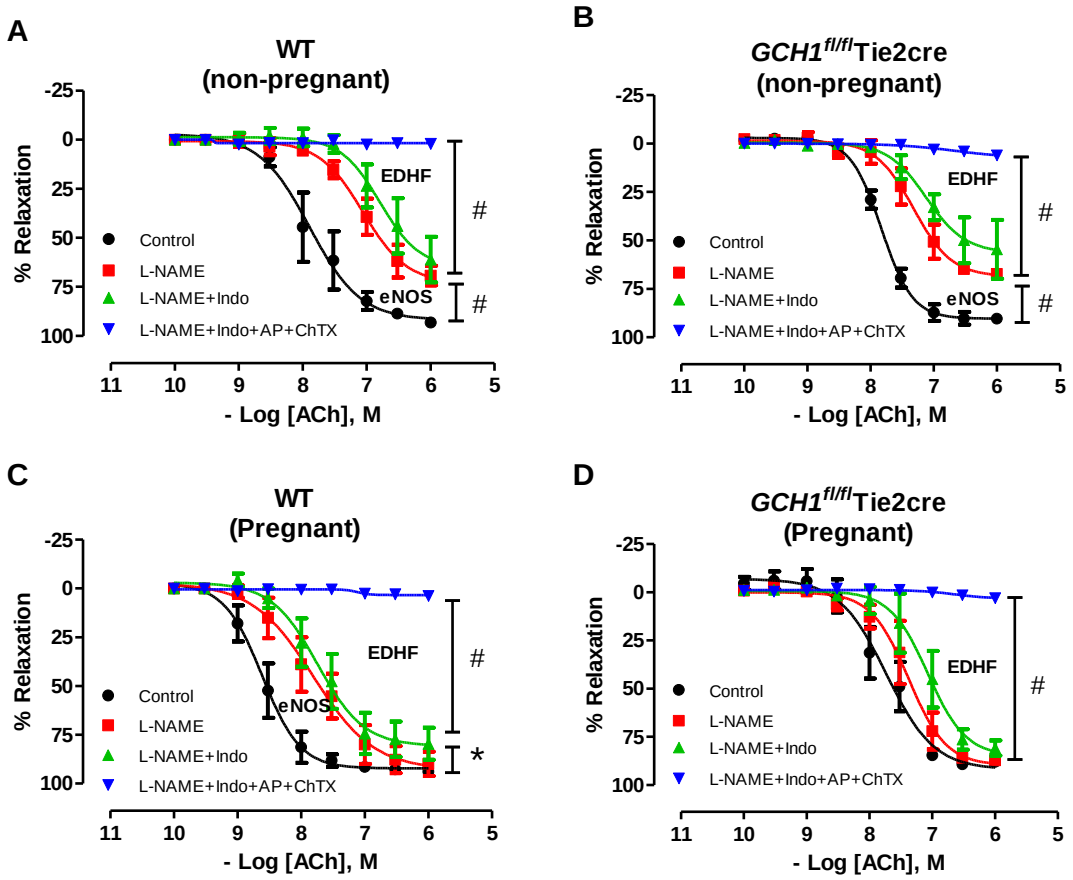


Figure 6.13. Contribution of prostacyclin, eNOS-derived vasodilators, and EDHF in non-pregnant and pregnant uterine arteries.

Isometric tension studies of uterine arteries from **A and B)** non-pregnant wild-type (WT) and *GCH1*$^{fl/fl}$Tie2cre mice and **C and D)** pregnant WT and *GCH1*$^{fl/fl}$Tie2cre mice were examined using a wire myograph. Endothelium-dependent vasodilatations to acetylcholine (ACh) were determined in the presence of the cyclooxygenase inhibitor, indomethacin (10 μM) alone, or indomethacin and the nitric oxide synthase inhibitor, L-NAME (100 μM), or indomethacin, L-NAME and EDHF blockers (apamin and charybdotoxin). Data are expressed as mean ± SEM. (*P<0.01, #P<0.001; n=5 to 6 animals per group).

6.4.4 Increased systolic blood pressure in *GCH1*$^{fl/fl}$Tie2cre female mice.

In chapter 5, I have previously shown that *GCH1*$^{fl/fl}$Tie2cre male mice have significantly higher systolic blood pressure compared to wild-type littermates. Heart rate in *GCH1*$^{fl/fl}$Tie2cre male mice was significantly lower compared to wild-type littermates. It is unknown whether increased systolic blood pressure in endothelial cell-targeted *GCH1* deficient mice is gender specific. To address this question, systolic blood pressure and heart rate in female *GCH1*$^{fl/fl}$Tie2cre and wild-type mice were determined by tail-cuff method in conscious mice as previously described in Section 5.3.3.1.

I have now shown that female *GCH1*$^{fl/fl}$Tie2cre mice also have significantly higher systolic blood pressure compared to wild-type littermates (Figure 6.14 A). Heart rate was also significantly lower in *GCH1*$^{fl/fl}$Tie2cre female mice compared to wild-type littermates (Figure 6.14 B). Together, I have shown that endothelial cell BH4 deficiency leads to an increase in systolic blood pressure in both *GCH1*$^{fl/fl}$Tie2cre male and female mice, suggesting that increased blood pressure in *GCH1*$^{fl/fl}$Tie2cre mice is not gender specific.

Figure 6.14

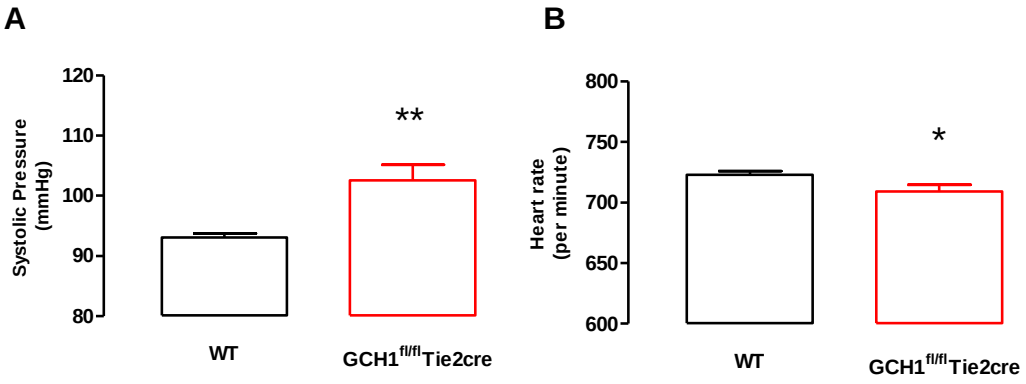


Figure 6.14. Haemodynamic measurements in *GCH1*$^{fl/fl}$Tie2cre and wild-type female mice. Systolic blood pressure and heart rate measurements were determined by tail-cuff method. A) Systolic blood pressure was significantly higher in *GCH1*$^{fl/fl}$Tie2cre females than wild-type littermates. B) Heart rate was significantly decreased in *GCH1*$^{fl/fl}$Tie2cre female mice compared to wild-type littermates. Data are expressed as mean ± SEM. (*$P<0.05$, **$P<0.01$; n=24 to 25 animals per group).

6.4.2 Pregnancy-induced Hypertension in *GCH1$^{fl/fl}$*Tie2cre mice.

To determine the requirement of endothelial cell BH4 biosynthesis in blood pressure regulation during pregnancy, blood pressure and heart rate were determined at gestation days, E0, E2.5, E5.5, E7.5, E10.5, E12.5, E15.5, E16.5, E17.5 and E18.5, using tail-cuff system as described in Section 5.3.1.1. Virgin *GCH1$^{fl/fl}$*Tie2cre and wild-type female mice were mated with wild-type male mice. Pregnancy was confirmed by the presence of a vaginal plug. Using a separate cohort of mice, I have shown that non-pregnant *GCH1$^{fl/fl}$*Tie2cre mice, as expected, have significantly higher systolic blood pressure compared to non-pregnant wild-type littermates. At E15.5 day of gestation, systolic blood pressure was significantly increased above basal levels and further elevated at E18.5 day of gestation in pregnant *GCH1$^{fl/fl}$*Tie2cre mice compared to that of *GCH1$^{fl/fl}$*Tie2cre mice at preconception (Figure 6.15 A). In contrast, no changes in blood pressure during pregnancy were seen in wild-type mice (Figure 6.15 C and D). Heart rate after E16.5 day of gestation onward was significantly reduced in pregnant *GCH1$^{fl/fl}$*Tie2cre mice compared to *GCH1$^{fl/fl}$*Tie2cre mice at baseline (Figure 6.15 B). Heart rate showed a trend towards a decrease in wild-type mice but was not significant at E18.5 day of gestation compared to that of wild-type at baseline.

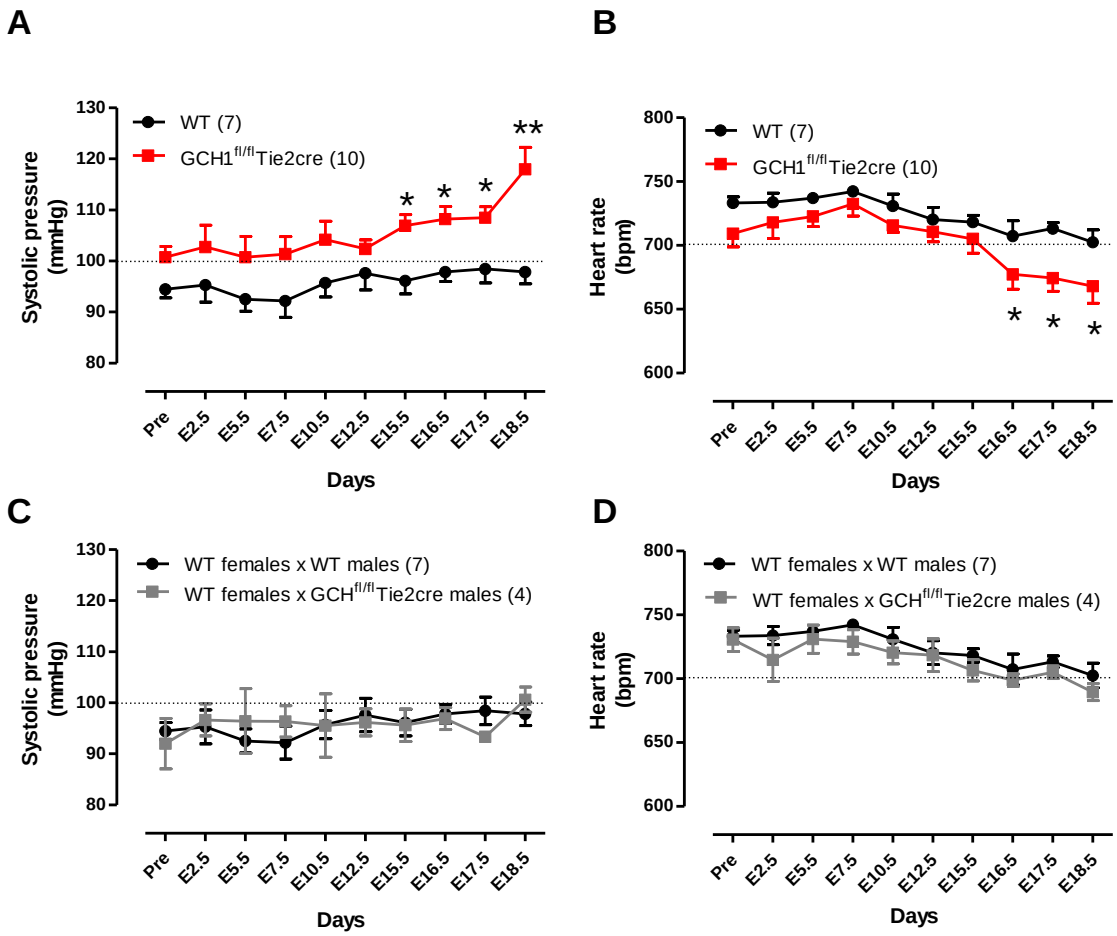


Figure 6.15. Haemodynamic measurements during pregnancy.

Virgin female wild-type and *GCH1*$^{fl/fl}$Tie2cre mice were mated with wild-type males. Systolic blood pressure and heart rate were determined prior to and during gestation by tail-cuff method. **A)** Prior to pregnancy, systolic blood pressure (SBP) was significantly higher compared to wild-type littermates and remained significantly elevated throughout pregnancy. After E15.5 day of gestation, SBP in *GCH1*$^{fl/fl}$Tie2cre female mice was significantly increased but unchanged in wild-type female mice. **B)** After gestation day E16.5, heart rate in *GCH1*$^{fl/fl}$Tie2cre mice was significantly decreased compared to heart rate of *GCH1*$^{fl/fl}$Tie2cre mice before pregnancy. No different was detected in heart rate before and at gestation day E18.5 in wild-type mice (*$P<0.05$; **$P<0.01$ n= 7 to 10 animals per group). **C and D)** No differences were detected in either SBP or heart rate before and during pregnancy between wild-type females mated with wild-type males and wild-type females mated with *GCH1*$^{fl/fl}$Tie2cre males (n= 4 to 7 animals per group). Data are expressed as mean ± SEM.

6.5 Discussion

In this chapter, I described a novel role of endothelial cell BH4-dependent NOS regulation in vascular adaptations and blood pressure regulation to normal pregnancy. The key findings were:

- Vascular adaptations to normal pregnancy were associated with increased endothelial cell BH4 biosynthesis and NOS-derived NO-mediated vasodilatation in uterine arteries from pregnant wild-type mice.
- Deficiency in endothelial cell BH4 biosynthesis during pregnancy led to a loss of NOS-derived NO mediated vasodilatation and impaired uterine vascular function in *GCH1*$^{fl/fl}$Tie2cre mice.
- Deficiency in endothelial cell BH4 biosynthesis led to a mild hypertension and bradycardia in female *GCH1*$^{fl/fl}$Tie2cre mice.
- Deficiency in endothelial cell BH4 biosynthesis during pregnancy led to a further increase in blood pressure and was associated with intrauterine growth restriction.

It has been shown previously that BH4 bioavailability is a key determinant of eNOS function and NO production (Crabtree et al., 2009b) and deficient endothelial cell BH4 biosynthesis, or loss of BH4 by oxidation (Landmesser et al., 2003), leads to eNOS uncoupling, vascular dysfunction and hypertension. Despite a marked decrease in BH4 levels in uterine arteries from non-pregnant *GCH1*$^{fl/fl}$Tie2cre mice, vasoconstriction, endothelium-dependent and independent vasodilatations are comparable to that of uterine arteries from non-pregnant wild-type mice, suggesting that endothelial cell BH4 biosynthesis does not play a significant role in non-pregnant uterine arteries (Linke et al., 2002).

During late pregnancy, the vasoconstrictor response to U46619 is reduced in wild-type uterine arteries compared to non-pregnant uterine arteries, which is reversed in the presence of L-NAME, suggesting increased NOS-derived NO mediated vascular tone in mouse pregnancy. These observations are compatible with recent findings in humans which demonstrated that acute administration of non-selectively NOS inhibitor L-NAME greatly reduced forearm blood flow in pregnant women compared to non-pregnant controls (Anumba et al., 1999; Williams et al., 1997). L-NAME treatment during pregnancy leads to decreased uterine blood flow in pregnant sheep and rats (Miller et al., 1999; Sladek et al., 1997). Consistent with this finding, I have shown that endothelial-dependent and independent vasodilatations are markedly enhanced in uterine arteries from pregnant wild-type mice compared to non-pregnant wild-type mice. Interestingly, the enhanced vasodilatation is accompanied by a 6-fold increase in vascular BH4 biosynthesis in uterine arteries of pregnant wild-type mice, suggesting for the first time that uterine vascular adaptation to normal pregnancy is associated with increased vascular BH4 biosynthesis. It is therefore likely that increased vascular BH4, eNOS expression and thus eNOS-derived NO production is responsible for the enhanced vasodilation. Although eNOS expression in uterine arteries has not been determined in this study, it is unlikely that increased vascular BH4 alone, without increased in eNOS expression, would increase NO-mediated vasodilatation. Consistent with this idea, mice with *GCH1* overexpressing specifically in the endothelial cell layer have a normal vascular function and blood pressure compared with wild-type littermates (Adlam et al., 2012; Alp et al., 2003a) These findings indicate that eNOS-derived NO is the key mediator in modulating vascular tone and vasodilatation during normal pregnancy. Indeed, increased eNOS protein and mRNA have been reported in uterine arteries (Rupnow et al., 2001), whereas iNOS and nNOS levels remain unchanged (Goetz et al., 1994; Linke et al., 2002)

In contrast to wild-type mice, pregnancy in *GCH1*$^{fl/fl}$Tie2cre mice did not alter either vasoconstrictor response to U46619 or endothelium-dependent vasodilatation in uterine arteries, despite enhanced endothelium-independent vasodilatation. Increased vascular BH4 levels are blunted in uterine arteries from *GCH1*$^{fl/fl}$Tie2cre mice, indicating that a significant portion of the increase in BH4 biosynthesis in wild-type uterine arteries is derived from the endothelium. These findings suggest that the endothelium is the major site of BH4 biosynthesis during pregnancy. Interestingly, L-NAME treatment has no significant effect on endothelium-dependent vasodilatation in uterine arteries from pregnant *GCH1*$^{fl/fl}$Tie2cre mice but markedly attenuated the response in uterine arteries from pregnant wild-type mice, suggesting the role of endothelial cell BH4 biosynthesis in eNOS regulation and NO generation in pregnancy. These findings suggest that deficiency in endothelial cell BH4 biosynthesis leads to an impairment of vascular function in uterine arteries during pregnancy. Impaired vascular function in uterine arteries of *GCH1*$^{fl/fl}$Tie2cre mice is likely to contribute to increased vascular resistance, reduced perfusion of the uterine circulation and thereby reduced nutrients and oxygen to growing fetuses. Indeed, deficiency in endothelial cell BH4 biosynthesis during pregnancy is associated with a low fetal and placental weight in *GCH1*$^{fl/fl}$Tie2cre mice. This is accompanied by reduced maternal weight gain during pregnancy in *GCH1*$^{fl/fl}$Tie2cre dams compared to pregnant wild-type mice. Despite reduced fetal and placental weights, litter sizes and onset of parturition are comparable between the wild-type and *GCH1*$^{fl/fl}$Tie2cre dams, indicating that litter sizes or parturition did not contribute to the reduction in fetal and placental weights. This finding is consistent with previous studies in eNOS knockout mice, which demonstrated that eNOS knockout mice gained significantly less weight during pregnancy than wild-type mice and have intrauterine growth restriction (Stanley et al., 2012a; Stanley et al., 2012b). In addition, there are no differences in fetal and placental weights of wild-type and *GCH1*$^{fl/fl}$Tie2cre

fetuses from *GCH1*$^{fl/fl}$Tie2cre dams, suggesting that the maternal genotype but not fetal genotype is responsible for the decrease in fetal and placental weights. These findings suggest for the first time that endothelial cell BH4 availability is implicated in the pathogenesis of intrauterine growth restriction.

The physiological requirement for endothelial cell BH4 biosynthesis in the regulation of blood pressure during pregnancy is unknown. First, I have shown that *GCH1*$^{fl/fl}$Tie2cre females have higher systolic blood pressure compared to wild-type littermates. This finding is consistent with previous findings in male *GCH1*$^{fl/fl}$Tie2cre mice. This finding suggests that increased blood pressure in *GCH1*$^{fl/fl}$Tie2cre mice is not gender specific. At late pregnancy, systolic blood pressure is augmented in *GCH1*$^{fl/fl}$Tie2cre mice but unchanged in wild-type mice. This increase in blood pressure is accompanied by bradycardia in *GCH1*$^{fl/fl}$Tie2cre mice. Consistent with this finding, eNOS knockout mice are hypertensive and have bradycardia in late pregnancy (Stauss HM et al 1999). These findings suggest that the baroreceptor reflex mechanisms responding to the increased blood pressure are likely to be responsible for reductions in heart rate in *GCH1*$^{fl/fl}$Tie2cre mice during pregnancy. To distinguish the role of maternal endothelial cell BH4 biosynthesis from that of fetus and placenta, wild-type females were mated with *GCH1*$^{fl/fl}$Tie2cre males, and *GCH1*$^{fl/fl}$Tie2cre females were mated with wild-type males, in both cases, resulting in wild-type and *GCH1*$^{fl/fl}$Tie2cre offspring. I have shown that pregnant wild-type females mated with *GCH1*$^{fl/fl}$Tie2cre males have normal blood pressure, suggesting lack of maternal endothelial cell BH4, but not fetal BH4, caused pregnancy-induced hypertension. To the best of our knowledge, this is the first study that demonstrates that deficiency in endothelial cell BH4 biosynthesis during pregnancy is alone sufficient to cause hypertension during pregnancy and fetal growth restriction, suggesting the critical role of endothelial cell BH4 biosynthesis in normal pregnancy. Whether pregnancy-induced hypertension in *GCH1*$^{fl/fl}$Tie2cre mice is

due to pre-existing high blood pressure is unclear. It has been reported that offspring from mothers with hypertensive disorders of pregnancy are likely to have a higher risk of hypertension and other cardiovascular disease in later life (Ferreira et al., 2009; Kajantie et al., 2009). Indeed, offspring born to mothers with hypertension during pregnancy is associated with elevated blood pressure in later in life (Lazdam et al., 2012; Lazdam et al., 2010). Whether offspring from *GCH1*$^{fl/fl}$Tie2cre mothers are developing cardiovascular disease in adulthood has yet to be determined.

Protein levels in uterine samples are comparable between pregnant wild-type and pregnant *GCH1*$^{fl/fl}$Tie2cre, as well as non-pregnant wild-type and non-pregnant *GCH1*$^{fl/fl}$Tie2cre mice. Because pre-eclampsia is characterised by hypertension and proteinuria during pregnancy, the characterisation of increased blood pressure alone without proteinuria during pregnancy would class as gestational hypertension instead of pre-eclampsia. Furthermore, there were no differences in plasma BH4 levels between non-pregnant wild-type and *GCH1*$^{fl/fl}$Tie2cre female mice, a finding consistent with biopterin data from male mice. Interestingly, plasma BH4 levels are markedly reduced in both wild-type and *GCH1*$^{fl/fl}$Tie2cre mice at late pregnancy. This finding indicates for the first time that a fall in plasma biopterins and BH4 levels is associated with a normal pregnancy in mice. Indeed, decreased plasma BH4 levels have been documented in a normal pregnancy in humans (Tachibana et al., 2002). It is unclear whether reduced plasma BH4 levels during pregnancy have a significant role or implication in a normal pregnancy. Furthermore, plasma BH4 levels are further reduced in pregnant *GCH1*$^{fl/fl}$Tie2cre mice compared to that from pregnant wild-type mice. Whether the decrease in plasma BH4 levels is implicated in the development of hypertension during pregnancy and intrauterine growth restriction in *GCH1*$^{fl/fl}$Tie2cre dams is unknown. In addition, it is unknown whether reduced plasma BH4 levels are

associated with human preeclampsia. Therefore, plasma BH4 levels may be useful as a biomarker for testing the development of preeclampsia and hypertension during pregnancy.

HMG CO-A reductase inhibition by statin therapy has been shown to be effective for primary and secondary cardiovascular prevention in high and moderate risk groups, at least in part through mechanisms which lead to restored eNOS activity. Indeed, statin therapy leads to an upregulation of vascular GTPCH expression, BH4 levels, and thereby improved endothelial function in humans with atherosclerosis (Antoniades et al., 2011a). Based from these observations, treatment with statins may be a potential therapeutic target for the prevention and treatment of pregnancy-induced hypertension and preeclampsia.

Taken together, this study demonstrated that deficiency in endothelial cell BH4 biosynthesis contributes to pregnancy-induced hypertension and intrauterine growth restriction. These findings suggest a novel role of endothelial cell BH4 biosynthesis in vascular adaptations and blood pressure regulation during pregnancy. Thus, targeting endothelial cell *GCH1* and BH4 biosynthesis may provide a novel therapeutic target for the prevention and treatment of pregnancy-related hypertension such as pre-eclampsia.

Chapter 7:
General discussion

Chapter 7: General Discussion

7.1 Principal findings and implications

The main findings of these studies presented in this thesis are:

1) Endothelial cell-targeted *GCH1* deletion led to endothelial cell BH4 deficiency, despite no significant change in plasma BH4, thus identifying a cell-autonomous requirement for endothelial cell *GCH1* and de novo BH4 biosynthesis.
2) Endothelial cell BH4 deficiency led to eNOS uncoupling, with loss of nitric oxide bioavailability and increased superoxide production in both primary endothelial cells and aortas.
3) In aortas, deficiency in endothelial cell BH4 biosynthesis led to aortic vascular dysfunction with eNOS-dependent vasodilatation mediated by eNOS-derived H_2O_2, acting through the soluble guanylate cyclase-dependent signalling pathway.
4) In mesenteric arteries, deficiency in endothelial cell BH4 biosynthesis led to a loss of eNOS-derived NO mediated vascular tone and impaired vascular function.
5) Deficiency in endothelial cell BH4 biosynthesis led to an increase in systemic blood pressure in both male and female, an effect which is normalised by L-NAME.
6) Deficiency in endothelial cell BH4 biosynthesis led to significantly increased incidence of abdominal aortic aneurysms in response to Ang II.
7) Deficiency in endothelial cell *GCH1* and BH4 biosynthesis is partially protective from LPS-induced vascular dysfunction and hypotension.
8) Vascular adaptations to normal pregnancy were associated with an increase in endothelial cell BH4 biosynthesis and enhanced NOS-derived NO mediated vasodilatation in uterine arteries.

9) Deficiency in endothelial cell BH4 biosynthesis during pregnancy led to a loss of NOS-derived NO mediated vasodilatation, impaired uterine vascular function, increased blood pressure and fetal growth restriction.

7.2 Future Work

The findings of this thesis identify several research areas which I believe warrant further investigation.

The work in this thesis discovered an important role of endothelial cell *GCH1* and BH4 biosynthesis in the regulation of vascular function and blood pressure in both health and disease. This is the first study to show that a deficiency in endothelial cell BH4 is alone sufficient to cause eNOS uncoupling, impaired vascular function and leads to hypertension even in the absence of vascular disease.

In this work I have also shown that endothelial cell *GCH1* and BH4 play a critical role in the pathogenesis of abdominal aortic aneurysm. The finding of increased incidence of aortic abdominal aneurysm in response to Ang II in *GCH1*$^{fl/fl}$Tie2cre mice opens several possible areas of investigation. Important roles for eNOS uncoupling and BH4 deficiency in AAA formation have recently been documented in hph-1 mice (Gao et al., 2012) and ApoE$^{-/-}$ knockout mice (Siu et al., 2014). Investigating aortic and plasma BH4 levels, as well as the expression of vascular *GCH1*, NOS isoforms and MMPs, in particular MMP2 and MMP9 which have been shown to play a role in the development of AAA, may provide a comprehensive understanding of the pathological process leading to AAA formation in *GCH1*$^{fl/fl}$Tie2cre mice. In clinical studies, it remains unknown whether vascular BH4 plays a role in the development of AAA. Thus plasma and vascular BH4 levels, as well as vascular

GCH1 mRNA and protein from patients with AAA should be measured. Indeed, circulating BH4 has recently been reported to be a biomarker for Ang II-induced AAA in hph-1 mice (Siu et al., 2014) and ApoE$^{-/-}$ mice. Human *GCH1* mutations are rare but do exist, causing severe BH4 deficiency syndromes such as hyperphenylalaninaemia. The incidence of AAA formation in these patients could be studied.

Although deficiency in endothelial cell *GCH1* and BH4 partially protects against LPS-induced vascular dysfunction and hypertension in *GCH1*$^{fl/fl}$Tie2cre mice at low dose of LPS (1 mg/kg), it is unknown whether deficiency in endothelial cell *GCH1*/BH4 is protective against LPS at higher doses that causes septic shock. Increased iNOS and *GCH1* expression in vascular smooth muscle cells have been reported to be associated with vascular dysfunction and hypotension induced by LPS. Investigation using vascular smooth muscle cell-specific *GCH1* deletion (e.g. *GCH1*$^{fl/fl}$SM22-cre mice) mice or knockout of *GCH1* in both endothelial cells and vascular smooth muscle cells may provide an insight into understanding the role of *GCH1* and BH4-dependent NOS regulation in different vessel wall cells in the pathogenesis of LPS-induced septic shock.

A novel role of endothelial cell BH4 biosynthesis in vascular adaptation and blood pressure regulation during pregnancy has been presented here for the first time. Deficiency in endothelial cell BH4 leads to abnormal vascular adaptation, hypertension and fetal growth restriction in *GCH1*$^{fl/fl}$Tie2cre mice during pregnancy. Investigation by supplementing *GCH1*$^{fl/fl}$Tie2cre mothers with BH4 or crossing *GCH1*$^{fl/fl}$Tie2cre mice with endothelial *GCH1* overexpressing mice may provide an insight into the pathological process leading to hypertension and fetal growth restriction in *GCH1*$^{fl/fl}$Tie2cre mice.

It has been reported that offspring from mothers with hypertensive disorders of pregnancy are likely to have a higher risk of hypertension and other cardiovascular disease in later life (Ferreira et al., 2009; Kajantie et al., 2009). It is unknown whether offspring born to *GCH1*$^{fl/fl}$Tie2cre mothers exhibit cardiovascular phenotypes in adulthood. In addition, plasma BH4 levels are markedly reduced in both wild-type and *GCH1*$^{fl/fl}$Tie2cre mice at late pregnancy and further reduced in *GCH1*$^{fl/fl}$Tie2cre mothers. Whether circulating BH4 levels are reduced in preeclamptic women is unknown. Thus, circulating BH4 levels may be used in clinic as a novel and powerful biomarker for the prevention or treatment of preeclampsia.

7.3 Concluding Remarks

These are the first studies to show that deficiency in endothelial cell *GCH1* and BH4 biosynthesis is alone sufficient to cause eNOS uncoupling, increased superoxide production, reduced NO generation, impaired vascular function and hypertension. The findings of this thesis confirm the hypothesis that endothelial cell BH4 is a pivotal regulator of eNOS function and vascular homeostasis under physiological states as well as in the pathogenesis of cardiovascular disease states. Thus, targeting vascular *GCH1* and BH4 biosynthesis may provide a novel therapeutic target for the treatment of vascular dysfunction in patients with hypertension, AAA formation, septic shock and in women with preeclampsia.

Chapter 8:
References

Chapter 8: References

Adlam, D., N. Herring, G. Douglas, J.P. De Bono, D. Li, E.J. Danson, A. Tatham, C.J. Lu, K.A. Jennings, S.J. Cragg, B. Casadei, D.J. Paterson, and K.M. Channon. 2012. Regulation of beta-adrenergic control of heart rate by GTP-cyclohydrolase 1 (GCH1) and tetrahydrobiopterin. *Cardiovasc Res* 93:694-701.

Aggarwal, S., A. Qamar, V. Sharma, and A. Sharma. 2011. Abdominal aortic aneurysm: A comprehensive review. *Experimental and clinical cardiology* 16:11-15.

Alderton, W.K., C.E. Cooper, and R.G. Knowles. 2001. Nitric oxide synthases: structure, function and inhibition. *The Biochemical journal* 357:593-615.

Aley, P.K., K.E. Porter, J.P. Boyle, P.J. Kemp, and C. Peers. 2005. Hypoxic modulation of Ca2+ signaling in human venous endothelial cells. Multiple roles for reactive oxygen species. *J Biol Chem* 280:13349-13354.

Ali, Z.A., R. Rinze, G. Douglas, Y. Hu, Q. Xiao, W. Qi, E. McNeill, C. Bursill, I. George, D.R. Greaves, Q. Xu, and K.M. Channon. 2013. Tetrahydrobiopterin determines vascular remodeling through enhanced endothelial cell survival and regeneration. *Circulation* 128:S50-58.

Alp, N.J., M.A. McAteer, J. Khoo, R.P. Choudhury, and K.M. Channon. 2004. Increased endothelial tetrahydrobiopterin synthesis by targeted transgenic GTP-cyclohydrolase I overexpression reduces endothelial dysfunction and atherosclerosis in ApoE-knockout mice. *Arterioscler Thromb Vasc Biol* 24:445-450.

Alp, N.J., S. Mussa, J. Khoo, S. Cai, T. Guzik, A. Jefferson, N. Goh, K.A. Rockett, and K.M. Channon. 2003a. Tetrahydrobiopterin-dependent preservation of nitric oxide-mediated endothelial function in diabetes by targeted transgenic GTP-cyclohydrolase I overexpression. *J Clin Invest* 112:725-735.

Alp, N.J., S. Mussa, J. Khoo, T.J. Guzik, S. Cai, A. Jefferson, K.A. Rockett, and K.M. Channon. 2003b. Tetrahydrobiopterin-dependent preservation of nitric oxide-mediated endothelial function in diabetes by targeted transgenic GTP-cyclohydrolase I overexpression. *J Clin Invest* 112:725-735.

Antoniades, C., C. Bakogiannis, P. Leeson, T.J. Guzik, M.H. Zhang, D. Tousoulis, A.S. Antonopoulos, M. Demosthenous, K. Marinou, A. Hale, A. Paschalis, C. Psarros, C. Triantafyllou, J. Bendall, B. Casadei, C. Stefanadis, and K.M. Channon. 2011a. Rapid, direct effects of statin treatment on arterial redox state and nitric oxide bioavailability in human atherosclerosis via tetrahydrobiopterin-mediated endothelial nitric oxide synthase coupling. *Circulation* 124:335-345.

Antoniades, C., C. Cunnington, A. Antonopoulos, M. Neville, M. Margaritis, M. Demosthenous, J. Bendall, A. Hale, R. Cerrato, D. Tousoulis, C. Bakogiannis, K. Marinou, M. Toutouza, C. Vlachopoulos, P. Leeson, C. Stefanadis, F. Karpe, and K.M. Channon. 2011b. Induction of vascular GTP-cyclohydrolase I and endogenous tetrahydrobiopterin synthesis protect against inflammation-induced endothelial dysfunction in human atherosclerosis. *Circulation* 124:1860-1870.

Antoniades, C., C. Shirodaria, M. Crabtree, R. Rinze, N. Alp, C. Cunnington, J. Diesch, D. Tousoulis, C. Stefanadis, P. Leeson, C. Ratnatunga, R. Pillai, and K.M. Channon. 2007. Altered plasma versus vascular biopterins in human atherosclerosis reveal relationships between endothelial nitric oxide synthase coupling, endothelial function, and inflammation. *Circulation* 116:2851-2859.

Anumba, D.O., S.C. Robson, R.J. Boys, and G.A. Ford. 1999. Nitric oxide activity in the peripheral vasculature during normotensive and preeclamptic pregnancy. *Am J Physiol* 277:H848-854.

Ayabe, N., V.R. Babaev, Y. Tang, T. Tanizawa, A.B. Fogo, M.F. Linton, I. Ichikawa, S. Fazio, and V. Kon. 2006. Transiently heightened angiotensin II has distinct effects on atherosclerosis and aneurysm formation in hyperlipidemic mice. *Atherosclerosis* 184:312-321.

Balligand, J.L., and P.J. Cannon. 1997. Nitric oxide synthases and cardiac muscle. Autocrine and paracrine influences. *Arterioscler Thromb Vasc Biol* 17:1846-1858.

Barker, J.E., Y.S. Bakhle, J. Anderson, T. Treasure, and P.J. Piper. 1996. Reciprocal inhibition of nitric oxide and prostacyclin synthesis in human saphenous vein. *Br J Pharmacol* 118:643-648.

Bauersachs, J., A. Bouloumi, D. Fraccarollo, K. Hu, R. Busse, and G. Ertl. 1999. Endothelial dysfunction in chronic myocardial infarction despite increased vascular endothelial nitric oxide synthase and soluble guanylate cyclase expression : role of enhanced vascular superoxide production. *Circulation* 100:292-298.

Beinder, E., M.G. Mohaupt, D. Schlembach, T. Fischer, R.B. Sterzel, N. Lang, and C. Baylis. 1999. Nitric oxide synthase activity and Doppler parameters in the fetoplacental and uteroplacental circulation in preeclampsia. *Hypertens Pregnancy* 18:115-127.

Bellamy, L., J.P. Casas, A.D. Hingorani, and D.J. Williams. 2007. Pre-eclampsia and risk of cardiovascular disease and cancer in later life: systematic review and meta-analysis. *BMJ* 335:974.

Bendall, J.K., N.J. Alp, N. Warrick, S. Cai, D. Adlam, K. Rockett, M. Yokoyama, S. Kawashima, and K.M. Channon. 2005. Stoichiometric relationships between endothelial tetrahydrobiopterin, eNOS activity and eNOS coupling in vivo: Insights from transgenic mice with endothelial-targeted GTPCH and eNOS over-expression. *Circ Res* 97:864-871.

Bendall, J.K., R. Rinze, D. Adlam, A.L. Tatham, J. de Bono, and K.M. Channon. 2007. Endothelial Nox2 overexpression potentiates vascular oxidative stress and hemodynamic response to angiotensin II: studies in endothelial-targeted Nox2 transgenic mice. *Circ Res* 100:1016-1025.

Beverelli, F., M.L. Bea, L. Puybasset, J.F. Giudicelli, and A. Berdeaux. 1997. Chronic inhibition of NO synthase enhances the production of prostacyclin in coronary arteries through upregulation of the cyclooxygenase type 1 isoform. *Fundamental & clinical pharmacology* 11:252-259.

Billiar, T.R., R.D. Curran, B.G. Harbrecht, D.J. Stuehr, A.J. Demetris, and R.L. Simmons. 1990. Modulation of nitrogen oxide synthesis in vivo: NG-monomethyl-L-arginine inhibits endotoxin-induced nitrate/nitrate biosynthesis while promoting hepatic damage. *J Leukoc Biol* 48:565-569.

Bitar, M.S., S. Wahid, S. Mustafa, E. Al-Saleh, G.S. Dhaunsi, and F. Al-Mulla. 2005a. Nitric oxide dynamics and endothelial dysfunction in type II model of genetic diabetes. *Eur J Pharmacol* 511:53-64.

Bitar, M.S., S. Wahid, S. Mustafa, E. Al-Saleh, G.S. Dhaunsi, and F. Al-Mulla. 2005b. Nitric oxide dynamics and endothelial dysfunction in type II model of genetic diabetes. *European Journal of Pharmacology* 511:53.

Budhiraja, R., R.M. Tuder, and P.M. Hassoun. 2004. Endothelial dysfunction in pulmonary hypertension. *Circulation* 109:159-165.

Bune, A.J., M.P. Brand, S.J. Heales, J.K. Shergill, R. Cammack, and H.T. Cook. 1996. Inhibition of tetrahydrobiopterin synthesis reduces in vivo nitric oxide production in experimental endotoxic shock. *Biochem Biophys Res Commun* 220:13-19.

Burgoyne, J.R., M. Madhani, F. Cuello, R.L. Charles, J.P. Brennan, E. Schroder, D.D. Browning, and P. Eaton. 2007. Cysteine redox sensor in PKGIa enables oxidant-induced activation. *Science* 317:1393-1397.

Burgoyne, J.R., O. Prysyazhna, O. Rudyk, and P. Eaton. 2012. cGMP-dependent activation of protein kinase G precludes disulfide activation: implications for blood pressure control. *Hypertension* 60:1301-1308.

Busse, R., G. Edwards, M. Feletou, I. Fleming, P.M. Vanhoutte, and A.H. Weston. 2002. EDHF: bringing the concepts together. *Trends Pharmacol Sci* 23:374-380.

Campbell, W.B., D. Gebremedhin, P.F. Pratt, and D.R. Harder. 1996. Identification of epoxyeicosatrienoic acids as endothelium-derived hyperpolarizing factors. *Circ Res* 78:415-423.

Carvajal, J.A., A.M. Germain, J.P. Huidobro-Toro, and C.P. Weiner. 2000. Molecular mechanism of cGMP-mediated smooth muscle relaxation. *Journal of cellular physiology* 184:409-420.

Channon, K.M. 2012. Tetrahydrobiopterin: a vascular redox target to improve endothelial function. *Current vascular pharmacology* 10:705-708.

Chataigneau, T., M. Feletou, P.L. Huang, M.C. Fishman, J. Duhault, and P.M. Vanhoutte. 1999. Acetylcholine-induced relaxation in blood vessels from endothelial nitric oxide synthase knockout mice. *Br J Pharmacol* 126:219-226.

Chauhan, S.D., H. Nilsson, A. Ahluwalia, and A.J. Hobbs. 2003. Release of C-type natriuretic peptide accounts for the biological activity of endothelium-derived hyperpolarizing factor. *Proc Natl Acad Sci U S A* 100:1426-1431.

Chen, G., H. Suzuki, and A.H. Weston. 1988. Acetylcholine releases endothelium-derived hyperpolarizing factor and EDRF from rat blood vessels. *Br J Pharmacol* 95:1165-1174.

Chen, Z.P., K.I. Mitchelhill, B.J. Michell, D. Stapleton, I. Rodriguez-Crespo, L.A. Witters, D.A. Power, P.R. Ortiz de Montellano, and B.E. Kemp. 1999. AMP-activated protein kinase phosphorylation of endothelial NO synthase. *FEBS Lett* 443:285-289.

Chiao, C.W., J.E. da Silva-Santos, F.R. Giachini, R.C. Tostes, M.J. Su, and R.C. Webb. 2013. P2X7 receptor activation contributes to an initial upstream mechanism of lipopolysaccharide-induced vascular dysfunction. *Clin Sci (Lond)* 125:131-141.

Cho, H.J., E. Martin, Q.W. Xie, S. Sassa, and C. Nathan. 1995. Inducible nitric oxide synthase - identification of amino acid residues essential for dimerization and binding of tetrahydrobiopterin. *Proc Natl Acad Sci USA* 92:11514-11518.

Connelly, L., M. Madhani, and A.J. Hobbs. 2005. Resistance to endotoxic shock in endothelial nitric-oxide synthase (eNOS) knock-out mice: a pro-inflammatory role for eNOS-derived no in vivo. *J Biol Chem* 280:10040-10046.

Conrad, K.P., and A.K. Davis. 1995. Nitric oxide synthase activity in placentae from women with pre-eclampsia. *Placenta* 16:691-699.

Cooke, C.L., and S.T. Davidge. 2003. Pregnancy-induced alterations of vascular function in mouse mesenteric and uterine arteries. *Biol Reprod* 68:1072-1077.

Cosentino, F., J.E. Barker, M.P. Brand, S.J. Heales, E.R. Werner, J.R. Tippins, N. West, K.M. Channon, M. Volpe, and T.F. Luscher. 2001. Reactive oxygen species mediate endothelium-dependent relaxations in tetrahydrobiopterin-deficient mice. *Arterioscler Thromb Vasc Biol* 21:496-502.

Cosentino, F., K. Hishikawa, Z.S. Katusic, and T.F. Luscher. 1997. High glucose increases nitric oxide synthase expression and superoxide anion generation in human aortic endothelial cells. *Circulation* 96:25-28.

Crabtree, M.J., and K.M. Channon. 2009. Dihydrofolate reductase and biopterin recycling in cardiovascular disease. *J Mol Cell Cardiol* 47:749-751.

Crabtree, M.J., C.L. Smith, G. Lam, M.S. Goligorsky, and S.S. Gross. 2008. Ratio of 5,6,7,8-tetrahydrobiopterin to 7,8-dihydrobiopterin in endothelial cells determines glucose-elicited changes in NO vs. superoxide production by eNOS. *Am J Physiol Heart Circ Physiol* 294:H1530-1540.

Crabtree, M.J., A.L. Tatham, Y. Al-Wakeel, N. Warrick, A.B. Hale, S. Cai, K.M. Channon, and N.J. Alp. 2009a. Quantitative regulation of intracellular endothelial nitric oxide synthase (eNOS) coupling by both tetrahydrobiopterin-eNOS stoichiometry and biopterin redox status: Insights from cells with tet-regulated GTP cyclohydrolase I expression. *J Biol Chem* 284:1136-1144.

Crabtree, M.J., A.L. Tatham, A.B. Hale, N.J. Alp, and K.M. Channon. 2009b. Critical role for tetrahydrobiopterin recycling by dihydrofolate reductase in regulation of endothelial nitric-oxide synthase coupling: relative importance of the de novo biopterin synthesis versus salvage pathways. *J Biol Chem* 284:28128-28136.

Creager, M.A., J.P. Cooke, M.E. Mendelsohn, S.J. Gallagher, S.M. Coleman, J. Loscalzo, and V.J. Dzau. 1990. Impaired vasodilation of forearm resistance vessels in hypercholesterolemic humans. *J Clin Invest* 86:228-234.

Cunha, F.Q., J. Assreuy, D.W. Moss, D. Rees, L.M. Leal, S. Moncada, M. Carrier, C.A. O'Donnell, and F.Y. Liew. 1994. Differential induction of nitric oxide synthase in various organs of the mouse during endotoxaemia: role of TNF-alpha and IL-1-beta. *Immunology* 81:211-215.

Darley-Usmar, V.M., N. Hogg, V.J. O'Leary, M.T. Wilson, and S. Moncada. 1992. The simultaneous generation of superoxide and nitric oxide can initiate lipid peroxidation in human low density lipoprotein. *Free Radical Res Comm* 17:9-20.

Daugherty, A., M.W. Manning, and L.A. Cassis. 2000. Angiotensin II promotes atherosclerotic lesions and aneurysms in apolipoprotein E-deficient mice. *The Journal of clinical investigation* 105:1605-1612.

Davis, F.M., D.L. Rateri, and A. Daugherty. 2014. Mechanisms of aortic aneurysm formation: translating preclinical studies into clinical therapies. *Heart* 100:1498-1505.

de Bono, J.P., N. Warrick, J.K. Bendall, K.M. Channon, and N.J. Alp. 2007. Radiochemical HPLC detection of arginine metabolism: measurement of nitric oxide synthesis and arginase activity in vascular tissue. *Nitric Oxide* 16:1-9.

Dikalov, S., K.K. Griendling, and D.G. Harrison. 2007. Measurement of Reactive Oxygen Species in Cardiovascular Studies. *Hypertension* 49:717-727.

Dimmeler, S., I. Fleming, B. Fisslthaler, C. Hermann, R. Busse, and A.M. Zeiher. 1999a. Activation of nitric oxide synthase in endothelial cells by Akt- dependent phosphorylation. *Nature* 399:601-605.

Dimmeler, S., I. Fleming, B. Fisslthaler, C. Hermann, R. Busse, and A.M. Zeiher. 1999b. Activation of nitric oxide synthase in endothelial cells by Akt-dependent phosphorylation. *Nature* 399:601-605.

Dinerman, J.L., J.P. Steiner, T.M. Dawson, V. Dawson, and S.H. Snyder. 1994. Cyclic nucleotide dependent phosphorylation of neuronal nitric oxide synthase inhibits catalytic activity. *Neuropharmacology* 33:1245-1251.

Dora, K.A., N.T. Gallagher, A. McNeish, and C.J. Garland. 2008. Modulation of endothelial cell KCa3.1 channels during endothelium-derived hyperpolarizing factor signaling in mesenteric resistance arteries. *Circ Res* 102:1247-1255.

Dora, K.A., S.L. Sandow, N.T. Gallagher, H. Takano, N.M. Rummery, C.E. Hill, and C.J. Garland. 2003. Myoendothelial gap junctions may provide the pathway for EDHF in mouse mesenteric artery. *J Vasc Res* 40:480-490.

Droge, W. 2002. Free radicals in the physiological control of cell function. *Physiological reviews* 82:47-95.

Du, Y.H., Y.Y. Guan, N.J. Alp, K.M. Channon, and A.F. Chen. 2008. Endothelium-specific GTP cyclohydrolase I overexpression attenuates blood pressure progression in salt-sensitive low-renin hypertension. *Circulation* 117:1045-1054.

Dumont, O., L. Loufrani, and D. Henrion. 2007. Key role of the NO-pathway and matrix metalloprotease-9 in high blood flow-induced remodeling of rat resistance arteries. *Arterioscler Thromb Vasc Biol* 27:317-324.

Edwards, G., K.A. Dora, M.J. Gardener, C.J. Garland, and A.H. Weston. 1998. K+ is an endothelium-derived hyperpolarising factor in rat arteries. *Nature* 396:269-271.

Elsner, D., A. Muntze, E.P. Kromer, and G.A. Riegger. 1992. Inhibition of synthesis of endothelium-derived nitric oxide in conscious dogs. Hemodynamic, renal, and hormonal effects. *American journal of hypertension* 5:288-291.

Evans, T.J., A. Carpenter, D. Moyes, R. Martin, and J. Cohen. 1995. Protective effects of a recombinant amino-terminal fragment of human bactericidal/permeability-increasing protein in an animal model of gram-negative sepsis. *J Infect Dis* 171:153-160.

Fadel, P.J., W. Zhao, and G.D. Thomas. 2003. Impaired vasomodulation is associated with reduced neuronal nitric oxide synthase in skeletal muscle of ovariectomized rats. *J Physiol* 549:243-253.

Fan, L.M., G. Douglas, J.K. Bendall, E. McNeill, M.J. Crabtree, A.B. Hale, A. Mai, J.-M. Li, M.A. McAteer, J.E. Schneider, R.P. Choudhury, and K.M. Channon. 2014. Endothelial Cell–Specific Reactive Oxygen Species Production Increases Susceptibility to Aortic Dissection. *Circulation* 129:2661-2672.

Feletou, M., Y. Huang, and P.M. Vanhoutte. 2010. Vasoconstrictor prostanoids. *Pflugers Archiv : European journal of physiology* 459:941-950.

Ferreira, I., L.L. Peeters, and C.D. Stehouwer. 2009. Preeclampsia and increased blood pressure in the offspring: meta-analysis and critical review of the evidence. *J Hypertens* 27:1955-1959.

Fleming, I., J. Bauersachs, B. Fisslthaler, and R. Busse. 1998. Ca2+-independent activation of the endothelial nitric oxide synthase in response to tyrosine phosphatase inhibitors and fluid shear stress. *Circ Res* 82:686-695.

Fleming, I., and R. Busse. 2003. Molecular mechanisms involved in the regulation of the endothelial nitric oxide synthase. *American journal of physiology. Regulatory, integrative and comparative physiology* 284:R1-12.

Forstermann, U., A. Mulsch, E. Bohme, and R. Busse. 1986 Stimulation of soluble guanylate cyclase by an acetylcholine-induced endothelium-derived factor from rabbit and canine arteries. *Circ Res* 58:531-538.

Forstermann, U., H.H. Schmidt, J.S. Pollock, H. Sheng, J.A. Mitchell, T.D. Warner, M. Nakane, and F. Murad. 1991. Isoforms of nitric oxide synthase. Characterization and purification from different cell types. *Biochem Pharmacol* 42:1849-1857.

Fujimoto, S., M. Mori, and H. Tsushima. 2003. Mechanisms underlying the hydrogen peroxide-induced, endothelium-independent relaxation of the norepinephrine-contraction in guinea-pig aorta. *Eur J Pharmacol* 459:65-73.

Furchgott, R.F., and J.V. Zawadzki. 1980. The obligatory role of endothelial cells in the relaxation of arterial smooth muscle by acetylcholine. *Nature* 288:373-376.

Galley, H.F., A.E. Le Cras, K. Yassen, I.S. Grant, and N.R. Webster. 2001. Circulating tetrahydrobiopterin concentrations in patients with septic shock. *Br J Anaesth* 86:578-580.

Gao, L., K.L. Siu, K. Chalupsky, A. Nguyen, P. Chen, N.L. Weintraub, Z. Galis, and H. Cai. 2012. Role of uncoupled endothelial nitric oxide synthase in abdominal aortic aneurysm formation: treatment with folic acid. *Hypertension* 59:158-166.

Garland, C.J. 2010. Compromised vascular endothelial cell SK(Ca) activity: a fundamental aspect of hypertension? *Br J Pharmacol* 160:833-835.

Garland, C.J., and G.A. McPherson. 1992. Evidence that nitric oxide does not mediate the hyperpolarization and relaxation to acetylcholine in the rat small mesenteric artery. *Br J Pharmacol* 105:429-435.

Gavazzi, G., C. Deffert, C. Trocme, M. Schappi, F.R. Herrmann, and K.-H. Krause. 2007. NOX1 Deficiency Protects From Aortic Dissection in Response to Angiotensin II. *Hypertension* 50:189-196.

Goetz, R.M., I. Morano, T. Calovini, R. Studer, and J. Holtz. 1994. Increased expression of endothelial constitutive nitric oxide synthase in rat aorta during pregnancy. *Biochem Biophys Res Commun* 205:905-910.

Goode, H.F., P.D. Howdle, B.E. Walker, and N.R. Webster. 1995. Nitric oxide synthase activity is increased in patients with sepsis syndrome. *Clin Sci (Lond)* 88:131-133.

Griendling, K.K., and D.G. Harrison. 1999. Dual role of reactive oxygen species in vascular growth. *Circ Res* 85:562-563.

Griffith, O.W., and D.J. Stuehr. 1995. Nitric oxide synthases: properties and catalytic mechanism. *Annual review of physiology* 57:707-736.

Groves, J.T., and C.C. Wang. 2000. Nitric oxide synthase: models and mechanisms. *Current opinion in chemical biology* 4:687-695.

Guzik, T.J., S. Mussa, D. Gastaldi, J. Sadowski, C. Ratnatunga, R. Pillai, and K.M. Channon. 2002a. Mechanisms of increased vascular superoxide production in human diabetes mellitus: Role of NAD(P)H oxidase and endothelial nitric oxide synthase. *Circulation* 105:1656-1662.

Guzik, T.J., N. West, R. Pillai, D. Taggart, and K.M. Channon. 2002b. Nitric oxide modulates superoxide release and peroxynitrite formation in human blood vessels. *Hypertension* 39:1088-1094.

Hansson, G.K. 2005. Inflammation, Atherosclerosis, and Coronary Artery Disease. *N Engl J Med* 352:1685-1695.

Hattori, Y., S. Hattori, X. Wang, H. Satoh, N. Nakanishi, and K. Kasai. 2007. Oral administration of tetrahydrobiopterin slows the progression of atherosclerosis in apolipoprotein E-knockout mice. *Arterioscler Thromb Vasc Biol* 27:865-870.

Heales, S., and K. Hyland. 1989. Determination of quinonoid dihydrobiopterin by high-performance liquid chromatography and electrochemical detection. *J Chromatogr* 494:77-85.

Heitzer, T., C. Brockhoff, B. Mayer, A. Warnholtz, H. Mollnau, S. Henne, T. Meinertz, and T. Munzel. 2000a. Tetrahydrobiopterin improves endothelium-dependent vasodilation in chronic smokers : evidence for a dysfunctional nitric oxide synthase. *Circ Res* 86:E36-E41.

Heitzer, T., H. Just, and T. Munzel. 1996. Antioxidant vitamin C improves endothelial dysfunction in chronic smokers. *Circulation* 94:6-9.

Heitzer, T., K. Krohn, S. Albers, and T. Meinertz. 2000b. Tetrahydrobiopterin improves endothelium-dependent vasodilation by increasing nitric oxide activity in patients with Type II diabetes mellitus. *Diabetologia* 43:1435-1438.

Higashi, Y., S. Sasaki, K. Nakagawa, Y. Fukuda, H. Matsuura, T. Oshima, and K. Chayama. 2002. Tetrahydrobiopterin enhances forearm vascular response to acetylcholine in both normotensive and hypertensive individuals. *American journal of hypertension* 15:326-332.

Hink, U., H. Li, H. Mollnau, M. Oelze, E. Matheis, M. Hartmann, M. Skatchkov, F. Thaiss, R.A. Stahl, A. Warnholtz, T. Meinertz, K. Griendling, D.G. Harrison, U. Forstermann, and T. Munzel. 2001a. Mechanisms underlying endothelial dysfunction in diabetes mellitus. *Circ Res* 88:E14-22.

Hink, U., H. Li, H. Mollnau, M. Oelze, E. Matheis, M. Hartmann, M. Skatchkov, F. Thaiss, R.A.K. Stahl, A. Warnholtz, T. Meinertz, K. Griendling, D.G. Harrison, U. Forstermann, and T. Munzel. 2001b. Mechanisms Underlying Endothelial Dysfunction in Diabetes Mellitus. *Circ Res* 88:e14-22.

Hobbs, A., P. Foster, C. Prescott, R. Scotland, and A. Ahluwalia. 2004. Natriuretic peptide receptor-C regulates coronary blood flow and prevents myocardial ischemia/reperfusion injury: novel cardioprotective role for endothelium-derived C-type natriuretic peptide. *Circulation* 110:1231-1235.

Holzmann, S. 1982. Endothelium-induced relaxation by acetylcholine associated with larger rises in cyclic GMP in coronary arterial strips. *J Cyclic Nucleotide Res* 8:409-419.

Hong, H.J., G. Hsiao, T.H. Cheng, and M.H. Yen. 2001. Supplementation with tetrahydrobiopterin suppresses the development of hypertension in spontaneously hypertensive rats. *Hypertension* 38:1044-1048.

Hopkins, F.G. 1895. The pigments of the pieridae: A contribution to the study of excretory substrances which function in ornament. *Philosophical Transactions of the Royal Society of London B* 186:661-682.

Howells, D.W., I. Smith, and K. Hyland. 1986. Estimation of tetrahydrobiopterin and other pterins in cerebrospinal fluid using reversed-phase high-performance liquid chromatography with electrochemical and fluorescence detection. *J Chromatogr* 381:285-294.

Huie, R.E., and S. Padmaja. 1993. The reaction of NO with superoxide. *Free Radic Res Commun* 18:195-199.

Ishii, M., S. Shimizu, T. Nagai, K. Shiota, Y. Kiuchi, and T. Yamamoto. 2001. Stimulation of tetrahydrobiopterin synthesis induced by insulin: possible involvement of phosphatidylinositol 3-kinase. *Int J Biochem Cell Biol* 33:65-73.

Kajantie, E., J.G. Eriksson, C. Osmond, K. Thornburg, and D.J. Barker. 2009. Pre-eclampsia is associated with increased risk of stroke in the adult offspring: the Helsinki birth cohort study. *Stroke* 40:1176-1180.

Kashiwagi, A., K. Shinozaki, Y. Nishio, H. Maegawa, Y. Maeno, A. Kanazawa, H. Kojima, M. Haneda, H. Hidaka, H. Yasuda, and R. Kikkawa. 1999. Endothelium-specific activation of NAD(P)H oxidase in aortas of exogenously hyperinsulinemic rats. *Am J Physiol* 277:E976-983.

Katada, J., and M. Majima. 2002. AT(2) receptor-dependent vasodilation is mediated by activation of vascular kinin generation under flow conditions. *Br J Pharmacol* 136:484-491.

Katusic, Z.S., A. Stelter, and S. Milstien. 1998. Cytokines stimulate GTP cyclohydrolase I gene expression in cultured human umbilical vein endothelial cells. *Arterioscler Thromb Vasc Biol* 18:27-32.

Kelly, B.A., B.C. Bond, and L. Poston. 2003. Gestational profile of matrix metalloproteinases in rat uterine artery. *Mol Hum Reprod* 9:351-358.

Kelly, B.A., S. Stone, and L. Poston. 2000. Cardiovascular adaptation to pregnancy: the role of altered vascular structure. *Fetal and Maternal Medicine Review* 11:105-116.

Kelly, R.A., and T.W. Smith. 1996. de modulatione cordis. *Circulation* 94:2361-2363.

Khoo, J.P., N.J. Alp, J.K. Bendall, S. Kawashima, M. Yokoyama, Y.H. Zhang, B. Casadei, and K.M. Channon. 2004. EPR quantification of vascular nitric oxide production in genetically modified mouse models. *Nitric Oxide* 10:156-161.

Khoo, J.P., L. Zhao, N.J. Alp, J.K. Bendall, T. Nicoli, K. Rockett, M.R. Wilkins, and K.M. Channon. 2005. A pivotal role for tetrahydrobiopterin in pulmonary hypertension. *Circulation* 111:2126-2133.

Kilbourn, R.G., A. Jubran, S.S. Gross, O.W. Griffith, R. Levi, J. Adams, and R.F. Lodato. 1990. Reversal of endotoxin-mediated shock by NG-methyl-L-arginine, an inhibitor of nitric oxide synthesis. *Biochemical and Biophysical Research Communications* 172:1132-1138.

Kinlay, S., P. Libby, and P. Ganz. 2001. Endothelial function and coronary artery disease. *Curr Opin Lipidol* 12:383-389.

Krivi, G.G., and G.M. Brown. 1979. Purification and properties of the enzymes from Drosophila melanogaster that catalyze the synthesis of sepiapterin from dihydroneopterin triphosphate. *Biochem Genet* 17:371-390.

Kubes, P., M. Suzuki, and D.N. Granger. 1991. Nitric Oxide: An Endogenous Modulator of Leukocyte Adhesion. *PNAS* 88:4651-4655.

Kublickiene, K.R., A.P. Cockell, H. Nisell, and L. Poston. 1997. Role of nitric oxide in the regulation of vascular tone in pressurized and perfused resistance myometrial arteries from term pregnant women. *Am J Obstet Gynecol* 177:1263-1269.

Kublickiene, K.R., B. Lindblom, K. Kruger, and H. Nisell. 2000. Preeclampsia: evidence for impaired shear stress-mediated nitric oxide release in uterine circulation. *Am J Obstet Gynecol* 183:160-166.

Kunsch, C., and R.M. Medford. 1999. Oxidative stress as a regulator of gene expression in the vasculature. *Circ Res* 85:753-766.

Kwon, N.S., C.F. Nathan, and D.J. Stuehr. 1989. Reduced biopterin as a cofactor in the generation of nitrogen oxides by murine macrophages. *J. Biol. Chem.* 264:20496-20501.

Landmesser, U., S. Dikalov, S.R. Price, L. McCann, T. Fukai, S.M. Holland, W.E. Mitch, and D.G. Harrison. 2003. Oxidation of tetrahydrobiopterin leads to uncoupling of endothelial cell nitric oxide synthase in hypertension. *J Clin Invest* 111:1201-1209.

Landmesser, U., B. Hornig, and H. Drexler. 2004. Endothelial function: A critical determinant in atherosclerosis? *Circulation* 109:II-27-33.

Lapize, C., C. Pluss, E.R. Werner, A. Huwiler, and J. Pfeilschifter. 1998. Protein kinase C phosphorylates and activates GTP cyclohydrolase I in rat renal mesangial cells. *Biochem Biophys Res Commun* 251:802-805.

Laursen, J.B., M. Somers, S. Kurz, L. McCann, A. Warnholtz, B.A. Freeman, M. Tarpey, T. Fukai, and D.G. Harrison. 2001. Endothelial regulation of vasomotion in apoE-deficient mice: implications for interactions between peroxynitrite and tetrahydrobiopterin. *Circulation* 103:1282-1288.

Lazdam, M., A. de la Horra, J. Diesch, Y. Kenworthy, E. Davis, A.J. Lewandowski, C. Szmigielski, A. Shore, L. Mackillop, R. Kharbanda, N. Alp, C. Redman, B. Kelly, and P. Leeson. 2012. Unique blood pressure characteristics in mother and offspring after early onset preeclampsia. *Hypertension* 60:1338-1345.

Lazdam, M., A. de la Horra, A. Pitcher, Z. Mannie, J. Diesch, C. Trevitt, I. Kylintireas, H. Contractor, A. Singhal, A. Lucas, S. Neubauer, R. Kharbanda, N. Alp, B. Kelly, and P. Leeson. 2010. Elevated blood pressure in offspring born premature to hypertensive pregnancy: is endothelial dysfunction the underlying vascular mechanism? *Hypertension* 56:159-165.

Li, H., T. Wallerath, and U. Forstermann. 2002. Physiological mechanisms regulating the expression of endothelial-type NO synthase. *Nitric Oxide* 7:132-147.

Libby, P. 2002. Inflammation in atherosclerosis. *Nature* 420:868-874.

Libby, P., S.J. Warner, and G.B. Friedman. 1988. Interleukin 1: a mitogen for human vascular smooth muscle cells that induces the release of growth-inhibitory prostanoids. *J Clin Invest* 81:487-498.

Linke, A., W. Li, H. Huang, Z. Wang, and T.H. Hintze. 2002. Role of cardiac eNOS expression during pregnancy in the coupling of myocardial oxygen consumption to cardiac work. *Am J Physiol Heart Circ Physiol* 283:H1208-1214.

Linscheid, P., A. Schaffner, N. Blau, and G. Schoedon. 1998. Regulation of 6-pyruvoyltetrahydropterin synthase activity and messenger RNA abundance in human vascular endothelial cells. *Circulation* 98:1703-1706.

Lu, T., T. He, Z.S. Katusic, and H.C. Lee. 2006. Molecular mechanisms mediating inhibition of human large conductance Ca2+-activated K+ channels by high glucose. *Circ Res* 99:607-616.

Lund, D.D., R.M. Brooks, F.M. Faraci, and D.D. Heistad. 2007. Role of angiotensin II in endothelial dysfunction induced by lipopolysaccharide in mice. *Am J Physiol Heart Circ Physiol* 293:H3726-3731.

Lusis, A.J. 2000. Atherosclerosis. *Nature* 407:233-241.

Maeda, T., S. Haeno, K. Oda, D. Mori, H. Ichinose, T. Nagatsu, and T. Suzuki. 2000. Studies on the genotype-phenotype relation in the hph-1 mouse mutant deficient in guanosine triphosphate (GTP) cyclohydrolase I activity. *Brain Dev* 22 Suppl 1:50-53.

Maier, W., F. Cosentino, R.B. Lutolf, M. Fleisch, C. Seiler, O.M. Hess, B. Meier, and T.F. Luscher. 2000. Tetrahydrobiopterin improves endothelial function in patients with coronary artery disease. *J Cardiovasc Pharmacol* 35:173-178.

Masters, B.S., K. McMillan, E.A. Sheta, J.S. Nishimura, L.J. Roman, and P. Martasek. 1996. Neuronal nitric oxide synthase, a modular enzyme formed by convergent evolution: structure studies of a cysteine thiolate-liganded heme protein that hydroxylates L-arginine to produce NO. as a cellular signal [published erratum appears in FASEB J 1996 Jul;10(9):1107]. *FASEB J.* 10:552-558.

Matoba, T., H. Shimokawa, H. Kubota, K. Morikawa, T. Fujiki, I. Kunihiro, Y. Mukai, Y. Hirakawa, and A. Takeshita. 2002. Hydrogen peroxide is an endothelium-derived hyperpolarizing factor in human mesenteric arteries. *Biochem Biophys Res Commun* 290:909-913.

Matoba, T., H. Shimokawa, M. Nakashima, Y. Hirakawa, Y. Mukai, K. Hirano, H. Kanaide, and A. Takeshita. 2000a. Hydrogen peroxide is an endothelium-derived hyperpolarizing factor in mice. *J Clin Invest* 106:1521-1530.

Matoba, T., H. Shimokawa, M. Nakashima, Y. Hirakawa, Y. Mukai, K. Hirano, H. Kanaide, and A. Takeshita. 2000b. Hydrogen peroxide is an endothelium-derived hyperpolarizing factor in mice. *J Clin Invest* 106:1521-1530.

McDonald, S.D., A. Malinowski, Q. Zhou, S. Yusuf, and P.J. Devereaux. 2008. Cardiovascular sequelae of preeclampsia/eclampsia: a systematic review and meta-analyses. *Am Heart J* 156:918-930.

Meher, S., and L. Duley. 2007. Nitric oxide for preventing pre-eclampsia and its complications. *Cochrane Database Syst Rev* CD006490.

Miller, S.L., G. Jenkin, and D.W. Walker. 1999. Effect of nitric oxide synthase inhibition on the uterine vasculature of the late-pregnant ewe. *Am J Obstet Gynecol* 180:1138-1145.

Milstien, S., and Z. Katusic. 1999. Oxidation of tetrahydrobiopterin by peroxynitrite: implications for vascular endothelial function. *Biochem Biophys Res Commun* 263:681-684.

Mitchell, B.M., L.G. Cook, S. Danchuk, and J.B. Puschett. 2007. Uncoupled endothelial nitric oxide synthase and oxidative stress in a rat model of pregnancy-induced hypertension. *American journal of hypertension* 20:1297-1304.

Mitchell, B.M., A.M. Dorrance, and R.C. Webb. 2003. GTP cyclohydrolase 1 inhibition attenuates vasodilation and increases blood pressure in rats. *Am J Physiol Heart Circ Physiol* 285:H2165-2170.

Moncada, S., R. Gryglewski, S. Bunting, and J.R. Vane. 1976. An enzyme isolated from arteries transforms prostaglandin endoperoxides to an unstable substance that inhibits platelet aggregation. *Nature* 263:663-665.

Moncada, S., R.M. Palmer, and E.A. Higgs. 1991. Nitric oxide: physiology, pathophysiology, and pharmacology. *Pharmacol Rev* 43:109-142.

Moncada, S., and J.R. Vane. 1981. Prostacyclin: its biosynthesis, actions and clinical potential. *Philosophical transactions of the Royal Society of London. Series B, Biological sciences* 294:305-329.

Morikawa, K., H. Shimokawa, T. Matoba, H. Kubota, T. Akaike, M.A. Talukder, M. Hatanaka, T. Fujiki, H. Maeda, S. Takahashi, and A. Takeshita. 2003. Pivotal role of Cu,Zn-superoxide dismutase in endothelium-dependent hyperpolarization. *J Clin Invest* 112:1871-1879.

Muirhead, E.E., B. Brooks, and W.L. Brosius. 1976. Indomethacin and blood pressure control. *The Journal of laboratory and clinical medicine* 88:578-583.

Murata, T., F. Ushikubi, T. Matsuoka, M. Hirata, A. Yamasaki, Y. Sugimoto, A. Ichikawa, Y. Aze, T. Tanaka, N. Yoshida, A. Ueno, S. Oh-ishi, and S. Narumiya. 1997. Altered pain perception and inflammatory response in mice lacking prostacyclin receptor. *Nature* 388:678-682.

Mustafa, A.K., G. Sikka, S.K. Gazi, J. Steppan, S.M. Jung, A.K. Bhunia, V.M. Barodka, F.K. Gazi, R.K. Barrow, R. Wang, L.M. Amzel, D.E. Berkowitz, and S.H. Snyder. 2011. Hydrogen sulfide as endothelium-derived hyperpolarizing factor sulfhydrates potassium channels. *Circ Res* 109:1259-1268.

Myatt, L., R.B. Rosenfield, A.L. Eis, D.E. Brockman, I. Greer, and F. Lyall. 1996. Nitrotyrosine residues in placenta. Evidence of peroxynitrite formation and action. *Hypertension* 28:488-493.

Nandi, M., A. Miller, R. Stidwill, T.S. Jacques, A.A. Lam, S. Haworth, S. Heales, and P. Vallance. 2005. Pulmonary hypertension in a GTP-cyclohydrolase 1-deficient mouse. *Circulation* 111:2086-2090.

Nelson, S.H., O.S. Steinsland, Y. Wang, C. Yallampalli, Y.L. Dong, and J.M. Sanchez. 2000. Increased nitric oxide synthase activity and expression in the human uterine artery during pregnancy. *Circ Res* 87:406-411.

Nichol, C.A., C.L. Lee, M.P. Edelstein, J.Y. Chao, and D.S. Duch. 1983. Biosynthesis of tetrahydrobiopterin by de novo and salvage pathways in adrenal medulla extracts, mammalian cell cultures, and rat brain in vivo. *Proc Natl Acad Sci U S A* 80:1546-1550.

Noronha, B.T., J.M. Li, S.B. Wheatcroft, A.M. Shah, and M.T. Kearney. 2005. Inducible nitric oxide synthase has divergent effects on vascular and metabolic function in obesity. *Diabetes* 54:1082-1089.

Ozaki, M., S. Kawashima, T. Yamashita, T. Hirase, M. Namiki, N. Inoue, K.-i. Hirata, H. Yasui, H. Sakurai, Y. Yoshida, M. Masada, and M. Yokoyama. 2002. Overexpression of endothelial nitric oxide synthase accelerates atherosclerotic lesion formation in apoE-deficient mice. *J Clin Invest* 110:331-340.

Palmer, R.M.J., D.S. Ashton, and S. Moncada. 1988. Vascular endothelial cells synthesize nitric oxide from L-arginine. *Nature* 333:664-666.

Petros, A., D. Bennett, and P. Vallance. 1991. Effect of nitric oxide synthase inhibitors on hypotension in patients with septic shock. *Lancet* 338:1557-1558.

Pieper, G.M. 1997. Acute amelioration of diabetic endothelial dysfunction with a derivative of the nitric oxide synthase cofactor, tetrahydrobiopterin. *J Cardiovasc Pharmacol* 29:8-15.

Plane, F., and C.J. Garland. 1996. Influence of contractile agonists on the mechanism of endothelium-dependent relaxation in rat isolated mesenteric artery. *Br J Pharmacol* 119:191-193.

Poston, L., A.L. Briley, P.T. Seed, F.J. Kelly, and A.H. Shennan. 2006. Vitamin C and vitamin E in pregnant women at risk for pre-eclampsia (VIP trial): randomised placebo-controlled trial. *Lancet* 367:1145-1154.

Prabhakar, P., H.S. Thatte, R.M. Goetz, M.R. Cho, D.E. Golan, and T. Michel. 1998. Receptor-regulated translocation of endothelial nitric-oxide synthase. *J Biol Chem* 273:27383-27388.

Prysyazhna, O., O. Rudyk, and P. Eaton. 2012. Single atom substitution in mouse protein kinase G eliminates oxidant sensing to cause hypertension. *Nat Med* 18:286-290.

Rafikov, R., F.V. Fonseca, S. Kumar, D. Pardo, C. Darragh, S. Elms, D. Fulton, and S.M. Black. 2011. eNOS activation and NO function: structural motifs responsible for the posttranslational control of endothelial nitric oxide synthase activity. *The Journal of endocrinology* 210:271-284.

Raijmakers, M.T., R. Dechend, and L. Poston. 2004. Oxidative stress and preeclampsia: rationale for antioxidant clinical trials. *Hypertension* 44:374-380.

Rateri, D.L., J.J. Moorleghen, A. Balakrishnan, A.P. Owens, 3rd, D.A. Howatt, V. Subramanian, A. Poduri, R. Charnigo, L.A. Cassis, and A. Daugherty. 2011. Endothelial cell-specific deficiency of Ang II type 1a receptors attenuates Ang II-induced ascending aortic aneurysms in LDL receptor-/- mice. *Circulation research* 108:574-581.

Ray, R., C.E. Murdoch, M. Wang, C.X. Santos, M. Zhang, S. Alom-Ruiz, N. Anilkumar, A. Ouattara, A.C. Cave, S.J. Walker, D.J. Grieve, R.L. Charles, P. Eaton, A.C. Brewer, and A.M. Shah. 2011. Endothelial Nox4 NADPH Oxidase Enhances Vasodilatation and Reduces Blood Pressure In Vivo. *Arteriosclerosis, Thrombosis, and Vascular Biology* 31:1368-1376.

Roggensack, A.M., Y. Zhang, and S.T. Davidge. 1999. Evidence for peroxynitrite formation in the vasculature of women with preeclampsia. *Hypertension* 33:83-89.

Rosenfeld, M.E., P. Polinsky, R. Virmani, K. Kauser, G. Rubanyi, and S.M. Schwartz. 2000. Advanced atherosclerotic lesions in the innominate artery of the ApoE knockout mouse. *Arterioscler Thromb Vasc Biol* 20:2587-2592.

Ross, R. 1999. Atherosclerosis--an inflammatory disease. *N Engl J Med* 340:115-126.

Rubanyi, G.M., and P.M. Vanhoutte. 1986. Oxygen-derived free radicals, endothelium, and responsiveness of vascular smooth muscle. *Am J Physiol* 250:H815-821.

Rudyk, O., A. Phinikaridou, O. Prysyazhna, J.R. Burgoyne, R.M. Botnar, and P. Eaton. 2013. Protein kinase G oxidation is a major cause of injury during sepsis. *Proc Natl Acad Sci U S A* 110:9909-9913.

Rupnow, H.L., T.M. Phernetton, C.E. Shaw, M.L. Modrick, I.M. Bird, and R.R. Magness. 2001. Endothelial vasodilator production by uterine and systemic arteries. VII. Estrogen and progesterone effects on eNOS. *Am J Physiol Heart Circ Physiol* 280:H1699-1705.

Rutherford, R.A., A. McCarthy, M.H. Sullivan, M.G. Elder, J.M. Polak, and J. Wharton. 1995. Nitric oxide synthase in human placenta and umbilical cord from normal,

intrauterine growth-retarded and pre-eclamptic pregnancies. *Br J Pharmacol* 116:3099-3109.

Sagripanti, A., and A. Carpi. 2000 Antithrombotic and prothrombotic activities of the vascular endothelium. *Biomed Pharmacother.* 54:107-111.

Sallstrom J, C.M., Persson AEG. 2006. The role of neuronal nitric oxide synthase in blood pressure regulation. In DSI conference abstract.

Santhanam, A.V., L.V. d'Uscio, L.A. Smith, and Z.S. Katusic. 2012. Uncoupling of eNOS causes superoxide anion production and impairs NO signaling in the cerebral microvessels of hph-1 mice. *J Neurochem* 122:1211-1218.

Schroder, K., M. Zhang, S. Benkhoff, A. Mieth, R. Pliquett, J. Kosowski, C. Kruse, P. Luedike, U.R. Michaelis, N. Weissmann, S. Dimmeler, A.M. Shah, and R.P. Brandes. 2012. Nox4 is a protective reactive oxygen species generating vascular NADPH oxidase. *Circ Res* 110:1217-1225.

Shimizu, S., M. Ishii, Y. Kawakami, Y. Kiuchi, K. Momose, and T. Yamamoto. 1999. Presence of excess tetrahydrobiopterin during nitric oxide production from inducible nitric oxide synthase in LPS-treated rat aorta. *Life Sci* 65:2769-2779.

Shimizu, S., M. Ishii, Y. Kawakami, K. Momose, and T. Yamamoto. 1998. Protective effects of tetrahydrobiopterin against nitric oxide-induced endothelial cell death. *Life Sci* 63:1585-1592.

Siu, K.L., and H. Cai. 2014. Circulating Tetrahydrobiopterin as a Novel Biomarker for Abdominal Aortic Aneurysm. *Am J Physiol Heart Circ Physiol*

Siu, K.L., X.N. Miao, and H. Cai. 2014. Recoupling of eNOS with folic acid prevents abdominal aortic aneurysm formation in angiotensin II-infused apolipoprotein E null mice. *PLoS One* 9:e88899.

Sladek, S.M., R.R. Magness, and K.P. Conrad. 1997. Nitric oxide and pregnancy. *Am J Physiol* 272:R441-463.

Spiekermann, S., U. Landmesser, S. Dikalov, M. Bredt, G. Gamez, H. Tatge, N. Reepschlager, B. Hornig, H. Drexler, and D.G. Harrison. 2003. Electron Spin Resonance Characterization of Vascular Xanthine and NAD(P)H Oxidase Activity in Patients With Coronary Artery Disease: Relation to Endothelium-Dependent Vasodilation. *Circulation* 107:1383-1389.

Stamler, J.S., E. Loh, M.-A. Roddy, K.E. Currie, and M.A. Creager. 1994. Nitric oxide regulates basal systemic and pulmonary vascular resistance in healthy humans. *Circulation* 89:2035-2040.

Stanley, J.L., I.J. Andersson, C.J. Hirt, L. Moore, M.R. Dilworth, A.R. Chade, C.P. Sibley, S.T. Davidge, and P.N. Baker. 2012a. Effect of the anti-oxidant tempol on fetal growth in a mouse model of fetal growth restriction. *Biol Reprod* 87:25, 21-28.

Stanley, J.L., I.J. Andersson, R. Poudel, C.F. Rueda-Clausen, C.P. Sibley, S.T. Davidge, and P.N. Baker. 2012b. Sildenafil citrate rescues fetal growth in the catechol-O-methyl transferase knockout mouse model. *Hypertension* 59:1021-1028.

Stauss, H.M., A. Godecke, R. Mrowka, J. Schrader, and P.B. Persson. 1999. Enhanced blood pressure variability in eNOS knockout mice. *Hypertension* 33:1359-1363.

Stroes, E., J. Kastelein, F. Cosentino, W. Erkelens, R. Wever, H. Koomans, T. Luscher, and T. Rabelink. 1997. Tetrahydrobiopterin restores endothelial function in hypercholesterolemia. *J Clin Invest* 99:41-46.

Stuehr, D.J., H.J. Cho, N.S. Kwon, M.F. Weise, and C.F. Nathan. 1991. Purification and characterization of the cytokine-induced macrophage nitric oxide synthase: An FAD- and FMN-containing flavoprotein. *Proc Natl Acad Sci U S A* 88:7773-7777.

Stuehr, D.J., and M. Ikeda-Saito. 1992. Spectral characterization of brain and macrophage nitric oxide synthases: cytochrome P-450-like hemeproteins that contain a flavin semiquinone radical. *J Biol Chem* 267:20547-20550.

Sullivan, J.A., M.A. Grummer, F.X. Yi, and I.M. Bird. 2006. Pregnancy-enhanced endothelial nitric oxide synthase (eNOS) activation in uterine artery endothelial cells shows altered sensitivity to Ca2+, U0126, and wortmannin but not LY294002--evidence that pregnancy adaptation of eNOS activation occurs at multiple levels of cell signaling. *Endocrinology* 147:2442-2457.

Szabo, C., C. Csaki, Z. Benyo, J. Marczis, M. Reivich, and A.G. Kovach. 1994a. Effect of superoxide dismutase on hemorrhagic hypotension and retransfusion-evoked middle cerebral artery endothelial dysfunction. *Circulatory shock* 44:104-110.

Szabo, C., C. Thiemermann, C.C. Wu, M. Perretti, and J.R. Vane. 1994b. Attenuation of the induction of nitric oxide synthase by endogenous glucocorticoids accounts for endotoxin tolerance in vivo. *Proc Natl Acad Sci U S A* 91:271-275.

Tachibana, D., H. Fukumasu, H. Shintaku, Y. Fukumasu, S. Yamamasu, O. Ishiko, T. Yamano, and S. Ogita. 2002. Decreased plasma tetrahydrobiopterin in pregnant women is caused by impaired 6-pyruvoyl tetrahydropterin synthase activity. *International journal of molecular medicine* 9:49-52.

Takaki, A., K. Morikawa, Y. Murayama, H. Yamagishi, M. Hosoya, J. Ohashi, and H. Shimokawa. 2008a. Roles of endothelial oxidases in endothelium-derived hyperpolarizing factor responses in mice. *J Cardiovasc Pharmacol* 52:510-517.

Takaki, A., K. Morikawa, M. Tsutsui, Y. Murayama, E. Tekes, H. Yamagishi, J. Ohashi, T. Yada, N. Yanagihara, and H. Shimokawa. 2008b. Crucial role of nitric oxide synthases system in endothelium-dependent hyperpolarization in mice. *J Exp Med* 205:2053-2063.

Tatham, A.L., M.J. Crabtree, N. Warrick, S. Cai, N.J. Alp, and K.M. Channon. 2009. GTP cyclohydrolase I expression, protein, and activity determine intracellular tetrahydrobiopterin levels, independent of GTP cyclohydrolase feedback regulatory protein expression. *J Biol Chem* 284:13660-13668.

Tayeh, M.A., and M.A. Marletta. 1989. Macrophage oxidation of L-arginine to nitric oxide, nitrite, and nitrate. Tetrahydrobiopterin is required as a cofactor. *J Biol Chem* 264:19654-19658.

Thomas, G., and P. Ramwell. 1986. Induction of vascular relaxation by hydroperoxides. *Biochem Biophys Res Commun* 139:102-108.

Thony, B., G. Auerbach, and N. Blau. 2000. Tetrahydrobiopterin biosynthesis, regeneration and functions. *The Biochemical journal* 347:1-16.

Todaka, T., C. Yokoyama, H. Yanamoto, N. Hashimoto, I. Nagata, T. Tsukahara, S. Hara, T. Hatae, R. Morishita, M. Aoki, T. Ogihara, Y. Kaneda, and T. Tanabe. 1999. Gene transfer of human prostacyclin synthase prevents neointimal formation after carotid balloon injury in rats. *Stroke* 30:419-426.

Tojo, A., M.L. Onozato, N. Kobayashi, A. Goto, H. Matsuoka, and T. Fujita. 2002. Angiotensin II and oxidative stress in Dahl Salt-sensitive rat with heart failure. *Hypertension* 40:834-839.

Tronc, F., Z. Mallat, S. Lehoux, M. Wassef, B. Esposito, and A. Tedgui. 2000. Role of matrix metalloproteinases in blood flow-induced arterial enlargement: interaction with NO. *Arterioscler Thromb Vasc Biol* 20:E120-126.

Ueda, S., H. Matsuoka, H. Miyazaki, M. Usui, S. Okuda, and T. Imaizumi. 2000. Tetrahydrobiopterin restores endothelial function in long-term smokers. *J Am Coll Cardiol* 35:71-75.

van Amsterdam, J.G., C. van den Berg, J. Zuidema, J.D. te Biesebeek, and H. Rokos. 1996. Effect of septicaemia on the plasma levels of biopterin and nitric oxide metabolites in rats and rabbits. *Biochem Pharmacol* 52:1447-1451.

van der Heijden, O.W., Y.P. Essers, G. Fazzi, L.L. Peeters, J.G. De Mey, and G.J. van Eys. 2005. Uterine artery remodeling and reproductive performance are impaired in endothelial nitric oxide synthase-deficient mice. *Biol Reprod* 72:1161-1168.

Vasquez-Vivar, J., D. Duquaine, J. Whitsett, B. Kalyanaraman, and S. Rajagopalan. 2002a. Altered tetrahydrobiopterin metabolism in atherosclerosis: implications for use of oxidized tetrahydrobiopterin analogues and thiol antioxidants. *Arterioscler Thromb Vasc Biol* 22:1655-1661.

Vasquez-Vivar, J., B. Kalyanaraman, and P. Martasek. 2003. The role of tetrahydrobiopterin in superoxide generation from eNOS: enzymology and physiological implications. *Free Radic Res* 37:121-127.

Vasquez-Vivar, J., B. Kalyanaraman, P. Martasek, N. Hogg, B.S. Masters, H. Karoui, P. Tordo, and K.A. Pritchard, Jr. 1998. Superoxide generation by endothelial nitric oxide synthase: the influence of cofactors. *Proc Natl Acad Sci U S A* 95:9220-9225.

Vasquez-Vivar, J., P. Martasek, J. Whitsett, J. Joseph, and B. Kalyanaraman. 2002b. The ratio between tetrahydrobiopterin and oxidized tetrahydrobiopterin analogues controls superoxide release from endothelial nitric oxide synthase: an EPR spin trapping study. *The Biochemical journal* 362:733-739.

Wallerath, T., I. Gath, W.E. Aulitzky, J.S. Pollock, H. Kleinert, and U. Forstermann. 1997. Identification of the NO synthase isoforms expressed in human neutrophil granulocytes, megakaryocytes and platelets. *Thromb Haemost* 77:163-167.

Wang, C.H., S.H. Li, R.D. Weisel, P.W. Fedak, A. Hung, R.K. Li, V. Rao, K. Hyland, W.J. Cherng, L. Errett, Y. Leclerc, D. Bonneau, D.A. Latter, and S. Verma. 2005. Tetrahydrobiopterin Deficiency Exaggerates Intimal Hyperplasia After Vascular Injury. *American journal of physiology. Regulatory, integrative and comparative physiology* Epub Mar 17 ahead of print.

Wang, S., J. Xu, P. Song, Y. Wu, J. Zhang, H. Chul Choi, and M.-H. Zou. 2008. Acute Inhibition of Guanosine Triphosphate Cyclohydrolase 1 Uncouples Endothelial Nitric Oxide Synthase and Elevates Blood Pressure. *Hypertension* 52:484-490.

Warnholtz, A., G. Nickenig, E. Schulz, R. Macharzina, J.H. Brasen, M. Skatchkov, T. Heitzer, J.P. Stasch, K.K. Griendling, D.G. Harrison, M. Bohm, T. Meinertz, and T. Muenzel. 1999. Increased NADH-oxidase-mediated superoxide production in the early stages of atherosclerosis : evidence for involvement of the renin- angiotensin system. *Circulation* 99:2027-2033.

Watt, W.B. 1964. Pteridine Components Of Wing Pigmentation In The Butterfly Colias Eurytheme. *Nature* 201:1326-1327.

Werner, E.R., G. Werner-Felmayer, and B. Mayer. 1998. Tetrahydrobiopterin, cytokines, and nitric oxide synthesis. *Proc Soc Exp Biol Med* 219:171-182.

Widder, J.D., W. Chen, L. Li, S. Dikalov, B. Thony, K. Hatakeyama, and D.G. Harrison. 2007. Regulation of Tetrahydrobiopterin Biosynthesis by Shear Stress. *Circ Res*

Widdop, R.E., S.M. Gardiner, P.A. Kemp, and T. Bennett. 1992. The influence of atropine and atenolol on the cardiac haemodynamic effects of NG-nitro-L-arginine methyl ester in conscious, Long Evans rats. *Br J Pharmacol* 105:653-656.

Williams, D.J., P.J. Vallance, G.H. Neild, J.A. Spencer, and F.J. Imms. 1997. Nitric oxide-mediated vasodilation in human pregnancy. *Am J Physiol* 272:H748-752.

Wolin, M.S., and T.M. Burke. 1987. Hydrogen peroxide elicits activation of bovine pulmonary arterial soluble guanylate cyclase by a mechanism associated with its metabolism by catalase. *Biochem Biophys Res Commun* 143:20-25.

Woo, H.J., J.Y. Kang, Y.K. Choi, and Y.S. Park. 2002. Production of sepiapterin in Escherichia coli by coexpression of cyanobacterial GTP cyclohydrolase I and human 6-pyruvoyltetrahydropterin synthase. *Appl Environ Microbiol* 68:3138-3140.

Xia, Y., A.L. Tsai, V. Berka, and J.L. Zweier. 1998. Superoxide generation from endothelial nitric-oxide synthase. A Ca2+/calmodulin-dependent and tetrahydrobiopterin regulatory process. *J Biol Chem* 273:25804-25808.

Xiong, W., J. Mactaggart, R. Knispel, J. Worth, Z. Zhu, Y. Li, Y. Sun, B.T. Baxter, and J. Johanning. 2009. Inhibition of reactive oxygen species attenuates aneurysm formation in a murine model. *Atherosclerosis* 202:128-134.

Xu, J., K.D. Kochanek, S.L. Murphy, and B. Tejada-Vera. 2010. Deaths: final data for 2007. *National vital statistics reports : from the Centers for Disease Control and Prevention, National Center for Health Statistics, National Vital Statistics System* 58:1-19.

Yanagisawa, M., H. Kurihara, S. Kimura, Y. Tomobe, M. Kobayashi, Y. Mitsui, Y. Yazaki, K. Goto, and T. Masaki. 1988. A novel potent vasoconstrictor peptide produced by vascular endothelial cells. *Nature* 332:411-415.

Yang, H., L.J. Roberts, M.J. Shi, L.C. Zhou, B.R. Ballard, A. Richardson, and Z.M. Guo. 2004. Retardation of Atherosclerosis by Overexpression of Catalase or Both Cu/Zn-Superoxide Dismutase and Catalase in Mice Lacking Apolipoprotein E. *Circulation Research* 95:1075-1081.

Yang, X.P., Y.H. Liu, E.G. Shesely, M. Bulagannawar, F. Liu, and O.A. Carretero. 1999. Endothelial nitric oxide gene knockout mice: cardiac phenotypes and the effect of angiotensin-converting enzyme inhibitor on myocardial ischemia/reperfusion injury. *Hypertension* 34:24-30.

Youn, J.Y., T. Wang, J. Blair, K.M. Laude, J.H. Oak, L.A. McCann, D.G. Harrison, and H. Cai. 2012. Endothelium-specific sepiapterin reductase deficiency in DOCA-salt hypertension. *Am J Physiol Heart Circ Physiol* 302:H2243-2249.

Yuill, K.H., P. Yarova, B.K. Kemp-Harper, C.J. Garland, and K.A. Dora. 2011. A novel role for HNO in local and spreading vasodilatation in rat mesenteric resistance arteries. *Antioxid Redox Signal* 14:1625-1635.

Zuurbier, C.J., V.M. Emons, and C. Ince. 2002. Hemodynamics of anesthetized ventilated mouse models: aspects of anesthetics, fluid support, and strain. *Am J Physiol Heart Circ Physiol* 282:H2099-2105.

Chapter 9: Appendices

Chapter 9: Appendices

9.1 Timing and venue of research

The work described in this thesis was conducted continuously between October 2010 to September 2014, in the British Heart Foundation (BHF) Molecular Cardiology Laboratory and Functional Genetics Facility, Division of Cardiovascular Medicine, Centre for Human Genetics, Oxford, UK.

9.2 Research funding

The author was funded by a British Heart Foundation (BHF) 4-year DPhil studentship. The laboratory of Prof Keith Channon is supported by a programme grant from the British Heart Foundation

9.3 Attributions

The author is very grateful to invaluable practical contributors to this body of research made by colleagues. Apart from the exclusions listed below, the author is directly responsible for the design, planning, execution and analyses of all experiments, and the data presentation of this thesis and related publication with first authorships.

Dr Eileen McNeill performed flow cytometry experiments and LPS injection. Mini-pump surgery of angiotensin II infusion was performed by Dr Gillian Douglas. Dr Mark Crabtree performed the L-arginine to L-citrulline conversion experiments. Mr Ashley Hale assisted in the genotyping and BH4 assays in early experiments.

9.4 Acknowledgements

I would like to firstly thank my supervisor Prof Keith Channon for giving me the opportunity to complete a DPhil in his research group. I am extremely grateful for his generous support, expert advice and guidance, encouragement and enthusiasm throughout this research. I would also like to extend my appreciation to Dr Eileen McNeill for her support and day-to-day help, and for all the countless discussions on my work. I truly appreciate the time, knowledge and support that she has given to me over the last four years.

I would like to express my deepest gratitude to all members of the Channon Group for their helpful discussion in lab meetings, advice with experimental work and proof reading my thesis. A special thank you to Dr Gillian Douglas for help with the *in vivo* work, Dr Mark Crabtree for his help with *in vitro* work, to Mr Ashley Hale for always lending a helping hand, to Dr Jyoti Patel, Dr Lampson Fan, and Miss Jade Bailey for keeping me entertained. I would like to thank James Brown for technical support around the lab and to Viv Clark and the technicians at the FGF for providing animal care. I also acknowledge the British Heart Foundation for the DPhil studentship and Magdalen College for generous travel allowances.

Finally, I would like to thank my family and friends, most importantly my parents for constantly supporting me throughout all my studies and for their faith and encouragement.

9.5 Publications arising from research

9.5.1 Publications arising from this thesis

Chuaiphichai, S., E. McNeill, G. Douglas, M.J. Crabtree, J.K. Bendall, A.B. Hale, N.J. Alp, and K.M. Channon. Cell-autonomous role of endothelial GTP cyclohydrolase 1 and tetrahydrobiopterin in blood pressure regulation. 2014. *Hypertension* 64:530-540

Chuaiphichai, S., Starr, A., Nandi, M., Channon, K.M., McNeill, M. Endothelial cell tetrahydrobiopterin deficiency attenuates LPS-induced vascular dysfunction and hypotension. (In Preparation).

9.5.2 Publications arising from other research work

Benson, M.A., H. Batchelor, **S. Chuaiphichai**, J. Bailey, H. Zhu, D.J. Stuehr, S. Bhattacharya, K.M. Channon, and M.J. Crabtree. A pivotal role for tryptophan 447 in enzymatic coupling of human endothelial nitric oxide synthase (eNOS): effects on tetrahydrobiopterin-dependent catalysis and eNOS dimerization. 2013. *J Biol Chem* 288:29836-29845

Cardini, B., Watschinger, K., Hermann, M., Oberhber, R, Obrist, P., Brandacher, G., **Chuaiphichai, S.**, Cardini, B., Channon, K.M., Pratschke, J., Maglion, M., Werner, E.R. Crucial role for neuronal nitric oxide synthase in early microcirculatory derangement and recipient survival following murine pancreas transplantation. 2014. *PloS One*. Nov 12;9(11):e112570.

M^{c}Neill, E., Crabtree, M.J., Sahgal, N., Patel, J., **Chuaiphichai, S**., Iqbal, A.J., Hale, A.B., Greaves, D.R., Channon, K.M. Regulation of iNOS Function, Redox State and NRF2 Activation by Macrophage *GCH1* and Tetrahydrobiopterin. 2015. *Free Radical Biology and Medicine.* Feb;79:206-16.

Latrémolière, A., Andrews, N., Latini, A., Cronin, S., Gorska, K., Tegeder,I., Romero, C., Painter, M., Babaniyi, O., Remor, AP., **Chuaiphichai, S.**, Miracca, G., Duong, K., Riva, P., Barrett, L., Ferreiròs, N., Naylor, A., Zhong, J., Blagg, J., Channon, K., Johnsson, K., Costigan, M. Reduction of neuropathic pain through the genetic and pharmacological inhibition of the tetrahydrobiopterin (BH4) pathway. (In Press).

9.5.3 Abstracts presented at scientific conferences

Chuaiphichai S, McNeill E, Bendall JK, Douglas D, Crabtree MJ, Hale AB, Alp NK, Channon KM. A Cell-Autonomous Role for Endothelial GTP Cyclohydrolase 1 and Tetrahydrobiopterin in Blood Pressure Regulation. *Frontiers in CardioVascular Biology Conference, Barcelona, July 2014*. (Oral Presentation).

Chuaiphichai S, McNeill E, Bendall JK, Douglas D, Crabtree MJ, Hale AB, Alp NK, Channon KM. A Cell-Autonomous Role for Endothelial GTP Cyclohydrolase 1 and Tetrahydrobiopterin in Blood Pressure Regulation. *Arteriosclerosis, Thrombosis and Vascular Biology Conference, Toronto, Canada, May 2014* (Poster Presentation, awarded **ATVB Award for Young Investigators**)

Chuaiphichai S, McNeill E, Bendall JK, Douglas D, Crabtree MJ, Hale AB, Alp NK, Channon KM. Deficiency in Endothelial Cell Tetrahydrobipterin Reveals Hydrogen Peroxide Mediated Changes in Vascular Function and Blood Pressure *In Vivo*. *European Society for Microcirculation and the European vascular biology Organisation, Birmingham, July 2013*. (Poster Presentation, awarded **Poster Prize**)